POLY(NORBORNENE) SUPPORTED SIDE-CHAIN COORDINATION COMPLEXES: AN EFFICIENT ROUTE TO FUNCTIONALIZED POLYMERS

A Dissertation
Presented to
The Academic Faculty

by

Joseph Raymond Carlise

In Partial Fulfillment
of the Requirements for the Degree
Doctor of Philosophy in the
School of Chemistry and Biochemistry

Georgia Institute of Technology
May 2006

POLY(NORBORNENE) SUPPORTED SIDE-CHAIN COORDINATION COMPLEXES: AN EFFICIENT ROUTE TO FUNCTIONALIZED POLYMERS

Approved by:

Dr. Marcus Weck, Advisor
School of Chemistry and Biochemistry
Georgia Institute of Technology

Dr. Charles L. Liotta
School of Chemistry and Biochemistry
Georgia Institute of Technology

Dr. E. Kent Barefield
School of Chemistry and Biochemistry
Georgia Institute of Technology

Dr. William S. Rees, jr.
Materials Science and Engineering
Georgia Institute of Technology

Dr. David Collard
School of Chemistry and Biochemistry
Georgia Institute of Technology

Date Approved:

To my family, for their words of encouragement, support, and faith in me.

ACKNOWLEDGEMENTS

I would like to thank my advisor, Professor Marcus Weck, for without his guidance, patience, scientific insights, motivation, and enthusiasm, all of the work presented herein would not have been possible. Marcus has been a terrific mentor to me ever since my first semester here at Georgia Tech when I enrolled in a class he was teaching during what was also his first semester here as well. Both his enthusiasm for science and sense of humor have been inspiring to me over the years. From Marcus I learned what it means to be a good scientist, to think like one, to write like one, and to communicate like one. For all of this I am very grateful.

I also wish to thank the members of my Ph.D. committee: Professors Kent Barefield, David Collard, Charles Liotta, and Will Rees. I have greatly appreciated all the times that they have been willing to lend their time and insights into my various scientific endeavors. Their thoughts and suggestions have also been an integral part of the successful completion of my work here at Georgia Tech.

My fellow colleagues have also had a strong positive impact on my experience here at Tech. I would like to thank everyone in my research group for keeping such a positive, fun attitude around our labs. It has really been enjoyable to come to work into this environment for the past several years as a result, and I would like to thank my entire group for that. Over the years I have had a great number of stimulating scientific discussions with many of my colleagues. Dr. Paul Stubbs (Homie), Dr. Robert Kriegel, Dr. Michael Holbach, Dr. Xian-Yong Wang, Dr. Joel Pollino, Warren Gerhardt, William Sommer, Clint South, and many others including Kamlesh Nair, MaryNell Higley,

Caroline Burd, Matija Crne, Alpay Kimyonok, Dr. Kunsang Yoon, Dr. Xiaolai Zheng, Poorva Tayal, were also for joining me in the many random scientific discussions that occurred so frequently. Also, I benefitted from my interactions with Dr. Javier Concepcion (a post-doc from the Rees lab at the time), who was a great help for me when I was just getting started. For these reasons I wish to thank them all for greatly enhancing my time here at Tech and making graduate school everything that I had hoped it would be.

I of course would like to thank my family for the patience, support, and inspiration they have given me through these years as a graduate student at Georgia Tech. Specifically, I would like to thank my parents, Chuck and Cathy, who have always had faith in me and are no doubt the reason that I have learned to have faith in myself. They have been outstanding role models for me through my entire life. If I can even come close to doing as good of a job at being a parent to my own children as they have been to me, I will know true success. My father's impressive cool-headedness and strong work ethic, somehow combined with a general lighthearted attitude, have always inspired me tremendously. My mother's passionate, humorous, understanding, patient attitude toward me during all of my ups and downs has been enough to lift my spirits more times than I can count. My brother, Chuck jr., having grown up only 1 ½ years younger than me, has really become one of my best friends – if nobody else anywhere seems like they understand me, somehow he and I are is always on the same page about nearly everything. My sister Maggie has both amazed and inspired me with her fun, unspoiled, positive, generous, silly, good-natured attitude towards life, she truly is one of a kind. I am very lucky to have such a wonderful brother and sister.

Finally, I wish to thank the two main ladies in my life, my partner Rebecca, and our daughter Celia, for keeping my life filled with love and joy. Not a single day goes by that Celia does not amaze me with her creativity and intelligence, as well as make me laugh. I feel truly lucky to be her Daddy, and to have her in my life. I met Rebecca here at Georgia Tech as a graduate student, and I can also add her to the list of people with whom I have enjoyed invigorating scientific discussions with, since she received her Ph.D. from this same department, and is always interested in discussing science with me. Rebecca's hard work, tireless dedication, and devotion to our family have amazed me. She has been a great help to me in the successful completion of my work here at Tech as well. I am very grateful for the few years that we have been together, and look forward to many many more happy years to come.

TABLE OF CONTENTS

Page

ACKNOWLEDGEMENTS iv

LIST OF TABLES xii

LIST OF FIGURES xiii

LIST OF SCHEMES xvii

LIST OF SYMBOLS AND ABBREVIATIONS xix

SUMMARY xxii

CHAPTER

1 INTRODUCTION TO SIDE-CHAIN FUNCTIONALIZED POLYMERS 1

1.1 Abstract 1

1.2 Introduction 1

1.3 Synthetic routes to side-chain functionalized polymers 2

1.3.1 Strategy 1: Functionalization of monomer units (Pre-Polymerization) 2

1.3.2 Strategy 2: Direct polymer functionalization (Post-Polymerization) 6

1.3.3 Strategy 3: Combinations of Strategies 1 and 2 8

1.4 Modern designs of SCFPs 9

1.5 Conclusion 17

1.6 References 18

2 METAL COORDINATION AS A STRATEGY FOR POLYMER AND MATERIAL FUNCTIONALIZATION 26

2.1 Abstract 26

2.2 Introduction 26

2.3 Metal Coordination in Polymer Chemistry 27

2.3.1 Advantages of metal coordination 28

2.3.2 Techniques and Applications of Metal Coordination in Polymer and Materials Chemistry 29

Supramolecular Design and Architecture 30

Organic Light-Emitting Diodes (OLEDs) and Photovoltaics 37

Supported Catalysts 42

2.4 Conclusion 43

2.5 References 44

3 SIDE-CHAIN FUNCTIONALIZED POLYMERS CONTAINING BIPYRIDINE COORDINATION SITES: POLYMERIZATION AND METAL COORDINATION STUDIES 50

3.1 Abstract 50

3.2 Introduction 50

3.3 Monomer Synthesis 52

3.4 Coordination Studies 55

3.5 Polymerization 58

3.6 Discussion 59

3.7 Living Tests 61

3.8 Conclusion 62

3.9 Experimental Section 63

3.10 References 81

4 FUNCTIONALIZATION OF GUAR AND SUBSEQUENT CROSS-LINKING VIA TRANSITION-METAL ION CHELATION 85

4.1 Abstract 85

4.2 Introduction 85

4.3 Project Design 87

4.4 Results and Discussion Section 87

4.4.1 Ligand Modification 87

4.4.2 Functionalization of Guar 88

4.4.3 Cross-linking of Guar Using Transition Metal Cations 90

4.5 Experimental Section 92

4.6 Conclusion 94

4.7 References 95

5 PHOSPHORESCENT SIDE-CHAIN FUNCTIONALIZED POLY(NORBORNENE)S CONTAINING IRIDIUM COMPLEXES 96

5.1 Abstract 96

5.2 Introduction 96

5.3 Monomer Design 98

5.4 Monomer Synthesis 99

5.5 Polymerization 103

5.6 Photophysical Properties 107

5.7 Conclusions 115

5.8 Experimental Section 116

5.9 References 128

6 MULTIFUNCTIONAL POLYMER BACKBONES FOR REVERSIBLE SELF-ASSEMBLY, CROSS-LINKING, AND GRAFTING 131

6.1 Abstract 131

6.2 Introduction 131

6.3 Synthetic Strategy 134

6.4 Small Molecule Synthesis 138

6.5 Macroinitiator Synthesis 139

6.6 Graft Copolymer Synthesis 140

6.7 Cross-Linking Studies 141

6.8 Conclusions 144

6.9 Experimental Section 145

6.10 References 152

7 POLYMERS WITH SIDE-CHAIN FUNCTIONALIZATION VIA METAL COORDINATION: CONCLUSIONS AND POTENTIAL FUTURE DIRECTIONS 154

7.1 Abstract 154

7.2 Introduction 154

7.3 Overall Summary and Conclusions 154

7.4 Potential Future Directions 157

7.4.1 Self-Assembly-Based Tuning of Luminescence 157

7.4.2 Solving the Problems of Polymer-Bound Alq_3 159

7.4.3 Potential Directions for Macromolecular Cross-Linking 161

7.5 Conclusions 165

7.6 References 167

APPENDIX A: SYNTHESIS AND HYDROLYSIS BEHAVIOR OF SIDE-CHAIN FUNCTIONALIZED NORBORNENES 169

A.1 Abstract 169

A.2 Introduction 169

A.3 Design Strategy 171

A.4 Monomer Syntheses 173

A.4.1 Synthesis of Norbornene PEG Esters 1 - 3. 173

A.4.2 Synthesis of Norbornene monomers containing PEG-Ester and Acid-Ester in their side-chains: Monomers 6 and 7 174

A.4.3 Synthesis of Norbornene linked to galactose *via* triethylene glycol ester: Monomer 8 175

A.4.4 Synthesis of Monomer 9 175
A.5 Hydrolysis 176
A.5.1 Hydrolysis of 4 and 5. 177
A.5.2 Hydrolysis of 6 182
A.5.3 Hydrolysis of 7 186
A.5.4 Hydrolysis of 9 190
A.5.5 Hydrolysis of 8. 192
A.6 Conclusion 196
A.7 Experimental Section 197
A.8 References 205

LIST OF TABLES

Page

Table 3.1: Polymerization data for the ROMP of monomer **1** with initiators **9**, **13** and **14** 59

Table 5.1: Polymer characterization data. 106

Table 5.2: Solution photophysical data for compounds **1 - 3** and their corresponding polymers. [*a*, acetonitrile; *b*, dichloromethane; *c*, toluene; *d*, dimethylsulfoxide; *e*, THF, ambient conditions; *f*, THF, degassed; * most samples showed broad absorbance range with no clear local maximum; ** relative to $Ru(bpy)_3(PF_6)_2$]; ‡, lifetimes measured in dichloromethane.] 108

Table 5.3: Solid-state photophysical data for all polymers. 109

Table 5.4: Lifetimes measured for *mer*-**2** and poly-*mer*-**2** in various solvents, both in ambient conditions and degassed. Lifetimes are displayed in microseconds (μs). 114

Table 6.1: Data for macroinitiators with ATRP initiator densities of 2.5 %, 5.0 %, and 10.0 %. 140

Table A1: Building blocks **1** and **2**, along with monomers **3 - 9**, for which the hydrolysis behavior was investigated in this study. The compound number on the left corresponds with a specific combination of tethers to norbornene, hydrolysable linkages, and functional groups, which are depicted in Figure 1 († synthesized by R. Kriegel[1]). 172

Table A2: Hydrolysis data for a mixture of compounds **4** and **5**. 177

Table A3: Hydrolysis data of compound **3**. 180

Table A4: Hydrolysis data for compound **6**. 183

Table A5: Hydrolysis data for compound **7**. 187

Table A6: Hydrolysis data for compound **9**. 191

Table A7: Hydrolysis data for compound **8**. 193

LIST OF FIGURES

Page

Figure 1.1:Fraser's bis-chloromethyl substituted bipyridine-based macroinitiator designs and subsequent block copolymers. 5

Figure 1.2: Post-polymerization strategy used by Bicak and co-workers to form graft copolymers. 6

Figure 1.3: Functionalization of poly(styrene) via Fréchet's lithiation method. 7

Figure 1.4: Multifunctional random terpolymer synthesized by Weck and co-workers. 10

Figure 1.5: Stepwise and orthogonal routes to functionalization of the Universal Polymer Backbone using DAP/thiamine and pincer/pyridine complimentary self-recognition units 11

Figure 1.6: Conceptual depiction of the multiple stepwise and orthogonal self-assembly strategies employed by Weck and co-workers. Clockwise from left: Universal Polymer Backbone (UPB) functionalized with multiple recognition motifs (left); UPB functionalized with single recognition unit (top); cross-linked and fully functionalized UPB system via addition of a difunctional substrate (top right); UPB fully functionalized with small molecule substrates (lower right); UPB functionalized with single recognition unit (bottom). 12

Figure 1.7: Hydrogen-bonding units designed to exhibit self-sorting when present in the same polymer backbone. 13

Figure 1.8: Stepwise and orthogonal routes to functionalization of the Universal Polymer Backbone using thiamine/DAP and isophthalamide/cyanuric acid complimentary self-recognition units. 14

Figure 1.9: Self-assembled hairy-rod polymers based on metal coordination and ionic interaction. 16

Figure 2.1: Chemical structures and cartoons of multifunctional ligands containing both pyridine (blue) and terpyridine (red) coordination sites. Left: meta-pyridine building block. Right: para-pyridine building block. 30

Figure 2.2: Formation of supramolecular building block via iron(II) coordination. 31

Figure 2.3: Metal coordination-based suprastructures from combination of meta- or para-iron-based building blocks and a second class of metal salts. 31

Figure 2.4: Metal coordination-mediated stacking of flattened, ruptured vesicles. 33

Figure 2.5: Multi-step main-chain self-assembly to form a flexible, high molecular weight polymer. Step 1: dimerization of difunctional unit via the self-complimentary ureidopyrimidinone end (top); Step 2: Addition of a metal salt such as iron(II) initiates metal coordination-based self-assembly of the trpy-functionalized ends to form extended polymer chains (bottom). 35

Figure 2.6: Abstraction of iron(II) ion from the bis-terpyridine complex with HEEDTA. 37

Figure 2.7: Triblock platimun-based polymer for use in OLED. 40

Figure 2.8: Alq_3 containing polymer synthesized by Weck and Meyers. 41

Figure 3.1: Dichlorobis(2'2-bipyridine)Ruthenium(II) derivatives 54

Figure 3.2: Metathesis catalysts used. 54

Figure 4.1: Schematic of guar, a poly(galactomannan). 86

Figure 4.2: Demonstration of "lipping" phenomena: Solution of guar (bpy/mannose ratio of 1:100), in the presence of RuCl3, and shaking for 10 seconds produces full gellation.. 91

Figure 4.3: Cross-linking of modified guar via transition metal ion chelation. 92

Figure 5.1: Top: Monomers employed in this study: **1**, bpy-based, charged iridium complex; **2**, ppy-based, neutral iridium complex; **3**, alkyl spacer-based monomer. Bottom: Grubbs' 3rd generation catalyst. 99

Figure 5.2: Copolymers poly-**1**-*co*-**3** (top) and poly-**2**-*co*-**3** (bottom). 104

Figure 5.3: Photoluminescence emission spectra of (from top to bottom): **1**, poly-**1**, poly-**1**-*co*-**3** (1:2)**,** poly-**1**-*co*-**3** (1:20) in dichloromethane (ex. 400 nm)**.** 109

Figure 5.4: Solid state PL emission spectra of (right to left): poly-**1**, poly-**1**-*co*-**3** (1:2), and poly-**1**-*co*-**3** (1:20) (ex. 400 nm). 110

Figure 5.5: Solid-state PL emission spectra of (from right to left): *mer*-poly-**2**, *mer*-poly-**2**-*co*-**3** (1:2)**,** *mer*-poly-**2**-*co*-**3** (1:20) (ex. 380 nm). 110

Figure 5.6: Solid-state PL emission spectra of (from right to left): *fac* -poly-**2**-*co*-**3** (1:2)**,** *fac*-poly-**2**-*co*-**3** (1:20) (ex. 380 nm). 111

Figure 5.7: Solution PL emission spectrum of (from top to bottom): *mer*-**2**, *mer*-poly-**2**, *mer*-poly-**2**-*co*-**3** (1:2)**,** *mer*-poly-**2**-*co*-**3** (1:20) in dichloromethane (ex. 380 nm). 112

Figure 5.8: Solution PL emission spectrum of (from top to bottom): *fac*-**2**, *fac*-poly-**2**-*co*-**3** (1:2)**,** *fac*-poly-**2**-*co*-**3** (1:20) in dichloromethane (ex. 380 nm). 112

Figure 5.9: Solvent dependence for *mer*-poly-**2**. A (toluene), C (acetonitrile), D (dichloromethane), E (dimethylsulfoxide), B (*fac*-**2** in dichloromethane, for comparison). 113

Figure 6.1: Monomers used to synthesize the macroinitiator via ROMP: triethylene glycol-based spacer monomer **1**, α-bromoester-containing monomer **2**, palladium-based pincer-containing monomer **3**. 135

Figure 6.2: Modified triblock copolymer design of the multifunctional polymer system. 136

Figure 6.3: Schematics of both organic soluble (left) and water soluble (right) graft copolymers 137

Figure 6.4: Multi-pyridine-containing cross-linking agents: tris-pyridine glycerol-based cross-linking agent **4**, and pentakis-pyridine galactose-based cross-linking agent **5**. 138

Figure 6.5: GPC traces of 10 % initiator density polymers: **G100** (left), **MI100** (right). 141

Figure 6.6: Viscosimetry data for corss-linking of **G100**: ♦ **4**, 5mg/mL, $CHCl_3$; Δ **4**, 20mg/mL, $CHCl_3$; € **4**, 24mg/mL, $CHCl_3$; x **5**, 20mg/mL, $CHCl_3$; * **4**, 20mg/mL, CH_2Cl_2; ♦ **4**, 20mg/mL, CH_2Cl_2 after ion exchange resin; - PVPy, 20mg/mL, CH_2Cl_2. 142

Figure 7.1: Design of self-assembly-tunable emissive polymeric metal complexes. 158

Figure 7.2: Schematic of the "claw" motif for polymer-bound Alq_3 complexes. 159

Figure 7.3: Formation of the improved Alq_3 monomer (top); 3-dimensional representation of the coordination environment (bottom) (on bottom picture: norbornenes left out for clarity) 160

Figure 7.4. Altenative cross-linking methodology using 2,2',2"-terpyridine (shown) or 2,2'-bipyridine units in place of the palladium pincer moiety. (M = transition metal) 162

Figure 7.5. Placement of cross-linking moities on ends of gratf chains instead of on the ends of the parent backbone. 163

Figure 7.6. Synthesis of potential hydrogen-bond "guided" monomers for use in metal coordinated high molecular weight polymers. Possible sequence order would be (1) diaminopyridine monomer (A) on left (synthesis shown), followed by a water soluble spacer such as a triethylene glycol monomer, followed by thiamine monomer (B) on left (synthesis not shown, analogous to A). 164

Figure 7.7. Schematic of polymer designed for metal coordination-based chain extension via end-to-end coupling. Hydrogen bonding moities are included to assist in end-to-end coupling once the chain becomes significantly long. 165

Figure A1: Structures corresponding with combinations in Table A.1 173

Figure A2: Pseudo-first order hydrolysis kinetics for compounds **4** and **5** at 37 ºC. € pH 3.1, • pH 4.6, Δ pH 5.6, ∇ pH 6.9, ♦ pH 7.4, + pH 8.9. 178

Figure A3: Pseudo-first order hydrolysis kinetics for compounds **4** and **5** at 37 ºC. € pH 3.1, • pH 4.6, Δ pH 5.6, ∇ pH 6.9, ♦ pH 7.4, + pH 8.9. 179

Figure A4: Pseudo-first order hydrolysis kinetics for compounds **4** and **5** at 80 ºC. € pH 3.1, • pH 4.6, Δ pH 5.6, ∇ pH 6.9, ♦ pH 7.4, + pH 8.9. 179

Figure A5: Pseudo-first order hydrolysis kinetics for compound **3** at 80 ºC. € pH 3.1, • pH 4.6, Δ pH 5.6, ∇ pH 6.9, ♦ pH 7.4, + pH 8.9. 181

Figure A6: Pseudo-first order hydrolysis kinetics for compound **3** at 60 ºC. € pH 3.1, • pH 4.6, Δ pH 5.6, ∇ pH 6.9, ♦ pH 7.4, + pH 8.9. 182

Figure A7: Pseudo-first order hydrolysis kinetics for compound **6** at 80 ºC. € pH 3.1, • pH 4.6, Δ pH 5.6, ∇ pH 6.9, ♦ pH 7.4. 183

Figure A8: Pseudo-first order hydrolysis kinetics for compound **6** at 60 ºC. € pH 3.1, • pH 4.6, Δ pH 5.6, ∇ pH 6.9, ♦ pH 7.4. 184

Figure A9: Pseudo-first order hydrolysis kinetics for compound **6** at 37 ºC. € pH 3.1, • pH 4.6, Δ pH 5.6, ∇ pH 6.9, ♦ pH 7.4. 185

Figure A10: Pseudo-first order hydrolysis kinetics for compound **7** at 37 ºC. € pH 3.1, • pH 4.6, Δ pH 5.6, ∇ pH 6.9, ♦ pH 7.4. 188

Figure A11: Pseudo-first order hydrolysis kinetics for compound **7** at 60 ºC. € pH 3.1, • pH 4.6, Δ pH 5.6, ∇ pH 6.9, ♦ pH 7.4, + pH 8.9. 189

Figure A12: Hydrolysis kinetics for compound **7** at 80 ºC. € pH 3.1, • pH 4.6, Δ pH 5.6, ∇ pH 6.9, ♦ pH 7.4, + pH 8.9. 189

Figure A13: Pseudo-first order hydrolysis kinetics for compound **9** at 37 ºC. • pH 4.6, Δ pH 5.6, ∇ pH 6.9, ♦ pH 7.4, + pH 8.9. 191

Figure A14: Hydrolysis kinetics for compound **8** at 37 ºC. € pH 3.1, • pH 4.6, Δ pH 5.6, ∇ pH 6.9, ♦ pH 7.4. 194

Figure A15: Hydrolysis kinetics for compound **8** at 60 ºC. € pH 3.1, • pH 4.6, Δ pH 5.6, ∇ pH 6.9, ♦ pH 7.4, + pH 8.9. 195

Figure A16: Hydrolysis kinetics for compound **8** at 80 ºC. ∈ pH 3.1, • pH 4.6, Δ pH 5.6, ∇ pH 6.9, ♦ pH 7.4. 195

LIST OF SCHEMES

Page

Scheme 3.1: MeLi, THF, 0 ^{o}C; (b) sat. $KMnO_4$/acetone; (c) LDA, THF, -20 ^{o}C; (d) $Br(CH_2)_{11}OTBS$ (**1**), THF, -95 ^{o}C; (e) TBAF, CH_2Cl_2; 33% overall yield. 53

Scheme 3.2: Formation of 75:25 *endo/exo* **1**: (a) reflux; (b) **4**, NEt_3, CH_2Cl_2; 80% overall yield. 53

Scheme 3.3: Formation of *exo* **1**: (a) **4**, DCC, DMAP (cat), CH_2Cl_2; 85% overall yield.53

Scheme 3.4: *Formation of **10***: (a) $RuCl_2(dmso)_4$, $CHCl_3$; *Formation of **8***: (b) 2 equiv. dnBpy, 1:1 EtOH/H_2O, reflux 12 hrs; (c) NH_4PF_6; 43% overall yield. *Formation of **15***: (a) $PdCl_2$(benzonitrile)$_2$, acetone; *Formation of **12***: (b) 1 equiv. dnBpy, MeOH; (c) AgOTf, 3hrs, dark. 55

Scheme 3.5: (a) $RuCl_2(dmso)_4$, $CHCl_3$, reflux; (b) 4,4'-dinonyl-2,2'-bipyridine, EtOH/H_2O, reflux; (c) NH_4PF_6; (d) 3-octyl-2,4-pentanedione, EtOH, reflux; (e) **7b**, MeOH; (f) AgOTf. 57

Scheme 4.1: Oxidation of 4,4'-dimethyl-2,2'-bipyridine using Jones' reagent. 88

Scheme 4.2: Modification of guar with 2,2'-bipyridinyl-4,4'-dicarbonyl chloride dihydrochloride. 89

Scheme 5.1: Synthesis of **1**: a.) Lithium diisopropylamide, THF, -78 ^{o}C; b.) propylene oxide, THF, 0 ^{o}C, 73%; c.) *exo*-5-norbornene-2-carboxylic acid, DCC, DMAP, CH_2Cl_2, 42%; d.) $[Ir(ppy)_2Cl]_2$, ethylene glycol, 150 ^{o}C, 72 %; e.) NH_4PF_6 (aq.). 101

Scheme 5.2: Synthesis of *mer*-**2**: a.) Lithium aluminum hydride, THF, 94%; b.) *exo*-5-norbornene-2-carboxylic acid, DCC, DMAP (cat.), CH_2Cl_2, 80%; c.) $[Ir(ppy)_2OTf]_2$, acetone, ambient temp., 43 %. 102

Scheme 5.3: Synthesis of *fac*-**2**: a.) Lithium aluminum hydride, THF, 99%; b.) *exo*-5-norbornene-2-carboxylic acid, DCC, DMAP, THF, 40%. 103

Scheme 6.1: Synthesis of ATRP initiating monomer **2**. 138

Scheme 6.2: Synthesis of tris-pyridine cross-linking agent **4**. 139

Scheme 6.3: Synthesis of pentakis-pyridine cross-linker **5**. 139

Scheme A1: Synthesis of norbornene spacer molecules **1**, **2**, and **3**. **1**: a = triethylene glycol (excess), THF, triethyamine; **2**: chloroethoxyethanol, triethylamine, THF; **3**: triethylene glycol monomethyl ether, triethylamine, THF. 174

Scheme A2: Synthesis of compounds **6** and **7**: a.) DCC, DMAP, CH_2Cl_2; b.) pyridine, THF. 175

Scheme A3: Synthesis of compound **8**. 175

Scheme A4: Synthesis of compound **9**. 176

LIST OF SYMBOLS AND ABBREVIATIONS

Alq_3	Aluminum tris-8-hydroxyquinoline
ATRP	Atom-transfer free radical polymeriazation
BCP	2,9-dimethyl-4,7-diphenyl-1,10-phenanthroline
bpy	2,2'-bipyridine
CGC	constrained geometry catalyst
CTA	chain-transfer agent
DAD	donor-acceptor-donor
DAP	diaminopyridine
DCC	dicyclohexylcarbodiimide
DDAA	donor-donor-acceptor-acceptor
DMAP	diaminopyridine
DMF	dimethylformamide
DNA	deoxyribonucleic acid
dNbpy	4,4'-dinonyl-2,2'-bipyridine
DSCs	dye-sensitized solar cells
EDTA	ethylene diamine tetraacetic acid
fac	facial
GPC	gel-permeation chromatography
HEEDTA	hexaethyl(ethylenediamine)tetraacetic acid
HOMO	highest occupied molecular orbital
K_a	association constant
LDA	lithium diisopropylamide
LEC	light-emitting electrochemical cell

LED	light-emitting diode
LUMO	lowest unoccupied molecular orbital
mer	meridional
NMP	nitroxide-mediated polymerization
NMR	nuclear magnetic resonance
OLED	organic light-emitting diode
OTf	triflate (trifluoromethanesulfonate)
PAA	poly(acrylic acid)
PCL	poly(caprolactone)
PDI	polydispersity index
PEG	poly(ethylene glycol)
PLA	poly(lactide)
PMMA	poly(methyl methacrylate)
ppy	phenylpyridine
PS	poly(styrene)
PVPy	poly(vinyl pyridine)
py	pyridine
RAFT	reversible addition-fragmentation chain-transfer polymerization
RNA	ribonucleic acid
ROMP	ring-opening metathesis polymerization
SANS	small angle neutron scattering
SAXS	small angle X-ray scattering
SCS	sulfur-carbon-sulfur
SCFP	side-chain functionalized polymer
TBAF	tetrabutyl ammonium fluoride

THF	tetrahydrofuran
TLC	thin-layer chromatography
TREN	tris(ethylene amine) amine
trpy	2,2',2"-terpyridine
UPB	Universal Polymer Backbone
UV-vis	ultraviolet-visible

SUMMARY

This thesis begins with a brief overview of current strategies used in the synthesis of side-chain functionalizad polymers and materials. The discussion then focuses more explicitly on transition metal-based motifs and methodologies that are employed in polymer functionalization and continues with a more detailed overview of this field.

The primary hypothesis that is addressed herein is that combining the versatility and strength of metal-ligand interactions with the efficiency and functional group tolerance of ROMP comprises a useful method of generating a variety of functionalized polymers and materials via side-chain metal coordination. Thus, the goal is to test this hypothesis by synthesizing functionalized polymers with a range of useful properties to demonstrate the relevance and importance of this methodology, by employing several different strategies to show the synthetic ease by which the materials can be realized.

The strategies and methods discussed in the synthesis of side-chain functionalized polymers are divided into three subgroups: (1) pre-polymerization functionalization, in which all of the modifications take place on the monomer with polymerization as the last step, (2) post-polymerization functionalization, in which the polymer itself is subsequently modified, and (3) combinations of the first two strategies.

It is shown that useful functional polymers and materials can be synthesized by any of the above strategies, and representative examples of each are given in both the introduction and in the body of work presented.

Modes of functionalization are all based on transition metal coordination, and polymerizations are primarily carried out via ROMP. Metal coordination is shown to be

a useful technique for functionalizing polymers, to creating supported emissive complexes, to modulating solution viscosity.

Finally, conclusions are drawn regarding the various strategies presented herein, and potential future directions are discussed.

CHAPTER 1

INTRODUCTION TO SIDE-CHAIN FUNCTIONALIZED POLYMERS

1.1 Abstract

This chapter introduces the concept of side-chain functionalized polymers, divides them into categories based on synthetic methodology and design motif, and puts them into the context of their respective applications both industrially as well as in the academic laboratory. The current research trends are described, and respective advantages and disadvantages to each strategy are outlined.

1.2 Introduction

Polymers and polymer-based materials are ubiquitous in modern society. From the plastic in a disposable pen, to the Kevlar in a bulletproof vest, to the synthetic rubber in tires, to the nylon in everything from clothing to carpets – synthetic polymers have become a ubiquitous part of our culture since they were first created over a century ago.

Until the advent of Merrifield's "solid phase technique" for the synthesis of peptides,[1] which functioned via an insoluble polymeric support acting as a protecting group in each consecutive condensation step, synthetic polymers were used primarily for their macroscopic properties for use as fibers, textiles, and plastics. In 1963, Merrifield's invention demonstrated the utility of functionalized polymers in organic synthesis, and the scientific community has reflected this revolutionary discovery ever since in the creative ways that functionalized polymers have been both synthesized and utilized [2-23]

Functionalized polymers have been defined as synthetic macromolecules to which are chemically bound functional groups that can be utilized as reagents, catalysts, protecting groups, etc.[3] A straightforward method to create polymers that have these functional

groups bound to them is through the use of side-chains in order to link the polymerizable group to the functional group, resulting in side-chain functionalized polymers (SCFPs). This understanding of the concept of SCFPs, by which the functional groups can often be easily modified, directly facilitates the ability to alter the macroscopic properties of the resulting polymers as well, thus paving the way to the optimization of functional materials commonly in use today.[17,24-35]

This thesis focuses primarily upon the concept of side-chain functionalized polymers, and the utilization of this concept to design new materials and improve upon current systems in use today.

1.3 Synthetic routes to side-chain functionalized polymers

Throughout the past several decades several distinct strategies have emerged for the synthesis of SCFPs. Depending on both the abilities of the starting reagents, as well as the desired properties of the final products, these strategies have been categorized primarily by the question of which order the synthetic steps are performed; and subsequently by the mode or modes of functionalization that will be employed. To arrive at a functionalized polymer, two distinct events must take place: (1) combination of monomer units to form a macromolecular structure, and (2) establishment of functional groups within the construct of this polymeric species. This gives rise to two possible synthetic strategies: functionalization of monomer units followed by polymerization, or direct functionalization of a polymer. Within these two groups exist subsets that stem from the mode of functionalization that will be utilized: either covalent or non-covalent. The focus of this section will be to illustrate the general concept of SCFPs based on the above-mentioned categorizations.

1.3.1 Strategy 1: Functionalization of monomer units (Pre-Polymerization)

A straightforward method that generates generally well-defined functionalized polymers is the strategy of synthesizing functionalized monomer units for use in subsequent polymerization. This method includes adding the functionality to the monomer unit and thus performing all of the synthesis on the small molecule prior to the polymerization reaction. It has several advantages – for instance, (1) it ensures that every single repeat unit will be identically adorned with the desired functional group, giving specifically a functionalized homopolymer (unless more than one type of monomer is employed), (2) it simplifies the functionalization process by eliminating the need for purification or separation of impurities that generally arise from incomplete reactions of large polymers with small molecules, and (3) it facilitates characterization of the resulting polymer in that there is no need to quantify whether a small percent of the monomer units did not get functionalized, especially if unreacted sites along the backbone are problematic for the intended use of the polymer. For instance, the presence of unwanted hydroxyls or other handles used for post-polymerization functionalization can be problematic as they introduce hydrogen-bonding and defects in a system in which these may not have been intended. Pre-polymerization functionalization ensures that this type of problem will not occur.

This strategy has been used extensively for a wide variety of polymer systems,[7,36-42] and is also commonly expanded upon by following the polymerization step with further functionalization of the polymer via self-assembly using non-covalent interactions such as metal coordination, hydrogen-bonding, or ionic interactions, thus ultimately incorporating both pre- and post-polymerization functionalization.[22,26,43-55] This topic of additional functionalization via self-assembly will be discussed in greater detail in a later section (**1.3.3)**.

When designed for use with a functional group-tolerant polymerization method, pre-polymerization functionalization can be a very useful tool for polymer synthesis. As suggested, an important factor in the utilization of this method is the amount of

interaction between the functional group and the catalyst, or more specifically, the non-participation of the functional group in the polymerization process. This method has proven useful for an extremely large number of applications, including emissive polymers,[40,46,56-60] graft copolymers,[61-67] side-chain liquid crystals,[53,68-73] and supported catalysts,[61,67,74-82] among others. Atom-transfer free radical polymerization (ATRP),[61,83-87] ring-opening metathesis polymerization (ROMP), nitroxide-mediated polymerization (NMP),[61,87,88] and reversible addition-fragmentation chain-transfer polymerization (RAFT),[87,89-94] are among the common modern polymerization techniques used today that are well known for their functional group tolerance. They have facilitated the rapid expansion of the field of polymer science that employs the pre-polymerization functionalization approach to functional materials. For example, in 2003, Fraser and co-workers reported a system where multiple modes of polymerization were initiated from the same 2,2'-bipyridine-based functional group, which was subsequently used for coordination in a later step.[95] Fraser's method, based on 4,4'-dimethyl-2,2'-bipyridine, relied on the chlorination of these methyl groups, and the subsequent selective unsymmetric functionalization of these chloromethyl groups to create different unique polymer initiation sites (Figure 1.1).

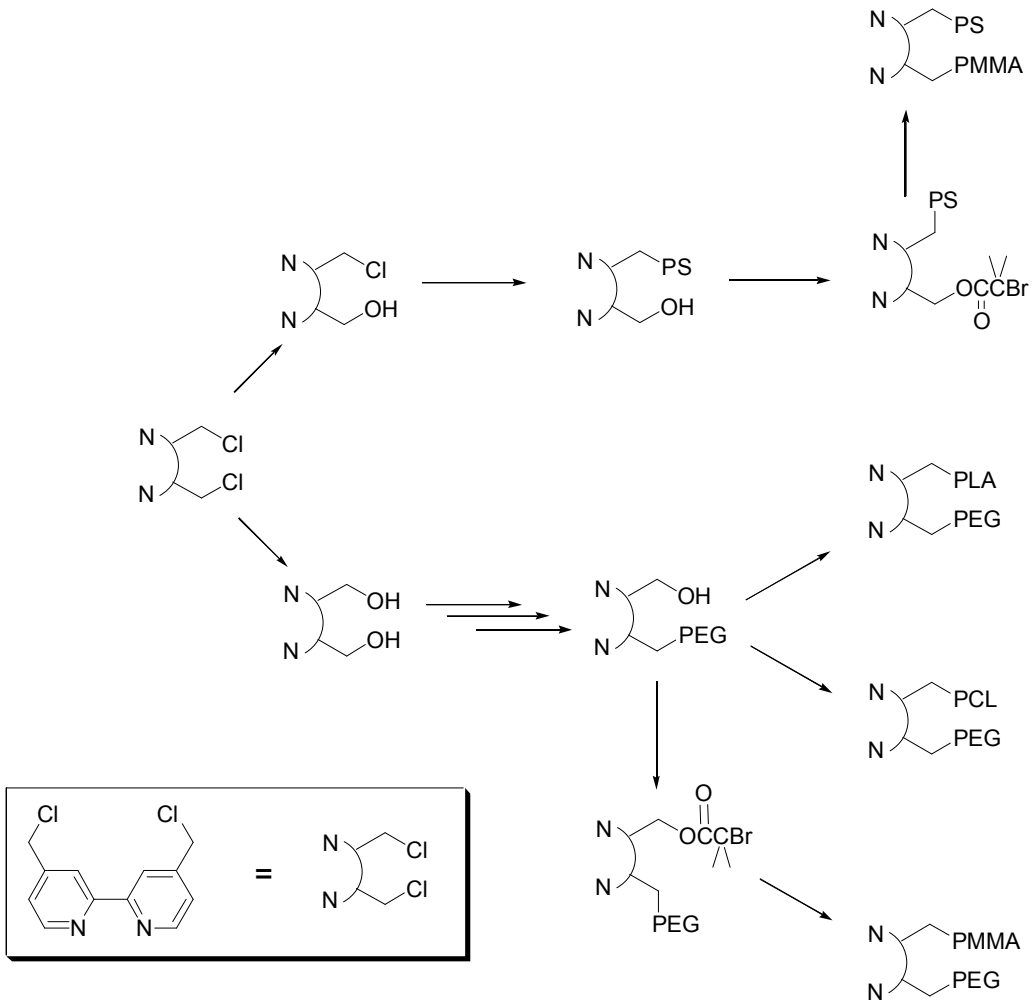

Figure 1.1. Fraser's bis-chloromethyl substituted bipyridine-based macroinitiator designs and subsequent block copolymers.

The strategy of selectively functionalizing the bis-chloromethyl bipyridine unit enables the synthesis of several pairs of polymers, including poly(styrene) (PS), poly(methyl methacrylate) (PMMA), poly(caprolactone) (PCL), poly(ethylene glycol) (PEG), and poly(lactide) (PLA). The polymerizations are all occurring on a functional group that is intended for use later as a ligand to form star polymers via transition metal coordination, so it is imperative that the polymerizations do not interfere with the ligand, and the reverse as well. This work demonstrates that these methods are indeed all functioning independently of one another, and it would not have been possible were it not for the

ability to gently polymerize functionalized monomers or functional groups without (1) interference of the monomer in the polymerization or (2) decomposition of the functional groups on the monomers.

1.3.2 Strategy 2: Direct Polymer Functionalization (Post-Polymerization)

A large number of polymers that have been modified solely through post-polymerization techniques have been reported.[2,78,79,81,96] This method was significantly more common relative to Strategy 1 (Pre-Polymerization Functionalization) before the advent of the controlled polymerization methods that incorporate functional group-tolerant catalysts and methods such as ROMP and ATRP mentioned in the above section. Traditional free-radical polymerization techniques have a much more narrow scope of functional groups that are tolerant of the harsh conditions of the polymerization, and as a result, post-polymerization modifications are often the only viable choice when restricted to uncontrolled free-radical polymerization techniques. Notwithstanding, there have nonetheless been several examples of post-polymerization functionalization reactions of polymers that have had average to very good results. For example, in 2003, Bicak and co-workers demonstrated the post-polymerization functionalization of poly(styrene) with N-chlorosulfonamide groups, followed by graft polymerization from these groups via the copper-mediated ATRP of methyl methacrylate (Figure 1.2).[67]

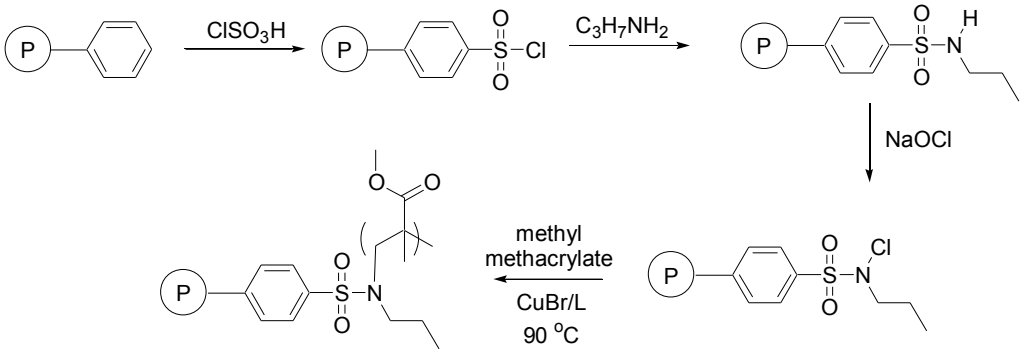

Figure 1.2. Post-polymerization strategy used by Bicak and co-workers to form graft copolymers.

It is of fundamental importance in cases where grafts are desired that a graft copolymerization method is employed that produces only the desired graft copolymer and no homopolymer side products. The major drawback of free radical methods of graft copolymerization lies in the fact that considerable amounts of wasteful non-grafted homopolymer are generated as by-product. This hurdle is successfully avoided by choosing a controlled grafting method such as ATRP.

Functionalization of poly(styrene) is not new, however. For example, in 1976, Fréchet and co-workers reported on the versatility resulting from lithiation of poly(styrene) (Figure 1.3).[96]

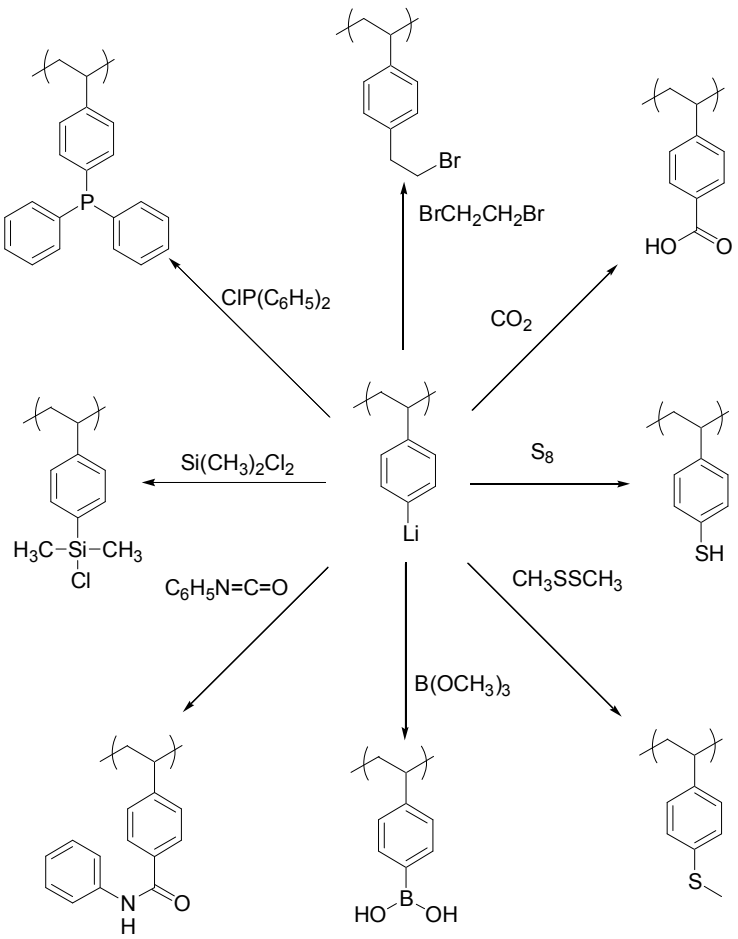

Figure 1.3. Functionalization of poly(styrene) via Fréchet's lithiation method.

They demonstrated that once lithiated, the reactive lithium sites could be easily and quantitatively transformed into carboxylic acids, thiols, sulfides, boronic acids, amides, silyl chlorides, phosphines, alkyl bromides, aldehyde, alcohols, or trityl functional groups, thereby opening the door to a wide variety of chemical transformations.

1.3.3 Strategy 3: Combinations of Strategies 1 and 2

Evidenced in the discussion above in the previous two sections, there are advantages as well as disadvantages to each of the two methods of polymer functionalization. Depending on the desired outcome, one method might appear more desirable than the other or vice versa. It stands to reason that often a mixture of these two techniques is ultimately the best route to take, and the task of designing this hybrid functionalization strategy has generated some very interesting and creative examples. There are several types of circumstances that warrant combination of these two techniques: (1) protected functional monomers that are deprotected after polymerization and can thus undergo further chemical transformations as a polymer, (2) recognition motifs for self-assembly of small molecules post-polymerization, (3) engineered polymer degradation once exposed to appropriate environmental conditions, (4) recycling of polymer backbones, and many others, including various combinations of the points just listed here.

Since it can be difficult to quantitatively control the location and density obtained via direct functionalization of polymers such as poly(styrene), etc., it has become increasingly common to employ non-covalent methods to further extend the reach of post-polymerization functionalization, with a delicacy that was not possible in the past using traditional covalent methods. If post-polymerization functionalization is desired, it is obviously beneficial to incorporate a site into the backbone that is easy to functionalize or modify. There are a large number of polymer-bound functional groups that can undergo further chemical transformations, but perhaps the simplest of this type to functionalize with a high degree of control is one that can participate in self-assembly or

self-organization, either through metal-ligand binding, hydrogen-bonding, or other interactions.

The concept of hierarchical self-organization observed in Nature has been the inspiration for a wide variety of potential applications as well as new methodologies in the field of chemistry. As a result, many synthetic polymers have been made that exhibit similar self-assembly behavior, including main-chain extension based on intermolecular interactions resulting in the formation of high molecular weight polymers, side-chain self-assembly of small molecules onto molecular recognition sites along polymers, and macroscopic polymer self-assembly and self-organization/alignment. While these non-covalent techniques have been utilized and investigated in small molecules for over a century, the employment of these methods in non-natural polymer science has been only researched extensively over the last two decades.[28,45,49,97-102] Over the next several pages, some very recent developments in the field will be introduced via presentation of selective examples of side-chain functionalization of polymers via multiple types of interactions.

1.4 Modern designs of SCFPs

A major class of supramolecular polymers are side-chain systems where the self-assembly receptors have been positioned on the side-chains of polymers. The self-assembly event then creates a function along the polymer backbone. This creates the potential for an enormous range of possible modifications to the polymer by rapid, straightforward self-assembly-based methodology. A primary goal of this strategy is to generate vast libraries of materials for a wide variety of applications since side-chain functionalized polymers have been employed or suggested for applications in electro-optics, biomaterials, liquid crystals etc.[18,43,103-106]

Over the past two decades, a wide variety of scientists have employed the basic design strategy of side-chain functionalized supramolecular polymers to synthesize

polymers that contain hydrogen-bonding as well as metal coordination receptor molecules in their side-chain.[21,22,26,38-42,44,45,49,50,97,107-109] Using basic self-assembly strategies, a number of functional polymers such as liquid crystalline polymers have been synthesized.[103-106,110-113] While highly successful, the employed strategies does not allow for the controlled multifunctionalization of side-chain supramolecular polymers. Over the past five years it became clear that a controlled multifunctionalization can only be achieved if multiple non-covalent recognition units are engineered into a single polymer backbone and if these multiple non-covalent recognition units can be addressed in an orthogonal fashion. To date only two basic polymer systems have been reported in the literature that follow these design guidelines.[22,44,45]

In 2004, Weck and co-workers demonstrated that both single as well as multifunctional self-assembly could be employed simultaneously, independently, and reversibly on the same side-chain functionalized polymer.[44] A random terpolymer of poly(norbornene) was synthesized consisting of diaminopyridine (DAP) hydrogen-bonding receptors and a palladium-functionalized SCS-type pincer ligand for metal coordination-based self-assembly (Figure 1.4).

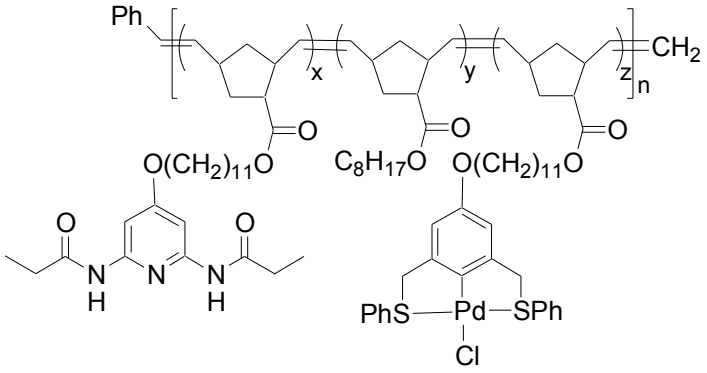

Figure 1.4. Multifunctional random terpolymer synthesized by Weck and co-workers.

The different unique properties and behaviors of the metal coordination site versus the hydrogen-bonding sites give the system a high degree of control. For instance, the thermoreversability of a hydrogen-bonded linkage versus the chemoreversability of

the metal coordination bond allows for independent control, tunability, and optimization of the polymer properties.

Initially, Weck and co-workers demonstrated that controlled, multi self-assembly in this system can be achieved either in a stepwise fashion or in a one-pot procedure (Figure 1.5).

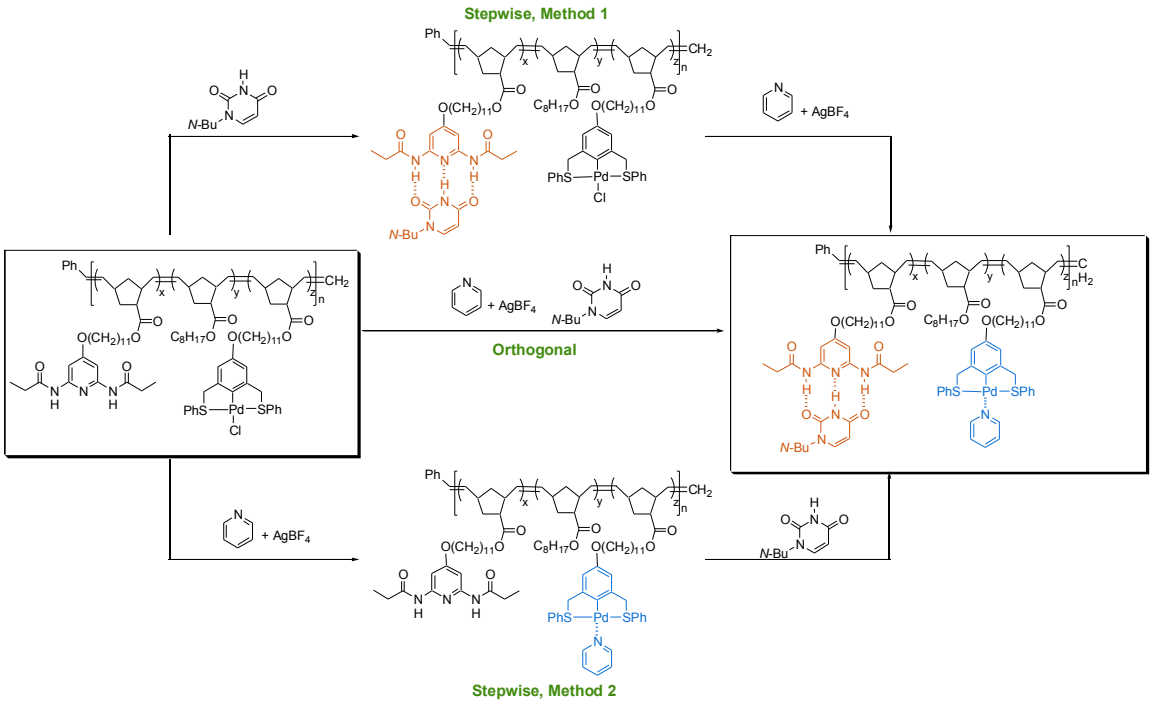

Figure 1.5. Stepwise and orthogonal routes to functionalization of the Universal Polymer Backbone using DAP/thiamine and pincer/pyridine complimentary self-recognition units

Their first report on the system clearly demonstrated that both recognition units function independently of each other and can be addressed selectively. Finally they demonstrated that the polymer properties of the fully self-assembled polymer are independent of the functionalization route. A variety of requirements are essential in this system. First, the two recognition motifs employed have to be independent of each other, second the polymerization method for the synthesis of the polymer backbone has to be

highly functional group tolerant since most self-assembly receptors have a high functional group and heteroatom content and finally the interactions have to be strong enough to allow for the controlled polymer functionalization. Since the introduction of their first random copolymer system based on DAP and palladated pincer complexes, Weck and coworkers have extended their concept to other polymer architectures (block copolymers) and self-assembly receptors.[22] Recently, they have combined the concepts of polymer architectural control with multifunctionalization.[44] They have synthesized a number of poly(norbornene)-based block copolymers containing two distinct self-assembly receptor molecules at the two polymer blocks. Again, through simple small molecule self-assembly, these block copolymers can be functionalized in an orthogonal fashion yielding highly functional block copolymers in a straightforward fashion (Figure 1.6).

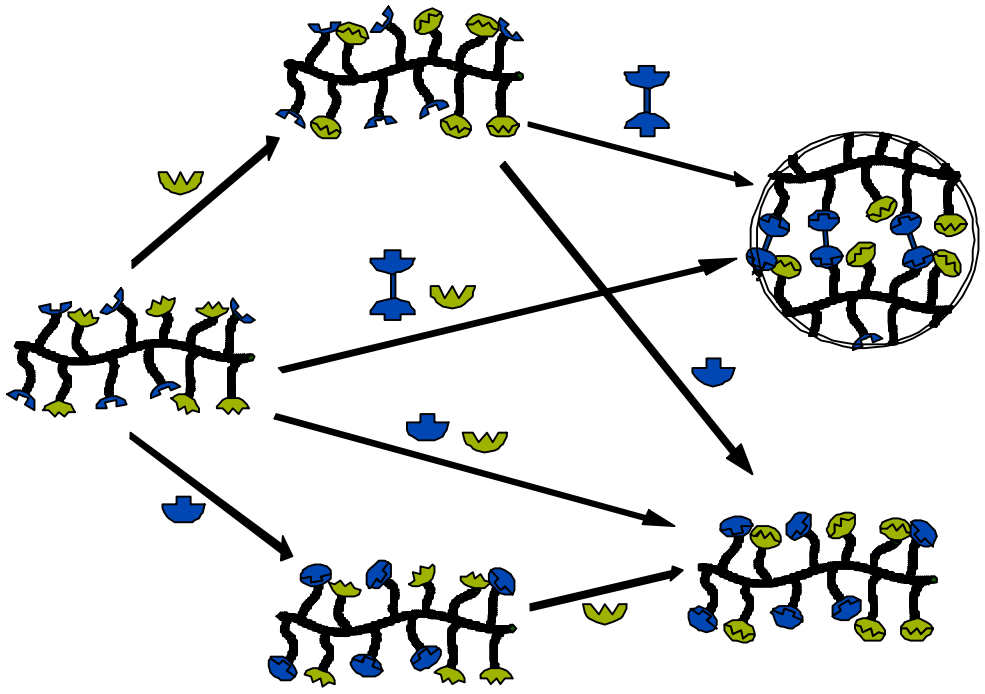

Figure 1.6. Conceptual depiction of the multiple stepwise and orthogonal self-assembly strategies employed by Weck and co-workers. Clockwise from left: Universal Polymer Backbone (UPB) functionalized with multiple recognition motifs (left); UPB functionalized with single recognition unit (top); cross-linked and fully functionalized

UPB system via addition of a difunctional substrate (top right); UPB fully functionalized with small molecule substrates (lower right); UPB functionalized with single recognition unit (bottom).

Finally, the Weck group has also investigated the incorporation of two distinct hydrogen-bonding receptors (Figure 1.7) along a single polymer backbone (both random and block copolymers were investigated).[22,50]

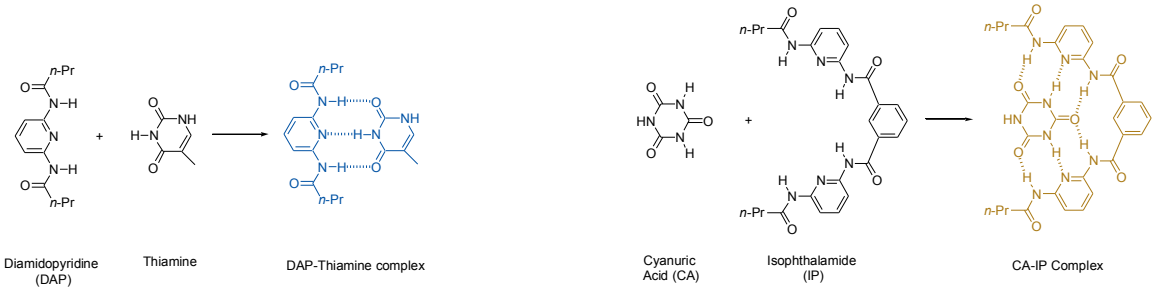

Figure 1.7. Hydrogen-bonding units designed to exhibit self-sorting when present in the same polymer backbone.

The selective self-assembly of a receptor molecule with its complementary recognition unit in the presence of a competitive recognition unit has been described as self-sorting in the literature. DNA and RNA are the prime examples of this concept. Using the above described copolymers containing two hydrogen-bonding units, Weck and Burd were able to prove this concept of self-sorting also in synthetic polymer systems (Figure 1.8).

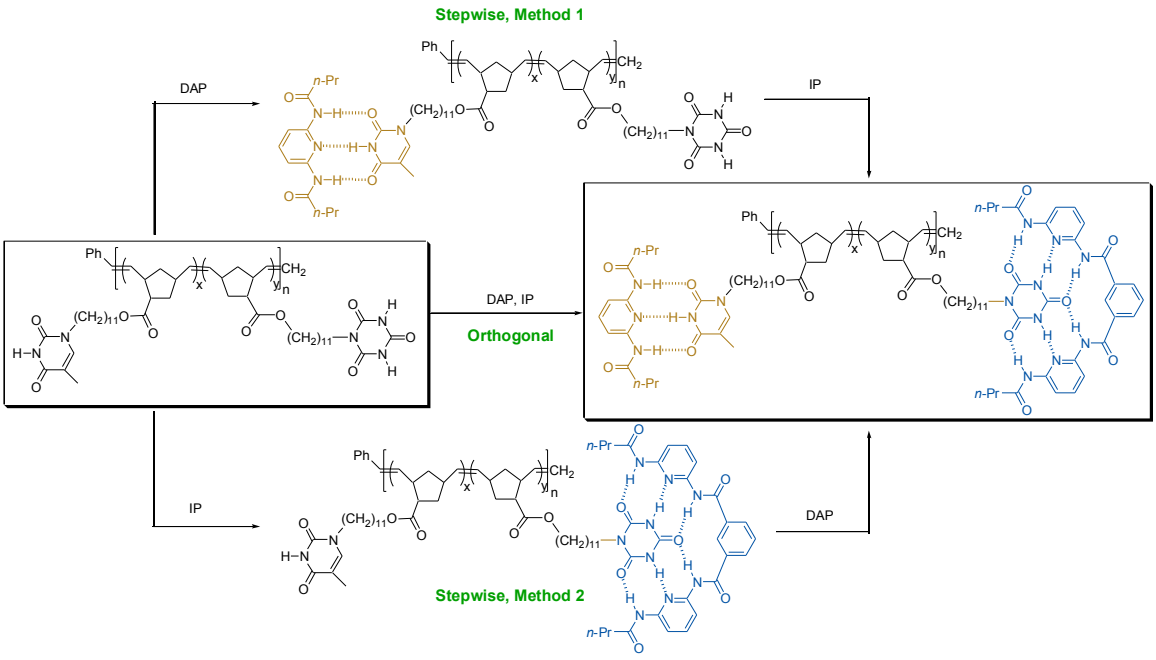

Figure 1.8. Stepwise and orthogonal routes to functionalization of the Universal Polymer Backbone using thiamine/DAP and isophthalamide/cyanuric acid complimentary self-recognition units.

To demonstrate the practicality and potential importance of their multifunctionalization concept, Weck and coworkers have investigated the formation of functional and cross-linked polymeric networks.[44] When employing terpolymers containing monomers with hydrogen-bonding receptor molecules and ones with palladated pincer complexes for metal coordination that are diluted in a matrix of alkyl-based spacer monomers, reversible cross-linking could be achieved through either the hydrogen-bonding unit or the metal coordination unit by employing either a bis-thymine or bis-perylene unit to crosslink through the side-chain DAP moieties via hydrogen-bonding, as well as a bis-pyridine molecule for cross-linking through the pincer groups via metal coordination. Extensive cross-linking was observed in all cases. Interestingly, the viscosity increases of the pincer-based cross-linked system were two orders of magnitude higher than that of the hydrogen-bonded systems. However, when the side-

chain hydrogen-bonding unit attached to the polymer was changed from DAP to cyanuric acid, a stronger interaction with the cross-linker, and thus higher solution viscosities, were achieved. This is in large part due to the increase in number of the participating hydrogen-bonding interactions involved with the corresponding cross-linker. In the case of the DAP unit, there are three hydrogen bonds involved per self-assembly site, interacting in a DAD fashion, for either of the cross-linkers employed (bis-thiamine or bis-perylene). However, when cyanuric acid is used instead, there are six hydrogen bonds involved at each self-assembly site.

The independent, non-interacting behaviors of these two modes of self-assembly allowed for the creation of a self-assembled, multifunctional, reversible, cross-linked material in one self-assembly step. This simultaneous self-assembly strategy, based on the results outlined above enables the creation of a fully functionalized, cross-linked system. Simultaneous addition of a small metal-complexing molecule such as pyridine, along with a hydrogen-bonding cross-linker such as the bis-thiamine unit, results in the fully cross-linked, fully functionalized terpolymer. The converse of this method was equally successful, *i.e.* addition of a small molecule hydrogen-bonding unit such as thiamine, along with a bis-pyridine cross-linker results again in a fully cross-linked, fully functionalized material. Interestingly, polymers could be fully de-functionalized and de-cross-linked by (1) heating to disrupt the hydrogen bonds, and (2) addition of PPh_3 to break the Pd-pyridine dative bond via competitive ligand interaction.

An interesting dimension of metal coordinated self-assembly that is quite often ignored, or at least not exploited to its fullest extent, occurs when the resulting coordination complex is a charged species, and as such, in need of a counterion. This counterion itself presents yet another subtle instance of ionic self-assembly, which often is overshadowed by its partner, the coordination complex. The second multi-functional side-chain supramolecular polymer system is based on this simple but important concept.[25,114-119] In 2003, Ikkala and co-workers reported a study in which they exploited

(1) a side-chain functionalized polymer, poly(vinyl pyridine), (2) metal coordination self-assembly via a tridentate Zn^{2+} complex, and (3) ionic self-assembly through functionalized counterions, *i.e.* dodecylbenzenesulfonate ions, to form multiple self-assembled complexes which adopted a cylindrical morphology (Figure 1.9).[120]

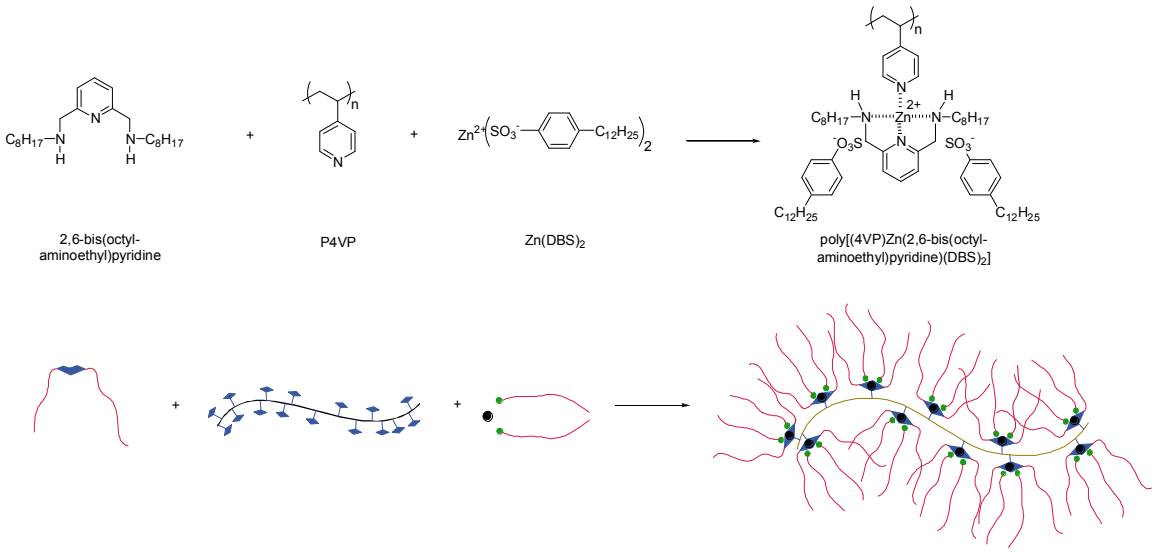

Figure 1.9. Self-assembled hairy-rod polymers based on metal coordination and ionic interaction.

The authors' goal was to synthesize self-assembled polymeric structures closely resembling dendron-modified polymers, but entirely through self-assembly. Ordinarily, during metal coordination-based self-assembly, if a charged species is the result, there will be any of a number of small counterions such as PF_6^-, Cl^-, BF_4^-, etc., to balance the positive residual charge of the metal ion. Ikkala and co-workers use of dodecylbenzene-functionalized counterions leads to control over solubility, as well as contributes significantly to the resulting conformation of the final self-assembled supramolecular structure via steric crowding. Several characterization methods, including (1) SAXS data showing self-organization in the mixture, (2) the lack of macroscopic phase separation, and (3) characteristic FT-IR shifts indicative of the coordination event, allowed Ikkala

and co-workers to conclude that mutually repulsive moieties are physically bonded within the supramolecular structures.[120]

1.5 Conclusion

The selected examples described herein are intended to give an indication of the potential utility of side-chain functionalized polymers, and the broad spectrum of possibilities that become available when multiple modes of functionalization are employed. This thesis focuses primarily on the ability to functionalize a polymer in a covalent manner, either before or after polymerization, and then add more complex functionality to the system through the use of a second type of interaction, namely metal coordination, which will be covered in more detail in the next chapter. The concept of combining side-chain functionalization methods introduces a high degree of flexibility to the system, enabling the adaptation of these polymers to a wide array of applications.

One of the primary goals of this thesis is to describe the concept of side-chain polymer functionalization based on multiple tiers of molecular association, both covalent and non-covalent, and demonstrate the complexity and flexibility that is possible when functionalization methods are combined in such a way. Often the polymer is functionalized covalently at first, with a group that is designed for interaction with a subsequent substrate via a non-covalent interaction such as metal coordination or hydrogen-bonding. This thesis focuses on the former as the primary method of adding complexity to a polymer design. The next chapter will discuss the concept of metal coordination as a means to add further functionality to polymers.

1.6 References

(1) Merrifield, R. B. *J. Am. Chem. Soc.* **1963**, *85*, 2149-2154.

(2) Leznoff, C. C. *Acc. Chem. Res.* **1978**, *11*, 327-33.

(3) Akelah, A.; Sherrington, D. C. *Chem. Rev.* **1981**, *81*, 557-8.

(4) Calvert, J. M.; Caspar, J. V.; Binstead, R. A.; Westmoreland, T. D.; Meyer, T. J. *J. Am. Chem. Soc.* **1982**, *104*, 6620-6627.

(5) Deronzier, A.; Moutet, J. C. *Acc. Chem. Res.* **1989**, *22*, 249-55.

(6) Aldinger, F.; Cherdron, H.; Kuehlein, K.; Riggs, J. *Adv. Mater.* **1992**, *4*, 138-42.

(7) Zentel, R. *Polymer* **1992**, *33*, 4040-4046.

(8) Archer, R. D. *Coord. Chem. Rev.* **1993**, *128*, 49-68.

(9) Frechet, J. M. J. *Science* **1994**, *263*, 1710-15.

(10) Wulff, G. *Angew. Chem. Int. Ed. Engl.* **1995**, *34*, 1812-32.

(11) McGrath, M. P.; Sall, E. D.; Tremont, S. J. *Chem. Rev.* **1995**, *95*, 381-98.

(12) Kiessling, L. L.; Strong, L. E. *Top. Organomet. Chem.* **1998**, *1*, 199-231.

(13) Biagini, S. C. G.; Davies, R. G.; Gibson, V. C.; Giles, M. R.; Marshall, E. L.; North, M.; Robson, D. A. *Chem. Commun.* **1999**, 235-236.

(14) Furstner, A. *Angew. Chem. Int. Ed.* **2000**, *39*, 3012-3043.

(15) Nummelin, S.; Skrifvars, M.; Rissanen, K. *Top. Curr. Chem.* **2000**, *210*, 1-67.

(16) McQuade, D. T.; Pullen, A. E.; Swager, T. M. *Chem. Rev.* **2000**, *100*, 2537-2574.

(17) Manners, I. *Science* **2001**, *294*, 1664-1666.

(18) Hagen, R.; Bieringer, T. *Adv. Mater.* **2001**, *13*, 1805-1810.

(19) Gohy, J.-F.; Lohmeijer, B. G. G.; Schubert, U. S. *Chem. Eur. J.* **2003**, *9*, 3472-3479.

(20) Grubbs, R. H. *Tetrahedron* **2004**, *60*, 7117-7140.

(21) Wang, X.-Y.; Weck, M. *Macromolecules* **2005**, *38*, 7219-7224.

(22) Burd, C.; Weck, M. *Macromolecules* **2005**, *38*, 7225-7230.

(23) Crespo-Biel, O.; Dordi, B.; Reinhoudt, D. N.; Huskens, J. *J. Am. Chem. Soc.* **2005**, *127*, 7594-7600.

(24) de Jong, J. J. D.; Lucas, L. N.; Kellogg, R. M.; van Esch, J. H.; Feringa, B. L. *Science* **2004**, *304*, 278-281.

(25) Faul, C. F. J.; Antonietti, M. *Adv. Mater.* **2003**, *15*, 673-683.

(26) Ikkala, O.; ten Brinke, G. *Science* **2002**, *295*, 2407-2409.

(27) Kippelen, B. *Nature Mater.* **2004**, *3*, 841-843.

(28) Klok, H.-A.; Lecommandoux, S. *Adv. Mater.* **2001**, *13*, 1217-1229.

(29) Liu, X. Y.; Sawant, P. D. *Adv. Mater.* **2002**, *14*, 421-426.

(30) Marks, T. J.; Ratner, M. A. *Angew. Chem. Int. Ed. Engl.* **1995**, *34*, 155-73.

(31) Shenhar, R.; Norsten, T. B.; Rotello, V. M. *Adv. Mater.* **2005**, *17*, 657-669.

(32) ten Brinke, G.; Ikkala, O. *Macromol. Symp.* **2003**, *203*, 103-109.

(33) Van Esch, J. H.; Feringa, B. L. *Angew. Chem. Int. Ed.* **2000**, *39*, 2263-2266.

(34) Wouters, D.; Hoppener, S.; Lunkwitz, R.; Chi, L.; Fuchs, H.; Schubert, U. S. *Adv. Funct. Mater.* **2003**, *13*, 277-280.

(35) Yabuuchi, K.; Rowan, A. E.; Nolte, R. J. M.; Kato, T. *Chem. Mater.* **2000**, *12*, 440-443.

(36) Dickerson, T. J.; Reed, N. N.; Janda, K. D. *Chem. Rev.* **2002**, *102*, 3325-3343.

(37) Kirschning, A.; Monenschein, H.; Wittenberg, R. *Angew. Chem. Int. Ed.* **2001**, *40*, 650-679.

(38) Pollino, J. M.; Weck, M. *Synthesis* **2002**, 1277-1285.

(39) Pollino, J. M.; Weck, M. *Org. Lett.* **2002**, *4*, 753-756.

(40) Meyers, A.; Weck, M. *Macromolecules* **2003**, *36*, 1766-1768.

(41) Meyers, A.; Weck, M. *Chem. Mater.* **2004**, *16*, 1183-1188.

(42) Carlise, J. R.; Weck, M. *J. Polym. Sci. Part A: Polym. Chem.* **2004**, *42*, 2973-2984.

(43) Pollino, J. M.; Weck, M. *Chem. Soc. Rev.* **2005**, *34*, 193-207.

(44) Pollino, J. M.; Nair, K. P.; Stubbs, L. P.; Adams, J.; Weck, M. *Tetrahedron* **2004**, *60*, 7205-7215.

(45) Pollino, J. M.; Stubbs, L. P.; Weck, M. *J. Am. Chem. Soc.* **2004**, *126*, 563-567.

(46) Valkama, S.; Kosonen, H.; Ruokolainen, J.; Haatainen, T.; Torkkeli, M.; Serimaa, R.; Ten Brinke, G.; Ikkala, O. *Nature Mater.* **2004**, *3*, 872-6.

(47) Ikkala, O.; ten Brinke, G. *Chem. Commun.* **2004**, 2131-2137.

(48) Bondzic, S.; De Wit, J.; Polushkin, E.; Schouten, A. J.; Ten Brinke, G.; Ruokolainen, J.; Ikkala, O.; Dolbnya, I.; Bras, W. *Macromolecules* **2004**, *37*, 9517-9524.

(49) Gerhardt, W.; Crne, M.; Weck, M. *Chem. Eur. J.* **2004**, *10*, 6212-6221.

(50) Stubbs, L. P.; Weck, M. *Chem. Eur. J.* **2003**, *9*, 992-999.

(51) Stepanyan, R.; Subbotin, A.; Knaapila, M.; Ikkala, O.; ten Brinke, G. *Macromolecules* **2003**, *36*, 3758-3763.

(52) Knaapila, M.; Ruokolainen, J.; Torkkeli, M.; Serimaa, R.; Horsburgh, L.; Monkman, A. P.; Bras, W.; ten Brinke, G.; Ikkala, O. *Synth. Met.* **2001**, *121*, 1257-1258.

(53) Weck, M.; Mohr, B.; Maughon, B. R.; Grubbs, R. H. *Macromolecules* **1997**, *30*, 6430-6437.

(54) Reinhoudt, D. N.; Timmerman, P.; Van Veggel, F. C. J. M. *NATO Ser. C: Math. Phys. Sci.* **1999**, *519*, 51-66.

(55) Mahalingam, V.; Onclin, S.; Peter, M.; Ravoo, B. J.; Huskens, J.; Reinhoudt, D. N. *Langmuir* **2004**, *20*, 11756-11762.

(56) Jiang, C.; Yang, W.; Peng, J.; Xiao, S.; Cao, Y. *Adv. Mater.* **2004**, *6*, 537-541.

(57) Furuta, P. T.; Deng, L.; Garon, S.; Thompson, M. E.; Frechet, J. M. J. *J. Am. Chem. Soc.* **2004**, *126*, 15388-15389.

(58) Sandee, A. J.; Williams, C. K.; Evans, N., R; Davies, J. E.; Boothby, C. E.; Kohler, A.; Friend, R. H.; Holmes, A. B. *J. Am. Chem. Soc.* **2004**, *126*, 7041-7048.

(59) Boyd, T. J.; Geerts, Y.; Lee, J.-K.; Fogg, D. E.; Lavoie, G. G.; Schrock, R. R.; Rubner, M. F. *Macromolecules* **1997**, *30*, 3553-3559.

(60) Wang, P.; Zakeeruddin, S. M.; Moser, J. E.; Nazeeruddin, M. K.; Sekiguchi, T.; Graetzel, M. *Nature Mater.* **2003**, *2*, 402-407.

(61) Hutchison, J. B.; Stark, P. F.; Hawker, C. J.; Anseth, K. S. *Chemistry of Materials* **2005**, *17*, 4789-4797.

(62) Yu, W. H.; Kang, E. T.; Neoh, K. G. *Langmuir* **2004**, *20*, 8294-8300.

(63) Grubbs, R. B.; Hawker, C. J.; Dao, J.; Frechet, J. M. J. *Angew. Chem., Int. Ed. Engl.* **1997**, *36*, 270-272.

(64) Murphy, J. J.; Kawasaki, T.; Fujiki, M.; Nomura, K. *Macromolecules* **2005**, *38*, 1075-1083.

(65) Kriegel, R. M.; Rees, W. S., Jr.; Weck, M. *Macromolecules* **2004**, *37*, 6644-6649.

(66) Sonmez, H. B.; Senkal, B. F.; Sherrington, D. C.; Bicak, N. *Reactive & Functional Polymers* **2003**, *55*, 1-8.

(67) Filiz Senkal, B.; Bicak, N. *Eur. Polym. J.* **2002**, *39*, 327-331.

(68) Demel, S.; Riegler, S.; Wewerka, K.; Schoefberger, W.; Slugovc, C.; Stelzer, F. *Inorg. Chim. Acta* **2003**, *345*, 363-366.

(69) Arehart, S. V.; Pugh, C. *J. Am. Chem. Soc.* **1997**, *119*, 3027-3037.

(70) Ungerank, M.; Winkler, B.; Eder, E.; Stelzer, F. *Macromol. Chem. Phys.* **1997**, *198*, 1391-1410.

(71) Wewerka, K.; Wewerka, A.; Stelzer, F.; Gallot, B.; Andruzzi, L.; Galli, G. *Macromol. Rapid Commun.* **2003**, *24*, 906-910.

(72) Li, M.-H.; Keller, P.; Albouy, P.-A. *Macromolecules* **2003**, *36*, 2284-2292.

(73) Percec, V.; Chu, P.; Asandei, A. D. *Polym. Mater. Sci. Eng.* **1999**, *80*, 223-224.

(74) Yang, L.; Mayr, M.; Wurst, K.; Buchmeiser, M. R. *Chem. Eur. J.* **2004**, *10*, 5761-5770.

(75) Mayr, M.; Buchmeiser, M. R. *Macromol. Rapid Commun.* **2004**, *25*, 231-236.

(76) Krause, J. O.; Lubbad, S. H.; Nuyken, O.; Buchmeiser, M. R. *Macromol. Rapid Commun.* **2003**, *24*, 875-878.

(77) Kroll Roswitha, M.; Schuler, N.; Lubbad, S.; Buchmeiser Michael, R. *Chem. Commun.* **2003**, 2742-3.

(78) Krause, J. O.; Lubbad, S.; Nuyken, O.; Buchmeiser, M. R. *Adv. Synth. Catal.* **2003**, *345*, 996-1004.

(79) Schubert, U. S.; Weidl, C. H.; Eschbaumer, C.; Kroell, R.; Buchmeiser, M. R. *Polym. Mater. Sci. Eng.* **2001**, *84*, 514-515.

(80) Arstad, E.; Barrett, A. G. M.; Tedeschi, L. *Tetrahedron Lett.* **2003**, *44*, 2703-2707.

(81) Buchmeiser, M. R. *Bioorg. Med. Chem. Lett.* **2002**, *12*, 1837-1840.

(82) Skaff, H.; Ilker, M. F.; Coughlin, E. B.; Emrick, T. *J. Am. Chem. Soc.* **2002**, *124*, 5729-5733.

(83) Kaneyoshi, H.; Inoue, Y.; Matyjaszewski, K. *Macromolecules* **2005**, *38*, 5425-5435.

(84) Tsarevsky, N. V.; Pintauer, T.; Matyjaszewski, K. *Macromolecules* **2004**, *37*, 9768-9778.

(85) Nguyen, J. V.; Jones, C. W. *Macromolecules* **2004**, *37*, 1190-1203.

(86) Matyjaszewski, K.; Patten, T. E.; Xia, J. *J. Am. Chem. Soc.* **1997**, *119*, 674-680.

(87) Matyjaszewski, K. *ACS Symp. Ser.* **2003**, *854*, 2-9.

(88) Shipp, D. A. *J. Macromol. Sci., Polym. Rev.* **2005**, *C45*, 171-194.

(89) Takolpuckdee, P. *Aust. J. Chem.* **2005**, *58*, 66.

(90) Moad, G.; Chong, Y. K.; Postma, A.; Rizzardo, E.; Thang, S. H. *Polymer* **2005**, *46*, 8458-8468.

(91) Barner, L.; Barner-Kowollik, C.; Davis, T. P.; Stenzel, M. H. *Aust. J. Chem.* **2004**, *57*, 19-24.

(92) Coote, M. L. *Aust. J. Chem.* **2004**, *57*, 1125-1132.

(93) Barner-Kowollik, C.; Davis, T. P.; Heuts, J. P. A.; Stenzel, M. H.; Vana, P.; Whittaker, M. *J. Polym. Sci., Part A: Polym. Chem.* **2003**, *41*, 365-375.

(94) Moad, G.; Mayadunne, R. T. A.; Rizzardo, E.; Skidmore, M.; Thang, S. H. *Macromol. Symp.* **2003**, *192*, 1-12.

(95) Smith, A. P.; Fraser, C. L. *Macromolecules* **2003**, *36*, 2654-2660.

(96) Farrall, M. J.; Frechet, J. M. J. *J. Org. Chem.* **1976**, *41*, 3877-82.

(97) Ten Brinke, G.; Ikkala, O. *Chem. Rec.* **2004**, *4*, 219-230.

(98) Bladon, P.; Griffin, A. C. *Macromolecules* **1993**, *26*, 6604-10.

(99) Bronich, T. K.; Ouyang, M.; Kabanov, V. A.; Eisenberg, A.; Szoka, F. C., Jr.; Kabanov, A. V. *J. Am. Chem. Soc.* **2002**, *124*, 11872-11873.

(100) Li, L.; Beniash, E.; Zubarev, E. R.; Xiang, W.; Rabatic, B. M.; Zhang, G.; Stupp, S. I. *Nature Mater.* **2003**, *2*, 689-694.

(101) Percec, V.; De, B. B.; Cho, W.-D.; Singer, K. D.; Zhang, J. *Polym. Mater. Sci. Eng.* **1999**, *80*, 262-263.

(102) Termonia, Y. *Biomacromolecules* **2004**, *5*, 2404-2407.

(103) Demikhov, E. I.; Kozlovsky, M. V. *Liq. Cryst.* **1995**, *18*, 911-14.

(104) Helgee, B.; Hjertberg, T.; Skarp, K.; Andersson, G.; Gouda, F. *Liq. Cryst.* **1995**, *18*, 871-8.

(105) Keith, C.; Reddy, R. A.; Tschierske, C. *Chem. Commun.* **2005**, 871-873.

(106) Lee, J.-H.; Lee, S.-D.; Choi, D. H. *Mol. Cryst. Liq. Cryst. Sci. Tech.* **1999**, *329*, 933-940.

(107) Kosonen, H.; Valkama, S.; Ruokolainen, J.; Torkkeli, M.; Serimaa, R.; ten Brinke, G.; Ikkala, O. *Eur. Phys. J. E: Soft Mat.* **2003**, *10*, 69-75.

(108) Meyers, A.; South, C.; Weck, M. *Chem. Commun.* **2004**, 1176-1177.

(109) Pollino, J. M.; Stubbs, L. P.; Weck, M. *Macromolecules* **2003**, *36*, 2230-2234.

(110) Ishii, T.; Hirayama, T.; Murakami, K.; Tashiro, H.; Thiemann, T.; Kubo, K.; Mori, A.; Yamasaki, S.; Akao, T.; Tsuboyama, A.; Mukaide, T.; Ueno, K.; Mataka, S. *Langmuir* **2005**, *21*, 1261-1268.

(111) Kato, T.; Kihara, H.; Ujiie, S.; Uryu, T.; Frechet, J. M. J. *Macromolecules* **1996**, *29*, 8734-8739.

(112) Kato, T.; Kihara, H.; Uryu, T.; Fujishima, A.; Frechet, J. M. J. *Macromolecules* **1992**, *25*, 6836-41.

(113) Kumar, U.; Kato, T.; Frechet, J. M. J. *J. Am. Chem. Soc.* **1992**, *114*, 6630-9.

(114) Guan, Y.; Yu, S.-H.; Antonietti, M.; Boettcher, C.; Faul, C. F. J. *Chem. Eur. J.* **2005**, *11*, 1305-1311.

(115) Kadam, J.; Faul, C. F. J.; Scherf, U. *Chem. Mater.* **2004**, *16*, 3867-3871.

(116) Wang, Z.; Medforth, C. J.; Shelnutt, J. A. *J. Am. Chem. Soc.* **2004**, *126*, 15954-15955.

(117) Wei, Z.; Laitinen, T.; Smarsly, B.; Ikkala, O.; Faul, C. F. J. *Angew. Chem. Int. Ed.* **2005**, *44*, 751-756.

(118) Zakrevskyy, Y.; Faul, C. F. J.; Guan, Y.; Stumpe, J. *Adv. Funct. Mater.* **2004**, *14*, 835-841.

(119) Zhang, T.; Spitz, C.; Antonietti, M.; Faul, C. F. J. *Chem. Eur. J.* **2005**, *11*, 1001-1009.

(120) Valkama, S.; Lehtonen, O.; Lappalainen, K.; Kosonen, H.; Castro, P.; Repo, T.; Torkkeli, M.; Serimaa, R.; ten Brinke, G.; Leskelae, M.; Ikkala, O. *Macromol. Rapid Commun.* **2003**, *24*, 556-560.

CHAPTER 2

METAL COORDINATION AS A STRATEGY FOR POLYMER AND MATERIAL FUNCTIONALIZATION

2.1 Abstract

This chapter introduces the concept of metal coordination, and focuses on its role in polymer and material functionalization and design. This includes metal-mediated induction of well-defined suprastructures, as well as luminescent and photochemical properties. The categories discussed below are based on synthetic methodology, design motif, and function. The examples described attempt to put the research into context based on each respective application either industrially or in the academic laboratory. The state of the current research is described, and respective advantages and disadvantages to each strategy are outlined.

2.2 Introduction

It is the primary goal of this thesis to discuss the functionalization of polymers and polymeric materials via side-chain metal coordination, and to demonstrate the utility of this methodology. Thus, the hypothesis that will be addressed is that combining multidentate metal complexes with living polymerization is useful for materials applications. This hypothesis will be tested through studying a variety of materials applications such as fluorescent materials and cross-linked materials. In order to provide a more comprehensive understanding of this strategy, the concept of metal coordination in polymer chemistry will be described and discussed, based on selected examples from the current literature. This chapter will build on the concepts introduced in Chapter 1, and add the focus of incorporation of metal coordination into the design of functionalized polymers.

Transition metal-ligand interactions form the basis for a large number of processes in Nature, from performing catalytic functions in enzymes, to oxygen transport in the blood stream, to photosynthesis in plants, and many more. It is not simply the site specificity of metal-ligand interactions that make it an attractive candidate for use in the laboratory, but also the wide range of resulting binding strengths arising from variation of the metal and/or the ligand employed in the binding event, as well as the variations in coordination geometry. These factors give the synthetic chemist a significantly high degree of control when designing molecular interactions based on metal coordination. Of course metal complexes, especially transition metal complexes, have demonstrated a profound propensity in the world of catalysis as well; however this section will focus primarily on the role of metal complexes in designing functionalized materials, including site specific and highly controlled binding events, photoluminescent and photovoltaic applications, and tuning of materials properties.

2.3 Metal Coordination in Polymer Chemistry

Metal-ligand interactions, although widely studied and utilized for centuries in the field of inorganic chemistry, have become increasingly popular in the field of polymer and materials science in the past half-century. This recent surge in interest in the metal coordination phenomena is complementary to the increasing need for smaller, more flexible, durable, functional materials, as metal coordination enables a high degree of flexibility in polymer and materials synthesis.

As mentioned in Chapter 1, chemists have harnessed the capability of molecules to self-assemble into organized materials, via non-covalent forces such as metal coordination and hydrogen bonding. In a seemingly unrelated arena, Nature uses photosynthesis to enable plants to harness the energy of sunlight to convert photons into usable energy. Scientists have studied this concept and are able to mimic it in the laboratory for photovoltaic applications such as solar cells.[1-7] The reverse of this concept

has also been utilized with a great deal of success; that is, putting energy into molecules in order to get light back out.[8-18] Just as is the case with supramolecular chemistry however, these fascinating phenomena are also often highly dependant on the existence of metal-ligand interactions and their resulting unique electronic properties.

In order to gain an understanding of the utility of metal-ligand bonding and its wide scope of applications, an introduction to the concept of metal coordination is of fundamental importance, and will be briefly introduced and discussed in the following section, followed by a description of the variety of ways that it has been incorporated into materials chemistry.

2.3.1 Advantages of Metal Coordination

Metal coordination in the *d*- and *f*- block is built on the concept of Lewis acid - Lewis base interactions, with additional cooperative orbital interactions often becoming significantly involved.[19,20] The focus herein will be specifically on the transition metals however, as it is their polyvalent cationic character and wide variation in preferred coordination geometries that allow for the vast spectrum of possible interactions with the ligands, and subsequent freedom of design in the field of materials chemistry.[20] Many transition metals can experience a wide range of oxidation states, can bind six or more ligands at once, and are capable of participating in pi- bonding with ligands that have a vacant pi* molecular orbital. These unique properties have given the transition metals the ability to greatly enhance the fields of polymer and materials chemistry, as their broad utility is apparent in the production of many important materials.[16,21-27] This unique behavior stems largely from the variation in electron configuration, and resulting preferred geometry, that is observed from one side of the *d*-block to the other.[19,20] This flexibility (relative to the alkali and alkaline earth metals) of the valence electrons enables both sigma- and pi- bonding, as well as a large window of available oxidation states for many of the members of this group. Many metals in the d-block prefer an

octahedral coordination geometry. However, it is also very common for some metals to adopt tetrahedral, tetragonal, and square-planar orientations as well. These attributes are among the many advantages that coordination chemistry lends to the field of polymeric and materials design

Besides the flexibility inherent in the various coordination geometries exhibited by the transition metals, there is also the ability to tune the energy gap between the HOMO and the LUMO of the coordination complex by changing the ligands around the metal. There are several macroscopic ways that changes in the HOMO-LUMO gap manifest themselves, including changes in color, emission, absorption, and magnetization, among others. Because the HOMO-LUMO gap is directly representative of the energetic "distance" that an excited electron must travel, emission of a photon upon relaxation of this exciton results in light of a wavelength directly related to this gap as well. It directly follows therefore that if changing the ligands in metal complex can dramatically alter the HOMO-LUMO gap, this should then lead to similar changes in the wavelength of the photons emitted upon excitation of the electrons in the complex, and it indeed does. This phenomenon has been substantially harnessed for use in many applications including emissive devices such as OLEDs. All colors of the spectrum have been achieved by manipulation of this HOMO-LUMO gap, creating the ability to make white light, which is required for many applications in flat-screen display technology.

2.3.2 Techniques and Applications of Metal Coordination in Polymer and Materials Chemistry

Metal coordination is a highly versatile technique, and can be utilized for a number of different aims including synthesis of light-emitting materials, supported catalysts, sensor technology, photovoltaics, self-assembly of well-defined superstructures, and a great many others. Depending on the strength, specificity, and coordination geometry of the particular metal-ligand interaction, a wide range of architectures, design motifs, and

functional materials can be attained. This section will elaborate on several interesting representative examples of ways in which metal coordination has played an integral role in achieving the desired material design and function.

Supramolecular Design and Architecture

Metal coordination can be employed as a self-assembly motif, often leading to highly organized and complex superstructures.[28-32] An interesting example of this architectural capability was reported in 2005 by Lehn and co-workers, in which they synthesized several multifunctional ligands, designed for selective complexation of specific metals, and demonstrated the ability of these self-assembled interactions to build both one- and two- dimensional architectures, which ultimately exhibited magnetic properties.[33] The ligands consisted of a series of several linked N-heterocyclic pyridine-type rings, which resulted in two terpyridine (trpy)-like coordination sites, as well as two single pyridine coordination sites. (Figure 2.1)

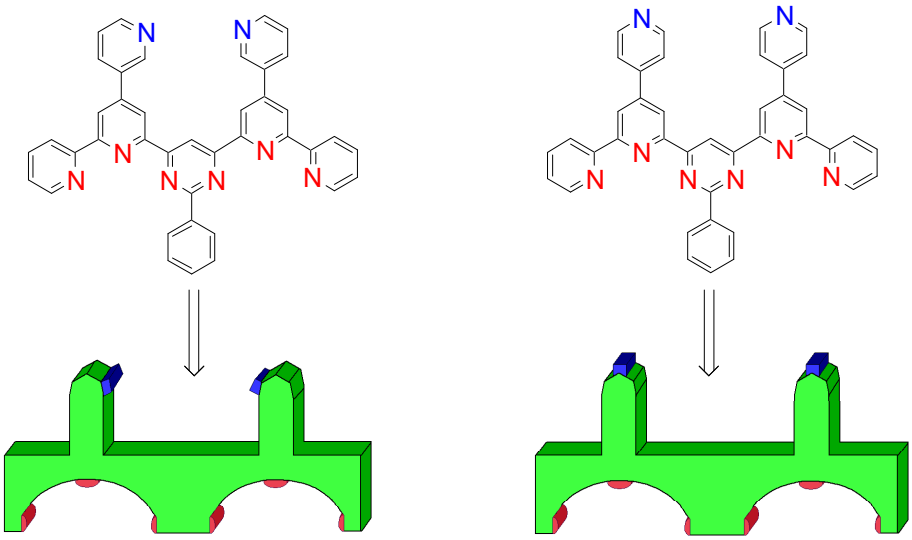

Figure 2.1. Chemical structures and cartoons of multifunctional ligands containing both pyridine (blue) and terpyridine (red) coordination sites. Left: meta-pyridine building block. Right: para-pyridine building block.

The single pyridine sites were designed with both a meta- and a para- pyridine for varying metal specificity. Upon introduction of an iron(II) salt, and subsequent binding of iron ions into two of the terpyridine-like sites, a square-shaped tetramer results with a metal:ligand ratio of 1:1.(Figure 2.2)

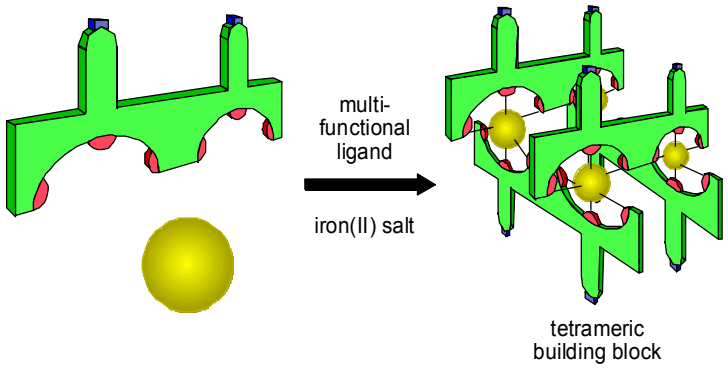

Figure 2.2. Formation of supramolecular building block via iron(II) coordination.

This can be done for either type of ligand, and the resulting square tetramer possesses on both the top and bottom face a new coordination site created by several of the single pyridines confined together in close proximity. This tetramer comprises the initial unit of what Lehn and co-workers refer to as a modular approach to supramolecular assembling and architecture. Next, depending upon the configuration of the single pyridine portion of the resulting modules, various orientations and structures can be obtained. For instance, addition of a lanthanide salt, such as lanthanum(III) perchlorate, to the module containing the meta-pyridine sites, creates one-dimensional rods as a result of one lanthanide ion binding to either the entire top or bottom face in a ratio of 8:1 pyridine:lanthanide.(Figure 2.3)

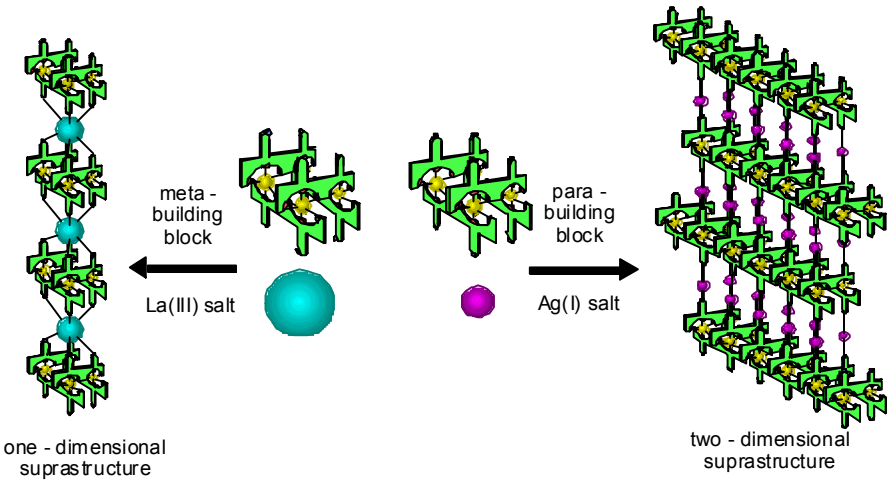

Figure 2.3. Metal coordination-based suprastructures from combination of meta- or para- iron-based building blocks and a second class of metal salts.

Alternatively, adding a silver salt such as silver tetrafluoroborate to the module based upon the para-pyridine-containing ligands, creates large two-dimensional networks. These networks arise from a pyridine:silver ratio of 1:2, the two pyridines arranged in a para- arrangement around each silver ion (Figure 11). Thus, for both the one- and the two- dimensional suprastructures formed, a multistep, completely metal coordination-based series of events leads to the desired architectures. Interestingly, these superstructures were found to exhibit magnetic properties as well once fully self-assembled.

Another interesting example that demonstrates the utility of metal coordination in a complex system resulting in organization of macromolecular structures was performed in 2001 by Sasaki and co-workers, in which they combined two self-assembly techniques to create reversible columns of stacked lipid bilayers.[34] First, vesicles were formed by amphiphilic lipids in water, followed by metal coordination to assemble the vesicles. The metal coordination was strong enough to cause flattening of the vesicles, and ultimately rupturing them, leading to two stacked discs per original vesicle (Figure 2.4).

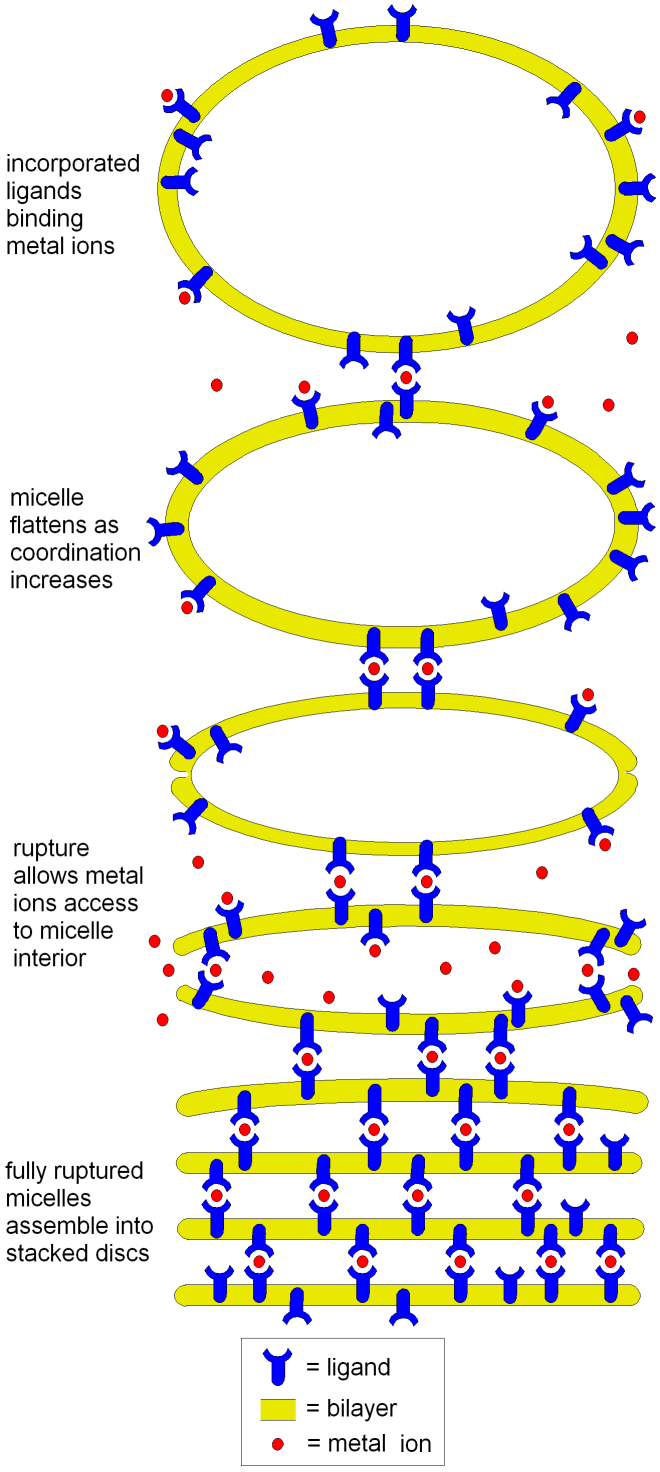

Figure 2.4. Metal coordination-mediated stacking of flattened, ruptured vesicles.

Sasaki and co-workers report columns of up to 45 stacked bilayers, which they observed using electron microscopy. The vesicles were made with a mixture of two different

lipids: 95% distearylphosphatidylcholine (DSPC), which is a zwitterionic lipid, and 5% PSIDA (a Cu^{2+} specific metal-chelating lipid). Once the vesicles were formed, addition of Cu^{2+} caused aggregation, which Sasaki and co-workers found to contain approximately 15-20% of the material in the columnar formation. This Cu^{2+} - mediated aggregation was entirely reversible by addition of EDTA to the mixture. This combination of reversible self-assembly techniques is yet another exciting example of the enormous variety of self-organizational phenomena which are ubiquitously employed by Nature, seemingly effortlessly, in all biological systems.

Multifunctional supramolecular main-chain polymers, *i.e.* multifunctional polymers that are based on non-covalent interactions including metal coordination, have the advantage of being reversible. This reversibility allows one to tailor molecular weights through a variety of variables including the strength of the non-covalent interactions between individual monomer units as well as the incorporation of terminal 'stopper' molecules, *i.e.* monofunctionalized monomers that terminate a polymer chain. While the incorporation of multiple non-covalent interactions along a polymer main-chain is conceptually simple, the realization of this concept has only been achieved very recently. In 2005, Schubert and co-workers reported such a system by combining trpy-based metal coordination with hydrogen-bonding. The system is based on poly(ε-caprolactone) that contains terminal self-assembly groups: on the one side a multidentate trpy ligand that can coordinate to a variety of metals including Ru and Co while the other end-group contains an ureidopyrimidinone unit (a self-complimentary, quadruple hydrogen-bonding unit with a DDAA motif).[43] The resulting macromonomers can be self-assembled into linear main-chain supramolecular polymers using both, hydrogen-bonding and metal coordination. The properties of the polymers can be tuned easily through (1) the choice of metal ion, (2) the temperature, and (3) monomer and/or metal concentration. The trpy ligand is a versatile candidate for this type of supramolecular system due to the tunability inherent in the very wide range of trpy-metal binding strengths (from 10^5 for Zn and Cd

to 10^{18} for Ru).[44,45] Schubert has investigated the potential of the trpy ligand in supramolecular polymers and synthesized a wide variety of polymers for a number of applications including light-emitting devices,[46] molecular switches,[47] and solar cells.[48] Furthermore, hydrogen-bonding, though it is typically weaker than metal coordination, is also widely tunable due to a) the dramatic increase in K_a as the number of hydrogen-bonding interactions increases, b) the dependence of the hydrogen-bond strength on the solvent, and c) the dramatic decrease of the hydrogen-bond strength at elevated temperatures.[49-53] The quadruple hydrogen-bonding unit employed by Schubert in this study, ureidopyrimidinone, has been investigated in detail over the last decade by Meijer and coworkers and has a K_a of $6*10^7$ M^{-1} in halogenated solvents.[54] Therefore, the macromolecular building block in the Schubert system exists as a dimer before metal coordination due to the high association constant for the quadruple hydrogen bonds. Addition of a solution of a metal salt such as $FeCl_2$ or $Zn(OAc)_2$ initiates, *via* self-assembly, a spontaneous polymerization which afforded, after precipitation with ammonium hexafluorophosphate, a supramolecular polymer with unique physical properties (Figure 2.5). For example, the hydrogen-bonded dimers are brittle and opaque, while the final metal-coordinated polymers are flexible. Furthermore, Schubert and coworkers were able to form transparent thin films of these polymers.

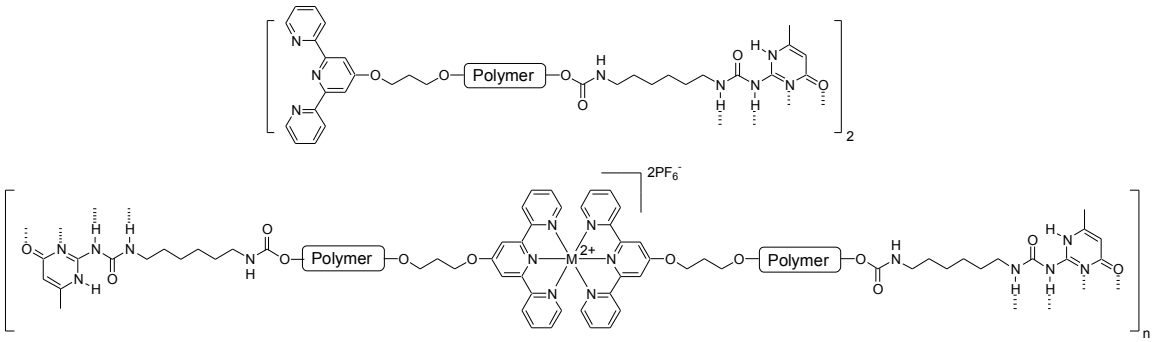

Figure 2.5. Multi-step main-chain self-assembly to form a flexible, high molecular weight polymer. Step 1: dimerization of difunctional unit via the self-complimentary ureidopyrimidinone end (top); Step 2: Addition of a metal salt such as iron(II) initiates

metal coordination-based self-assembly of the trpy-functionalized ends to form extended polymer chains (bottom).

In contrast to covalent-based polymers, characterization of supramolecular polymers is often challenging since basic polymer characterization methods such as gel-permeation chromatography for the determination of molecular weights and polydispersities are incompatible with hydrogen-bonding and often coordination chemistry (in particular if charged species are involved).[55] As a result, alternative methods for determining the size of the supramolecules in question are often employed, including small-angle neutron scattering (SANS), small-angle X-ray scattering (SAXS),[56-61] and various light-scattering techniques.[62-64] The supramolecular polymers reported by Schubert were characterized by several methods, including UV-vis spectroscopy, which confirmed the coordination event, and viscometry, which evidenced the presence of high molecular weight polymers. Interestingly, due to the reversibility of the self-assembled interactions, an exponential dependence of the viscosity on the polymer concentration was observed, instead of the linear dependence that might be expected from a polymer possessing irreversible linkages throughout. Schubert attributes this effect to a ring-chain equilibrium, *i.e.* the formation of high molecular weight cyclic structures at lower concentrations, which would cause a slower increase in viscosity with increasing concentration. Once a critical concentration is reached, the concentration of cyclic polymers remains constant and the viscosity begins to rise rapidly due to the formation of high molecular weight linear supramolecular polymers.

The reversibility of the system through metal-trpy decomplexation was also investigated through the addition of the strong transition metal-chelating ligand hydroxyethyl ethlyenediaminetetraacetic acid (HEEDTA).[65] This ligand has been shown to be capable of opening bis-trpy-iron(II) complexes by abstracting the iron ion in a ligand-exchange process (Figure 2.6).[65] Indeed, addition of HEEDTA to the iron-

complexed supramolecular polymer caused full decomplexation within two minutes, as was evident by loss of the characteristic color of the iron-trpy complex resulting in the depolymerization of the supramolecular polymer into dimers.

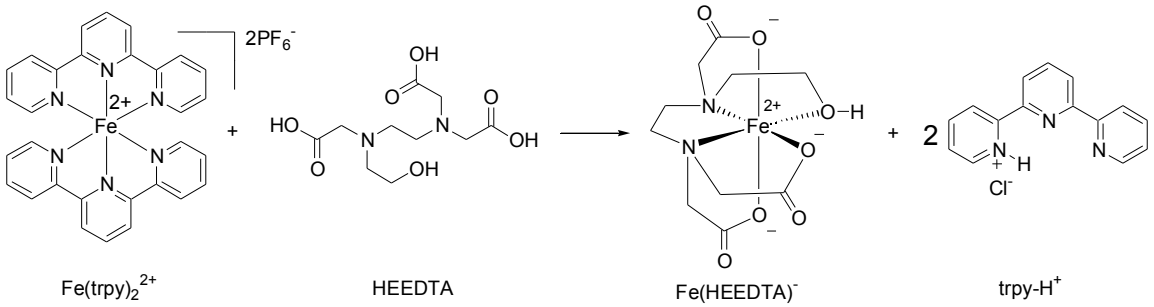

Figure 2.6. Abstraction of iron(II) ion from the bis-terpyridine complex with HEEDTA.

The reports discussed above provide examples of how transition metal coordination can be used to control the design of materials on a molecular level as well as a more global, macroscopic level, often giving higher order to the systems that it has been employed. This thesis will continue to focus on how materials and polymers can be functionalized via metal coordination and will now move to the arena of polymers and materials for optical and photovoltaic applications.

Organic Light-Emitting Diodes (OLEDs) and Photovoltaics

Besides the broad utility of metal coordination in the field of supramolecular chemistry, the technique enjoys just as wide of an array of applications in photochemical material design including both emissive materials (OLEDs)[8,13,66,67] and photovoltaics (solar cells).[2,3,6,68,69] As these two applications are essentially the reverse of one another, and thus rely on very similar chemistries, they will be discussed together in this section.

Modern civilization has relied on non-renewable coal and petroleum-based natural resources as the primary source of energy for centuries. This is still the case today, and as a result, the prospect of a global energy shortage is becoming increasingly apparent.[70] For this reason, in the last several decades there has been increasing interest in finding

efficient alternative renewable energy sources such as harnessing the power of the wind (windmills), water (hydrodynamics), or the sun (photovoltaics). The first two of the three alternative sources listed above rely on converting mechanical force into electricity. However, the third item, photovoltaics, is a specifically chemistry-based problem to solve.

The art of creating materials that generate an electric current as a result of the absorption of photons from sunlight has been optimized somewhat in the last several decades, although efficiencies are still much lower than what can be reached theoretically.[2] Organic solar cells, including dye-sensitized solar cells (DSCs), have become increasingly more efficient in the last ten years, although some drawbacks still exist. For instance, DSCs are typically not thermally stable at elevated temperatures.[2] However, it is becoming increasingly apparent that materials that are solution processible are desirable, as they can be adapted to fit nearly any design or niche in which the particular functional material is applicable, and they are also simpler and more cost effective to produce. In order to achieve this goal, polyelectrolyte-based dye-sensitized solar cells have been proposed as a possible solution.[71-73] Although this strategy eliminates the rigid crystalline component used in past designs, there remains the issue of leakage of polyelectrolyte solution if the device is damaged. Graetzel, Samuelson, and others have reported solutions to this problem, which consist of neither solid-state nor liquid-based materials, but a hybrid material made up of a polyelectrolyte gel supported on a flexible polymer.[71-73] The dye incorporated into this polymeric device is most commonly based on $Ru(bpy)_3$, often in the form of derivatives such as *cis*-$RuL_2(SCN)_2$ or *cis*-$RuLL'(SCN)_2$ (L = 4,4′-dicarboxylic acid-2,2′-bipyridine, L′ = 4,4′-dinonyl-2,2′-bipyridine).[2] This technology, which enables clean energy conversion from sunlight using a flexible substrate that can be made more economically than the traditional single crystal alternatives, represents another example of how metal coordination has come into play in the creative and efficient design of modern functional materials.

While photovoltaics rely on a light source in order to produce energy, light-emitting diodes (LEDs) essentially perform in the opposite direction, emitting photons upon excitation by an outside source such as an electric current (electroluminescence), a chemical reaction (chemiluminescence), or even light (photoluminescence). LEDs have traditionally consisted of emissive metal coordination complexes such as $Ir(ppy)_3$, Alq_3, and many others, as well as certain highly conjugated organic molecules. The aforementioned current trend towards solution processible materials has profoundly impacted the field of emissive materials as well, with the result being the synergistic combination of organic chemistry and emissive molecules, resulting in the so-called organic light-emitting diode (OLED). These materials are indeed solution processible, due to incorporation of a sufficient amount of a soluble organic component combined with the often-insoluble emissive material. The chromophore has been incorporated into the organic matrix by (1) doping it into a polymer,[9,17,74-76] (2) adding alkyl groups to the small molecule,[17] and (3) attaching the chromophore to a polymer backbone.[66,67,77-82] The most commonly utilized method thus far has been the doping method. A large number of reports on this method have emerged in the last 20 years. The doping method suspends the luminescent material in the polymer matrix so as to enable solution processing. However, phase separation can be a significant problem due to the vast differences in the properties of the chromophore and the matrix. As a result, alternative methods have been devised to improve the solubility of the luminescent species, such as the strategy of simply adding alky groups to the chromophore. This strategy has been successful at improving material solubility, although any additional additives must also be alkylated in order to maintain homogeneity of the system, or some phase separation may still occur. To overcome this hurdle, scientists have begun to covalently attach the luminescent molecules directly to a polymer backbone, which achieves essentially the same results as the simple alkylation strategy, but also has the advantage of incorporating all active species including chromophores and additives directly into the copolymer, immobilizing

the molecules and eliminating the problem of phase separation, while greatly simplifying and facilitating the solution processing of the final materials.

For example, in 2004, Thompson, Fréchet, and co-workers reported their synthesis of platinum-functionalized random copolymers that included along the same polymer backbone all necessary materials to create an efficient, near-white light emitting material (Figure 2.7).[66]

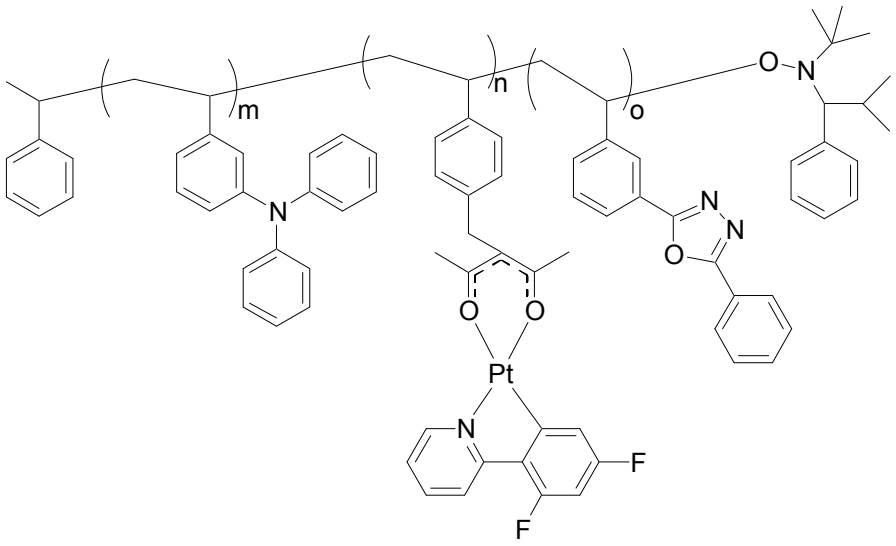

Figure 2.7. Triblock platinum-based polymer for use in OLED.

This report was a significant step forward in the improvement of emissive device technology, as it has become desirable to move away from rigid, many-layer devices, towards simplification and flexibility. The phosphorescent material synthesized in this study consisted of electron-transporting moieties, hole-transporting moieties, and emitter complexes all tethered to a single polymer that was simply spin coated for device fabrication. It was, however, necessary to vacuum deposit an Alq_3 layer on top of this film, along with 2,9-dimethyl-4,7-diphenyl-1,10-phenanthroline (BCP), in order to complete the device. As technology continues to progress, vacuum deposition may completely give way to solution processing, greatly facilitating the fabrication of thin, flexible, emissive materials.

Another significant step forward in this direction, perhaps complimentary to the work described above, was reported by Weck and Meyers in 2003 when they introduced an effective alternative to the traditional process of vacuum-depositing Alq_3, an important emission and electron-transport layer in light-emitting devices.[77] By covalently attaching the Alq_3 complex to a polymerizable unit (norbornene), they were able to synthesize the first Alq_3-containing polymer via ring-opening metathesis polymerization (ROMP) (Figure 2.8).

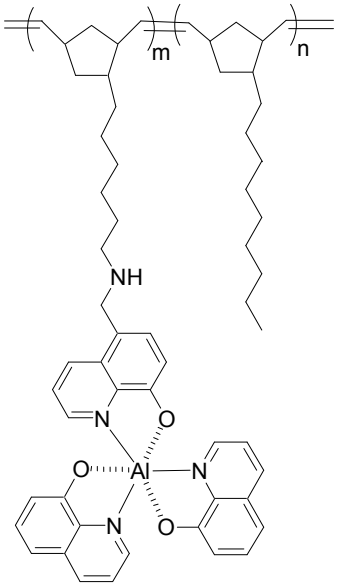

Figure 2.8. Alq_3 containing polymer synthesized by Weck and Meyers.

It was shown that the polymerization of this complex did not hinder the original emissive output of the analogous small molecule. In a later report, they also demonstrated the utility of this system in the solid state, by the fabrication and characterization of uniform thin films of this polymer.[80] It was also shown that the emission wavelength could be tuned significantly both by modifying the hydroxyquinoline ligand as well as changing the ratio of Alq_3 monomer to spacer monomer. This research is representative of the trend away from bulky, rigid emissive materials towards flexible, solution processable polymeric alternatives, and perhaps might be combined with similar work as described by

Thompson, Fréchet, and co-workers above, where Alq_3 is still vacuum deposited on top of a solution processed OLED, thereby nearly eliminating the need for vacuum deposition techniques altogether.

Supported Catalysts

Homogeneous catalysts have the advantage of being in the same phase as the reactants, thereby allowing for significantly more interaction with the substrates than a heterogeneous composition. However, a common problem with homogeneous catalysts is removal of the catalyst from the products, and if economically important, recoverability of the catalyst as well. An effective way to circumvent this issue is to employ a heterogeneous catalyst system. To achieve this, the catalyst must either be insoluble in the reaction medium, or it must be immobilized onto something that is insoluble. In the case of the latter, if the tether with which the catalyst is immobilized is long enough, the catalyst may still have enough flexibility to have a significant amount of interaction with the substrates to achieve a reasonable reaction rate. For example, in 2005, Jones and co-workers reported an efficient heterogeneous organometallic catalyst that had been immobilized on a spatially patterned silica surface.[83] The spatial patterning technique, demonstrated by the same authors in an earlier work, ensures that the immobilized species remain isolated from each other once tethered to the surface, thereby eliminating unwanted side reactions or diminished reactivity resulting from interactions between catalyst molecules. Jones and co-workers showed that immobilization of a titanium-based constrained geometry catalyst (CGC) using their patterning technique could promote efficient copolymerization of norbornene and ethylene, an industrially important material currently synthesized on a large scale for applications in microelectronics, among others. Homogeneous CGCs are typically used for copolymerizations such as these, however it is advantageous to have a heterogeneous catalyst to facilitate removal of the species from the product, as well as recover the CGC

for repeated use. The work reported by Jones and co-workers is yet another representative example of the utility inherent in metal coordination-based functionalization of materials.

2.4 Conclusion

This section sought to give some background and insight into the enormously broad range of possibilities available to scientists through invoking the concept of functionalization of materials via metal coordination-based interactions. The wide spectrum of roles played by metal complexes, the variation in binding strengths, the site-specificity of the interactions between ligand and metal, and the ability of these complexes to often lend themselves to self-assembly techniques all combine to create a powerful toolbox for chemists in virtually all fields. As the creative and efficient uses of this technology continue to grow and progress, and these techniques become increasingly deeper and intricately involved in chemists' laboratory arsenal, metal coordination is rapidly beginning to appear ubiquitous in the field of chemistry.

The two introductory chapters of this thesis thus far have aimed to provide an adequate background for the research to be presented in the chapters to come, which is all based on polymer functionalization through the use of side-chain metal coordination complexes. Now the focus of the discussion will turn to more specific, recent research regarding the both the process of incorporating functional sites along polymer backbones, as well as using polymers as supports for industrially relevant small molecules.

2.5 References

(1) Roncali, J. *Chem. Soc. Rev.* **2005**, *34*, 483-495.

(2) Wang, P.; Zakeeruddin, S. M.; Moser, J. E.; Nazeeruddin, M. K.; Sekiguchi, T.; Graetzel, M. *Nat. Mater.* **2003**, *2*, 402-407.

(3) Wang, P.; Zakeeruddin, S. M.; Moser, J. E.; Humphry-Baker, R.; Graetzel, M. *J. Am. Chem. Soc.* **2004**, *126*, 7164-7165.

(4) Kumar, R.; Sharma, A. K.; Parmar, V. S.; Watterson, A. C.; Chittibabu, K. G.; Kumar, J.; Samuelson, L. A. *Chem. Mater.* **2004**, *16*, 4841-4846.

(5) Kalyanasundaram, K. *Coord. Chem. Rev.* **1982**, *46*, 159.

(6) Sullivan, B. P.; Salmon, D. J.; Meyer, T. J. *Inorg. Chem.* **1977**, *17*, 3334.

(7) Schultze, X.; Serin, J.; Adronov, A.; Fréchet, J. M. J. *Chem. Commun* **2001**, 1160–1161.

(8) Veinot, J. G. C.; Marks, T. J. *Acc. Chem. Res.* **2005**, *38*, 632-643.

(9) Jiang, C.; Yang, W.; Peng, J.; Xiao, S.; Cao, Y. *Adv. Mater.* **2004**, *6*, 537-541.

(10) Lo, S.-C.; Male, N. A. H.; Markham, J. P. J.; Magennis, S. W.; Burn, P. L.; Salata, O. V.; Samuel, I. D. W. *Adv. Mater.* **2002**, *14*, 975-979.

(11) D'Andrade, B. W.; Brooks, J.; Adamovich, V.; Thompson, M. E.; Forrest, S. R. *Adv. Mater.* **2002**, *14*, 1032-1036.

(12) Al Attar, H. A.; Monkman, A. P.; Tavasli, M.; Bettington, S.; Bryce, M. R. *Appl. Phys. Lett.* **2005**, *86*, 121101.

(13) Suzuki, M.; Tokito, S.; Sato, F.; Igarashi, T.; Kondo, K.; Koyama, T.; Yamaguchi, T. *Appl. Phys. Lett.* **2005**, *86*, 103507.

(14) Bard, A. J.; Gao, F. G. *J. Am. Chem. Soc.* **2000**, *122*, 7426-7427.

(15) Gao, F. G. B., A. J. *J. Am. Chem. Soc.* **2000**, *122*, 7426-7427.

(16) Sandee, A. J.; Williams, C. K.; Evans, N., R; Davies, J. E.; Boothby, C. E.; Kohler, A.; Friend, R. H.; Holmes, A. B. *J. Am. Chem. Soc.* **2004**, *126*, 7041-7048.

(17) Zhu, W.; Liu, C.; Su, L.; Yang, W.; Yuan, M.; Cao, Y. *J. Mater. Chem.* **2003**, *13*, 50-55.

(18) Boyd, T. J.; Geerts, Y.; Lee, J.-K.; Fogg, D. E.; Lavoie, G. G.; Schrock, R. R.; Rubner, M. F. *Macromolecules* **1997**, *30*, 3553-3559.

(19) Crabtree, R. H. *The Organometallic Chemistry of the Transition Metals*; 3rd ed.; Wiley-Interscience: New York, 2001.

(20) Shriver, D.; Atkins, P. *Inorganic Chemistry*; 3rd ed.; W. H. Freeman and Company: New York, 1999.

(21) Percec, V.; Chu, P.; Asandei, A. D. *Polym. Mater. Sci. Eng.* **1999**, *80*, 223-224.

(22) Schubert, U. S.; Alexeev, A.; Andres, P. R. *Macro. Mater. Eng.* **2003**, *288*, 852-860.

(23) Kurth, D. G.; Meister, A.; Thuenemann, A. F.; Foerster, G. *Langmuir* **2003**, *19*, 4055-4057.

(24) Raimundo, J.-M.; Lecomte, S.; Edelmann, M. J.; Concilio, S.; Biaggio, I.; Bosshard, C.; Guenter, P.; Diederich, F. *J. Mater. Chem.* **2004**, *14*, 292-295.

(25) Stang, P. J.; Olenyuk, B. *Handbook of Nanostructured Materials and Nanotechnology* **2000**, *5*, 167-224.

(26) Buchmeiser, M. R. *Chem. Rev.* **2000**, *100*, 1565-1604.

(27) Ikkala, O.; ten Brinke, G. *Chem. Commun.* **2004**, 2131-2137.

(28) Kuehl, C.; Yamamoto, T.; Seidel, S. R.; Stang, P. J. *Org. Lett.* **2002**, *4*, 913 – 915.

(29) Holliday, B. J.; Mirkin, C., A. *Angew. Chem. Int. Ed.* **2001**, *40*, 2022 – 2053.

(30) Swiegers, G. F.; Malefetse, T. J. *Chem. Rev.* **2000**, *100*, 3483 – 3537.

(31) Balzani, V.; Credi, A.; Raymo, F. M.; Stoddart, J., F. *Angew. Chem. Int. Ed.* **2000**, *39*, 3348 – 3391.

(32) Collier, C. P.; Mattersteig, G.; Wong, E. W.; Luo, Y.; Sampaio, J.; Raymo, F. M.; Stoddart, J. F.; Health, J. R. *Science* **1999**, *285*, 391 - 395.

(33) Ruben, M. Z., U.; Lehn, J.-M.; Ksenofontov, V.; Gutlich, P.; Vaughan, G. B. M. *Chem. Eur. J.* **2005**, *11*, 94.

(34) Waggoner, T. A.; Last, J. A.; Kotula, P. G.; Sasaki, D. Y. *J. Am. Chem. Soc.* **2001**, *123*, 496-497.

(35) Faul, C. F. J.; Antonietti, M. *Adv. Mater.* **2003**, *15*, 673-683.

(36) Guan, Y.; Yu, S.-H.; Antonietti, M.; Boettcher, C.; Faul, C. F. J. *Chem. Eur. J.* **2005**, *11*, 1305-1311.

(37) Kadam, J.; Faul, C. F. J.; Scherf, U. *Chem. Mater.* **2004**, *16*, 3867-3871.

(38) Wang, Z.; Medforth, C. J.; Shelnutt, J. A. *J. Am. Chem. Soc.* **2004**, *126*, 15954-15955.

(39) Wei, Z.; Laitinen, T.; Smarsly, B.; Ikkala, O.; Faul, C. F. J. *Angew. Chem. Int. Ed.* **2005**, *44*, 751-756.

(40) Zakrevskyy, Y.; Faul, C. F. J.; Guan, Y.; Stumpe, J. *Adv. Funct. Mater.* **2004**, *14*, 835-841.

(41) Zhang, T.; Spitz, C.; Antonietti, M.; Faul, C. F. J. *Chem. Eur. J.* **2005**, *11*, 1001-1009.

(42) Valkama, S.; Lehtonen, O.; Lappalainen, K.; Kosonen, H.; Castro, P.; Repo, T.; Torkkeli, M.; Serimaa, R.; ten Brinke, G.; Leskelae, M.; Ikkala, O. *Macromol. Rapid Commun.* **2003**, *24*, 556-560.

(43) Hofmeier, H.; Hoogenboom, R.; Wouters, M. E. L.; Schubert, U. S. *J. Am. Chem. Soc.* **2005**, *127*, 2913-2921.

(44) Hogg, R.; Wilkins, R. G. *J. Chem. Soc.* **1962**, 341.

(45) Holyer, R. H.; Hubbard, C. D.; Kettle, S. F. A.; Wilkins, R. G. *Inorg. Chem.* **1966**, *5*, 622.

(46) Tekin, E.; Holder, E.; Marin, V.; de Gans, B.-J.; Schubert, U. S. *Macromol. Rapid Commun.* **2005**, *26*, 293-297.

(47) Hofmeier, H.; Schubert, U. S. *Chem. Soc. Rev.* **2004**, *33*, 373-399.

(48) Andres, P. R.; Schubert, U. S. *Adv. Mater.* **2004**, *16*, 1043-1068.

(49) Beta, I. A.; Sorensen, C. M. *J. Phys. Chem. A,* ACS ASAP.

(50) Bian, L. *J. Phys. Chem. A* **2003**, *107*, 11517-11524.

(51) Grabowski, S. J. *J. Phys. Chem. A* **2001**, *105*, 10739-10746.

(52) Remer, L. C.; Jensen, J. H. *J. Phys. Chem. A* **2000**, *104*, 9266-9275.

(53) Silverstein, K. A. T.; Haymet, A. D. J.; Dill, K. A. *J. Am. Chem. Soc.* **2000**, *122*, 8037-8041.

(54) El-ghayoury, A.; Peeters, E.; Schenning, A. P. H. J.; Meijer, E. W. *Chem. Commun.* **2000**, 1969-1970.

(55) Meier, M. A. R.; Lohmeijer, B. G. G.; Schubert, U. S. *Macromol. Rapid Commun.* **2003**, *24*, 852–857.

(56) Tiitu, M.; Volk, N.; Torkkeli, M.; Serimaa, R.; ten Brinke, G.; Ikkala, O. *Macromolecules* **2004**, *37*, 7364-7370.

(57) Ikkala, O.; ten Brinke, G. *MRS Symp. Proc.* **2003**, *775*, 213-223.

(58) Knaapila, M.; Torkkeli, M.; Makela, T.; Horsburgh, L.; Lindfors, K.; Serimaa, R.; Kaivola, M.; Monkman, A. P.; ten Brinke, G.; Ikkala, O. *MRS Symp. Proc.* **2001**, *660*, JJ5 21/1-JJ5 21/6.

(59) Kosonen, H.; Valkama, S.; Ruokolainen, J.; Knaapila, M.; Torkkeli, M.; Serimaa, R.; Monkman, A. P.; ten Brinke, G.; Ikkala, O. *Synth. Met.* **2003**, *137*, 881-882.

(60) Ruokolainen, J.; Tanner, J.; ten Brinke, G.; Ikkala, O.; Torkkeli, M.; Serimaa, R. *Macromolecules* **1995**, *28*, 7779-84.

(61) Valkama, S.; Ruotsalainen, T.; Kosonen, H.; Ruokolainen, J.; Torkkeli, M.; Serimaa, R.; ten Brinke, G.; Ikkala, O. *Macromolecules* **2003**, *36*, 3986-3991.

(62) Gohy, J.-F.; Lohmeijer, B. G. G.; Alexeev, A.; Wang, X.-S.; Manners, I.; Winnik, M. A.; Schubert, U. S. *Chem. Eur. J.* **2004**, *10*, 4315-4323.

(63) Gohy, J.-F.; Lohmeijer, B. G. G.; Schubert, U. S. *Macromol. Rapid Commun.* **2002**, *23*, 555-560.

(64) Xie, P.; Zhang, R. *J. Mater. Chem.* **2005**, *15*, 2529-2550.

(65) Schmatloch, S.; Gonzalez, M. F.; Schubert, U. S. *Macromol. Rapid Commun.* **2002**, *23*, 957-961.

(66) Furuta, P. T.; Deng, L.; Garon, S.; Thompson, M. E.; Frechet, J. M. J. *J. Am. Chem. Soc.* **2004**, *126*, 15388-15389.

(67) Gong, X.; Moses, D.; Heeger, A. J.; Xiao, S. *J. Phys. Chem. B* **2004**, *108*, 8601-8605.

(68) Yonemoto, E. H.; Saupe, G. B.; Schmehl, R. H.; Hubig, S. M.; Riley, R. L.; Iverson, B. L.; Mallouk, T. E. *J. Am. Chem. Soc.* **1994**, *116*, 4786-4795.

(69) Buda, M.; Kalyuzhny, G.; Bard, A. J. *J. Am. Chem. Soc.* **2002**, *124*, 6090-6098.

(70) Dresselhaus, M. S.; Thomas, I. L. *Nature* **2001**, *414*, 332-337.

(71) Graetzel, M. *Inorg. Chem.* **2005**, *44*, 6841-6851.

(72) Nelson, J. *Science* **2001**, *293*, 1059-1060.

(73) Tributsch, H. *Coord. Chem. Rev.* **2004**, *248*, 1511–1530.

(74) Yuichiro Kawamura, S. Y., Stephen R. Forrest *J. Appl. Phys.* **2002**, *92*, 87-93.

(75) Nazeeruddin, M. K.; Humphry-Baker, R.; Berner, D.; Rivier, S.; Zuppiroli, L.; Graetzel, M. *J. Am. Chem. Soc.* **2003**, *125*, 8790-8797.

(76) Lee, C.-L.; Kang, N.-G.; Cho, Y.-S.; Lee, J.-S.; Kim, J.-J. *Opt. Mater.* **2003**, *21*, 119-123.

(77) Meyers, A.; Weck, M. *Macromolecules* **2003**, *36*, 1766-1768.

(78) Wang, X.-Y.; Weck, M. *Macromolecules* **2005**, *38*, 7219-7224.

(79) Meyers, A.; South, C.; Weck, M. *Chem. Commun.* **2004**, 1176-1177.

(80) Meyers, A.; Weck, M. *Chem. Mater.* **2004**, *16*, 1183-1188.

(81) Carlise, J. R.; Weck, M. *J. Polym. Sci. Part. A: Polym. Chem.* **2004**, *42*, 2973-2984.

(82) Carlise, J. R.; Kriegel, R. M.; Rees, W. S., Jr.; Weck, M. *J. Org. Chem.* **2005**, *70*, 5550-5560.

(83) McKittrick, M. W.; Jones, C. W. *Chem. Mater.* **2005**, *17*, 4758-4761.

CHAPTER 3

SIDE-CHAIN FUNCTIONALIZED POLYMERS CONTAINING BIPYRIDINE COORDINATION SITES: POLYMERIZATION AND METAL COORDINATION STUDIES

3.1 Abstract

Monomers containing (tris-bipyridine) ruthenium (II), (bis-bipyridine) palladium (II), and heteroleptic ruthenium complexes were synthesized and polymerized *via* ruthenium catalyzed ring-opening metathesis polymerization in non-polar solvents. The solubility of the resulting polyelectrolytes in nonpolar solution could be tuned by alkyl functionalization of the ligands around the metal centers. These polymers present the first polynorbornenes containing a bpy-based metal complex at each repeating unit and might find numerous applications including luminescent and electroluminescent materials.

3.2 Introduction

The first two chapters thus far have sought to provide some background on the concepts of side-chain functionalized polymers (Chapter 1), and functionalization via metal coordination (Chapter 2). In the current chapter and the ones that follow, several specific examples of work done in the area of combining the above two concepts will be explained in detail. Ring-opening metathesis polymerization (ROMP) is chosen as the primary method of polymerization, and several different metal-ligand interactions are explored to test the hypothesis introduced in Chapter 2 that combining the versatility and strength of metal-ligand interactions with the efficiency and functional group tolerance of

ROMP comprises a useful method of generating a variety of functionalized polymers and materials.

Choosing the appropriate combination of metal and ligand for use as a polymer functionalization motif is of critical importance, and has the potential to significantly affect the properties of the resultant material. For instance, binding strength varies by many orders of magnitude from one complex to another, as noted in Chapter 2.[1,2] Additionally, coordination geometry and thus the number of ligands around a metal varies as well. There is also the possibility of variation in net charge from complex to complex, and thus the opportunity to engineer charges into an otherwise neutral polymer, or vice versa.

In order to explore the effects of varying both metal and ligand on an otherwise identical set of macromolecules, as well as to demonstrate the ability to functionalize these polymers with modified ligands as a model for other functional groups as well, a poly(norbornene)-based polymer with 2-2'-bipyridine as the coordination site was designed. Transition metals Ru^{2+} and Pd^{2+} were used to complex bipyridine analogues as well as acetylacetonato analogues to the polymer. The project demonstrates the synthesis of bipyridine (bpy) containing monomers for ring-opening metathesis polymerization (ROMP), coordination of ruthenium or palladium by the pendant bpy, subsequent functionalization of the metal center with multidentate ligands, and finally the ring-opening metathesis polymerization of these monomers in non-polar solutions using ruthenium-based initiators.

Multidentate nitrogen-donor ligands such as 2,2'-bipyridine are advantageous as they are often neutral, stable in solution, and form highly stable complexes with numerous transition metals.[3-18] The resulting multidentate nitrogen donor ligand-based metal complexes have a large number of potential applications. For example, $Ru(bpy)_3^{2+}$ complexes have been studied widely for potential uses in solar energy conversion,[19-26] light-emitting electrochemical cells (LECs),[27] luminescent and electroluminescent

materials,[20,28-31] and non-linear optical devices.[32] Incorporation of such complexes onto a polymer backbone improves processability and allows for the formation of materials in thin films.[33,34] Methods used to incorporate $Ru(bpy)_3^{2+}$ and similar coordination complexes into a polymer include free-radical polymerizations[35] and ATRP.[29,36] However, to this date no cases of the employment of ROMP have been reported, despite the fact that ROMP is often the polymerization method of choice for highly functionalized monomers due to its living character and high functional group tolerance.[37-40] Only the incorporation of terpyridine onto a solid substrate *via* ROMP for use in ATRP experiments has been reported, but formation of the metal complex occurred after the system had become heterogeneous.[41] Other ROMP polymers that include metal-containing systems with dative metal-ligand bonds and counterions are absent from the literature.

In non-polar media, $Ru(bpy)_3^{2+}$ containing monomers have been incorporated into copolymers for solubility reasons and have only constituted approximately 10-20% of the copolymer systems.[42] Due to the ionic character of the resulting polymer and its poor solubility in many common polymerization solvents, non-polar monomers have been needed. In this study, the synthesis of $Ru(bpy)L_x$ and $Pd(bpy)L_y$ (L = Oacac, dnBpy [3-octyl-2,4-pentanedione, 4,4'-dinonyl-2,2'-bipyridine, respectively]) containing monomers, and demonstrate the formation of the corresponding homopolymers in non-polar solvent *via* ROMP are reported.

3.3 Monomer Synthesis

The synthesis of monomer **1**, the building block for all of the bipyridine-based coordination complexes, started with the functionalization of the 2,2'-bipyridine (bpy) unit.[43,44] Methylation at the 6-position followed by lithiation of the methyl group and subsequent substitution reaction with *tert*-butyldimethylsilyl-protected bromoundecanol (**2**) built outward from the initial bpy unit to form **3** (Scheme 3.1).

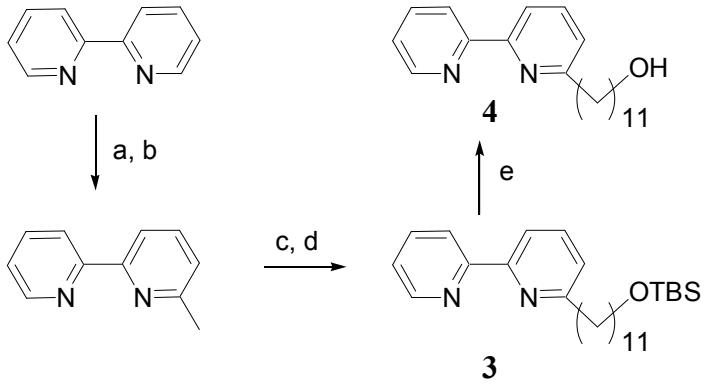

Scheme 3.1. (a) MeLi, THF, 0 ^{o}C; (b) sat. $KMnO_4$/acetone; (c) LDA, THF, -20 ^{o}C; (d) $Br(CH_2)_{11}OTBS$ (**2**), THF, -95 ^{o}C; (e) TBAF, CH_2Cl_2; 33% overall yield.

Deprotection of the alcohol gave compound **4**, and either condensation with norbornenyl acid chloride (**5**)[45] to form *endo/exo* **1**, or coupling with the corresponding exo-carboxylic acid (**6**)[46] to form *exo* **1**, yielded the target monomers (Schemes 3.2 & 3.3).

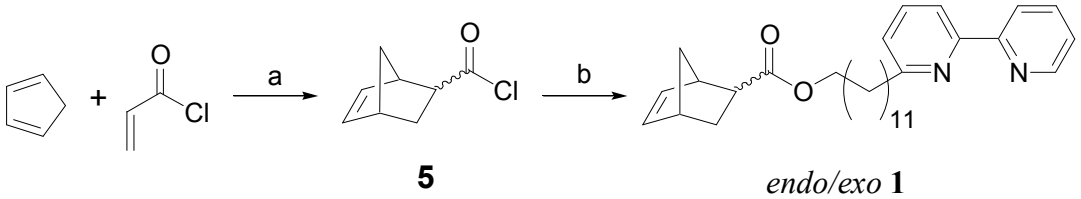

Scheme 3.2. Formation of 75:25 *endo/exo* **1**: (a) reflux; (b) **4**, NEt_3, CH_2Cl_2; 80% overall yield.

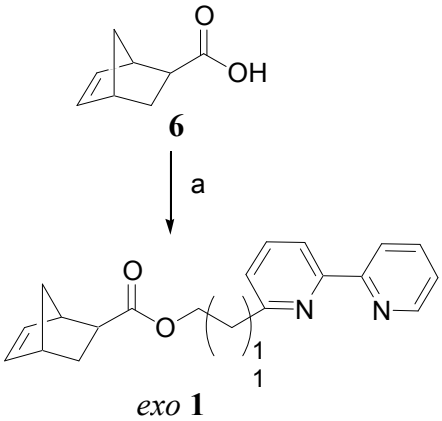

Scheme 3.3. Formation of *exo* **1**: (a) **4**, DCC, DMAP (cat), CH_2Cl_2; 85% overall yield.

The synthesis of $RuCl_2(dmso)_4$[47] and **7a**[48] followed literature procedures, with compound **7b** being analogous to **7a** with the substitution of 4,4'-dinonyl-2,2'-bipyridine (dnBpy) in place of the simple bpy (Figure 3.1).

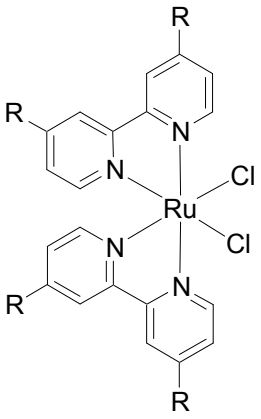

7a: R = H
7b: R = $(CH_2)_8CH_3$

Figure 3.1. Dichlorobis(2'2-bipyridine)Ruthenium(II) derivatives

The use of dnBpy instead of bpy became necessary to tailor solubility during the polymerization and of the final polymers. For instance, the polymerization of the $Ru(bpy)_3^{2+}$ analogue of **8,** in less polar solvents such as dichloromethane using **9**, (Figure 3.2)

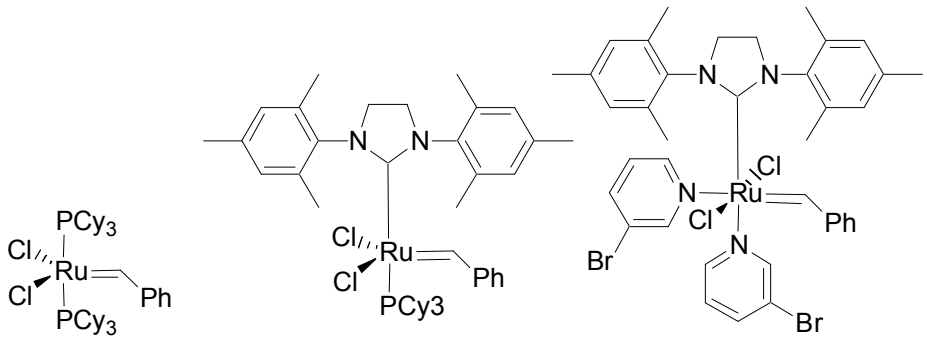

9 **13** **14**

Figure 3.2. Metathesis catalysts used.

proceeded slowly and only to approximately 20-30%. Though the monomers are fully soluble, the resulting polymers become rapidly insoluble and precipitate. As a result, the

catalytically active end of the polymer is removed from the liquid phase, and the polymerization effectively ceases at that point.

3.4 Coordination Studies

Monomer **1** has been reacted with $RuCl_2(dmso)_4$ in an equimolar ratio (Scheme 3.4),

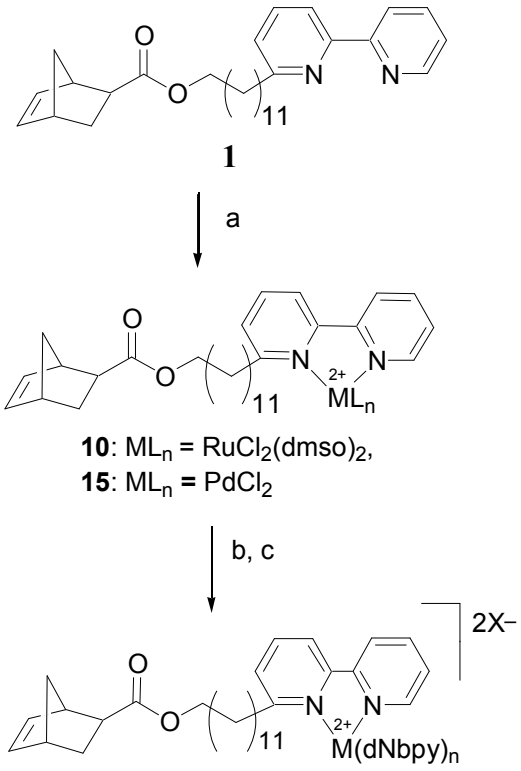

Scheme 3.4. *Formation of **10***: (a) $RuCl_2(dmso)_4$, $CHCl_3$; *Formation of **8***: (b) 2 equiv. dnBpy, 1:1 $EtOH/H_2O$, reflux 12 hrs; (c) NH_4PF_6; 43% overall yield. *Formation of **15***: (a) $PdCl_2(benzonitrile)_2$, acetone; *Formation of **12***: (b) 1 equiv. dnBpy, MeOH; (c) AgOTf, 3hrs, dark.

resulting in the formation of **10**, which serves as the precursor for all ruthenium-containing monomers. In **10**, the metal center is coordinated to one bpy (from the monomer) and two chlorides and two dimethyl sulfoxides, which allow for selective replacement with other ligands including two moles of dnBpy to form **8** or two moles of

2,4-pentanedione to form the heteroleptic monomer **11**. In the case of compound **12,** 4,4'-dinonyl-2,2'-bipyridine was metallated with $PdCl_2(benzonitrile)_2$, displacing the benzonitriles, followed by the reaction with **1** in the final step in the presence of silver triflate to form monomer **12** (Scheme 3.5).

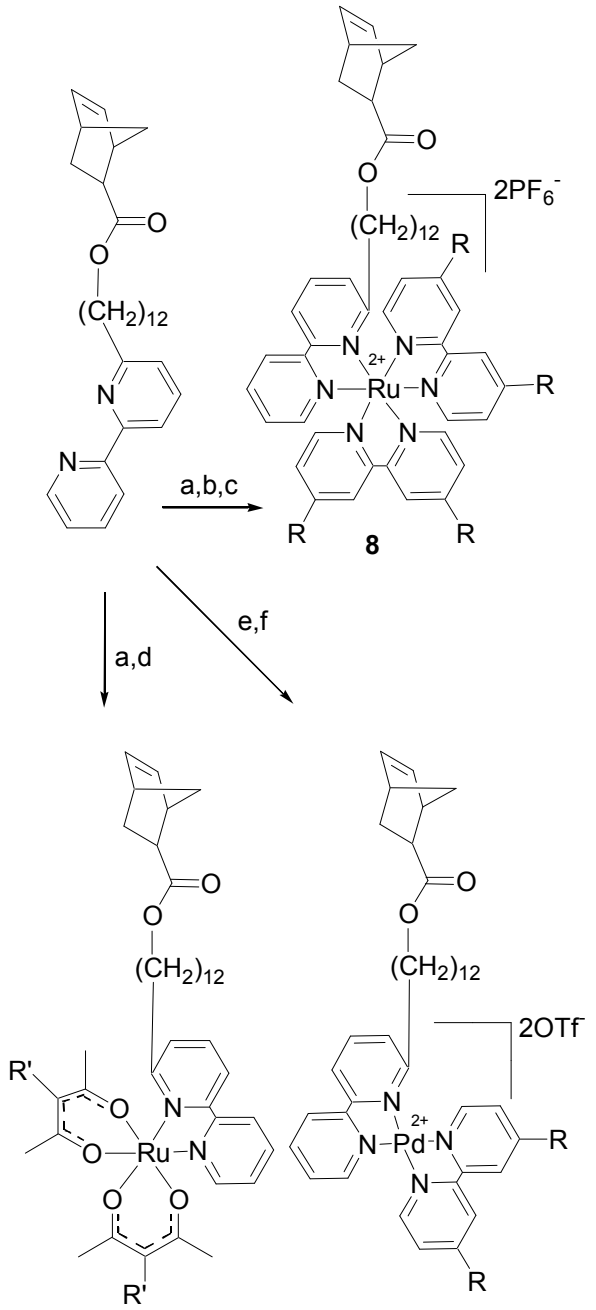

Scheme 3.5. (a) $RuCl_2(dmso)_4$, $CHCl_3$, reflux; (b) 4,4'-dinonyl-2,2'-bipyridine, EtOH/H_2O, reflux; (c) NH_4PF_6; (d) 3-octyl-2,4-pentanedione, EtOH, reflux; (e) **7b**, MeOH; (f) AgOTf.

3.5 Polymerization

We have studied the ROMP of all monomers using initiators **9, 13,** and **14** (Figure 2). In the case of **13** and **14**, one PCy_3 group has been replaced with the 4,5-dihydroimidazol-2-ylidene resulting in a dramatic increase in the rate of propagation (k_p).[49-51] However, it has been reported in the literature that the rate of initiation (k_i) of **13** is much slower than the rate of propagation, resulting in complete polymerization before full initiation has occurred, thereby limiting the control over the polymerization.[49-51] This shortcoming has been overcome with the recent emergence of catalyst **14**. It has been shown for **14** that the rate of initiation has been increased to the point where it is now comparable with the k_p, thus allowing for fast, efficient, functional group tolerant, and living polymerizations.[51]

Polymerizations of monomer **6** and the metal-containing monomers **8**, **11**, **12**, and **15** were carried out in dichloromethane. Using either **13** or **14**, all polymerizations with the exception of **11** were complete within minutes, while polymerizations using **9** took at least several hours, with some polymerizations never reaching completion. In the case of monomer **1**, polymerization was not observed using catalyst **9**. It was postulated that the typically strong binding between ruthenium and bipyridine was responsible for the catalyst poisoning. In contrast, catalysts **13** and **14** polymerized **6** easily within minutes. No polymerization was observed for either *endo/exo* **12** or *exo* **12**, using any of the catalysts. One possible limitation of **12** in being polymerized is the choice of counterion. No changes in monomer solubility were observed upon exchange of the counterion of **12** from triflate to hexafluorophosphate. However, this anion exchange allowed for the polymerizations of **12** to proceed quantitatively when using either **13** or **14**. This suggests that ROMP is inhibited by the presence of the triflate anion.

3.6 Discussion

This study allowed for exploration into the abilities of various transition metal containing norbornene-bipyridine monomers to undergo ring-opening metathesis polymerization. Efficiency of the polymerization was found to be strongly dependant upon the solubility of the resulting polymer, the choice of counterion, and the initiator. In all cases except for *exo* **8**, ROMP using **9** did not result in full or controlled polymerization. Monomers **1** and **11** did not polymerize at all under normal conditions with **9** while ROMP of **12** with **13** and **14** went slowly over a period of hours to days with visible catalyst decomposition as observed *in situ* by ^{1}H NMR of the carbene region. In contrast to **9**, ROMP of all monomers except **12** using either **13** or **14** was fast, efficient, and complete. However, due to a lack of full initiation, ROMP using **13** was uncontrolled. In the case of polymer **1**, the resulting polymers have high molecular weights and low polydispersities as outlined in Table 3.1.

Table 3.1. Polymerization data for the ROMP of monomer **1** with initiators **9**, **13** and **14**

	Catalyst	**$M_n/10^3$**	**$M_w/10^3$**	**PDI**
exo **1**	**9**	---	---	---
	13	2700	4900	1.83
	14	32.83	38.16	1.16
endo/exo **1**	**9**	---	---	---
	13	12700	13200	1.04
	14	13	34	2.67

The polymerizations are likely non-living, as only a small percentage of catalyst initiates with **9.** This causes the degree of polymerization to vary from experiment to experiment, and as a result no direct conclusions can be drawn from the GPC results.

Characterization of the highly charged polymers proved to be challenging. For the charged species, each monomer unit contains a +2 charge, thus making even a simple 20-mer into a polyelectrolyte with a +40 charge. This polyelectrolyte-like behavior made polymer characterization impossible using gel-permeation chromatography in methylene chloride, THF, or DMF, since the charges either interacted too strongly with the column packing material or simply formed aggregates in an ionomeric fashion and never eluted. Recently, Schubert and coworkers have shown that similar problems with charged polymers in methylene chloride or chloroform as the mobile phase could be circumvented by switching to a mobile phase consisting of 10 mM NH_4PF_6 in N,N-dimethylformamide.[52] However, the polymers in Schubert's case all contained a single charged species in the center of a long uncharged polymer, *i.e.* the polymers all had only a +2 charge. Our attempts at characterizing our polymers using the Schubert mobile phase proved to be unsuccessful, even with short chain lengths of only ten repeat units. However, the polymers are indefinitely soluble in non-polar solvents such as methylene chloride, which allows for solution spectroscopy such as NMR. The polymerization of all monomers, like all other poly(norbornene)s synthesized *via* ROMP, can easily be monitored *via* proton NMR spectroscopy. The alkene proton signals of the strained norbornene ring system appear approximately at $\delta = 6.0 - 6.3$ ppm. Upon ring-opening and subsequent polymerization, these proton signals shift upfield to approximately $\delta = 5.0 - 5.5$ ppm, with full baseline resolution, thus greatly facilitating monitoring the progress of the polymerization. The catalyst activity can also be directly monitored through observation of the carbene region of the proton NMR spectra. For example, in catalyst **9**, the single proton of the uninitiated carbene shows up at approximately 20.0 ppm, while the initiated carbene signal comes at approximately 18.8 ppm. Other signals

in this region are indicative of catalyst decomposition. Proton NMR spectroscopy proved that all monomers had been quantitatively converted to polymer over various polymerization times. The formation of polymer was supported by precipitation of the post-polymerization reaction mixture into 10 x excess of methanol, decanting, and collecting the purified polymer residue. All monomers were soluble in methanol.

Polymer solubility proved to be a major hurdle in the polymerization of most monomers. While polymerization of the bis 2,2'-bipyridine analog of **8** using **9** was complete within ten minutes, the polymer started to precipitate out after several minutes resulting in an insoluble solid. However, polymer solubility was tailored by using a more soluble bipyridine-type ligand, 4,4'-dinonyl-2,2'-bipyridine (dnBpy). Incorporation of two dnBpy ligands in place of the two bpy units per monomer (**8**) resulted in polymers that stayed fully soluble in methylene chloride. The uncharged polymer **11** displayed the same solubility advantages from ligand alkylation. However, due to the fact that the acac ligand is charged, there is no need for a counterion.

3.7 Living Tests

The living nature of polymers **1** and **8** polymerized with catalysts **9** and **14** was probed *via* ^{1}H NMR spectroscopy of the carbene region.[38] First, the uninitiated carbene signal of the catalyst was observed to completely disappear, giving rise to the fully initiated species. For the polymerizations of monomers *endo/exo* **1** and *exo* **1** with catalyst **14**, and *exo* **8**, with catalysts **9** and **14**, after complete disappearance of the norbornene alkene proton signals indicating conversion of all monomer to polymer, the initiated carbene signal was still present. The fully initiated carbene species was still present even thirty minutes after complete polymerization. During this period, no changes in the integration of the carbene signals were detected suggesting that no catalyst decompositions occurred and therefore that the polymerizations of *endo/exo* **1** and *exo* **1** with **14**, and *exo* **8**, with **9** and **14**, are living.

3.8 Conclusion

This work demonstrated both the synthesis and the subsequent polymerization in non-polar media of monomers with pendant bipyridine-containing metal complexes. Combining the functional group tolerance of ring-opening metathesis polymerization (ROMP) with the strategy of pre-polymerization functionalization enables the synthesis of complex macromolecules flanked with functional groups attached via a purely metal coordination-based motif. All monomers are fully soluble in non-polar solvents and can be polymerized *via* ROMP. Solubility of the polymers could be tuned through alkyl functionalization of the ligands around the metal center. These results present the first report of the polymerization of norbornene with pendant bpy M L_x side groups. The resulting polymers may find applications such as solar energy converters, light-emitting electrochemical cells (LECs), luminescent and electroluminescent materials, non-linear optical devices, and organic light-emitting diodes (OLEDs).

The modification of the bipyridine ligands and successful coordination and subsequent polymerization indicates that these polymers might be useful with other more complex functionalities tethered to them. Also, as is consistent with the main drive of this thesis, these polymers demonstrate the ability to use side-chain metal coordination to add functionalization to a polymer chain. Some interesting future directions for this work might involve further modifications of the bipyridine ligand besides simply the alkyl chain. Perhaps a mesogenic moiety that would induce a liquid crystalline component to the system, or a water soluble modification that would allow for incorporation into dye-sensitized solar cells would be useful modifications.

This concept is also well-suited for dendritic and cross-linking applications, since the ruthenium tris-bipyridine complex is both very strong and radiates outward in six directions. It is this last point that leads to the subject of the next chapter, which explores the cross-linking capabilities of ruthenium, among other transition metals, on a modified natural macromolecule in an aqueous system.

3.9 Experimental Section

All reagents were purchased either from Acros Organic, Aldrich, or Strem Chemicals, and were used without further purification unless otherwise noted. NEt_3 and DMF were distilled from CaH_2, and THF and CH_2Cl_2 were dried via passage through Cu_2O and alumina columns. NMR spectra were taken on a 300 MHz Varian Mercury spectrometer and were referenced to residual proton solvent. Mass spectral analysis was provided by the Georgia Tech Mass Spectrometry Facility using a VG-70se spectrometer. Gel permeation chromatography (GPC) analyses were carried out using a Waters 1525 binary pump coupled to a Waters 2414 refractive index detector. The GPC was calibrated using polystyrene standards on a Styragel® HR 4 and HR 5E column set with CH_2Cl_2 or THF as the eluent. Elemental analyses were performed by Galbraith Laboratories, Knoxville, Tennessee, or Atlantic Microlab, in Norcross, Georgia. Compounds **5**, bicyclo[2.2.1]hept-5-ene-2-carbonyl chloride,[45] **6**, exo-bicyclo[2.2.1]hept-5-ene-2-carboxylic acid,[46] **7a**,[48] and $RuCl_2(dmso)_4$[47] were prepared according to literature procedures.

Synthesis of *endo/exo*-Bicyclo[2.2.1]hept-5-ene-2-carboxylic acid 12-[2,2']bipyridinyl-6-yl-dodecyl ester (*endo/exo* 1)

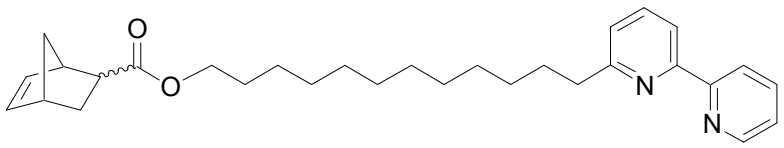

Compound **4** (1.47 g, 4.31 mmol) was dissolved in 20 mL of dry THF. Next, 809 mg (8 mmol) of dry triethylamine was added, followed by 783 mg (5 mmol) of acid chloride **5** and the reaction mixture was allowed to stir for eight hours, during which a white precipitate had formed and the liquid phase turned orange. The solvent was removed, the mixture dissolved in 40 mL of ethyl acetate and filtered. The filtrate was dried with

$MgSO_4$ and the solvent removed to yield an oil. The oil was purified *via* column chromatography using neutral, deactivated alumina (80-200 mesh) and a 10:1 hexane/ethyl acetate solvent system as the mobile phase. Compound **1** (1.47 g, 3.18 mmol, 74%) was recovered as a clear translucent oil. ^{1}H NMR ($CDCl_3$, 300 MHz): δ 1.27 (m, 18H, CH_2-C**H**$_2$-CH_2); 1.60 (m, 3H, alkyl); 1.81 (m, 4H, norbornene); 2.20 (dd, 0.25H, J_1=10.0 Hz, J_2=4.4 Hz; *exo*-norbornene); 2.84 (dd, 2H, J_1=7.8 Hz, J_2=7.8 Hz, Bpy-C**H**$_2$-CH_2); 2.94 (m, 1H, *endo*-norbornene); 3.01 (s, br, 0.25H, *exo*-norbornene); 3.19 (m, 0.75H, *endo*-norbornene); 3.98 (m, 1.5H, O-C**H**$_2$-CH_2, *endo*-isomer); 4.03 (t, 0.5H, *J*=6.6 Hz, O-C**H**$_2$-CH_2, *exo*-isomer); 5.92 (dd, 0.75H, J_1=5.6 Hz, J_2=3.3 Hz, alkene *endo*-isomer); 6.13 (m, 0.5H, alkene, exo-isomer); 6.16 ((dd, 0.75H, J_1=5.6 Hz, J_2=3.3 Hz, alkene, *endo*-isomer); 7.18 (d, 1H, *J*=7.6 Hz, bpy-5-C**H**); 7.31 (ddd, 1H, J_1=7.4 Hz, J_2=4.6 Hz, J_3=1.1 Hz, bpy-5'-C**H**); 7.73 (t, 1H, *J*=7.7 Hz, bpy-4-C**H**); 7.83 (td, 1H, J_1=7.6 Hz, J_2=1.9 Hz, bpy-3'-C**H**); 8.22 (d, 1H, *J*=7.7 Hz, bpy-3-C**H**); 8.47 (d, 1H, *J*=7.8 Hz, bpy-3'-C**H**); 8.66 (m, 1H, bpy-6'-C**H**). ^{13}C NMR ($CDCl_3$, 300 MHz): δ 26.3, 29.0, 29.5, 29.6, 29.9, 30.0, 31.1, 30.7, 38.8, 42.0, 42.9, 43.5, 43.7, 46.1, 46.9, 49.9, 64.6, 64.7, 64.9, 118.4, 121.4, 122.9, 123.6, 132.5, 135.9, 137.0, 137.2, 137.9, 138.2, 149.2, 156.7, 162.1. UV/vis in CH_2Cl_2 (λ_{max}): 279, 301 nm. MS: m/z calcd. (M) 460.66, found (electrospray) 461.3 (M^+). Anal. Found: C, 77.90; H, 9.10; N, 6.19. Calcd for $C_{30}H_{40}N_2O_2$: C, 78.22; H, 8.75; N, 6.08.

Synthesis of *exo*-Bicyclo[2.2.1]hept-5-ene-2-carboxylic acid 12-[2,2']bipyridinyl-6-yl-dodecyl ester (*exo* 1)

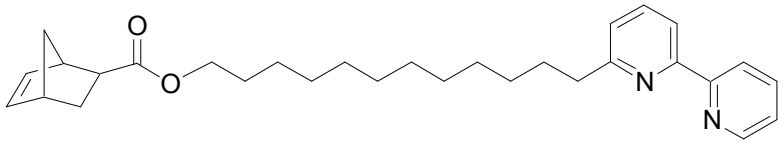

Compound **6** (406 mg, 2.9 mmol), compound **4** (1.00g, 2.9 mmol), and 4-N,N-dimethylaminopyridine (36 mg, 0.29 mmol) were dissolved in 20 mL of dichloromethane. Then dicyclohexylcarbodiimide (570 mg, 2.9 mmol) was added under argon, with a white precipitate forming approximately 2 minutes after addition of dicyclohexylcarbodiimide. The reaction was stirred overnight. The precipitate was then filtered off and the solvent removed to give the crude ester product, which was purified via column chromatography (20:1 hexane/ethyl acetate, deactivated neutral alumina) to give *exo* **1** as a partially crystalline translucent oil, (1.18 g, 2.6 mmol, 88% yield). ^{1}H NMR ($CDCl_3$, 300 MHz): δ 1.27 (m, 18H, CH_2-C**H**$_2$-CH_2); 1.60 (m, 3H, norbornene alkyl); 1.81 (m, 4H, norbornene alkyl); 2.20 (dd, 0.25H, J_1=10.0 Hz, J_2=4.4 Hz; norbornene alkyl); 2.84 (dd, 2H, J_1=7.8 Hz, J_2=7.8 Hz, Bpy-C**H**$_2$-CH_2); 2.91 (s, br, 1H, norbornene alkyl); 3.02 (s, br, 1H, norbornene alkyl); 4.06 (t, 2H, *J*=6.6 Hz, O-C**H**$_2$-CH_2); 6.13 (m, 2H, alkene); 7.18 (d, 1H, *J*=7.6 Hz, bpy-5-C**H**); 7.31 (ddd, 1H, J_1=7.4 Hz, J_2=4.6 Hz, J_3=1.1 Hz, bpy-5'-C**H**); 7.73 (t, 1H, *J*=7.7 Hz, bpy-4-C**H**); 7.83 (td, 1H, J_1=7.6 Hz, J_2=1.9 Hz, bpy-3'-C**H**); 8.22 (d, 1H, *J*=7.7 Hz, bpy-3-C**H**); 8.47 (d, 1H, *J*=7.8 Hz, bpy-3'-C**H**); 8.66 (m, 1H, bpy-6'-C**H**).

Synthesis of *tert*-Butyl-dimethyl-silanyloxy-11-bromo-1-undecanol (2)

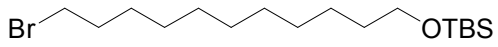

11-Bromo-1-undecanol (10 g, 39.8 mmol) was dissolved in 50 mL of N,N-dimethylformamide along with imidazole (2.72 g, 40 mmol) and *tert*-butyl-dimethylsilyl chloride (6.03 g, 40 mmol). The reaction was stirred for 12 hours at 25 ^{o}C. Afterwards the crude product was purified via column chromatography using silica gel and a 30:1 hexane/ethyl acetate solvent system. Compound **2** was collected as a clear oil (8.39 g, 22.9 mmol) in 58% yield. ^{1}H NMR ($CDCl_3$, 300 MHz): δ 0.04 (s, 6H, Si-C**H**$_3$); 0.89 (s,

9H, C-C**H**$_3$); 1.27 (m, 14H, CH_2-C**H**$_2$-CH_2); 1.50 (quint, 2H, *J*=6.6 Hz, Br-C**H**$_2$-CH_2); 1.85 (quint, 2H, *J*=6.7 Hz, O-CH_2-C**H**$_2$-CH_2); 3.40 (t, 2H, *J*=7.2 Hz, Br-C**H**$_2$-CH_2); 3.60 (t, 2H, *J*=6.6 Hz, O-C**H**$_2$-CH_2). ^{13}C NMR ($CDCl_3$, 300 MHz): δ -4.8, 18.8, 26.2, 27.3, 28.5, 29.3, 29.8, 29.9, 33.0, 33.2, 45.5, 63.6. MS: m/z calcd. (M) 364.18, found (electrospray) 365.1 (M^+).

Synthesis of 6-[12-(*tert*-Butyl-dimethyl-silanyloxy)-dodecyl]-[2,2']bipyridinyl (3)

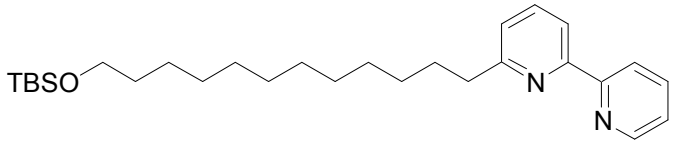

6-Methyl-2,2'-bipyridine[33] (2.75 g, 16.16 mmol) was dissolved in 10 mL dry THF and added dropwise to a solution of 17 mmol of lithium diisopropylamine (LDA) in 10 mL of THF at –95 °C under an Ar atmosphere. The solution turned dark blue immediately. The reaction was stirred for 30 min, allowed to warm to -30 °C, and then cooled back to –95 °C. A degassed solution of 5.90 g (16.16 mmol) of **2** in 10 mL dry THF was added dropwise and the solution was allowed to stir overnight at 25 °C. The reaction was cooled to -20° C and quenched with 15 mL water forming a bright yellow, biphasic mixture. The THF was removed, and the resultant mixture was washed with 3 x (40 mL) Et_2O. The organic phases were combined, dried with $MgSO_4$, the solvent removed, and the remaining yellow oil purified via column chromatography using 20:1 hexane/EtOAc on neutral alumina. Compound **3** was recovered as a clear oil in 48% yield (3.53 g, 7.76 mmol). ^{1}H NMR ($CDCl_3$, 300 MHz): δ 0.03 (s, 6H, Si-C**H**$_3$); 0.88 (s, 9H, C-C**H**$_3$); 1.27 (m, 16H, CH_2-C**H**$_2$-CH_2); 1.50 (m, 2H, Bpy-CH_2-C**H**$_2$-CH_2); 1.71 (quint, 2H, *J*=7.1 Hz, O-CH_2-C**H**$_2$-CH_2); 2.86 (dd, 2H, J_1=7.8 Hz, J_2=7.8 Hz, Bpy-C**H**$_2$-CH_2); 3.60 (t, 2H, *J*=6.6 Hz, O-C**H**$_2$-CH_2); 7.05 (d, 1H, *J*=7.6 Hz, bpy-5-C**H**); 7.28 (ddd, 1H, J_1=7.4 Hz, J_2=4.6 Hz, J_3=1.1 Hz, bpy-5'-C**H**); 7.66 (t, 1H, *J*=7.7 Hz, bpy-4-C**H**); 7.80 (td, 1H,

J_1=7.6 Hz, J_2=1.9 Hz, bpy-4'-C**H**); 8.16 (d, 1H, *J*=7.7 Hz, bpy-3-C**H**); 8.43 (d, 1H, *J*=7.8 Hz, bpy-3'-C**H**); 8.66 (m, 1H, bpy-6'-C**H**). ^{13}C NMR ($CDCl_3$, 300 MHz) δ -4.8, 26.2, 26.4, 27.9, 29.8, 29.9, 30.0, 30.1, 33.2, 36.1, 48.2, 63.6, 92.5, 118.3, 121.6, 123.0, 123.7, 137.0, 149.0, 156.9, 165.1. MS: m/z calcd. (M) 454.3, found (EI) 454.4 (M). Calcd for $C_{28}H_{46}N_2O_2Si$: C, 73.95; H, 10.20; N, 6.16. Found: C, 73.90; H, 10.33; N, 5.90.

Synthesis of 12-[2,2']Bipyridinyl-6-yl-dodecan-1-ol (4)

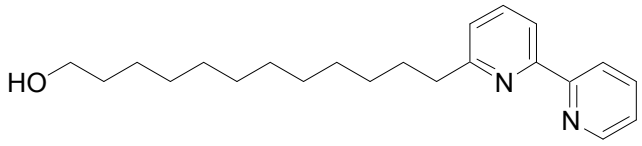

Compound **3** (1.71 g, 3.75 mmol) was added to a solution of 1.23 g (3.9 mmol) TBAF in 25 mL THF and stirred for one hour at 25 °C. The reaction was then quenched with 15 mL of water and extracted 3 x with 30 mL methylene chloride. The organic layers were combined, dried, the solvent removed, and the residue was placed under vacuum (0.1 Torr) to remove residual TBAF. The product was isolated as a white solid in >99% yield. ^{1}H NMR ($CDCl_3$, 300 MHz): δ 1.27 (m, 16H, CH_2-C**H**$_2$-CH_2); 1.53 (quint, 2H, *J*=6.7 Hz, Bpy-CH_2-C**H**$_2$-CH_2); 1.80 (quint, 2H, *J*=7.0 Hz, O-CH_2-C**H**$_2$-CH_2); 2.10 (s, br, 1H, O-**H**); 2.84 (dd, 2H J_1=7.8 Hz, J_2=7.8 Hz, Bpy-C**H**$_2$-CH_2); 3.61 (t, 2H, *J*=6.5 Hz, O-C**H**$_2$-CH_2); 7.08 (d, 1H, *J*=7.6 Hz, bpy-5-C**H**); 7.30 (ddd, 1H, J_1=7.4 Hz, J_2=4.6 Hz, J_3=1.1 Hz, bpy-5'-C**H**); 7.66 (t, 1H, *J*=7.7 Hz, bpy-4-C**H**); 7.82 (td, 1H, J_1=7.6 Hz, J_2=1.9 Hz, bpy-3'-C**H**); 8.16 (d, 1H, *J*=7.7 Hz, bpy-3-C**H**); 8.43 (d, 1H, *J*=7.8 Hz, bpy-3'-C**H**); 8.64 (m, 1H, bpy-6'-C**H**). ^{13}C NMR ($CDCl_3$, 300 MHz): δ 26.1, 27.9, 33.1, 38.7, 63.2, 118.4, 121.5, 122.9, 123.7, 137.2, 149.1, 155.4, 162.1. MS: m/z calcd. (M) 340.25, found (EI) 340.2 (M).

Synthesis of Dichlorobis(4,4'-dinonyl-2,2'-bipyridine)ruthenium(II) (7b)

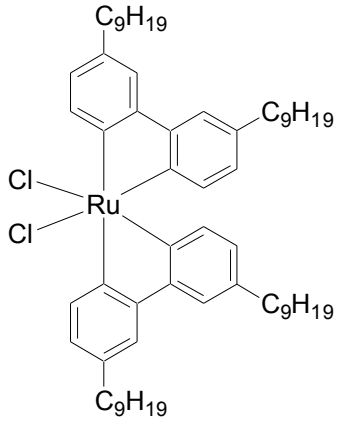

DnBpy (4,4'-dinonyl-2,2'-bipyridine, 323 mg, 0.79 mmol), $RuCl_3[H_2O]_x$ (103 mg, 0.40 mmol), and LiCl (167 mg, 3.95 mmol) were added to 5 mL of degassed N,N-dimethylformamide. The solution was refluxed under argon for eight hours, cooled to room temperature, and 50 mL of a 1:1 acetone/water solution was added forming a violet-black precipitate after one hour. The precipitate was filtered off and redissolved in 20 mL of methylene chloride, dried with $MgSO_4$, and the solvent was removed. Crude **7b** was collected as a dark violet oil (612 mg) and used without further purification.

Synthesis of Bis(4,4'-dinonyl-2,2'-bipyridine)ruthenium(II) di(hexafluorophosphate) bicyclo[2.2.1]hept-5-ene-2-carboxylic acid 12-[2,2']bipyridinyl-6-yl-dodecyl ester (8)

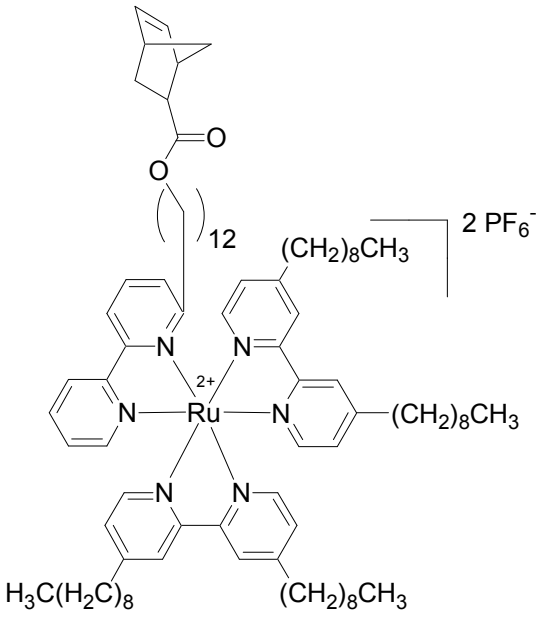

Method I: Compound **7** (294 mg, 0.373 mmol) and dnBpy (305 mg, 0.75 mmol) were suspended in 20 mL of a 1:1 water/ethanol solution. The mixture was refluxed, becoming homogeneous after 15 minutes, and turning orange-brown after one hour. After eight hours, the solution was concentrated to 4-5 mL, and 10 mL of water were added, resulting in a dark orange brown solution. A solution of NH_4PF_6(aq.) (0.5 mL, 3.0 M) was added, turning the solution from dark orange brown to bright orange. The mixture was extracted with 30 mL of methylene chloride, the water layer was washed with 2 x (20 mL) methylene chloride, the organic layers were combined, dried with $MgSO_4$, and the solvent removed, to give crude **8**, which was purified *via* column chromatography (50:1 CH_2Cl_2/MeOH, neutral deactivated alumina) yielding 409 mg of pure **8** (65%) as a bright orange oil. ^{1}H NMR ($CDCl_3$, 300 MHz): δ 0.89 (m, 12H, CH_2-C**H**$_3$); 1.28 (m, 72H, CH_2-C**H**$_2$-CH_2); 1.68 (m, 8H, alkyl); 1.84 (m, 2H, alkyl); 2.83 (m, 8H, dnBpy-C**H**$_2$-CH_2); 2.99 (dd, 2H, J_1=7.8 Hz; J_2=7.8 Hz, bpy-C**H**$_2$-CH_2); 3.26 (s, 1H, norbornene); 4.01 (m, 2H, O-C**H**$_2$-CH_2); 5.90 (m, 1H, norbornene alkenyl); 6.14 (m, 1H, norbornene alkenyl); [unsymmetric aromatic region of the Ru(bpy)$_3$ complex, 19 H total:] 7.06 (m, 1H); 7.23 (m, 3H); 7.43 (m, 1H); 7.53 (d, 3H, *J*=5.6 Hz); 7.62 (m, 1H); 7.76 (d,

1H, *J*=5.4 Hz); 8.05 (m, 1H); 8.11 (m, 1H); 8.18 (m, 3H); 8.23 (m, 1H); 8.27 (m. 1H); 8.45 (m, 1H); 9.74 (dd, 1H, J_1= Hz; J_2=6.0 Hz). ^{13}C NMR ($CDCl_3$, 300 MHz): δ 1.4, 11.0, 11.4, 11.8, 14.5, 23.0, 26.3, 29.0, 30.4, 30.5, 30.6, 32.2, 35.6, 41.9, 42.5, 43.5, 46.6, 46.9, 64.8, 95.8, 95.9, 123.7, 124.8, 126.4, 127.0, 127.7, 128.2, 135.9, 138.1, 143.3, 143.7, 144.1, 150.6, 154.7, 155.2, 155.9, 156.4, 156.8, 157.6, 168.6, 176.4. MS: m/z calcd. (M) 1668.9, found (electrospray) 1524 (M^+ - PF_6^- counterion). UV/vis in CH_2Cl_2 (λ_{max}): 281, 299, 454 nm. Anal. Found: C, 61.04; H, 7.87; N, 4.97; Ru, 7.38. Calcd for CHNRu: C, 61.89; H, 7.73; N, 5.04; Ru, 6.06.

Method II: Compound **7b** (612 mg, 0.62 mmol) was combined with **1** (285 mg, 0.62 mmol) in 15 mL of a 1:1 ethanol/water solution, and refluxed for eight hours under argon, during which time the solution changed from purple to orange-brown. The solution was cooled to room temperature, and 0.5 mL of a 3.0 M aqueous solution of NH_4PF_6 was added to precipitate the product, which was then extracted with methylene chloride and water. The water layer was washed with 3 x (25 mL) methylene chloride, and the organic layers combined, dried with $MgSO_4$, and the solvent removed to afford 833 mg of the crude product as a dark orange oil. The oil was purified via column chromatography using neutral, deactivated alumina (80-200 mesh) with a 20:1 methylene chloride/methanol solvent system as the mobile phase. Compound **8** (650 mg, 0.39 mmol) was recovered as a bright orange oil in 63 % yield.

Synthesis of Dichlorobis(dimethylsulfoxide)ruthenium(II)bicyclo[2.2.1]hept-5-ene-2-carboxylic acid 12-[2,2']bipyridinyl-6-yl-dodecyl ester (10)

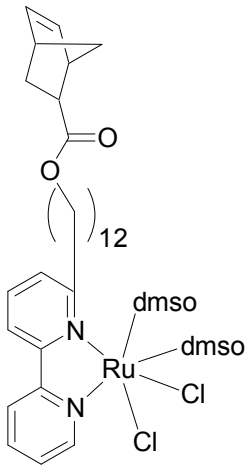

Compound **1** (400 mg, 0.87 mmol) was added to 10 mL degassed chloroform followed by the addition of $RuCl_2(dmso)_4$ (430 mg, 1.41 mmol). The solution was refluxed under argon for eight hours, turning reddish-brown after approximately 20 min. The reaction was removed from the heat, cooled to room temperature, concentrated to ca. 2-3 mL, and re-dissolved in 3 mL methylene chloride. Diethyl ether (40 mL) was then added, resulting in the formation of a heterogeneous mixture. The precipitate was filtered off, the filtrate was again concentrated to ca. 2-3 mL, and 3 mL methylene chloride was added, followed by 80 mL of hexanes, turning the solution cloudy with a purple material aggregating and settling to the bottom. The hexane was removed, yielding 294 mg of crude **10** as a purple oil which was used without further purification.

Synthesis of Bis(3-octyl-pentane-2,4-dione)ruthenium(II)bicyclo[2.2.1]hept-5-ene-2-carboxylic acid 12-[2,2']bipyridinyl-6-yl-dodecyl ester (11)

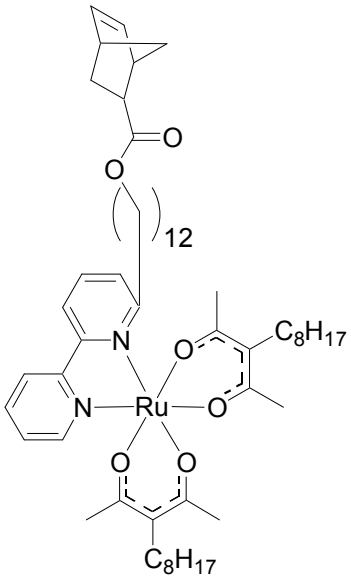

A solution of 193 mg (0.091 mmol) 3-octyl-pentane-2,4-dione in acetone was added to 143 mg (0.182 mmol) of compound **7** dissolved in 20 mL of acetone and refluxed overnight. The resulting purple solution was concentrated, re-dissolved in ethyl acetate (20 mL), and washed three times with aqueous calcium carbonate, then three times with water. The purple ethyl acetate solution was dried with magnesium sulfate, the solvent removed, and the crude purple oil was used for polymerization, as purification attempts resulted in monomer decomposition.

Synthesis of (4,4'-dinonyl-2,2'-bipyridine) palladium(II) di(trifluoromethanesulfonate) bicyclo[2.2.1]hept-5-ene-2-carboxylic acid 12-[2,2']bipyridinyl-6-yl-dodecyl ester (12)

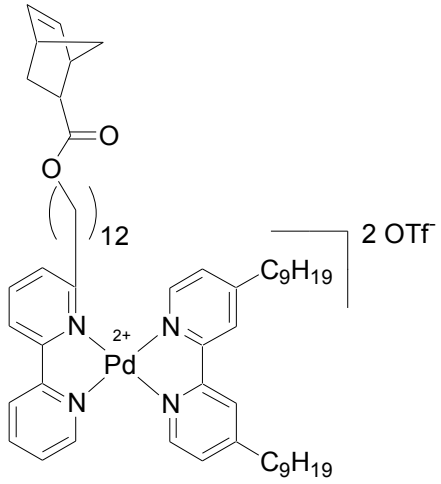

Compound **15** (221 mg, 0.346 mmol) was suspended in 50 mL of methanol and 4,4'-dinonyl-2,2'-bipyridine (141 mg, 0.346 mmol) and AgOTf (178 mg, 0.693 mmol) were added. The reaction was stirred at room temperature in the dark for eight hours, after which 10 mL of a suspension of Norit in methanol was added, and the reaction stirred for three more hours. The mixture was filtered, and the filtrate was washed with 40 mL of hexanes, dried with $MgSO_4$, and the solvent removed to afford crude **12,** which after purification by column chromatography (deactivated neutral alumina, 100:1 CH_2Cl_2/MeOH) gave 322 mg of pure **12** (73% yield). ^{1}H NMR ($CDCl_3$, 300 MHz): • 0.95 (m, 6H, C**H**$_2$-CH_3); 1.29 (m, 42H, CH_2-C**H**$_2$-CH_2); 1.52 (m, 1H, alkyl); 1.61 (m, 3H, alkyl); 1.72 (m, 5H, alkyl); 1.91 (dt, 1H, J_1=11.7 Hz; J_2=3.9 Hz; norbornene alkyl); 2.18 (dd, 1H, J_1=9.8 Hz; J_2=4.5 Hz; norbornene alkyl); 2.55 (m, 1H, alkyl); 2.83 (m, 6H, bpy-C**H**$_2$-CH_2); 3.03 (s, br, 1H, alkyl); 4.06 (t, 2H, J=7.1 Hz, O-C**H**$_2$-CH_2); [remaining protons from unsymmetric aromatic region of the Pd(bpy)$_2$ complex, 13 H total:] 7.18 (d, 1H, J=7.5 Hz); 7.33 (m, 1H); 7.45 (d, 1H, J=7.7 Hz); 7.53 (m, 1H); 7.73 (t, 1H, J=7.7

Hz); 7.82 (m, 2H); 7.91 (s, br, 1H); 8.04 (m, 1H); 8.21 (d, 1H, *J*=8.3 Hz); 8.46 (d, 1H, *J*=8.4); 8.65 (m, 1H); 9.11 (d, 1H, *J*=6.1 Hz). ^{13}C NMR ($CDCl_3$, 300 MHz): • 14.2, 23.0, 26.3, 29.0, 29.6, 29.8, 30.1, 30.9, 33.2, 35.8, 37.4, 38.6, 43.4, 46.6, 49.8, 63.1, 64.8, 85.6, 87.2, 118.0, 121.0, 121.2, 122.8, 123.6, 126.7, 129.2, 132.3, 132.5, 135.9, 136.8, 137.1, 137.7, 138.1, 149.0, 149.2, 153.0, 155.4, 157.0, 162.1. UV/vis in CH_2Cl_2 ($\bullet_{max}$): 279, 299 nm. MS: m/z calcd. (M) 1272.47, found (electrospray) 1272.5 (M^+).

Synthesis of Dichloro[palladium(II)]bicyclo[2.2.1]hept-5-ene-2-carboxylic acid 12-[2,2']bipyridinyl-6-yl-dodecyl ester (15)

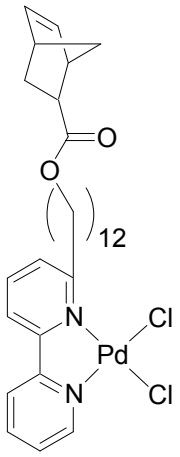

Dichlorobis(benzonitrile)palladium(II) (200 mg, 0.522 mmol) was combined with **1** (229 mg, 0.522 mmol) in 20 mL of acetone and stirred for fifteen minutes under argon, at which time the solution turned orange. Then 150 mL of hexanes were added and the solution became cloudy. The reaction mixture was allowed to sit for one hour to let the precipitate settle. The acetone was decanted off, the remaining orange powder dissolved in methylene chloride and filtered through celite, and the solvent was removed, yielding **15** as an orange oil (133 mg, 0.208 mmol, 42%). ^{1}H NMR ($CDCl_3$, 300 MHz): δ 1.26 (m, 19H, CH_2-C**H**$_2$-CH_2); 1.50 (m, 3H, alkyl); 1.83 (m, 3H, alkyl); 2.20 (m, 0.6H, norbornene exo-isomer); 2.89 (m, 2H, bpy-C**H**$_2$-CH_2); 3.00 (s, br, 0.6H, norbornene exo-

isomer); 3.17 (m, 0.6H, norbornene exo-isomer); 3.55 (m, 2H); 4.00 (m, 2H); 5.90 (m, 0.6H, endo isomer); 6.13 (m, 1.4H, endo/exo isomers); 7.37 (dd, 1H, J_1=7.8 Hz, J_2=1.2 Hz, bpy-5-C**H**); 7.45 (m, 1H, bpy-5'-C**H**); 7.66 (m, 1H, bpy-4'-C**H**); 7.99 (t, 1H, J=7.5 Hz, bpy-4-C**H**); 8.15 (m, 2H, bpy-3,3'-C**H**); 9.14 (dd, 1H, J_1=6.0 Hz, J_2=1.2 Hz, bpy-6'-C**H**). ^{13}C NMR ($CDCl_3$, 300 MHz): δ 26.3, 29.0, 29.5, 30.6, 31.5, 39.6, 42.0, 43.6, 46.1, 46.6, 46.9, 49.8, 64.8, 120.9, 123.5, 125.8, 128.2, 129.3, 132.3, 135.9, 137.7, 140.2, 140.7, 150.9, 156.4, 157.5, 170.3, 174.6, 176.1. UV/vis in CH_2Cl_2 (λ_{max}): 323 nm. MS: m/z calcd. (M) 636.15, found (electrospray) 636.2 (M^+).

Synthesis of Dichloro[4,4'-dinonyl-2,2'-bipyridine Palladium(II)] (16)

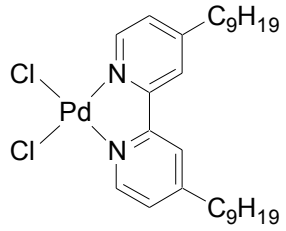

Dichlorobis(benzonitrile)palladium(II) (200 mg, 0.522 mmol) was combined with 4,4'-dinonyl-2,2'-bipyridine (213 mg, 0.522 mmol) in 20 mL of acetone and stirred for fifteen minutes under argon, giving an orange solution with crystals forming. Addition of hexane (50 mL) completed the precipitation of the product. The reaction mixture was allowed to sit for one hour. The solvent was decanted, the remaining orange crystals washed 2 x with hexane (20 mL), and the product was dried under high vacuum (50 mTorr) for one hour to give 297 mg (97 %) of pure **16**. ^{1}H NMR ($CDCl_3$, 300 MHz): δ 0.89 (t, 6H, J=7.1 Hz, CH_2-C**H**$_3$); 1.28 (m, 24H, CH_2-C**H**$_2$-CH_2); 1.69 (quint, 4H, J=7.6 Hz, bpy-CH_2-C**H**$_2$-CH_2); 2.85 (dd, 4H, J_1=8.5 Hz, J_2=7.6 Hz, bpy-C**H**$_2$-CH_2); 7.30 (dd, 2H, J_1=1.7 Hz, J_2=6.1 Hz, bpy-5,5'-C**H**); 7.94 (d, 2H, J=1.8 Hz, bpy-3,3'-C**H**); 8.96 (d, 2H, J=5.6 Hz, bpy-6,6'-C**H**). ^{13}C NMR ($CDCl_3$, 300 MHz): δ 14.5, 23.0, 29.6, 29.7, 29.8, 30.3,

32.2, 36.1, 123.9, 126.4, 149.6, 155.8, 157.8. MS: m/z calcd. (M) 584.19, found (electrospray) 584.2 (M^+). UV/vis in CH_2Cl_2 (λ_{max}): 282, 318 nm.

Synthesis of Bicyclo[2.2.1]hept-5-ene-2-carboxylic acid 12-dodecyl ester (17)

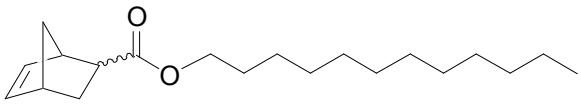

Acid chloride **5** (840 mg, 5.37 mmol), 1-dodecanol (1.00 g, 5.37 mmol), and triethylamine (1.09 g, 10.7 mmol) were dissolved in 20 mL dichloromethane and stirred for eight hours under argon. The solution was quenched with 3 mL of water and extracted with dichloromethane and water. The water layer was washed with dichloromethane (3 x 15 mL), and the organic layers were combined, dried with $MgSO_4$, and the solvent removed. Column chromatography with silica and a 20:1 hexane/ethyl acetate solvent system yielded **17**. (1.50 g, 4.89 mmol) as a clear oil in 91% yield. ^{1}H NMR ($CDCl_3$, 300 MHz): δ 0.86 (t, 3H, *J* =7.2 Hz, CH_2-C**H**$_3$); 1.24 (m, 19H, CH_2-C**H**$_2$-CH_2); 1.40 (m, 2H, alkyl); 1.57 (m, 2H, alkyl); 1.87 (m, 1H, alkyl); 2.89 (m, 2H, alkyl); 3.17 (s, br, 1H, alkyl); 3.98 (m, 2H, alkyl); 5.90 (m, 1H, norbornene alkenyl); 6.16 (m, 1H, norbornene alkenyl). ^{13}C NMR ($CDCl_3$, 300 MHz): δ 14.5, 23.0, 26.3, 27.7, 29.0, 29.7, 29.9, 30.0, 32.3, 33.1, 38.5, 42.8, 43.7, 43.9, 45.2, 46.0, 49.5, 49.9, 51.2, 63.3, 64.7, 87.2, 132.5, 137.9, 175.0. Anal. Found: C, 78.65; H, 10.58. Calcd. for $C_{20}H_{34}O_2$: C, 78.38; H, 11.18.

General Polymerization Procedure

The desired monomer (0.05 mmol) was dissolved in 0.75mL of CD_2Cl_2 and a portion of the initiator (0.001 mmol) was added. The reaction was shaken vigorously at room temperature. After the polymerization was complete by NMR, the polymer was

quenched with two to three drops of ethyl vinyl ether, and the polymer was precipitated by pouring into cold methanol. The polymer was purified by redissolving in 1 mL of dichloromethane and reprecipitation in methanol.

Polymer (1)

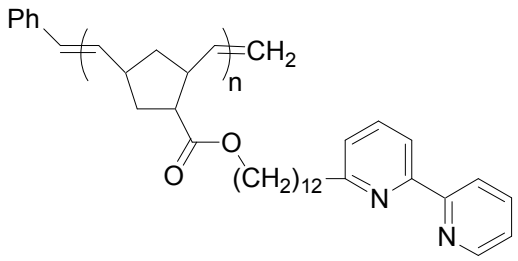

Isolated yield 65%. ^{1}H NMR (CD_2Cl_2): δ 1.26 (m, 16H); 1.58 (m, 4H, alkyl); 1.79 (m, 2H); 2.04 (m, 2H); 2.49 (m, 2H); 2.83 (t, 2H, *J*=7.1 Hz); 3.06 (m, 1H); 4.01 (m, 2H); 5.20 (m, 1H); 5.38 (m, 1H); 7.14 (d, 1H, *J*=7.3 Hz); 7.28 (m, 1H); 7.70 (t, 1H, *J*=7.6 Hz); 7.79 (t, 1H, *J*=8.2 Hz); 8.20 (d, 1H, *J*=6.6 Hz); 8.45 (d, 1H, *J*=8.0 Hz); 8.63 (d, 1H, *J*=3.7 Hz). ^{13}C NMR (CD_2Cl_2, 300 MHz): δ 26.32, 29.06, 29.66, 29.75, 29.90, 29.99, 30.08, 38.62, 46.47, 101.69, 118.02, 120.93, 122.81, 123.61, 128.73, 136.74, 137.02, 145.09, 149.13, 150.71, 155.35, 156.24, 156.57, 159.29, 163.94. IR (KBr, cm^{-1}): 780.7, 1044.3, 1146.1, 1286.4, 1332.2, 1428.7, 1457.6, 1581.5, 1728.1, 2852.5, 2922.0, 3080.4. UV/vis in CH_2Cl_2 (λ_{max}): 279, 301 nm.

Polymer (8)

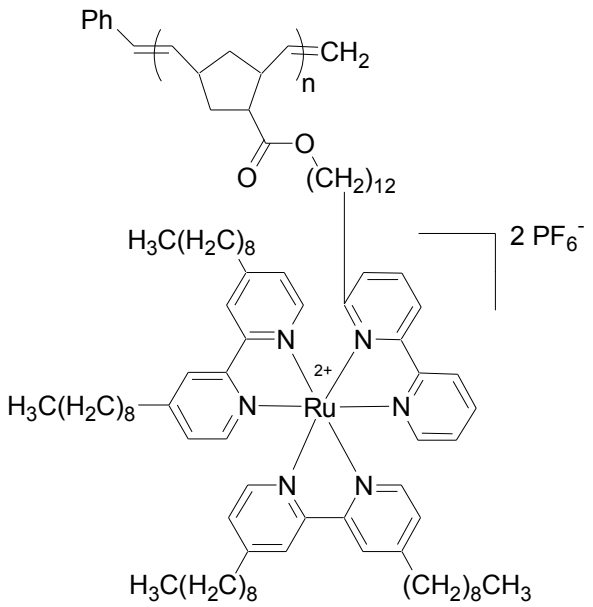

Isolated yield 71%. ^{1}H NMR (CD_2Cl_2): δ 0.87 (m, 12H); 1.28 (m, 69H); 1.69 (m, 11H); 2.09 (m, 2H); 2.42 (m, 1H); 2.84 (m, 8H); 3.25 (m, 2H); 4.02 (m, 2H); 5.40 (m, 2H); 7.06 (m, 2H); 7.184 (m, 1H); 7.26 (m, 2H); 7.40 (m, 1H); 7.53 (m, 2H); 7.64 (m, 1H); 8.07 (m, 4H); 8.22 (m, 3H); 8.47 (m, 1H); 9.53 (d, 1H, *J*=5.7 Hz); 9.98 (d, 1H, *J*=5.8 Hz). ^{13}C NMR (CD_2Cl_2, 300 MHz): δ 1.19, 9.99, 14.29, 19.04, 23.04, 26.41, 29.06, 29.45, 29.60, 29.71, 29.84, 30.44, 30.51, 32.09, 32.18, 35.52, 35.64, 42.38, 45.08, 77.22, 77.74, 92.19, 101.05, 112.37, 115.62, 122.97, 123.42, 124.15, 124.48, 126.46, 126.76, 127.30, 127.94, 128.00, 133.87, 146.24, 150.56, 152.32, 152.83, 154.34, 154.75, 154.84, 155.11, 155.75, 155.99, 156.05, 156.66, 156.71, 156.90, 156.96, 157.60, 157.83. IR (KBr, cm^{-1}): 836.1, 916.1, 1014.0, 1190.8, 1418.6, 1453.7, 1616.7, 1715.1, 2853.0, 2922.4, 3061.2. UV/vis in CH_2Cl_2 (λ_{max}): 281, 300, 454 nm.

Polymer (11)

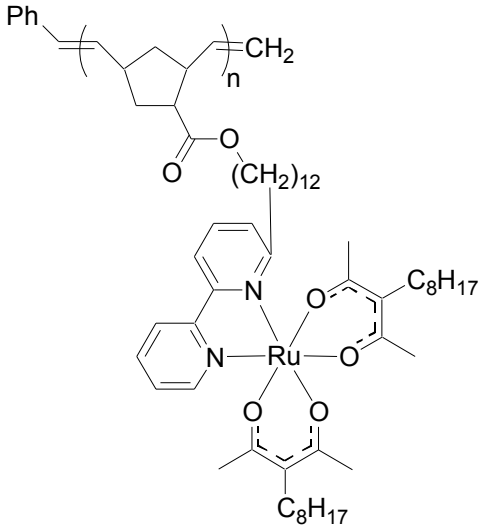

Isolated yield 47%. ^{1}H NMR (CD_2Cl_2): δ 0.88 (m, 6H); 1.24 (m, 45H); 1.60 (m, 6H); 1.77 (m, 3H); 2.04 (m, 1H); 2.31 (m, 8H); 2.92 (m, 12H); 4.03 (m, 4H); 5.21 (m, 2H); 7.07 (m, 1H); 7.42 (m, 2H); 7.84 (m, 2H); 8.43 (m, 2H). ^{13}C NMR (CD_2Cl_2, 300 MHz): δ 27.14, 29.57 (br), 33.36, 38.53, 65.87 (br), 67.24, 78.83, 87.58, 96.49 (br), 103.07, 110.85 (br), 120.30 (br), 135.81, 138.90, 144.31, 156.54 (br), 160.36, 164.64, 169.14, 181.31, 188.74, 206.41. IR (KBr, cm^{-1}): 801.8, 1033.3, 1097.8, 1178.4, 1259.9, 1453.7, 1621.5, 1713.2, 1985.7, 2853.0, 2961.3, 3055.4. UV/vis in CH_2Cl_2 (λ_{max}): 299, 365, 555 nm.

Polymer (12)

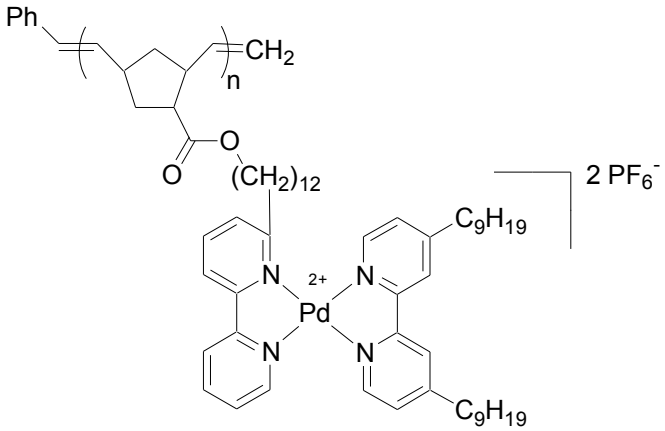

Isolated yield 53%. ^{1}H NMR (CD_2Cl_2): δ 0.89 (m, 6H); 1.28 (m, 40H); 1.59 (m, 2H); 1.71 (m, 5H); 1.97 (m, 6H); 2.56 (m, 2H); 2.83 (t, 4H, *J*=7.8 Hz); 3.05 (m, 2H); 4.02 (m, 2H); 5.22 (m, 1H); 5.35 (m, 1H); 7.15 (d, 1H, *J*=7.2 Hz); 7.29 (d, 2H, *J*=5.9 Hz); 7.36 (d, 1H, *J*=6.0 Hz); 7.67 (m, 1H); 7.79 (m, 1H); 7.90 (m, 1H); 8.07 (m, 1H); 8.14 (m, 1H); 8.19 (m, 1H); 8.62 (m, 1H); 9.10 (d, 1H, *J*=5.9 Hz); 9.21 (d, 1H, 5.5 Hz). • ^{13}C NMR (CD_2Cl_2, 300 MHz): δ 14.0, 23.0, 29.1, 29.5, 30.0, 30.5, 32.2, 35.8, 38.6, 38.9, 64.7, 118.1, 121.0, 121.6, 122.8, 123.7, 126.2, 126.8, 131.8, 134.8, 136.8, 137.0, 138.3, 141.8, 149.1, 150.1, 155.3, 156.3, 157.8. IR (KBr, cm^{-1}): 637.4, 773.4, 1030.4, 1175.8, 1255.6, 1332.7, 1428.2, 1453.7, 1563.6, 1581.5, 1724.7, 2852.5, 2922.9, 3083.2. UV/vis in CH_2Cl_2 (λ_{max}): 279, 301 nm.

Polymer (17)

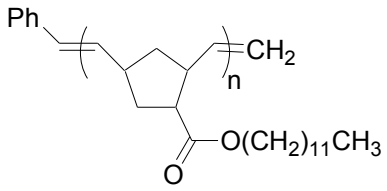

Isolated yield 88%. ^{1}H NMR (CD_2Cl_2): δ 0.91 (t, 3H, *J*=6.4 Hz); 1.28 (m, 21H); 1.60 (m, 2H); 2.01 (m, 1H); 2.45 (m, 1H); 2.79 (m, 1H); 3.13 (m, 1H); 4.06 (m, 2H); 5.24 (m, 1H); 5.46 (m, 1H). ^{13}C NMR (CD_2Cl_2, 300 MHz): δ 14.5, 23.0, 26.3, 29.1, 29.6, 32.1, 37.3 (br), 42.8 (br), 43.3 (br), 48.0 (br), 50.6 (br), 64.8, 131.9 (br), 133.7 (br), 135.1 (br), 176.0 (br).

3.10 References

(1) Hogg, R.; Wilkins, R. G. *J. Chem. Soc.* **1962**, 341.

(2) Holyer, R. H.; Hubbard, C. D.; Kettle, S. F. A.; Wilkins, R. G. *Inorg. Chem.* **1966**, *5*, 622.

(3) Lohmeijer, B. G. G.; Schubert, U. S. *J. Polym. Sci., Part A: Polym. Chem.* **2003**, *41*, 1413-1427.

(4) Ziessel, R. *Coord. Chem. Rev.* **2001**, *216–217*, 195–223.

(5) Lehn, J.-M.; Rigault, A.; Siegel, J.; Harrowfield, J.; Chervier, B.; Moras, D. *Proc. Nat. Acad. Sci.* **1987**, *84*, 2565-2569.

(6) Piguet, C.; Hopfgartner, G.; Bocquet, B.; Schaad, O.; Williams, A. F. *J. Am. Chem. Soc.* **1994**, *116*, 9092-9102.

(7) Psillakis, E.; Jeffery, J. C.; McCleverty, J. A.; Ward, M. D. *J. Chem. Soc., Dalton Trans.* **1997**, 1645.

(8) Suzuki, T.; Kotsuki, H.; Isobe, K.; Moriya, N.; Nakagawa, Y.; Ochilb, M. *Inorg. Chem.* **1995**, *34*, 530-531.

(9) Albrecht, M.; Frohlich, R. *J. Am. Chem. Soc.* **1997**, *119*, 1656-1661.

(10) Piguet, C. *Incl. Phen. Macro. Chem.* **1999**, *34*, 361.

(11) Mamula, O.; Von Zelewsky, A.; Bernardinelli, G. *Angew. Chem. Int. Ed.* **1998**, *37*, 289-293.

(12) Olenyuk, B.; Fechtenkotter, A.; Stang, P. J. *J. Chem. Soc., Dalton Trans.* **1998**, 1707.

(13) Lawrence, D. S.; Jiang, T.; Levett, M. *Chem. Rev.* **1995**, *95*, 2229-2260.

(14) Lindsey, J. S. *New J. Chem.* **1991**, *15*, 153.

(15) Hasenknopf, B.; Lehn, J. M.; Kneisel, B. O.; Baum, G.; Fenske, D. *Angew. Chem. Int. Ed. Engl.* **1996**, *35*, 1838-1840.

(16) Philp, D.; Stoddart, J. F. *Angew. Chem. Int. Ed. EngI.* **1996**, *35*, 1154-1196.

(17) Chambron, J.-C.; Dietrich-Buchecker, C. O.; Heitz, V.; Nierengarten, J.-F.; Sauvage, J.-P. *Transition Metals in Supramolecular Chemistry*; Kluwer Academic: Boston, 1993; Vol. 448.

(18) Chambron, J.-C.; Dietrich-Buchecker, C. O.; Sauvage, J.-P. *Top. Cur. Chem.* **1993**, *165*.

(19) Kalyanasundaram, K. *Coord. Chem. Rev* **1982**, *46*, 159.

(20) Wang, P.; Zakeeruddin, S. M.; Moser, J. E.; Nazeeruddin, M. K.; Sekiguchi, T.; Graetzel, M. *Nat. Mater.* **2003**, *2*, 402-407.

(21) Calvert, J. M.; Caspar, J. V.; Binstead, R. A.; Westmoreland, T. D.; Meyer, T. J. *J. Am. Chem. Soc.* **1982**, *104*, 6620-6627.

(22) Wang, P.; Zakeeruddin, S. M.; Moser, J. E.; Humphry-Baker, R.; Graetzel, M. *J. Am. Chem. Soc.* **2004**, *126*, 7164-7165.

(23) Kumar, R.; Sharma, A. K.; Parmar, V. S.; Watterson, A. C.; Chittibabu, K. G.; Kumar, J.; Samuelson, L. A. *Chem. Mater.* **2004**, *16*, 4841-4846.

(24) Graetzel, M. *Inorg. Chem.* **2005**, *44*, 6841-6851.

(25) Nelson, J. *Science* **2001**, *293*, 1059-1060.

(26) Tributsch, H. *Coord. Chem. Rev* **2004**, *248*, 1511–1530.

(27) Buda, M.; Kalyuzhny, G.; Bard, A. J. *J. Am. Chem. Soc.* **2002**, *124*, 6090-6098.

(28) Farah, A. A.; Pietro, W. J. *Polym. Bull.* **1999**, *43*, 135–142.

(29) Holder, E.; Meier, M. A. R.; Marin, V.; Schubert, U. S. *J. Polym. Sci., Part A: Polym. Chem* **.2003**, *41*, 3954 –3964.

(30) Tadokoro, M.; Kanno, H.; Kitajima, T.; Shimada-Umemoto, H.; Nakanishi, N.; Isobe, K.; Nakasuji, K. *Proc. Nat. Acad. Sci.* **2002**, *99*, 4950-4955.

(31) Bard, A. J.; Gao, F. G. *J. Am. Chem. Soc.* **2000**, *122*, 7426-7427.

(32) Balzani, V.; Juris, A. *Coord. Chem. Rev* **2001**, *211*, 97–115.

(33) Micheletto, R.; Yoshimatsu, N.; Yokokawa, M.; An, T.; Lee, H.; Okazaki, S. *Opt. Commun.* **2001**, *196*, 47-53.

(34) Schubert, U. S.; Eschbaumer, C. *Angew. Chem. Int. Ed.* **2002**, *41*, 2892-2926.

(35) Schultze, X.; Serin, J.; Adronov, A.; Fréchet, J. M. J. *Chem. Commun* **2001**, 1160–1161.

(36) Johnson, R. M.; Corbin, P. S.; Ng, C.; Fraser, C. L. *Macromolecules* **2000**, *33*, 7404-7412.

(37) Nguyen, S. T.; Grubbs, R. H. *J. Am. Chem. Soc.* **1993**, *115*, 9858-9859.

(38) Nguyen, S. T.; Johnson, L. K.; Grubbs, R. H. *J. Am. Chem. Soc.* **1992**, *114*, 3974-3975.

(39) Kanaoka, S.; Grubbs, R. H. *Macromolecules* **1995**, *28*, 4707-4713.

(40) Schwab, P.; France, M. B.; Ziller, J. W.; Grubbs, R. H. *Angew. Chem. Int. Ed. Engl.* **1995**, *34*, 2039-2041.

(41) Kroll, R.; Eschbaumer, C.; Schubert, U. S.; Buchmeiser, M. R.; Wurst, K. *Macromol. Chem. Phys.* **2001**, *202*, 645–653.

(42) Ennis, P. M.; Kelly, J. M.; O'Connell, C. M. *J. Chem. Soc., Dalton Trans.* **1986**, *11*.

(43) Garber, T.; Wallendael, S.; Rillema, D. P.; Kirk, M.; Hatfield, W. E.; Welch, J. H.; Singhi, P. *Inorg. Chem.* **1990**, *29*, 2863-2868.

(44) Newkome, G. R.; Patri, A. K.; Holder, E.; Schubert, U. S. *Eur. J. Org. Chem* **2004**, 235-254.

(45) Jacobine, A. F.; Glaser, D. M.; Nakos, S. T. *Polym. Mater. Sci. Eng.* **1989**, *60*, 211-216.

(46) Manning, D. D.; Strong, L. E.; Hu, X.; Beck, P. J.; Kiessling, L. L. *Tetrahedron* **1997**, *53*, 11937-11952.

(47) Evans, I. P.; Spencer, A.; Wilkinson, G. *J. Chem. Soc., Dalton Trans.* **1973**, 204.

(48) Sullivan, B. P.; Salmon, D. J.; Meyer, T. J. *Inorg. Chem.* **1977**, *17*, 3334.

(49) Bielawski, C. W.; Grubbs, R. H. *Angew. Chem. Int. Ed.* **2000**, *39*, 2903-2906.

(50) Courchay, F. C.; Sworen, J. C.; Wagener, K. B. *Macromolecules* **2003**, *36*, 8231-8239.

(51) Sanford, M. S.; Ulman, M.; Grubbs, R. H. *J. Am. Chem. Soc.* **2001**, *123*, 749-750.

(52) Meier, M. A. R.; Lohmeijer, B. G. G.; Schubert, U. S. *Macromol. Rapid Commun.* **2003**, *24*, 852–857.

CHAPTER 4

FUNCTIONALIZATION OF GUAR AND SUBSEQUENT CROSS-LINKING *VIA* TRANSITION-METAL ION CHELATION

4.1 Abstract

This chapter describes the functionalization of guar, a naturally occurring polysaccharide, with metal-chelating ligands based on 2,2'-bipyridine, in varying ratios. The modified guar was dissolved in water and subsequently cross-linked via addition of various aqueous transition metal salt solutions such as iron(II) sulfate, copper(II) chloride, ruthenium(II) chloride, and cobalt(II) chloride. The resulting cross-linked mixtures experienced viscosity increases that varied with choice of metal as well as bipyridine density.

4.2 Introduction

This work resulted from a collaborative effort with an industrial sponsor, and addresses the main hypothesis of this thesis by exploring both the functionalization of a naturally occurring macromolecule with chelating ligands, and the subsequent behavior of this material in the presence of metal cations. This strategy represents the method of "post-polymerization functionalization" since a large polysaccharide is chosen as the model for the polymer to functionalize.

The specific type of ligands presented in this work (2,2'-bipyridine) enable the material to cross-link and build viscosity in aqueous media when a metal ion is introduced, which is an industrially useful and desirable quality for aqueous polymer systems. Polymeric networks and gels formed by non-covalent interactions have been reported previously.[1-7] Although cross-linked and gelled materials have presented many

useful properties and applications, transition metal-ligand bonds have rarely been employed in terms of the design and construction of these materials, despite their frequent involvement in the arena of coordination polymers in crystal engineering. Reports on the pH dependant equilibrium between borate-based cross-linkers and polysaccharides are being currently investigated,[8-10] with promising results. However, these systems consist of rapidly exchanging, equilibrium-based interactions that remain somewhat ill defined due to the plethora of available hydroxyl groups on macromolecules of interest such as the large family of polysaccharides.

Guar is a polysaccharide with a molecular weight of ca. 1000 kD.[8] Structurally, guar consists of a poly(mannose) backbone, with galactose side-chains in a ratio of approximately 1.6:1 mannose to galactose (Figure 4.1). Thus, a simple calculation suggests that there are on average 7000 mannose repeat units per guar molecule.

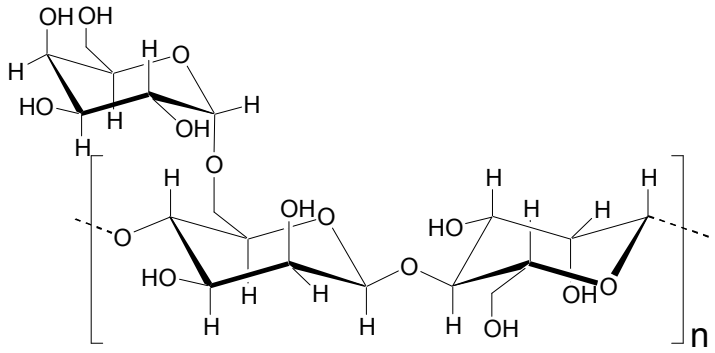

Figure 4.1. Schematic of guar, a poly(galactomannan).

This chapter describes the first time that a naturally occurring polysaccharide such as guar has been derivatized with a chelating ligand for the purpose of network formation via addition of a transition metal salt. A versatile ligand, 2,2'-bipyridine, was chosen since it has a medium to high affinity for a large number of transition metals. This led to cross-linkers that were transition-metal cations that could be introduced to a solution of the modified guar as aqueous solutions of the various metal salts. The transition metal salts chosen for the cross-linkers were $Fe(SO_4)_2$, $RuCl_3$, $CoCl_2$, and $CuCl_2$. Through functionalization of guar with various amounts of the 2,2'-bipyridine ligand, followed by

addition of cross-linker solution, a highly viscous cross-linked polymer network was created.

4.3 Project Design

Guar is essentially a polyhexose-based macromolecule whose periphery is virtually covered with primary and secondary hydroxyl groups. Once the challenge of thoroughly drying this polysaccharide is achieved, these hydroxyl groups are ideally suited for functionalization by an electrophilic unit such as an acyl chloride or an acid anhydride. This functionalization strategy was utilized by converting the 2'2-bipyridine ligand into a diacid chloride and reacting it with previously dried guar in various ratios so as to explore the effects of cross-linking density on the viscosity behavior of guar. Additionally, the use of a variety of metal cations allowed the strength of the cross-linking interactions to be monitored as well.

In order to modify the guar with metal coordination sites, portions of acyl chloride-modified 2,2'-bipyridine were added in the following ratios: (bpy:mannose % loading in parentheses) 1:3 (33%), 1:10 (10%), 1:50 (2%), 1:100 (1%), and 1:500 (0.2%).

Once the guar has been functionalized, it was cross-linked by addition of an aqueous solution containing a transition metal salt. These salts thus act directly as the cross-linking agents via multiple metal ion chelation or sequestration by the modified macromolecules. By using a variety of different transition metal salts, a range of binding strengths can be achieved, based on the analogous to the previously measured binding affinity of the small molecule analogues; i.e. complexes of the type $M(bpy)_x(L)_y$.

4.4 Results and Discussion Section

4.4.1 Ligand Modification

In order to minimize steric crowding in the vicinity of the coordination site, para-methylated 2,2'-bipicoline (4,4'-dimethyl-2,2'-bipyridine) was chosen as starting

material, rather than 2,2'-bipyridine itself, since methylation of 2,2'-bipyridine using reagents such as methyl lithium typically prefers substitution in the ortho- position over the para- position.[11] Methyl groups at the para- position of a pyridine ring are susceptible to strong oxidation conditions. Thus, following a literature procedure based on Jones' conditions, 2,2'-bipicoline was dissolved in concentrated sulfuric acid, and added CrO_3 to oxidize the methyl groups (Scheme 4.1).[12]

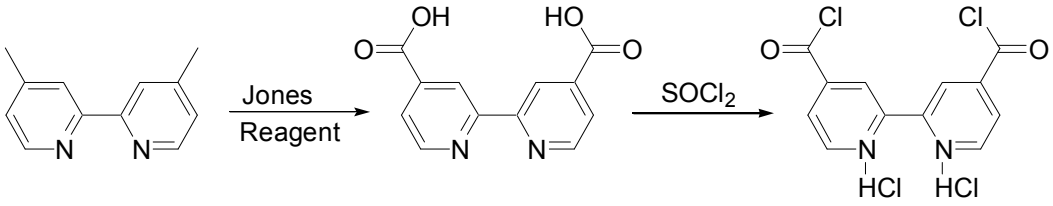

Scheme 4.1. Oxidation of 4,4'-dimethyl-2,2'-bipyridine using Jones' reagent.

Purification yielded the desired di-carboxylic acid in 77 % yield. Subsequent refluxing of this white solid in thionyl chloride for three hours provided the diacid chloride as a tan solid in the form of the dihydrochloride salt.

4.4.2 Functionalization of Guar

Guar, as with any poly-ol, must be thoroughly dry in order to effectively react with acyl chlorides so as to avoid re-hydrolysis of the acyl chloride back to the carboxylic acid. In order to dry the guar, the material was suspended it in toluene in a flask equipped with a Dean-Stark trap, and refluxed the mixture for two days. After draining of the collected water, anhydrous calcium chloride was added to the trap and refluxing was continued for an additional day, the toluene was distilled off, and the dried guar powder was put under vacuum (50 mTorr) overnight to remove any residual toluene.

The dried guar was stirred in dry dioxane, in which it was slightly soluble. To this mixture was added the ligand [2,2']bipyridinyl-4,4'-dicarbonyl dichloride and excess dry triethylamine. Five reactions were simultaneously conducted – the first with a mannose:ligand ratio of 3:1, corresponding to a ligand loading of 33% (numerical

average based on number of repeat units in the backbone). The other four reactions had mannose:ligand ratios of 10:1 (10%), 50:1 (2%), 100:1 (1%), and 500:1 (0.2%). The reactions were stirred overnight after which aliquots were taken from the completed reactions to be used directly in the following cross-linking step. The guar functionalization reactions were conducted in dioxane at an approximate concentration of 64 mg/mL (Scheme 4.2)

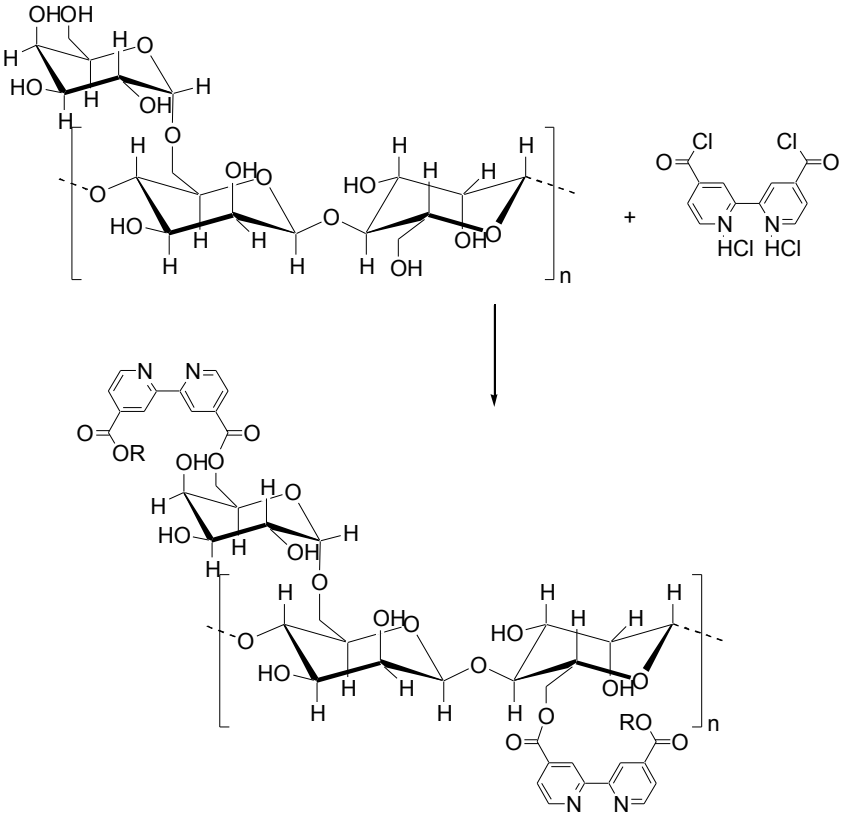

Scheme 4.2. Modification of guar with 2,2'-bipyridinyl-4,4'-dicarbonyl chloride dihydrochloride.

Contrary to previous reports of hydrophobically modified polymers,[13,14] the hydrophobic modification imparted on the guar matrix by introduction of the bipyridine units had little to no effect on the solution viscosity, prior to addition of the metal salt, once the pH of the solution had been adjusted to approximately 4.5 to 5.0.

4.4.3 Cross-linking of Guar Using Transition Metal Cations

The degree of cross-linking can vary depending both on the degree of ligand loading onto the guar, as well as the amount of metal cation present. Since the same amount of metal salt was added in each case relative to the ligand loading, the cross-linking was dependant upon the degree of loading, for each metal-ligand system. Depending on the degree of cross-linking, the modified guar can exhibit several different behaviors. For example, if there is very little cross-linking there might be no observable change in the macroscopic properties of the solution, such as viscosity, etc. However, once the cross-linking grows to an appreciable amount, the solution would be expected to thicken substantially. Continuing this progression and using an increasingly higher ligand loading should lead to full gellation, where very little to no fluid behavior is observed when a beaker of the material is inverted. The final stage of this progression leads to immediate gellation to a solid mass that expels water in a matter of seconds giving a clear solution containing a solid mass either floating of at the bottom of the flask resulting from what was recognized as "over cross-linking" within the specifications of these experiments. The optimal cross-linking behavior was that which was observed when there is gellation, but the material exhibits a pseudo-flowing characteristic that has become to be known as "lipping" – during this state, the material can flow about half way out of a flask, and stop, hanging suspended until the flask is turned further. This condition was the desired outcome for these cross-linking experiments, and comprised a qualitative, macroscopic method of determining the amount of cross-linking.

Once the guar was functionalized with the appropriate ratios of ligand, the samples were diluted into water in order to adjust the concentrations to 4.8 mg/mL. However, the derivatized guar did not dissolve in the aqueous solution until the pH was lowered to <5, which was accompanied by a color change from tan to light pink, and an increase in apparent solution viscosity. The dissolved guar solutions were stirred for one hour in order to fully dissolve the guar. Then a solution of 0.5 equivalents of metal salt (with

respect to ligand) in water was added and stirred for one hour in order to cross-link the guar. After one hour, there were no observable changes to the solution, so an additional 0.5 equivalents was added and stirred again for another hour, again showing no change in color or viscosity. At this point, the pH of the mixture was raised to approximately 10 by addition of a concentrated aqueous solution of sodium hydroxide. This change in pH triggered an immediate cross-linking reaction, suggesting that the same ligand-protonation reaction that facilitated the dissolution of the guar initially was responsible for blocking the coordination sites. Raising the pH was required in order to free up the chelating sites of the ligand, resulting in immediate sequestration of the surrounding metal cations, and the corresponding cross-linking of the guar directly followed (Figure 4.2).

Figure 4.2. Demonstration of "lipping" phenomena: Solution of guar (bpy/mannose ratio of 1:100), in the presence of RuCl3, and shaking for 10 seconds produces full gellation.

The thickness of the resulting solutions varied depending on both the ligand density as well as the choice of transition metal salt used (Figure 4.3).

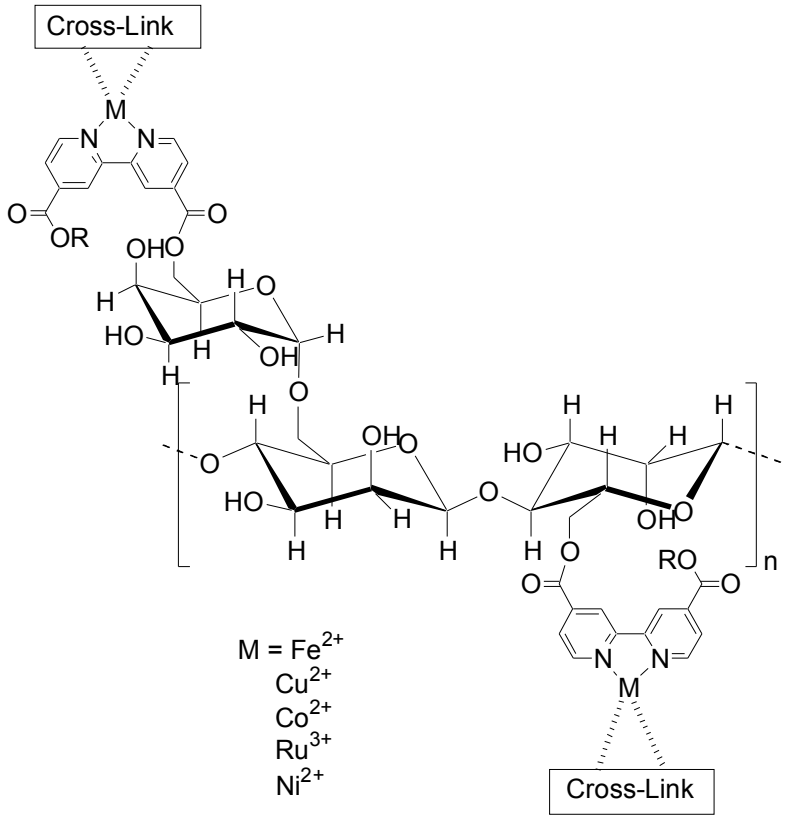

Figure 4.3. Cross-linking of modified guar via transition metal ion chelation.

4.5 Experimental Section

Synthesis of 2,2'-bipyridinyl-4,4'-dicarboxylic acid (1)

One gram (5.43 mmol) of 4,4'-dimethyl-2,2'-bipyridine was dissolved in 40 mL of concentrated sulfuric acid. The solution was cooled to 0 ^{o}C, and 3.3 g of CrO_3 was added slowly, forming a yellow solution. The solution was stirred for two days, after which the solution had turned dark green. The green solution was poured into ice water, forming a green precipitate that was filtered off and washed with water. This precipitate was then suspended in 50 mL of water, and a 10 M solution of potassium hydroxide was added until the solution was basic (ca. pH > 8). The solution was filtered, and the filtrate was acidified using HCl which precipitated the product as a white solid, which was washed

with water, methanol, and ether, and then dried to yield1.017 g (4.16 mmol, 77% yield) of **1**.

Synthesis of 2,2'-bipyridinyl-4,4'-dicarbonyl dichloride (2)

A solution of 1.017 g of 1 in thionyl chloride was refluxed for three hours. The excess thionyl chloride was then distilled off and the remaining orange – tan solid was dried under vacuum (20 mTorr) for three hours to completely remove the residual thionyl chloride. The product was then used immediately without further purification.

Derivatization of guar with 2,2'-bipyridinyl-4,4'-dicarbonyl dichloride (3a-e)

In five separate flasks, dried guar (958 mg per flask, approx. 3.7 mmol mannose content) was stirred in dry dioxane (15 mL), and 2 mL (27 mmol, 7x excess) of triethylamine was added to each vial. Appropriate portions of a 0.59 M solution of 2,2'-bipyridinyl-4,4'-dicarbonyl dichloride in dioxane (**3a**: 2.1 mL; **3b**: 0.6 mL; **3c**: 0.13 mL; **3d**: 63 μL; **3e**: 13 μL) were added to the guar mixtures slowly, and allowed to stir for 8 hours. The solutions were removed from stirring, and aliquots were used directly in the following step.

Cross-linking of Functionalized Guar

A 0.48% solution of derivatized guar was prepared by dissolving 0.5 mL of the solution from the previous step in 9.5 mL of water. The pH was adjusted to 4.5 by addition of HCl to solubilize the guar, causing the color to change to light pink and the solution to thicken. Then a solution of a transition metal salt ($FeSO_4$, $CuCl_2$, $CoCl_2$, or $RuCl_3$) in water was added and the vial was shaken for one minute. The pH was then adjusted to

approximately 10 by addition of 5 M sodium hydroxide, and the vial was shaken again for 10-15 seconds and allowed to sit for an additional five minutes.

4.6 Conclusion

This work has demonstrated the functionalization of guar with the ligand 2,2'-bipyridine, as well as cross-linking of this derivatized guar by addition of transition metal salts, resulting in solutions that were highly viscous compared with those of the un-cross-linked guar. An important aspect of the hypothesis of this thesis was tested in this work in that the polymerization step was circumvented so that the materials functionalization via metal coordination could be focused on specifically, both at a low cost, and a high yield. The strategy that was followed in this work consisted purely of direct polymer functionalization, instead of monomer functionalization, fitting entirely into what was described in Chapter 1 as "Strategy 2", or "post-polymerization functionalization." As a result, in order to achieve the desired results of high viscosity, while still maintaining some control over the methodology, two discreet post-polymerization steps were employed: (1) covalent functionalization using the modified bipyridine ligands, and (2) metal coordination and chelation of transition metal ions by these ligands to form the networks. This two-step process enables a wide array of possible motifs for cross-linking, via various metal-ligand combinations and ratios, and as stated in Chapters 1 and 2 of this thesis, it is indeed very often that multiple tiers of functionalization are ultimately required for better control over the polymeric system at hand. Just as Nature rarely, if ever, exhibits a single self-assembly or functionalization step, attempts at mimicking this theme in the lab continue to prove that if a high degree of control is desired, the synergistic strategy of multiple functionalization techniques are a promising path to take.

4.7 References

(1) Montembault, A.; Viton, C.; Domard, A. *Biomacromolecules* **2005**, *6*, 653-662.

(2) R. Cortesi; C. Nastruzzi; Davis, S. S. *Biomater.* **1998**, *19*, 1641-1649.

(3) Xing, B.; Choi, M.-F.; Xu, B. *Chem. Eur. J.* **2002**, *8*, 5028-5032.

(4) Xing, B.; Choi, M.-F.; Xu, B. *Chem. Commun.* **2002**, 362-363.

(5) Capitani, D.; Crescenzi, V.; De Angelis, A. A.; Segre, A. L. *Macromolecules* **2001**, *34*, 4136-4144.

(6) Carlucci, L.; Ciani, G.; Proserpio, D. M.; Sironi, A. *J. Chem. Soc., Dalton Trans.* **1997**, 1801-1803.

(7) Lewis, A. L.; Miller, J. D. *Polymer* **1993**, *34*, 2453-7.

(8) Bishop, M.; Shahid, N.; Yang, J.; Barron, A. R. *J. Chem. Soc., Dalton Trans.* **2004**, 2621-2634.

(9) Adams, H.; Batten, S. R.; Davies, G. M.; Duriska, M. B.; Jeffery, J. C.; Jensen, P.; Lu, J.; Motson, G. R.; Coles, S. J.; Hursthouse, M. B.; Ward, M. D. *J. Chem. Soc., Dalton Trans.* **2005**, 1910-1923.

(10) Schubert, D. M.; Alam, F.; Visi, M. Z.; Knobler, C. B. *Chem. Mater.* **2003**, *15*, 866-871.

(11) Carlise, J. R.; Weck, M. *J. Polym. Sci. Part. A: Polym. Chem.* **2004**, *42*, 2973-2984.

(12) Garelli, N.; Vierling, P. *J. Org. Chem.* **1992**, *57*, 3046-3051.

(13) Cram, S. L.; Brown, H. R.; Spinks, G. M.; Hourdet, D.; Creton, C. *Macromolecules* **2005**, *38*, 2981-2989.

(14) Liaw, D.-J.; Chen, T.-P.; Huang, C.-C. *Macromolecules* **2005**, *38*, 3533-3538.

CHAPTER 5

PHOSPHORESCENT SIDE-CHAIN FUNCTIONALIZED POLY(NORBORNENE)S CONTAINING IRIDIUM COMPLEXES

5.1 Abstract

Norbornenes containing phosphorescent iridium complexes based on $Ir(ppy)_3$ and $Ir(ppy)_2(bpy)(PF_6)$ were synthesized and copolymerized with alkyl-norbornenes via ring-opening metathesis polymerization in nonpolar solvents using ruthenium initiators. The luminescent properties of the resulting polymers both in solution and in the solid state were tested. The polymers were found to retain the optical properties of the phosphorescent small molecule analogues with emissions maxima in the yellow/green, quantum yields from 0.23 to 0.24 for $Ir(ppy)_2(bpy)(PF_6)$ analogues, 0.02 to 0.03 for *mer*-$Ir(ppy)_3$ analogues, 0.20 to 0.24 for *fac*-$Ir(ppy)_3$ analogues, and lifetimes of 0.41 to 0.55 μs for $Ir(ppy)_2(bpy)(PF_6)$ analogues, 0.22 to 0.62 μs for *mer*-$Ir(ppy)_3$ analogues, 1.28 to 1.48 μs for *fac*-$Ir(ppy)_3$ analogues. By combining the phosphorescent properties of these emissive molecules with the solution processability and ease of synthesis of polynorbornene backbones, these materials might be highly useful in the field of light-emitting devices and emissive display technology.

5.2 Introduction

A major advantage to using metal coordination to functionalize polymeric materials is that quite often the metal complexes created via the functionalization of the macromolecule exhibit interesting properties themselves, such as magnetism, light-emission, redox properties, and catalytic abilities. Based on the promising results described in Chapter 3 regarding solution stability, retention of photophysical properties,

and polymerizability using a variety of ROMP catalysts, it was advantageous to expand the concept to focus implicitly upon incorporating the properties of the newly formed complex into the resulting material, rather than simply using metal coordination to tether another group to a polymer. The hypothesis presented in this thesis is addressed fully in this chapter, by using metal coordination to add functionality to a polymer that is created via a living polymerization process, that ultimately will be useful in materials applications such as OLEDs, etc.

Phosphorescent coordination complexes, including the class of iridium compounds described in this chapter, already feature prominently in various materials and devices as the emissive species, as a result of their high quantum efficiencies and strong photo- and electroluminescence.[1-4] In current device technologies, the luminescent molecules are either vacuum deposited as low molecular weight compounds or doped into a polymeric matrix,[1,5-10] requiring lengthy and expensive fabrication of devices,[11] as well as introducing the possibility of phase separation during processing. In order to simplify this fabrication process, recent efforts have been aimed at direct incorporation of the emissive species, via covalent attachment, to a solution-processable polymer backbone.[12] Examples to date include the attachment to poly(dimethyl siloxane)s, poly(fluorene)s, and poly(styrene)s, showing promising results in areas such as solution processing and sensor technology.[13-17] To meet the needs of the rapidly expanding scope of applications that have been suggested for polymer-supported, highly emissive phosphorescent complexes, further optimization is necessary. This includes synthesizing increasingly robust and durable, yet easily modifiable polymeric scaffolds in order to facilitate the tuning of materials. Ring-opening metathesis polymerization (ROMP), as described earlier in Chapter 3, has been shown to fulfill these criteria.[18]

This work demonstrates the synthesis of phosphorescent iridium complexes covalently bound to norbornene, the homo- and co- polymerization of these monomers, and finally the persistent adherence of the luminescence activity to the known values of

the small molecule analogs throughout the entire process for both the polymers in solution as well as in the solid state.

5.3 Monomer Design

Monomers were designed based on choice of phosphorescent complex as well as durability and ease of synthesis. All monomers were synthesized in three steps or less from commercially available starting materials. The emissive complex is attached to the polymerizable unit by a short alkyl linker to a norbornenyl ester which has been shown to be highly stable under a variety of conditions.[22] To investigate the optical effects on the properties of the resulting polymers, both a charged monomer and a neutral monomer are included in this study, as well as an alkyl-chain based monomer that can serve to space out the luminescent inorganic complexes and aid polymer solubility (Figure 5.1).

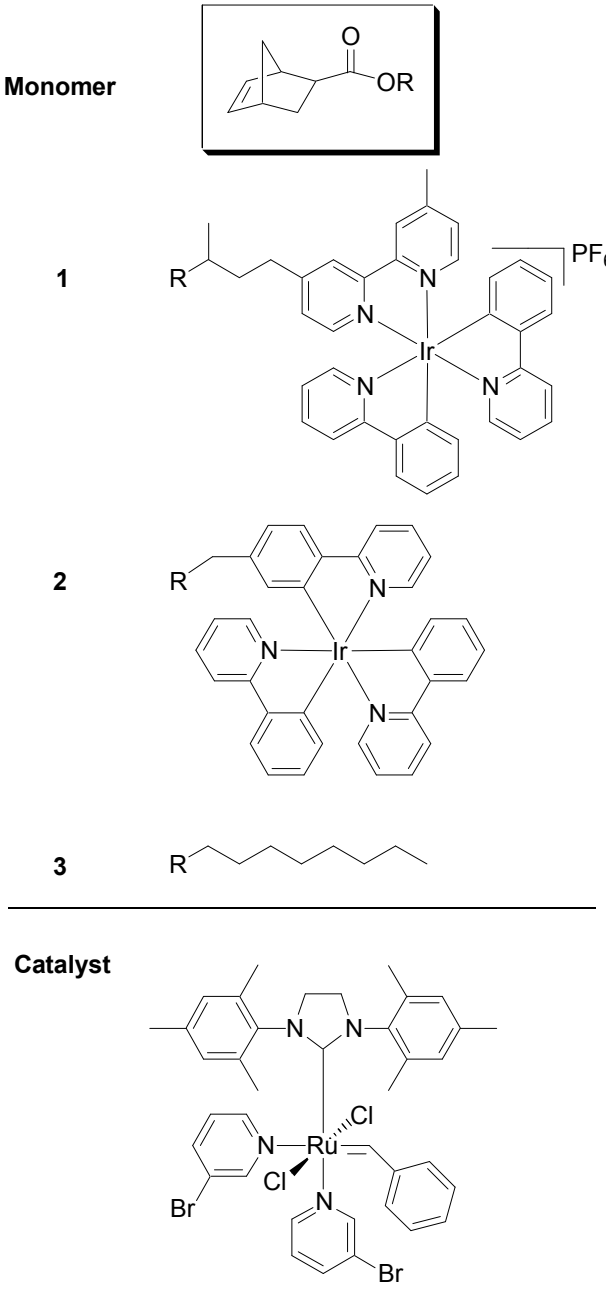

Figure 5.1. Top: Monomers employed in this study: **1**, bpy-based, charged iridium complex; **2**, ppy-based, neutral iridium complex; **3**, alkyl spacer-based monomer. Bottom: Grubbs' 3rd generation catalyst.

5.4 Monomer Synthesis

Monomers **1**, **2**, and **3** were readily synthesized in three steps or less in overall good yields. The synthesis of monomer **1** started with the treatment of commercially available

4,4'-dimethyl-2,2'-dipyridyl (dMbpy) with one equivalent of lithium diisopropylamide (LDA), followed by the addition of one equivalent of propylene oxide, to give compound **4** in 73 % yield. Ring-opening addition of the propylene oxide to form **4** occurred exclusively by the attack of the dMbpy anion on the less substituted carbon of the epoxide. No attack onto the more substituted carbon was detected. Compound **4** was esterified with *exo*-5-norbornene-2-carboxylic acid, using dicyclohexylcarbodiimide (DCC) and a catalytic amount of dimethylamino pyridine (DMAP) to afford compound **5** in 42 % yield. In a modification to a previously published procedure,[10] **5** was then combined with $[Ir(ppy)_2Cl]_2$ at 150 ^oC in ethylene glycol, followed by the addition of NH_4PF_6(aq) to provide iridium-containing monomer **1** in 72 % yield (Scheme 5.1).

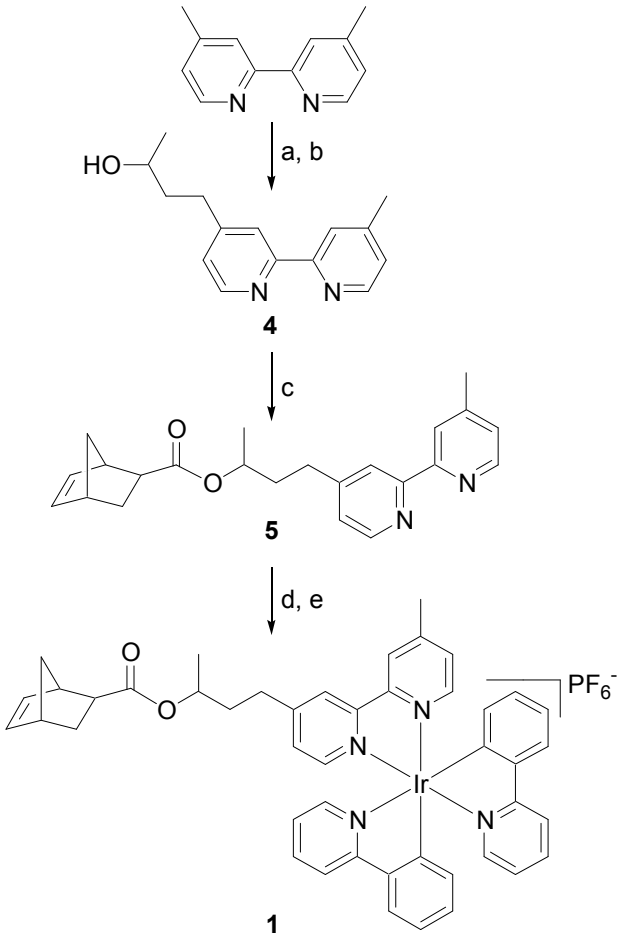

Scheme 5.1. Synthesis of **1**: a.) Lithium diisopropylamide, THF, -78 ^{o}C; b.) propylene oxide, THF, 0 ^{o}C, 73%; c.) *exo*-5-norbornene-2-carboxylic acid, DCC, DMAP, CH_2Cl_2, 42%; d.) $[Ir(ppy)_2Cl]_2$, ethylene glycol, 150 ^{o}C, 72 %; e.) NH_4PF_6 (aq.).

Commercially available 4-(2-pyridine)benzaldehyde was reduced with $LiAlH_4$ to give the corresponding alcohol **6** in 94 % yield, which was then esterified with *exo*-5-norbornene-2-carboxylic acid using DCC/DMAP, as described for **1**, to give compound **7** in 80 % yield. Simultaneously, $[Ir(ppy)_2Cl]_2$ was treated with silver trifluoromethane sulfonate (AgOTf) to transform the chloro-complex into the more labile iridium triflate species which is the precursor for the meridional coordination with a third ppy-type ligand. The resulting triflate complex was treated with **7** in acetone at room temperature

overnight to give the meridionally oriented iridium-containing monomer *mer*-**2** in 43% yield (Scheme 5.2).[23]

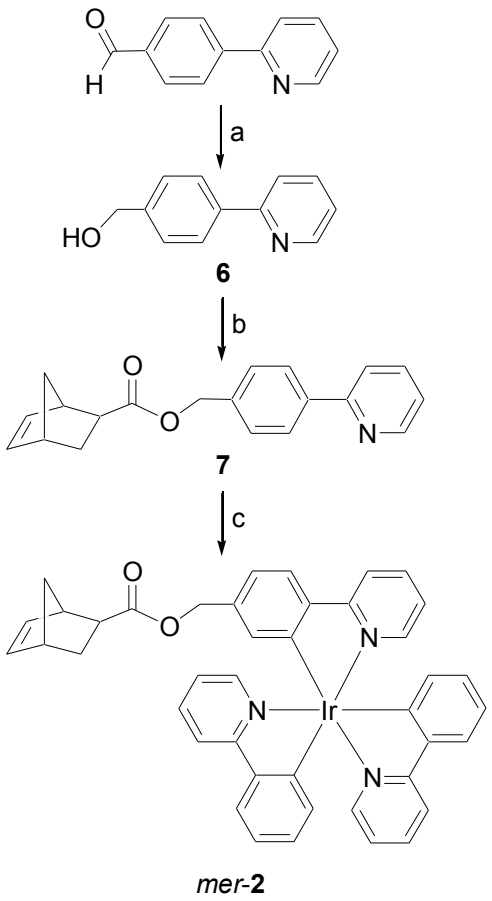

Scheme 5.2. Synthesis of *mer*-**2**: a.) Lithium aluminum hydride, THF, 94%; b.) *exo*-5-norbornene-2-carboxylic acid, DCC, DMAP (cat.), CH_2Cl_2, 80%; c.) $[Ir(ppy)_2OTf]_2$, acetone, ambient temp., 43 %.

Monomer *fac*-**2** was obtained by the reduction of the previously reported formylphenyl-substituted iridium complex $Ir(ppy)_2fppy$[5] with $LiAlH_4$ to give compound **8**, *fac*-$Ir(ppy)_2(hmppy)$ (hmppy = hydroxymethyl-ppy) that contains a single hydroxymethyl group as a chemical handle. Esterification with *exo*-5-norbornene-2-carboxylic acid using DMAP and DCC yielded the facially oriented monomer **2** in 40 % yield (Scheme 5.3).

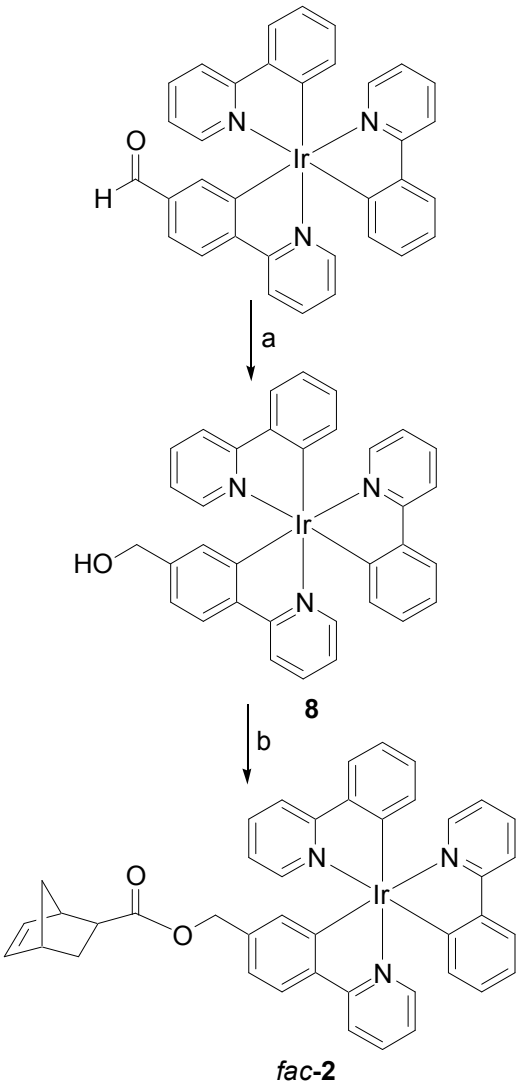

Scheme 5.3. Synthesis of *fac*-**2**: a.) Lithium aluminum hydride, THF, 99%; b.) *exo*-5-norbornene-2-carboxylic acid, DCC, DMAP, THF, 40%.

The yield-limiting step is the facial coordination of the ligands onto the iridium metal center. This step occurs typically in less than 30 % whereas meridional orientation can be achieved in yields as high as 70 %.[23] Monomer **3** was obtained as described in the literature.[24]

5.5 Polymerization

Homo- and co-polymerizations were carried out using a standard protocol for all monomers. Monomers **1** and **2** were homo- and copolymerized with **3** in various ratios in

dichloromethane and precipitated into either diethyl ether or methanol. All polymerizations were complete within 2-3 minutes, using Grubbs' 3rd generation benzyldine initiator as the ROMP catalyst (Figure 1).[25] The target degree of polymerization was 50 for poly- **1** and poly-**2** and all copolymers, and copolymer ratios consisted of both 20:1 and 2:1 for the mixtures of both monomers **3**:**1** and **3**:**2** (Figure 5.2).

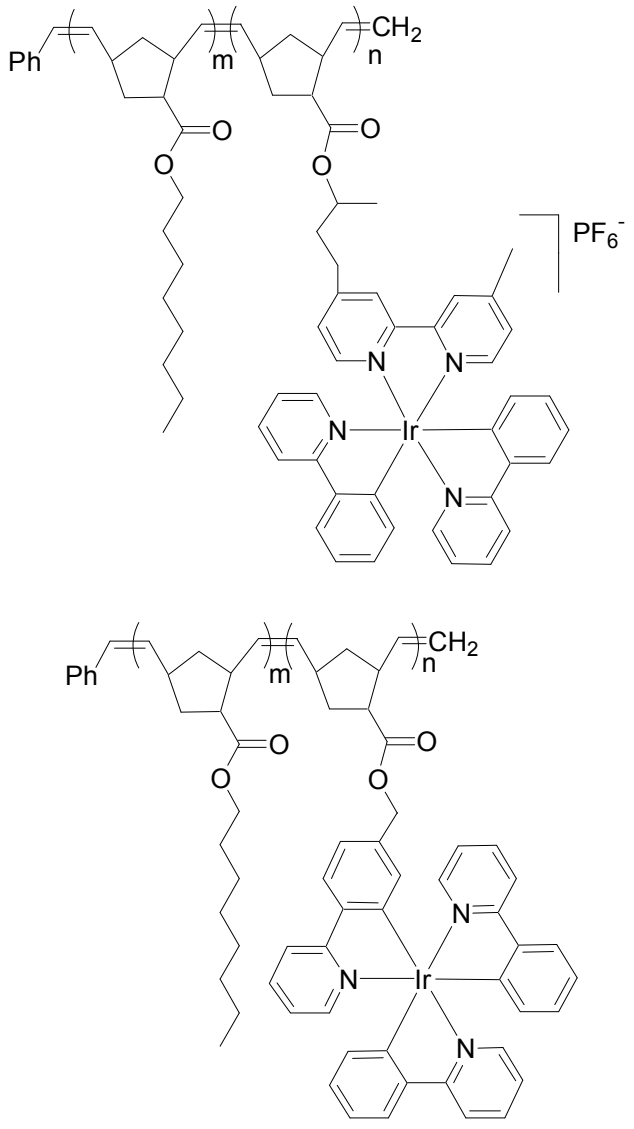

Figure 5.2. Copolymers poly-**1**-*co*-**3** (top) and poly-**2**-*co*-**3** (bottom).

Poly-**1** and poly-*mer*-**2**, in contrast to previously published homopolymers that contain charged transition metal-complexes on every repeating unit,[19-21] were fully

soluble in dichloromethane without the aid of alkyl spacers or alkylated ligands. In contrast, poly-*fac*-**2** precipitated out during the polymerization and could not be re-dissolved in any organic solvent. Monomer **3** was thus employed in this study both as a means of controlling the chromophore density in the solid state, as well as an aid to polymer solubility.

Although all homopolymers of **1**, *mer*-**2**, and **3**[24] are fully soluble in dichloromethane, dichloromethane solutions of poly-**1** or poly-**2** when mixed with a solution of poly-**3**, would either become turbid, or cause full precipitation of the iridium-containing polymers from solution. This is consistent with observations in the literature that polymers containing metal complexes are often insoluble in strongly non-polar environments,[26] although it is also possible that precipitation may have instead been caused by formation of polymer aggregates. However, attempts at block copolymerizations of **3** with either **1** or **2** caused the same phenomena, i.e. a 50-fold excess of monomer **3** was added to a homogeneous solution of short chain polymer (~20 mer, catalyst was still fully initiated and living as observed via ^{1}H NMR of the carbene signal) of **1** or **2**, and upon addition of this second portion of monomer, turbidity or precipitation occurred instantly. Both poly-**1** as well as poly-**2** also precipitate quickly in hexanes or diethyl ether, giving the same result as addition of an excess of alkyl monomer **3**. Copolymers of **1** or **2** with **3** only remained fully soluble when they were copolymerized in a random fashion. Therefore, although the rates of polymerization with the catalyst employed are very fast, the observed solubility of the copolymers, suggests a random nature for the copolymers used in this system.

Gel-permeation chromatography (GPC) was employed for all polymers (Table 5.1).

Table 5.1. Polymer characterization data.

Polymer	M_n	M_w	PDI	T_g, °C	T_d, °C
poly-**1**	31,000	43,100	1.39	--	330
poly-**1**-*co*-**3** (1:2)	11,200	19,300	1.71	10	339
poly-**1**-*co*-**3** (1:20)	18,500	47,000	2.55	--	347
poly-*mer*-**2**	--	--	--	--	248
poly-*mer*-**2**-*co*-**3** (1:2)	--	--	--	-43	298
poly-*mer*-**2**-*co*-**3** (1:20)	--	--	--	--	336
poly-*fac*-**2**	--	--	--	--	--
poly-*fac*-**2**-*co*-**3** (1:2)	26,300	30,500	1.16	-53	358
poly-*fac*-**2**-*co*-**3** (1:20)	44,100	54,300	1.23	-44	374

All GPC traces of poly-*mer*-**2** were multimodal, showing approximately the same elution times as their *fac*-counterparts, but in all cases for poly-*mer*-**2** and copolymers there were two highly overlapping, non-baseline resolved signals. Therefore, while clearly polymers were formed, it was not possible to determine molecular weights and polydispersities. The fact that all polymers eluted fully to give baseline-resolved mono- or multi- modal signals was unexpected, as it is commonly known for most charged metal-containing polymers that if any sample comes through the columns at all the data will likely be entirely undecipherable due to the formation of either aggregates or at least strong interactions of the metal complex with the stationary phase.[27] This problem can be circumvented for polymers containing a single metal complex by doping the mobile phase with ammonium hexafluorophosphate.[27] However, poly-**1** could be fully characterized using GPC in methylene chloride, with no dopant added to the mobile phase, even though every repeat unit contains a charged moiety. The homopolymer poly-**1** showed the lowest polydispersity index (PDI) with 1.39. A PDI of 1.71 was observed for the 1:2 copolymer of **1** with **3**, while a PDI of 2.55 was observed for the 1:20 copolymer. Copolymers of *fac*-**2** with **3** showed more narrow distributions and lower PDI's. The 1:2 copolymer had a PDI of 1.16 and the 1:20 copolymer had a PDI of 1.23.

The insolubility of the homopolymer of *fac*-**2** was unexpected based on the good solubility of poly-mer-**2**. This polymer insolubility may be due to several factors. First, due to the anionic nature of the phenylpyridine ligand, a relatively strong dipole is created in the facial configuration since the anionic carbon bound to the metal exists on the same face of the molecule for all three ligands. In fact, for the small molecule *fac*-$Ir(ppy)_3$, a quite large dipole moment of 6.5 D has been calculated.[28] In the homopolymer, when these complexes are forced to be in close proximity along the backbone, aggregation may occur as a result. Conversely, the meridional configuration has anionic carbons that are trans to each other, canceling out any dipolar effects created by two out of the three ligands. This trans effect also causes lengthening of these carbon-iridium organometallic bonds (2.07-2.08 Å),[29] thus distributing the anionic character of the ligands more evenly around the periphery of the complex while maintaining the positive metal center on the interior. These solubility problems were not observed in the case of the monomer *fac*-**2**, or any of its copolymers with **3**, indicating that the insolubility is directly an effect of restraining these complexes into very close proximity with each other in nonpolar solvents, as is the case with the homopolymer only.

There were no distinct glass transition temperatures observable for any of the homopolymers, as well as the 1:20 copolymers of **3** with **1** or **2**. However, for the 1:20 copolymer of *fac*-**2** with **3**, a glass transition of –44 ^{o}C was observed. The 1:2 copolymers of **3** with **1**, *mer*-**2**, and *fac*-**2** all exhibited distinct T_g values of 10, -43, and –53 ^{o}C, respectively. These values may reflect the differences caused by incorporation of a charged polymer (poly-**1** series) compared with a neutral polymer (*mer*- and *fac*- poly-**2** series). In all cases, the polymers exhibited progressively higher decomposition temperatures as the amount of co-monomer **3** increased.

5.6 Photophysical Properties

The agreement of the luminescent data between the well-studied small phosphorescent iridium complexes and our polymeric material in solution and in the solid state is crucial to the potential development and realization of polymeric OLEDs. In acetonitrile, $Ir(ppy)_2(bpy)(PF_6)$ has been reported to emit strongly at 606 nm,[30] while *tert*-butyl substitution at the bipyridinyl 4- and 4'- positions gives rise to an emission maximum at 581 nm,[10] suggesting that alkylation at the *para*-positions of the bipyridine has a blue-shifting effect on the emissive properties of the complex. An emission maximum of 555 nm was measured for compound **1** (Table 5.2, Figure 5.3), suggesting that the employment of the norbornenyl ester in close proximity to the emissive complex is responsible for the observed change in wavelength.

Table 5.2. Solution photophysical data for compounds **1** - **3** and their corresponding polymers. [*a*, acetonitrile; *b*, dichloromethane; *c*, toluene; *d*, dimethylsulfoxide; *e*, THF, ambient conditions; *f*, THF, degassed; * most samples showed broad absorbance range with no clear local maximum; ** relative to $Ru(bpy)_3(PF_6)_2$]; ‡, lifetimes measured in dichloromethane.]

Complex	λ_{abs}, nm*	λ_{em}, nm	F**	t (ms)[e]	t (ms)[f]
1	--	556[a], 551[b]	0.236[a]	0.145	0.534
poly-**1**‡	--	555[a], 551[b]	0.278[a]	0.207	0.549
poly-**1**-*co*-**3** (1:2)	--	556[a], 552[b]	0.225[a]	0.138	0.413
poly-**1**-*co*-**3** (1:20)	--	557[a], 554[b]	0.238[a]	0.148	0.486
mer-**2**	--	546[a], 543[b], 537[c], 540[d]	0.034[a]	0.049	0.498
mer-poly-**2**	388[a]	519[a], 538[b], 511[c], 545[d]	0.022[a]	0.031	0.619
mer-poly-**2**-*co*-**3** (1:2)	385[a]	517[a], 541[b]	0.025[a]	0.041	0.222
mer-poly-**2**-*co*-**3** (1:20)	385[b]	540[b]	0.022[b]	0.048	0.350
fac-**2**	373[a]	543[a], 515[b]	0.219[a]	0.033	1.48
fac-poly-**2**	--	--	--	--	--
fac-poly-**2**-*co*-**3** (1:2)	293[a], 377[a]	517[a], 515[b]	0.243[b]	0.045	1.28
fac-poly-**2**-*co*-**3** (1:20)	377[b]	514[b]	0.201[b]	0.045	1.43

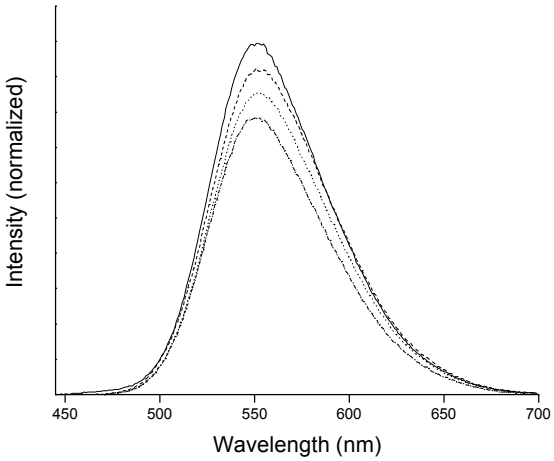

Figure 5.3. Photoluminescence emission spectra of (from top to bottom): **1**, poly-**1**, poly-**1**-*co*-**3** (1:2)**,** poly-**1**-*co*-**3** (1:20) in dichloromethane (ex. 400 nm)**.**

Poly-**1** has an emission maximum of 556 nm, as do all copolymers of **1** with alkyl spacer monomer **3** (Table 2, Figure 3). The emission quantum yield for **1** of 0.236 is nearly identical to previously reported values in the literature of 0.235 for the *tert*-butyl analogue,[10] while the luminescence lifetime for **1** (534 ns) was also similar to the small molecule analogue (557 ns). In the solid state, poly-**1** exhibited an emission at 545 nm for the homopolymer, and 540 nm and 531 nm respectively for the copolymers as incorporation of **3** increased (Table 5.3, Figure 5.4).

Table 5.3. Solid-state photophysical data for all polymers.

Polymer	λ_{em} **(nm)**
1	545
1-*co* -**3** (1:2)	540
1-*co* -**3** (1:20)	531
mer -**2**	550
mer -**2**-*co* -**3** (1:2)	543
mer -**2**-*co* -**3** (1:20)	534
fac -**2**	--
fac -**2**-*co* -**3** (1:2)	521
fac -**2**-*co* -**3** (1:20)	513

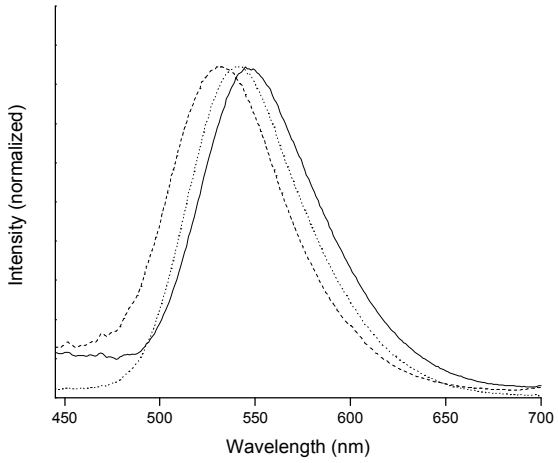

Figure 5.4. Solid-state PL emission spectra of (right to left): poly-**1**, poly-**1**-*co*-**3** (1:2), and poly-**1**-*co*-**3** (1:20) (ex. 400 nm).

This observation is consistent with previously reported trends that show that the emission wavelength is strongly dependent upon the local environment and that a blue shift is observed upon dilution of the luminescent monomer concentration in a copolymer.[10,21,31] Similar shifts in solid-state emission were observed for polymers of both *mer*-**2** (Figure 5.5) and *fac*-**2** (Figure 5.6) as well.

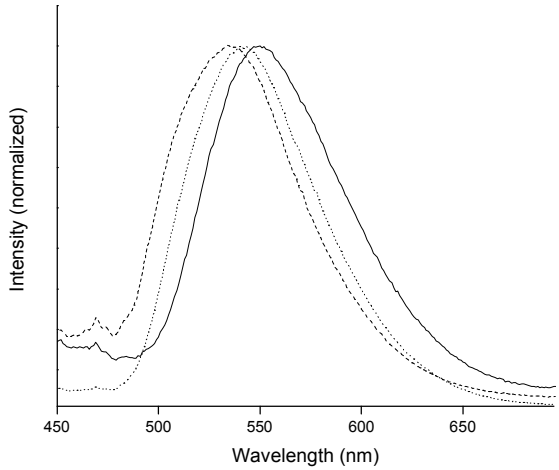

Figure 5.5. Solid-state PL emission spectra of (from right to left): *mer*-poly-**2**, *mer*-poly-**2**-*co*-**3** (1:2)**,** *mer*-poly-**2**-*co*-**3** (1:20) (ex. 380 nm).

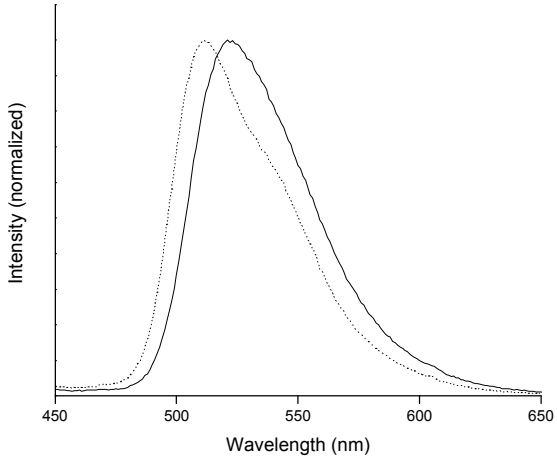

Figure 5.6. Solid-state PL emission spectra of (from right to left): *fac* -poly-**2**-*co*-**3** (1:2)**,** *fac*-poly-**2**-*co*-**3** (1:20) (ex. 380 nm).

It has been well documented that in dichloromethane, at room temperature, *fac*-$Ir(ppy)_3$ emits strongly at 510 nm,[32] with emission quantum yields as high as 0.40, while *mer*-$Ir(ppy)_3$ emits at 512 nm with lower quantum yields of 0.036.[29] This difference in emission quantum yields, brought about by the large discrepancy in non-radiative decay rates (more than an order of magnitude between facial and meridional $Ir(ppy)_3$), lessens significantly as the temperature decreases from 298 ^{o}C to 77 ^{o}C, where both complexes are strongly luminescent.[29] Similar differences were observed in observations of the luminescent intensities of polymers containing *mer*-**2** (Figure 5.7) vs. polymers containing *fac*-**2** (Figure 5.8), in solution as well as in the solid state at room temperature.

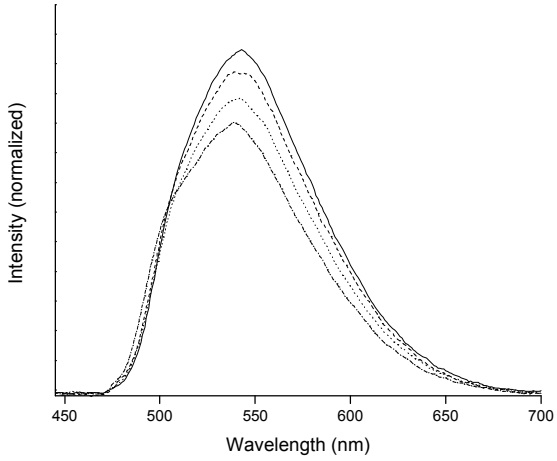

Figure 5.7. Solution PL emission spectrum of (from top to bottom): *mer*-**2**, *mer*-poly-**2**, *mer*-poly-**2**-*co*-**3** (1:2)**,** *mer*-poly-**2**-*co*-**3** (1:20) in dichloromethane (ex. 380 nm).

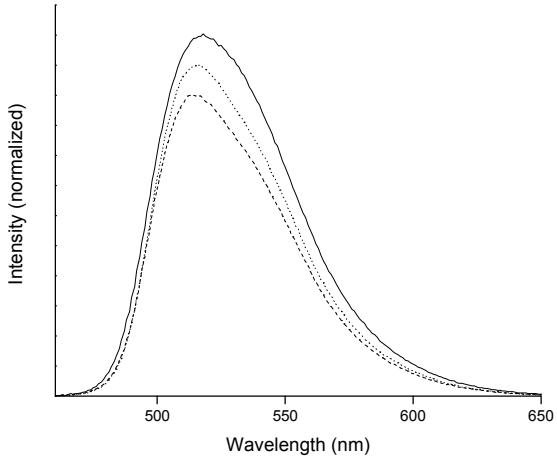

Figure 8. Solution PL emission spectrum of (from top to bottom): *fac*-**2**, *fac*-poly-**2**-*co*-**3** (1:2)**,** *fac*-poly-**2**-*co*-**3** (1:20) in dichloromethane (ex. 380 nm).

In accordance with the aforementioned literature trends, *fac*-**2** was significantly more emissive, with an emission quantum yield of 0.219 in acetonitrile. Copolymers of *fac*-**2** with **3** in a 1:2 ratio and 1:20 ratio gave quantum yields of 0.243 and 0.201 respectively. *Mer*-**2** however, showed a much lower emission quantum yield of 0.034 in acetonitrile.

Both homo- and co-polymers containing this complex showed slightly lower quantum yields of 0.022 to 0.025.

The emission maximum for *mer*-**2** and its polymers in acetonitrile was shifted substantially from that expected from the small molecule analogue *mer*-Ir(ppy)$_3$. The only structural difference between *mer*-**2** and the previously reported *mer*-Ir(ppy)$_3$ complex is the addition of the norbornenyl ester *para* to the pyridine on the phenyl group of one of the ppy ligands, although it is electronically separated from the metal complex by a methylene linkage. Despite the expected insulating effect of the methylene unit, a red shift of the emission wavelength from that reported in the literature for the unsubstituted *mer*-Ir(ppy)$_3$ complex (512 nm) to 543 nm is observed. However, when comparing emission spectra for *mer*-**2** and its polymers in various solvents, it becomes evident that the emission from the *mer* complex is comprised of two different emission maxima, one occurring in the expected range of 510 to 515 nm, and another occurring in the range from 538 to 546 nm. Depending on the choice of solvent, the intensities of each vary with respect to one another (Figure 5.9).

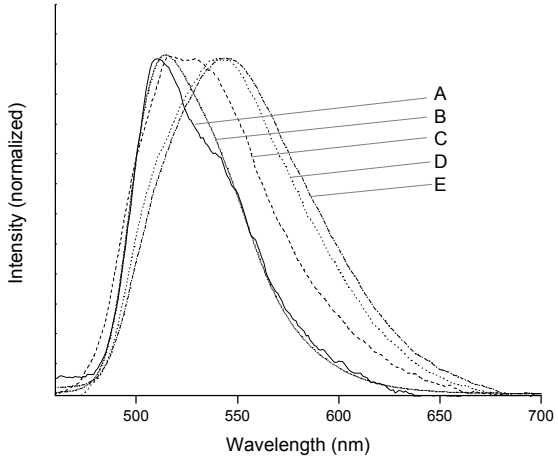

Figure 5.9. Solvent dependence for *mer*-poly-**2**. A (toluene), C (acetonitrile), D (dichloromethane), E (dimethylsulfoxide), B (*fac*-**2** in dichloromethane, for comparison).

In dichloromethane (538 nm) or dimethylsulfoxide (545 nm), the emission for poly-*mer*-**2** is broad and significantly red-shifted from that expected based on the literature reported small molecule by as much as 30 nm in some instances. There is a small shoulder to the left, appearing in the range normally expected for the major signal in the previously reported small molecule. Conversely, in toluene, the emission (510 nm) closely resembles that of the facial complex. It is narrower, with a shoulder to the right, in the range of the other signal observed for the more polar solvents described above. Finally, in acetonitrile, there is a broad emission maximum observed, which appears to span nearly equally the two different emissions observed for the other solvents (516-540 nm). It is interesting to note that in the case *mer*-**2**, this solvent dependence was not observed, and the emission maximum in all four solvents mentioned above remained in the range of 537 nm (toluene) to 546 nm (acetonitrile). Table 5.4 lists the corresponding lifetimes for each of the aforementioned solvents. In the case of the two solvents that exhibit the most strongly red-shifting effects on the emission, namely dichloromethane and dimethylsulfoxide, the lifetimes are also markedly different from the other entries, both showing a significant decrease.

Table 5.4. Lifetimes measured for *mer*-**2** and poly-*mer*-**2** in various solvents, both in ambient conditions and degassed. Lifetimes are displayed in microseconds (μs).

	mer-**2**		*mer*-poly-**2**	
Solvent	air	degassed	air	degassed
CH_2Cl_2	0.069	0.516	0.042	0.133
dmso	0.211	0.62	0.145	0.286
CH_3CN	0.022	0.481	0.002	0.717
Toluene	0.036	0.348	0.028	0.791

Neither toluene nor acetonitrile showed the same lowering effect on the excited state lifetimes for poly-*mer*-**2**.

In the *mer*-configuration of $Ir(ppy)_3$, when one ligand is modified as in the case with *mer*-**2**, there are two diastereomers possible. However, since the monomer *mer*-**2** does not show the same solvent dependent behavior as in the polymer, the observed differences in emission for *mer*-poly-**2** are more likely due to conformational differences in the polymer architecture brought about by the changes in the environment as a result of varying the solvent. Specifically, acetonitrile is a good solvent for the emissive complex, but a poor solvent for the poly(norbornene) backbone. Both dichloromethane and dimethylsulfoxide are good solvents for both the metal complex as well as the polymer backbone, and toluene is a poor to average solvent for both the complex and the backbone. The various combinations above can create a wide variety of polymer conformations in solution, causing differences in inter-chromophore distances, potentially giving rise to the observed variations in emission wavelength.

5.7 Conclusions

The ROMP polymerization of several iridium complex-containing monomers, their solubility in nonpolar solvents, and the retention of luminescent properties by the emissive complexes both as polymers in solution as well as in the solid state has been demonstrated. The results described herein lay the foundation for further steps into device fabrication using these materials, providing simplification and improvements to the process of polymerizing highly emissive phosphorescent iridium complexes. The methodology employed in this chapter relies heavily upon the strategy of "pre-polymerization functionalization" as described in Chapter 1. These polymers were fully functionalized via their side-chains using metal-ligand coordination, but in this case it was the properties of the actual complex that were desired, rather than the viscosity effects that come from structural changes such as those described in Chapter 4 in the guar system. In this study of potential materials for OLEDs, no further chemical modifications took place once the polymer was synthesized. This chapter addressed the

hypothesis of this thesis in several ways, specifically by using metal coordination to add functionality to a polymer, that was created via a living polymerization process, that ultimately will be useful in materials applications such as OLEDs, etc.

Throughout this thesis an emphasis has often been placed upon the advantages of employing variations in the types of functionalization strategies used, either occurring simultaneously along the same polymer backbone, or sequentially emanating from the same original functional groups. The next chapter will introduce a multifunctional polymer motif that incorporates (1) multiple polymerization techniques, (2) multiple types of functionalities along the same polymer backbone, and (3) graft copolymer chains that introduce another functionality into the system that has the potential to strongly influence the solubility of the system.

5.8 Experimental Section

All reagents were purchased either from Acros Organics or Aldrich and used without further purification. DMF and $CDCl_3$ were distilled from calcium hydride and degassed prior to use. THF was dried via passage through copper oxide and alumina columns. NMR spectra were taken using a 300 MHz Varian Mercury spectrometer. All spectra are referenced to residual proton solvent. Mass spectral analyses were provided by the Georgia Tech Mass Spectrometry Facility using a VG-70se spectrometer. Gel permeation chromatography (GPC) analyses were carried out using a Waters 1525 binary pump coupled to a Waters 2414 refractive index detector with methylene chloride as an eluant on American Polymer Standards 10 • m particle size, linear mixed bed packing columns. All GPCs were calibrated using polystyrene standards. Atlantic Microlabs, Norcross, GA, performed all elemental analyses. UV/vis absorption measurements were taken on a Shimadzu UV-2401 PC recording spectrophotometer. Emission measurements were acquired using a Shimadzu RF-5301 PC spectrofluorophotometer. Lifetime measurements were taken using a PTI model C-72 fluorescence laser spectrophotometer

with a PTI GL-3300 nitrogen laser. DSC data was collected using a Seiko model DSC 220C. TGA data was collected using a Seiko model TG/DTA 320.

Synthesis of *exo*-Bis(2-phenyl-pyridine)iridium(III) bicyclo[2.2.1]hept-5-ene-2-carboxylic acid 1-methyl-3-(3-methyl-[2,3']bipyridinyl-4'-yl)-propyl ester hexafluorophosphate (1)

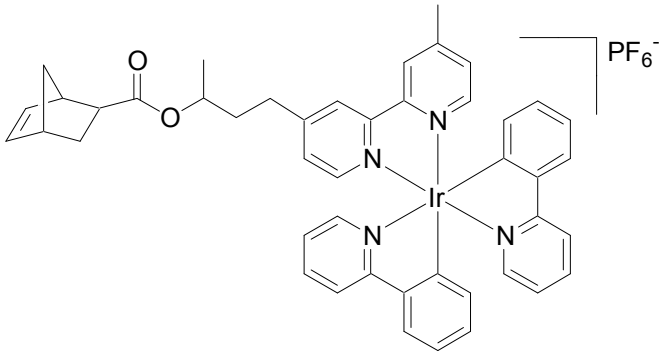

Compound **5** (910 mg, 2.51 mmol) and $[Ir(ppy)_2Cl]_2$ (615 mg, 1.14 mmol Ir) were combined in degassed ethylene glycol (10 mL) and refluxed for 24 hours under argon atmosphere. The reaction mixture was then removed from the heat and allowed to cool to room temperature followed by the addition of NH_4PF_6 (1.7 mL of a 1.0 mM aqueous solution). The reaction mixture was then extracted with methylene chloride and washed three times with water, dried with $MgSO_4$, and the solvent removed to give crude **1**, which was purified via column chromatography (silica, 98:2 CH_2Cl_2/EtOH) to give compound **1** as a bright yellow powder (830 mg, 0.82 mmol, 72 %). ^{1}H NMR ($CDCl_3$, 300 MHz) δ = 8.48 (m, 2H, *o*-bpy); (7.91-6.29 ppm range: aromatic protons, unassigned): 7.91 (s, br, 1H); 7.88 (s, br, 1H); 7.80-7.71 (m, 4H); 7.66 (d, 2H, J = 7.5 Hz); 7.54-7.49 (m, 2H); 7.21-7.17 (m, 2H); 7.06-7.02 (m, 2H); 6.99 (dt, 2H, J_1 = 7.4 Hz, J_2 = 0.9 Hz); 6.88 (dt, 2H, J_1 = 7.5 Hz, J_2 = 1.1 Hz); 6.29 (dd, 2H, J_1 = 7.4 Hz, J_2 = 3.8 Hz); 6.13-6.08 (m, 2H, norbornene vinyl); 4.93 (m, 1H, ester methine); 3.02 (s, 1H); 2.90 (m, 3H, CH-

C**H**$_3$); 2.57 (s, 3H, pyridine-C**H**$_3$); 2.08-1.96 (m, 2H); 1.92-1.85 (m, 1H, norbornene alkyl); 1.70 (s, br, 1H, norbornene bridgehead); 1.49 (m, 1H, norbornene alkyl); 1.36 (m, 2H, CH-C**H**$_2$-CH$_2$); 1.28 (dt, 3H, J_1 = 6.2 Hz, J_2 = 1.7 Hz, norbornene alkyl). ^{13}C NMR ($CDCl_3$, 100 MHz) δ = 176.2, 168.0, 167.9, 156.0, 155.5, 155.4, 152.5, 150.8, 150.0, 149.8, 148.8, 143.8, 138.3, 138.2, 136.0, 132.0, 131.9, 130.9, 129.1, 128.3, 128.3, 126.1, 125.2, 124.9, 123.6, 122.7, 119.8, 70.0, 46.9, 46.6, 46.5, 43.6, 41.9, 41.8, 35.7, 31.4, 30.6, 30.6, 21.6, 20.0. MS (ESI) 863.3 (M – loss of PF_6^-). Elemental analysis for $C_{45}H_{42}F_6IrN_4O_2P$ calculated: C, 53.62; H, 4.20; N, 5.56; found: C, 53.63; H, 4.21; N, 5.42.

Synthesis of *mer-exo*-Bis(2-phenyl-pyridine)iridium(II) Bicyclo[2.2.1]hept-5-ene-2-carboxylic acid 4-pyridin-2-yl-benzyl ester (*mer*-2)

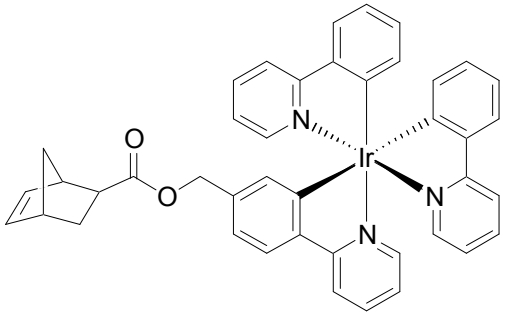

[Ir(ppy)$_2$Cl] $_2$ (100 mg, 0.187 mmol Ir) was treated with silver triflate in 5 mL refluxing acetone for two hours in the dark. The reaction mixture was then filtered, and the filtrate was combined with compound **7** (114 mg, 0.37 mmol). Immediately, 0.1 mL triethylamine was added, causing the reaction to turn instantly from light yellow to deep orange and turbid. The reaction was left to stir under argon at ambient temperature overnight. Then the solvent was removed, and the residue purified via column chromatography (neutral alumina, 1:1 hexane/dichloromethane) to give *mer*-**2** in 43 % yield. ^{1}H NMR ($CDCl_3$, 300 MHz) δ = (8.08-6.39 ppm: aromatic region, unassigned):

8.08 (d, 1H, *J* = 5.8 Hz); 7.92 (m, 2H); 7.78 (m, 3H); 7.63 (m, 3H); 7.63 (m, 1H); 7.57 (m, 2H); 7.49 (m, 3H); 6.93 (m, 3H); 6.81 (m, 1H); 6.71 (m, 1H); 6.60 (m, 1H); 6.39 (m, 1H); 6.11 (m, 2H, norbornene vinyl); 4.95 (m, 2H, ppy methylene); 2.97 (s, br, 1H, norbornene ester methine); 2.89 (s, br, 1H, norbornene methine); 2.18 (m, 1H, alkyl); 1.89 (m, 1H, unsymmetric norbornene bridgehead C**H**); 1.34 (m, 3H, norbornene alkyl). ^{13}C NMR ($CDCl_3$, 100 MHz) δ = 167.0, 166.5, 161.7, 161.3, 161.0, 147.3, 147.2, 143.9, 143.8, 137.5, 137.4, 137.3, 136.2, 136.1, 136.0, 133.1, 130.1, 130.0, 124.1, 124.0, 122.2, 122.1, 120.1, 120.0, 119.4, 119.0, 118.9, 66.6, 49.8, 45.9, 43.5, 42.8, 29.4. Elemental analysis for $C_{42}H_{34}IrN_3O_2$ calculated: C, 62.67; H, 4.26; N, 5.22; found: C, 62.19; H, 4.35; N, 4.89.

Synthesis of *fac-exo*-Bis(2-phenyl-pyridine)iridium(II) Bicyclo[2.2.1]hept-5-ene-2-carboxylic acid 4-pyridin-2-yl-benzyl ester (*fac*-2)

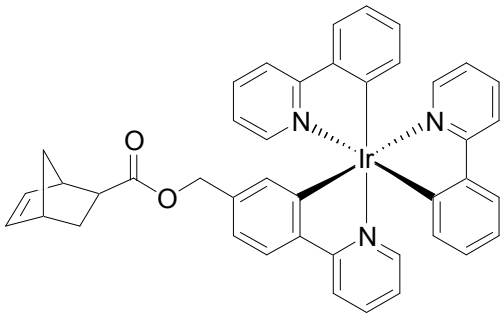

Compound **8** (200 mg, 0.24 mmol), *exo*-5-norbornene-2-carboxylic acid (40 mg, 0.24 mmol), and dimethylaminopyridine (DMAP) (17 mg, 0.12 mmol) were combined in 15 mL of dichloromethane. A solution of dicyclohexylcarbodiimide (DCC) (60 mg, 0.24 mmol) in 5 mL dichloromethane was added and the reaction stirred under argon at ambient temperature for 24 hours. The solvent was evaporated, and the residue was purified via column chromatography (neutral alumina, 1:1 hexane/dichloromethane) to give *fac*-**6** as a bright yellow powder in 40 % yield. ^{1}H NMR ($CDCl_3$, 300 MHz) δ =

7.79-7.75 (m, 3H, *o*-pyridine); 7.64-7.59 (m, 3H, *p*-pyridine); 7.50-7.39 (m, 6H, *m*-pyridine); 6.92-6.85 (m, 8H, phenyl); 6.83-6.77 (m, 3H, phenyl); 6.17-6.08 (m, 2H, norbornene vinyl); 4.98 (d, 1H, J = 12.8 Hz, ppy methylene unsymmetric C**H**); 4.92 (dd, 1H, J_1 = 12.7 Hz, J_2 =1.8 Hz, ppy methylene unsymmetric C**H**); 2.99 (s, br, 1H, norbornene ester methine); 2.90 (s, br, 1H, norbornene methine); 2.20 (dd, 1H, J_1 = 10.1 Hz, J_2 = 4.4 Hz, methine); 1.93-1.86 (m, 1H, norbornene bridgehead); 1.56 (m, 1H, norbornene); 1.47 (m, 2H, norbornene alkyl). ^{13}C NMR ($CDCl_3$, 100 MHz) δ = 176.3, 166.8, 166.4, 161.8, 161.3, 161.0, 147.2, 144.0, 143.9, 138.4, 138.2, 137.4, 137.3, 137.3, 136.2, 135.9, 130.1, 130.0, 129.9, 128.9, 124.1, 122.3, 122.2, 120.2, 120.1, 119.5, 119.0, 67.0, 64.1, 46.9, 46.7, 43.5, 43.4, 41.9, 30.7, 30.6, 30.5, 27.2. Elemental analysis for $C_{42}H_{34}IrN_3O_2$ calculated: C, 62.67; H, 4.26; N, 5.22; found: C, 62.30; H, 4.36; N, 4.88.

Synthesis of 4-(Methyl-[2,3']bipyridinyl-4'-yl)-butan-2-ol (4)

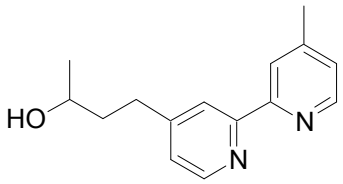

Diisopropylamine (1.41 g, 13.9 mmol) was dissolved in 30 mL of dry THF under argon and cooled to 0 ^{o}C. N-butyllithium (10 M solution in hexanes, 1.39 mL, 13.9 mmol) was added, and the reaction was stirred for 20 minutes. The resulting *in-situ*-generated lithium diisopropylamide was then cooled to -78 ^{o}C and a solution of 4,4'-dimethyl-2,2'-dipyridyl (2.5 g, 13.6 mmol) was added dropwise over a period of ten minutes. The reaction was stirred for 30 minutes, allowed to warm to 0 ^{o}C and then cooled to -20 ^{o}C. A solution of propylene oxide (788 mg, 13.6 mmol) in 70 mL THF was added dropwise over a period of 30 minutes and the reaction stirred for one hour. The reaction mixture was quenched by slow addition of 10 mL of water, followed by 70 mL of aqueous pH 7

phosphate buffer. The mixture was extracted three times with diethyl ether, the combined organic layers dried with $MgSO_4$, the solvent removed, and the resulting residue subject to column chromatography (neutral alumina, 1:1 hexane/EtOAc) to remove less polar impurities (r_f 0.5), while the product remained on the baseline. Pure **4** was subsequently eluted (r_f 0.5) by flushing the column with a 20:1 mixture of EtOAc/EtOH to give 2.40 g (9.90 mmol, 73 %) of the target compound as a slightly yellow oil. ^{1}H NMR ($CDCl_3$, 300 MHz): δ = 8.49 (dd, 2H, J_1 = 8.1 Hz, J_2 = 5.0 Hz, *o*-pyridine); 8.18 (d, 2H, J = 4.2 Hz, 5,5'-pyridine); 7.09 (dt, 2H, J_1 = 4.9 Hz, J_2 = 1.6 Hz, 3,3'-pyridine); 3.78 (sextet, 1H, J = 6.1 Hz, methine); 2.76 (m, 2H, pyridinyl methylene); 2.39 (s, 3H, pyridinyl methyl); 1.80 (m, 2H, CH-C**H**$_2$-CH_2), 1.17 (d, 3H, J = 6.2 Hz, alkyl CH-C**H**$_3$). ^{13}C NMR ($CDCl_3$, 100 MHz): δ = 156.3, 156.2, 152.6, 149.3, 149.1, 148.5, 124.9, 124.2, 122.3, 121.6, 67.2, 39.8, 31.9, 24.0, 21.4. MS (ESI) 243.1 (M+1).

Synthesis of *exo*-Bicyclo[2.2.1]hept-5-ene-2-carboxylic acid 1-methyl-3-(3-methyl-[2,3']bipyridinyl-4'-yl)-propyl ester (5)

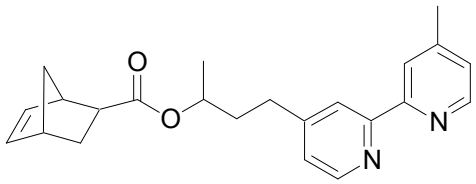

Compound **4** (2.00 g, 8.25 mmol), *exo*-5-norbornene-2-carboxylic acid (1.14 g, 8.25 mmol), and DMAP (50 mg, 0.41 mmol) were combined in 50 mL of dichloromethane at ambient temperature under argon. A solution of DCC (1.74 g, 8.42 mmol) in 30 mL of dichloromethane was added and the reaction mixture was stirred overnight. The resulting white precipitate was filtered off, and the solvent was removed. The residue was purified using column chromatography (neutral alumina, 5:1 hexane/EtOAc) to yield two distinct compounds that eluted together. The impurity was removed by repeated re-precipitation

from hot hexanes, while pure **5** remained fully soluble. Compound **5** was collected as a slightly yellow oil (1.27 g, 3.50 mmol, 42 %). ^{1}H NMR ($CDCl_3$, 300 MHz): δ = 8.55 (m, 2H, *o*-pyridine); 8.23 (s, br, 2H, 3,3'-pyridine); 7.13 (m, 2H, 5,5'-pyridine); 6.13 (m, 2H, norbornene vinyl); 4.98 (sextet, 1H, J = 6.3 Hz, ester methine); 3.03 (d, br, 1H, J = 4.5 Hz, CH=CH=C**H**); 2.92 (s, br, 1H, norbornene methine), 2.75 (m, 2H, pyridine methylene); 2.44 (s, 3H, pyridine methyl); 2.20 (m, 1H, CH=CH-C**H**); 1.96 (m, 3H, alkyl-methyl); 1.52 (m, 2H, alkyl methylene), 1.39 (m, 2H, norbornene methylene); 1.27 (dd, 2H, J_1 = 6.3 Hz, J_2 = 1.1 Hz, norbornene methylene). ^{13}C NMR ($CDCl_3$, 100 MHz): δ = 175.9, 156.4, 156.0, 151.8, 149.3, 149.0, 148.3, 138.2, 135.9, 124.9, 124.0, 122.2, 121.1, 70.4, 47.0, 46.7, 43.8, 43.7, 42.0, 37.0, 36.9, 31.9, 30.7, 21.6, 20.5. MS (ESI) 363.2 (M+1). Elemental Analysis for $C_{23}H_{26}N_2O_2$ calculated: C, 76.21; H, 7.23; N, 7.73; found: C, 75.56; H, 7.38; N, 7.73.

Synthesis of (4-pyridin-2-yl-phenyl)-methanol (6)

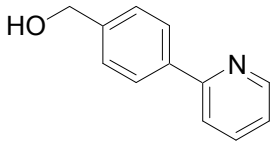

A solution of 4-pyridin-2-yl-benzaldehyde (2.00 g, 10.9 mmol) in 20 mL of dry THF was added dropwise over a period of ten minutes to a stirred suspension of lithium aluminum hydride (829 mg, 21.8 mmol) in 80 mL of dry THF at 0 ^{o}C under an argon atmosphere. After complete addition, the reaction mixture was allowed to warm to room temperature and stirred for four hours. The solution was then cooled again to 0 ^{o}C and the reaction mixture was carefully quenched by the slow addition of 10 mL of 1 N HCl. The mixture was diluted with diethyl ether, and washed twice with neutral phosphate buffer (pH 7.0), once with brine, dried over $MgSO_4$, the solvent removed, and the residue was purified by column chromatography (silica gel, ethyl acetate/hexanes 1:2) to yield **6** as a slightly

yellow oil (1.90 g, 10.2 mmol, 94 %). ^{1}H NMR ($CDCl_3$, 300 MHz): δ = 8.66 (ddd, 1H, J_1 = 4.9 Hz, J_2 = 1.7 Hz, J_3 = 0.9 Hz, *o*-pyridine); 7.91 (d, 2H, J = 8.3 Hz, phenyl 3,5-C**H**); 7.72 (m, 2H, pyridine 3,4-C**H**); 7.41 (d, 2H, J = 8.4 Hz, phenyl 2,6-C**H**); 7.22 (ddd, 1H, J_1 = 6.9 Hz, J_2 = 4.8 Hz, J_3 = 1.6 Hz, pyridine 5-C**H**); 4.71 (s, 2H, methylene); 2.82 (s, 1H, alcohol O**H**). ^{13}C NMR ($CDCl_3$, 100 MHz): δ = 157.4, 149.6, 142.3, 142.2, 138.5, 138.4, 137.1, 127.4, 127.2, 122.3, 121.0, 64.9. MS (ESI) 185.9 (M+1).

Synthesis of *exo*-Bicyclo[2.2.1]hept-5-ene-2-carboxylic acid 4-pyridin-2-yl-benzyl ester (7)

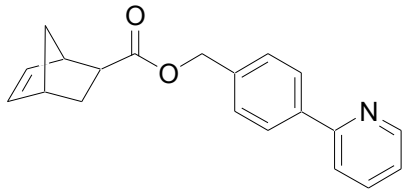

Compound **6** (1.50 g, 8.10 mmol), *exo*-5-norbornene-2-carboxylic acid (1.12 g, 8.10 mmol), and DMAP (10 mg, 0.081 mmol) were combined in 50 mL dichloromethane under argon. Then a solution of DCC (1.68 g, 8.18 mmol) in 30 mL of dichloromethane was added, and the reaction mixture was stirred overnight at ambient temperatures. A white precipitate formed during the reaction which was filtered off. The solvent was removed and the residue subject to column chromatography (basic alumina, 7:1 hexane/EtOAc) to yield **7** as a clear oil (1.98 g, 6.48 mmol, 80 %). ^{1}H NMR ($CDCl_3$, 300 MHz): δ = 8.69 (ddd, 1H, J_1 = 4.8 Hz, J_2 = 1.7 Hz, J_3 = 1.0 Hz, *o*-pyridine); 8.00 (d, 2H, J = 8.4 Hz, phenyl 3,5-C**H**); 7.74 (m, 2H, pyridine 3,4-C**H**); 7.45 (d, 2H, J = 8.4 Hz, phenyl 2,6-C**H**); 7.23 (ddd, 1H, J_1 = 7.1 Hz, J_2 = 4.9 Hz, J_3 = 2.2 Hz, pyridine 5-C**H**); 6.12 (m, 2H, norbornene vinyl); 5.19 (s, 2H, methylene); 3.08 (s, 1H, ester methine); 2.93 (s, 1H, CH=CH-C**H**); 2.30 (m, 1H, CH=CH-C**H**); 1.95 (dt, 1H, J_1 = 11.8 Hz, J_2 = 3.6 Hz, norbornene methylene); 1.54 (m, 1H, norbornene methylene bridgehead); 1.39 (m, 1H,

norbornene methylene bridgehead). ^{13}C NMR ($CDCl_3$, 100 MHz): δ = 176.1, 157.1, 149.9, 139.4, 138.3, 137.2, 137.0, 135.9, 128.6, 127.3, 122.4, 120.7, 66.2, 47.0, 46.7, 43.5, 42.0, 30.8. MS (ESI) 306.1 (M+1). Elemental analysis for $C_{20}H_{19}NO_2$ calculated: C, 78.66; H, 6.27; N, 4.59; found: C, 78.35; H, 6.36; N, 4.63.

Synthesis of *fac*-Bis(2-phenylpyridine)-p-hydroxymethyl-2-(pyridyl)benzene iridium (III) (8)

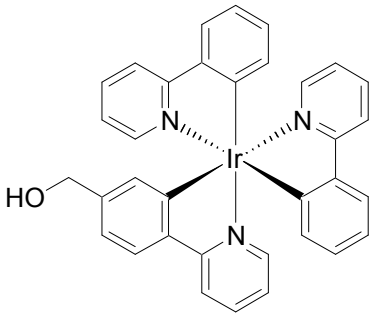

fac-Ir(ppy)$_2$(fppy) (0.20 mg, 0.29 mmol) was dissolved in 30 mL of tetrahydrofuran (THF) and 8.8 mL (3-fold excess) of lithium aluminum hydride (0.1 M solution in THF) was added dropwise, upon which the solution turned immediately from bright orange-red to yellow-green. The reaction mixture was stirred at ambient temperatures for one hour and then quenched by the addition of ethyl acetate. The crude material, which showed no remaining aldehyde signal by ^1H NMR, was dissolved in dichloromethane and washed three times with water, dried with $MgSO_4$, and used without further purification.

General Polymerization Procedure

The polymerizations were carried out under argon, at ambient temperatures, in dichloromethane, at concentrations of 0.2 M in monomer. All polymers were synthesized on an approximately 50 mg scale with a monomer to catalyst ratio of 50:1. All polymers were purified by precipitation into either methanol or diethyl ether.

Polymer (Poly-1)

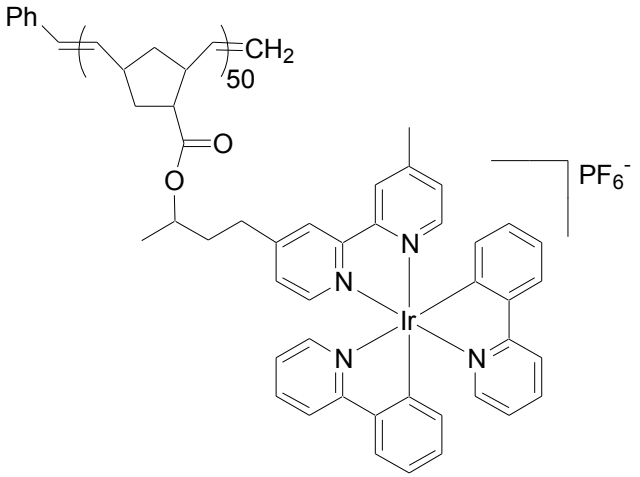

^{1}H NMR (CD_2Cl_2, 300 MHz): δ = 8.44 (m, 2H); 7.93-7.74 (m, 8H); 7.53 (m, 2H); 7.23 (m, 3H); 7.02 (m, 5H); 6.91 (m, 1H); 6.34 (m, 2H); 5.45-5.16 (m, 2H); 4.91 (m, 1H); 3.21-2.71 (m, 4H); 2.56 (m, 5H); 1.97 (m, 3H); 1.66 (m, 2H); 1.23 (m, 5H). ^{13}C NMR (CD_2Cl_2, 100 MHz): δ = 167.9, 155.9, 155.6, 152.3, 150.8, 150.3, 150.0, 148.8, 144.0, 138.4, 131.9, 130.7, 129.2, 128.4, 125.7, 125.0, 124.9, 123.6, 122.7, 120.0, 65.9, 37.3, 35.8, 31.5, 21.4, 21.3, 20.1, 19.9, 19.8.

Polymer (poly-1-*co*-3 (1:2))

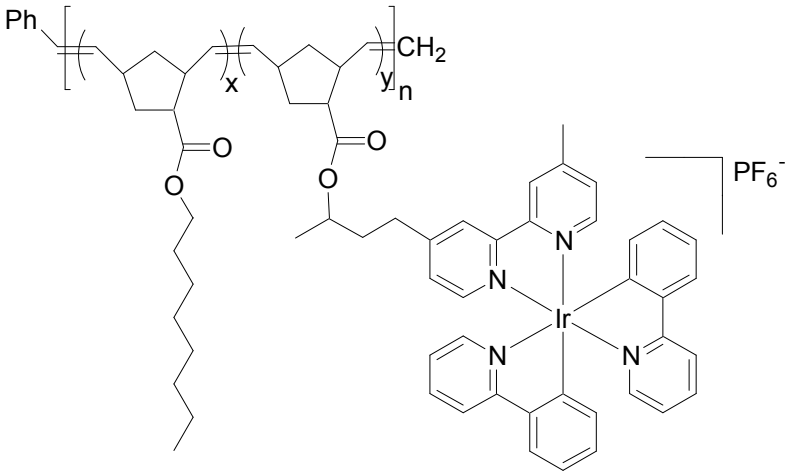

^{1}H NMR (CD_2Cl_2, 300 MHz): δ = 8.42 (m, 0.6H); 7.95 (m, 0.6H); 7.87-7.73 (m, 1.3H); 7.53 (m, 0.6H); 7.25 (m, 0.6H); 7.03 (m, 0.9H); 6.94 (m, 0.6H); 6.34 (m, 0.6H); 5.50-5.15 (m, 2H); 4.95 (m, 0.4H); 3.99 (m, 1.2H); 3.16 (0.6H); 2.90-2.65 (m, 1.8H); 2.41 (m, 1.5H), 1.97 (m, 2H); 1.82-1.48 (m, 2H); 1.30 (m, 5.5H); 0.91 (m, 1.9H). ^{13}C NMR ($CDCl_3$, 100 MHz): δ = 175.7, 174.8, 168.0, 156.0, 155.5, 152.3, 150.7, 150.4, 150.1, 148.8, 144.0, 138.3, 134.7, 133.6, 132.9, 131.9, 130.8, 129.2, 128.4, 125.7, 125.0, 124.7, 123.5, 122.7, 120.0, 64.4, 48.7, 41.5, 36.8, 32.0, 31.4, 29.4, 28.9, 26.3, 26.2, 22.9, 21.4, 15.3, 14.1.

Polymer (poly-*mer*-2)

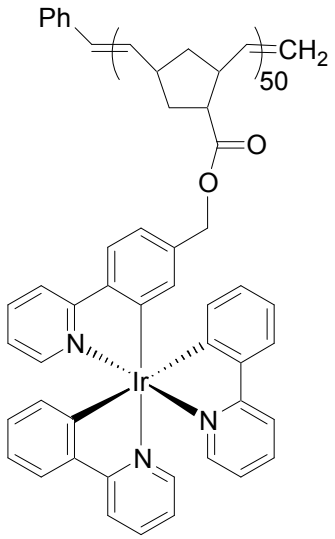

^{1}H NMR (CD_2Cl_2, 300 MHz): δ = 9.27 (d, 1H, *J* = 5.7 Hz); 8.05 (m, 1H); 7.97-7.88 (m, 2H); 7.82 (t, 1H, *J* = 7.7 Hz); 7.68 (m, 2H); 7.58 (d, 2H, *J* = 7.8 Hz); 7.46-7.07 (m, 2H); 7.00-6.71 (m, 7H); 6.65-6.50 (m, 3H); 6.38 (m, 1H); 5.90 (d, 1H, *J* = 7.7 Hz); 5.40-4.81 (m, 2H); 3.13 (m, 2H); 2.73-2.31 (m, 2H); 2.10-1.78 (m, 2H); 1.62 (m, 2H); 1.18 (m, 1H). ^{13}C NMR (CD_2Cl_2, 100 MHz): δ = 168.2, 151.7, 145.0, 144.2, 136.9, 130.6, 129.3, 124.4, 123.9, 122.8, 121.6, 118.9, 47.1, 8.7.

Poly-*mer*-2-*co*-3 (1:2)

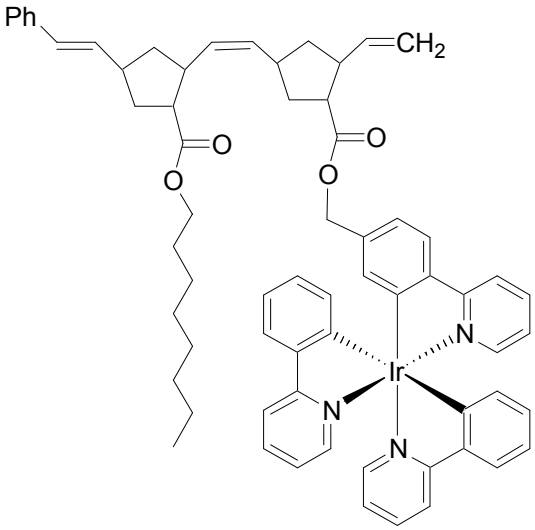

^{1}H NMR ($CDCl_3$, 300 MHz): δ = 9.22 (d, 0.3H, *J* = 5.5 Hz); 8.08 (m, 0.2H); 7.87 (m, 0.4H); 7.73 (m, 0.5H); 7.54 (m, 0.6H); 7.22 (m, 0.4H); 6.95-6.68 (m, 1.2H); 6.55 (m, 0.3H); 6.37 (m, 0.2H); 5.92 (d, 0.2H, *J* = 7.8 Hz); 5.50-4.79 (m, 2H); 3.99 (m, 1.3H); 3.06 (m, 0.8H); 2.85 (m, 0.9H); 2.50 (m, 0.5H); 1.98 (m, 1H); 1.74 (m, 0.4H); 1.60 (m, 1.1H); 1.32 (m, 7.1H); 0.88 (m, 1.8H). ^{13}C NMR ($CDCl_3$, 100 MHz): δ = 174.8, 168.7, 153.4, 151.8, 145.5, 143.9, 137.4, 136.5, 134.7, 133.5, 132.9, 130.8, 130.2, 129.9, 129.3, 126.5, 124.4, 123.9, 122.4, 121.5, 118.8, 118.6, 64.6, 48.7, 47.0, 43.1, 40.8, 36.3, 32.0, 29.4, 28.9, 26.3, 26.2, 22.9, 14.4, 8.9.

5.9 References

(1) D'Andrade, B. W.; Brooks, J.; Adamovich, V.; Thompson, M. E.; Forrest, S. R. *Adv. Mater.* **2002**, *14*, 1032-1036.

(2) Gong, X.; Robinson, M. R.; Ostrowski, J. C.; Moses, D.; Bazan, G. C.; Heeger, A. J. *Adv. Mater.* **2002**, *14*, 581-585.

(3) Kohler, A.; Wilson, J. S.; Friend, R. H. *Adv. Mater.* **2002**, *14*, 701-707.

(4) Lamansky, S.; Djurovich, P.; Murphy, D.; Abdel-Razzaq, F.; Lee, H.-E.; Adachi, C.; Burrows, P. E.; Forrest, S. R.; Thompson, M. E. *J. Am. Chem. Soc.* **2001**, *123*, 4304-4312.

(5) Beeby, A.; Bettington, S.; Samuel, I. D. W.; Wang, Z. *J. Mater. Chem.* **2003**, *13*, 80-83.

(6) Brunner, K.; van Dijken, A.; Borner, H.; Bastiaansen, J. J. A. M.; Kiggen, N. M. M.; Langeveld, B. M. W. *J. Am. Chem. Soc.* **2004**, *126*, 6035-6042.

(7) Inomata, H.; Goushi, K.; Masuko, T.; Konno, T.; Imai, T.; Sasabe, H.; Brown, J. J.; Adachi, C. *Chem. Mater.* **2004**, *16*, 1285-1291.

(8) Kawamura, Y.; Yanagida, S.; Forrest, S. R. *J. Appl. Phys.* **2002**, *92*, 87-93.

(9) Okumoto, K.; Shirota, Y. *Chem. Mater.* **2003**, *15*, 699-707.

(10) Slinker, J. D.; Gorodetsky, A. A.; Lowry, M. S.; Wang, J.; Parker, S.; Rohl, R.; Bernhard, S.; Malliaras, G. G. *J. Am. Chem. Soc.* **2004**, *126*, 2763-2767.

(11) Shinar, J. *Organic Light-Emitting Devices*; Springer-Verlag: New York, 2004.

(12) Suzuki, M.; Tokito, S.; Sato, F.; Igarashi, T.; Kondo, K.; Koyama, T.; Yamaguchi, T. *Appl. Phys. Lett.* **2005**, *86*, 103507.

(13) Chen, X. L., J.-L.; Liang, Y.; Ahmed, M. O.; Tseng, H.-E.; Chen, S.-A. *J. Am. Chem. Soc.* **2003**, *125*, 636-637.

(14) DeRosa, M. C.; Mosher, P. J.; Yap, G. P. A.; Focsaneanu, K. S.; Crutchley, R. J.; Evans, C. E. B. *Inorg. Chem.* **2003**, *42*, 4864-4872.

(15) Sandee, A. J.; Williams, C. K.; Evans, N., R; Davies, J. E.; Boothby, C. E.; Kohler, A.; Friend, R. H.; Holmes, A. B. *J. Am. Chem. Soc.* **2004**, *126*, 7041-7048.

(16) Tekin, E.; Holder, E.; Marin, V.; de Gans, B.-J.; Schubert, U. S. *Macromol. Rapid Commun.* **2005**, *26*, 293-297.

(17) Marin, V.; Holder, E.; Hoogenboom, R.; Schubert, U. S. *J. Polym. Sci., Part A: Polym. Chem.* **2004**, *42*, 4153.

(18) Grubbs, R. H. *Handbook of Metathesis*; Wiley-VCH: Weinheim, 2003; Vol. 3.

(19) Carlise, J. R.; Weck, M. *J. Polym. Sci. Part. A: Polym. Chem.* **2004**, *42*, 2973-2984.

(20) Meyers, A.; South, C.; Weck, M. *Chem. Commun.* **2004**, 1176-1177.

(21) Meyers, A.; Weck, M. *Chem. Mater.* **2004**, *16*, 1183-1188.

(22) Carlise, J. R.; Kriegel, R. M.; Rees, W. S., Jr.; Weck, M. *J. Org. Chem.* **2005**, *70*, 5550-5560.

(23) DeRosa, M. C.; Hodgson, D. J.; Enright, G. D.; Dawson, B.; Evans, C. E. B.; Crutchley, R. J. *J. Am. Chem. Soc.* **2004**, *126*, 7619-7626.

(24) Pollino, J. M.; Nair, K. P.; Stubbs, L. P.; Adams, J.; Weck, M. *Tetrahedron* **2004**, *60*, 7205-7215.

(25) Love, J. A.; Morgan, J. P.; Trnka, T. M.; Grubbs, R. H. *Angew. Chem.* **2002**, *114*, 4207-4209.

(26) Pollino, J. M.; Weck, M. *Synthesis* **2002**, 1277-1285.

(27) Meier, M. A. R.; Lohmeijer, B. G. G.; Schubert, U. S. *Macromol. Rapid Commun.* **2003**, *24*, 852–857.

(28) Breu, J.; Sto¨ssel, P.; Schrader, S.; Starukhin, A.; Finkenzeller, W. J.; Yersin, H. *Chem. Mater.* **2005**, *17*, 1745.

(29) Tamayo, A. B.; Alleyne, B. D.; Djurovich, P. I.; Lamansky, S.; Tsyba, I.; Ho, N. N.; Bau, R.; Thompson, M. E. *J. Am. Chem. Soc.* **2003**, *125*, 7377-7387.

(30) Kim, I.-B.; Wilson James, N.; Bunz Uwe, H. F. *Chem. Commun.* **2005**, 1273-5.

(31) Brinkmann, M.; Gadret, G.; Muccini, M.; Taliani, C.; Masciocchi, N.; Sirani, A. *J. Am. Chem. Soc.* **2000**, *122*, 5147.

(32) Colombo, M. G.; Brunold, T. C.; Riedener, T.; Güdel, H. U.; Fortsch, M.; Bürgi, H.-B. *Inorg. Chem.* **1994**, *33*, 545-550.

CHAPTER 6

MULTIFUNCTIONAL POLYMER BACKBONES FOR REVERSIBLE SELF-ASSEMBLY, CROSS-LINKING, AND GRAFTING

6.1 Abstract

This chapter describes the synthesis of multifunctional ring-opening metathesis polymerization (ROMP)-based modified triblock co-polymers that are endowed with a combination of metal coordination motifs in the form of the SCS-palladium-pincer complex, α-bromoesters for site-specific initiation of graft copolymerization via atom-transfer free radical polymerization (ATRP), and subsequently poly(*tert*-butyl acrylate) side-chains. Functionalization of the ROMP-based macroinitiators was successful via both the metal coordination sites as well as the grafting sites. The metal coordination sites did not exhibit the expected behavior once the graft copolymerization had taken place. The data acquired suggests that this is likely due to residual catalyst from the ATRP reaction interfering with the coordination process.

6.2 Introduction

Side-chain functionalized metal coordinated polymers have been shown to be useful for the creation of several different materials in this thesis thus far. With the success of the works described in Chapters 3 through 5 which focused on a single type of side-chain functionalization per system, it is logical at this point to explore a more complex strategy. In keeping with the major hypothesis and goal of this thesis, engineering multiple functions into a single polymer system would enhance the demonstration of the utility and potential of the concept of functionalizing polymers via side-chain metal

coordination. The system described in this chapter employs multiple modes of polymerization to form complex graft copolymers from block copolymers, and attempts to utilize metal coordination as a means to cross-link the graft copolymers. Both methods of polymerization, specifically ROMP and atom transfer free radical polymerization (ATRP) employ transition metal coordination complexes as the active catalysts, and as such, add an additional degree of complexity to this system which is uses metal coordination as a means of macromolecular assembly.

Atom-transfer free radical polymerization has become an important method of polymerization in the synthesis of many materials today.[1-5] The combination of ATRP with ROMP has already been shown to have some utility in designing block copolymers, graft copolymers, liquid crystals, and other systems where it is desirable to combine the elements of "*polymerizing from*" a specific point (ATRP), and "*polymerizing through*" (ROMP). Weck and co-workers exploited this discreet mechanistic difference by creating a ROMP backbone that contained ATRP initiators, and subsequently polymerizing from this backbone to create a graft copolymer.[6] Others have used the reverse of this process, polymerizing from a ROMP monomer that contained an ATRP initiator using ATRP, and then polymerizing through it via ROMP.[7-9]

The ruthenium carbene metathesis catalysts have been shown to be highly functional group tolerant, and even remain highly successful in the presence of a competitive chelating ligand such as 2,2'-bipyridine. However, the copper (I) – based ATRP catalysts do not show such robustness in the presence of a chelating ligand. To date, there are no examples in the literature where copper (I) mediated ATRP has been carried out to form a polymer that contains a copper-chelating ligand, when the ligand was intended to be used for chelating another metal in a subsequent step. Indeed, combining the technique of ATRP with the metal coordination-based method of material functionalization introduces some complexity due to the possibility of interference of the ATRP catalyst with the

ligands intended for subsequent functionalization, and so this must be taken into consideration when designing the system.

In order to circumvent this potential unwanted interaction, a method was chosen that incorporated the palladium-based pincer ligand. Since this ligand already contains the metal ion, it was postulated that there would be little to no interference with the ATRP catalyst. This palladium pincer complex, being a sufficiently stable species until activated by removal of the chloride ligand,[10,11] presents a promising opportunity to engineer a metal coordination site into a system that will ultimately be polymerized via copper-mediated ATRP.[12,13]

Macromolecular cross-linking via metal coordination was demonstrated in Chapter 4, and was shown to be an effective route to tuning and adjustment of solution viscosity via network formation. However, although the metal coordination based binding event is often well-defined, occurring via spontaneous sequestration of solvated metal cations, the pre-coordination step of macromolecular modification with the 2,2'-bipyridine binding site remains still somewhat ambiguous with regards to the location of the binding sites both on the macromolecule as well as with respect to one another.

Optimally, all steps of the macromolecular functionalization process would be well-defined so as to facilitate tuning of the properties of the system. In order to achieve this goal, a system was designed that met the following criteria: a well-defined, branched macromolecule with specifically placed metal coordination sites for functionalization. To best mimic natural macromolecules, which are both abundant and cost effective, a large branched structure such as a graft copolymer was chosen over straight-chain polymers as the model of choice. The combination of ROMP and ATRP blends facile synthetic elements and functional group tolerance with well controlled and defined superstructures. The parent backbone, or macroinitiator, was constructed via ROMP because of its functional group tolerance, and ability to produce polymers of low PDI's

that are often living. Additionally, ROMP was seen as an attractive polymerization method due to its ability to incorporate functional monomers in a random fashion.

The macroinitiator is composed primarily of triethylene glycol-based spacer monomers, with a small portion (2.5 – 10 %) of α-bromo ester-containing monomers included for subsequent initiation of graft copolymerization in a later step. Located on either end of this backbone are approximately trimers of palladium-containing pincer monomers for functionalization or cross-linking of the final polymer. Graft copolymers are synthesized using this ROMP-based macroinitiator, via copper-mediated ATRP of *tert*-butyl acrylate. This choice of graft co-monomer ultimately gives this system the option of solubility either in organic or aqueous media, since the nonpolar *tert*-butyl groups can easily be removed to convert the chains to poly(acrylic acid) (PAA). Thus the proposed system enables the construction of a well-defined macromolecule that has specifically designed coordination sites, that can be active in both aqueous and organic environments.

6.3 Synthetic Strategy

In order to create a macroinitiator with a narrow polydispersity index (PDI) (< 1.1), the use of a chain-transfer agent (CTA) was not an available option, as the PDI's of CTA-based ROMP polymers do not fall into this narrow regime.[14] As a result, in order to simulate the end-capping effect of a CTA, a triblock copolymer approach was decided upon, with the first and third blocks only consisting of approximately three repeat units of pincer-containing monomer, and the middle block being a random copolymer of the above mentioned triethylene glycol spacer monomer and the ATRP-initiating α-bromo ester monomer (Figure 6.1).

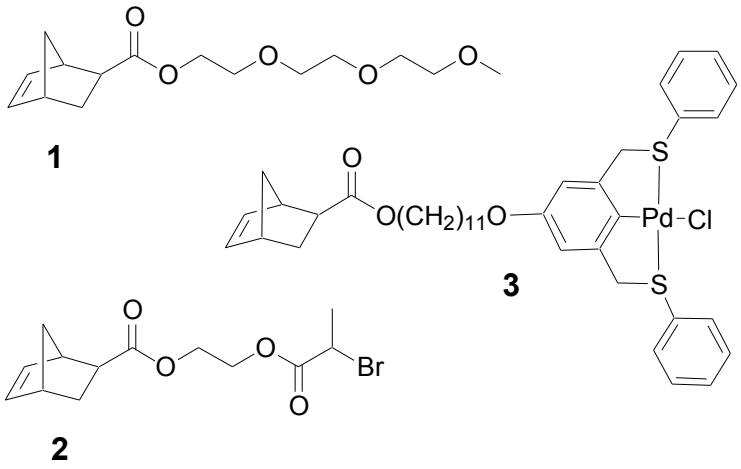

Figure 6.1. Monomers used to synthesize the macroinitiator via ROMP: triethylene glycol-based spacer monomer **1**, α-bromoester-containing monomer **2**, palladium-based pincer-containing monomer **3**.

The ability of the third generation Grubbs catalyst to initiate more quickly than its first and second generation counterparts enables full initiation of the catalyst even when there is a monomer:catalyst ratio as high as 3:1.[15] This efficiency of these catalysts allow for the polymerization of monomers such as the three above mentioned molecules in a controlled fashion, resulting in polymers with low PDI's. A schematic representation of the resulting macroinitiator is depicted in Figure 6.2.

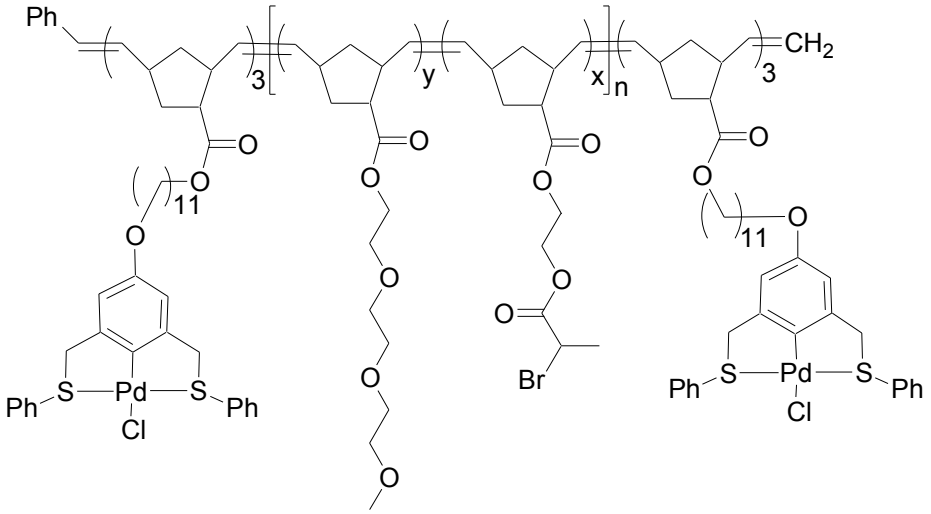

Polymer	y	x	% initiator
MI25	48.75	1.25	2.50%
MI50	47.5	2.5	5.00%
MI100	45	5	10.00%

Figure 6.2. Modified triblock copolymer design of the multifunctional polymer system.

The three macroinitiators used in this study consist of initiator densities of 2.5 % (**MI25**), 5.0 % (**MI50**), and 10.0 % (**MI100**).

Upon formation of the complete triblock copolymer, the incorporated ATRP initiator sites can then be utilized to grow graft copolymers via conventional Cu(I)-mediated ATRP polymerization techniques. The α-bromo ester is a common ATRP initiating moiety, as it undergoes homolytic C-Br cleavage in the presence of an appropriate low oxidation state transition metal complex such as the CuBr/Me_6TREN catalyst used in this work. *Tert*-butyl acrylate was chosen as the graft co-monomer, as it creates a nonpolar polymer chain that can be utilized as such, or deprotected by various reagents such as trifluoroacetic acid to form poly(acrylic acid) and hence transform into a water-soluble polymer system (Figure 6.3).

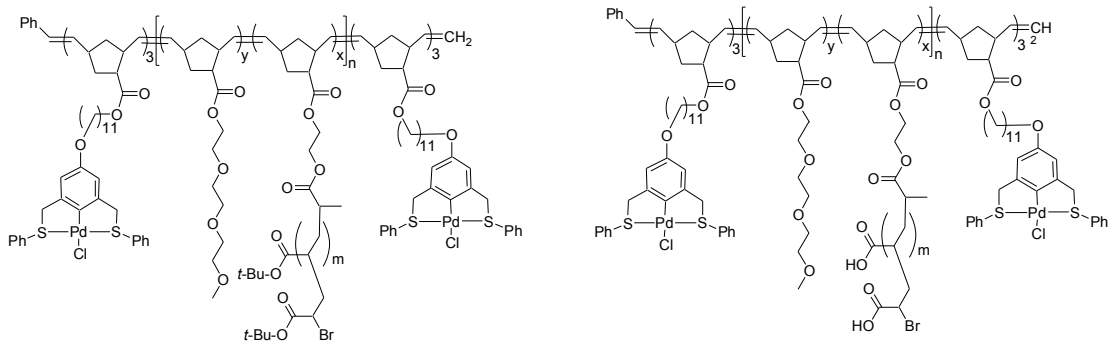

Figure 6.3. Schematics of both organic soluble (left) and water soluble (right) graft copolymers

Once the fully grafted polymers are created, this well-defined macromolecule can now be either simply functionalized (with a pyridine-containing molecule) or cross-linked (via a molecule containing two or more pyridines)(Figure 6.4).

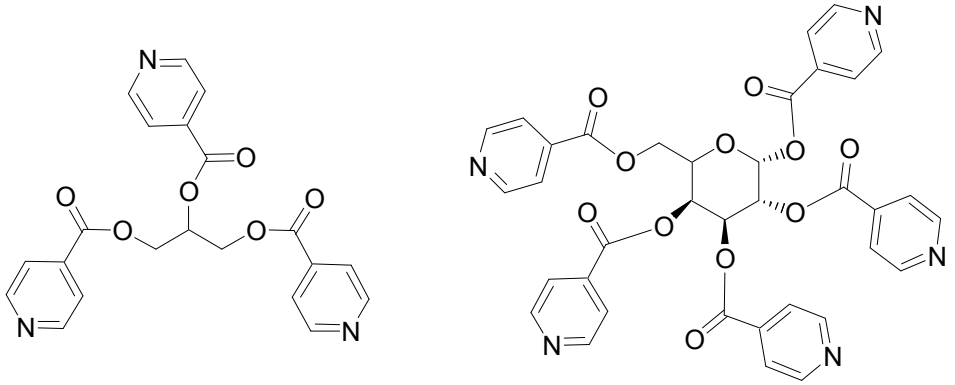

4 **5**

Figure 6.4. Multi-pyridine-containing cross-linking agents: tris-pyridine glycerol-based cross-linking agent **4**, and pentakis-pyridine galactose-based cross-linking agent **5**.

The cross-linking behavior can be effectively observed by several methods, including ^{1}H NMR in which diagnostic signals shift upon the palladium-pyridine coordination event, and simple viscosimetric measurements where solution viscosity should increase noticeably upon cross-linking. This cross-linking effect has been shown to be highly

effective using a bis-pyridine cross-linking agent and a non-grafted polymer, by Weck and co-workers.[10]

Lastly, the viscosity of the cross-linked system can be returned to approximately that of the pre-cross-linked polymer through simple addition of a phosphine such as PPh_3, etc., which binds more strongly to the palladium and displaces the pyridine.[11-13]

6.4 Small Molecule Synthesis

The syntheses of the pincer and triethylene glycol monomers were carried out according to literature procedures as described by Pollino[13] and Kriegel,[6] respectively. The α-bromo ester monomer was synthesized in two steps by coupling of the mono-substituted ethylene glycol ester of norbornene carboxylic acid **6**[16] with 2-bromopropionic acid using dicyclohexylcarbodiimide (DCC) and dimethylamino pyridine (DMAP), giving the desired monomer in 87 % yield (Scheme 6.1).

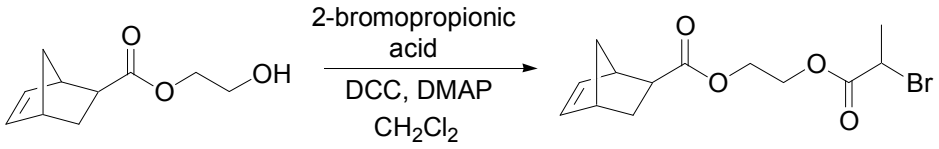

6 **2**

Scheme 6.1. Synthesis of ATRP initiating monomer **2**.

Syntheses of the tris- and pentakis- pyridine based cross-linking agents, were both carried out in a single step. The tris-pyridine cross-linking agent began with combining glycerol, isonicotinyl chloride hydrochloride, and triethylamine together and refluxing for 24 hours in THF to give the target tris-pyridine cross-linker in 80 % yield (Scheme 6.2).

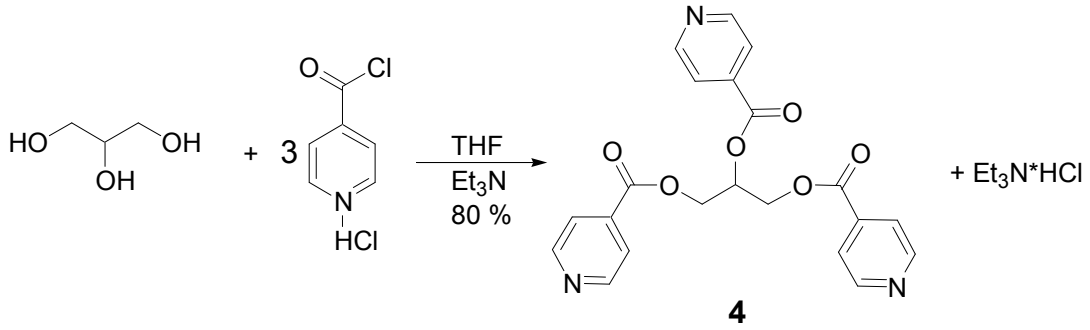

4

Scheme 6.2. Synthesis of tris-pyridine cross-linking agent **4**.

The pentakis-pyridine cross-linker was synthesized analogously, replacing glycerol with galactose, giving a yield of 17 % (Scheme 6.3).

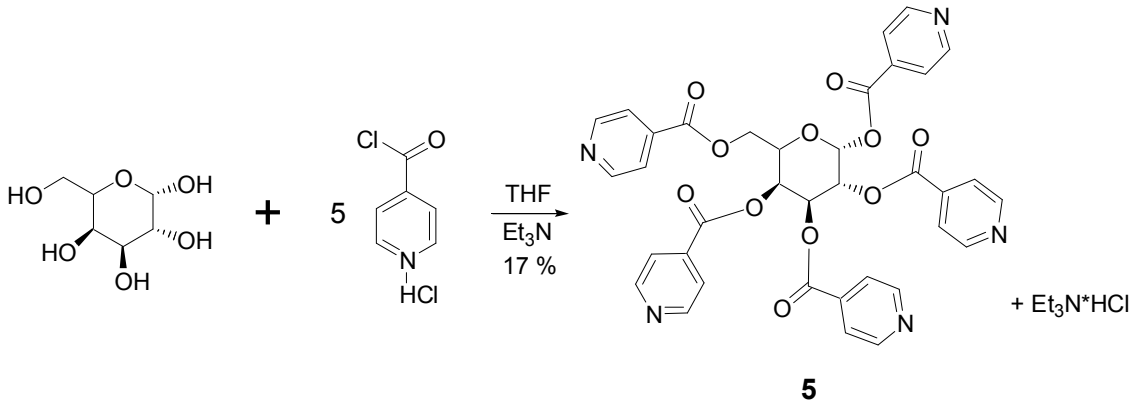

5

Scheme 6.3. Synthesis of pentakis-pyridine cross-linker **5**.

6.5 Macroinitiator Synthesis

The pincer monomer was added to a rapidly stirring solution of Grubbs' third generation catalyst and stirred for two minutes. Immediately thereafter a solution of a mixture of both triethylene glycol methyl ether monomer and the α-bromo ester monomer was added to the reaction mixture, and was stirred for five minutes. Finally, a solution of pincer monomer was once again added to the stirring polymer solution quickly, and stirred for five additional minutes, then quenched using ethyl vinyl ether. Each polymerization step monitored by TLC to observe complete monomer consumption.

The polymer was precipitated into methanol three times, and collected. All polymers were recovered in yields ranging from 58 % (**MI50**) to 71 % (**MI25**), and were pure by elemental analysis (± 0.40 %). Data for these polymers are shown in Table 6.1.

Table 6.1. Data for macroinitiators with ATRP initiator densities of 2.5 %, 5.0 %, and 10.0 %.

Polymer	M_n	M_w	PDI	Elem. Anal. (calc)	Elem. Anal. (found)
MI25	26800	29400	1.09	C, 62.45; H, 7.87	C, 62.56; H, 7.72
MI50	27200	28500	1.05	C, 62.15; H, 7.80	C, 61.58; H, 7.57
MI100	25900	27400	1.05	C, 61.57; H, 7.68	C, 61.55; H, 7.73

6.6 Graft Copolymer Synthesis

Initial explorations into the synthesis of the graft copolymers began with the macroinitiator **MI100**. Conventional ATRP was carried out using the CuBr/Me_6TREN catalyst system, which is reported by Matyjaszewski and co-workers to be one of the most efficient ATRP catalysts known to date.[3] The monomer *tert*-butyl acrylate was chosen for the graft copolymer chains, and a portion of toluene was added to the ATRP reaction mixture in order to solubilize the macroinitiator. After combining together in a monomer:catalyst:initiator ratio of 1300:0.5:1, and degassing (3 x freeze pump thaw), the reaction mixture was heated to 65 ^{o}C for 24 hours. After this time period the polymerization had progressed to 25 % conversion via ^{1}H NMR, and was quenched by opening to air and cooling. After precipitation into a 50/50 mixture of methanol and water the polymer was redissolved in methylene chloride and filtered through neutral alumina in order to remove any residual copper.

Formation of the graft copolymer was confirmed by ^{1}H NMR and GPC analysis. Comparison of the GPC traces for both **MI100** with that of **G100** shows that the molecular weight increased significantly (Figure 6.5), with no remaining non-grafted polymer left over.

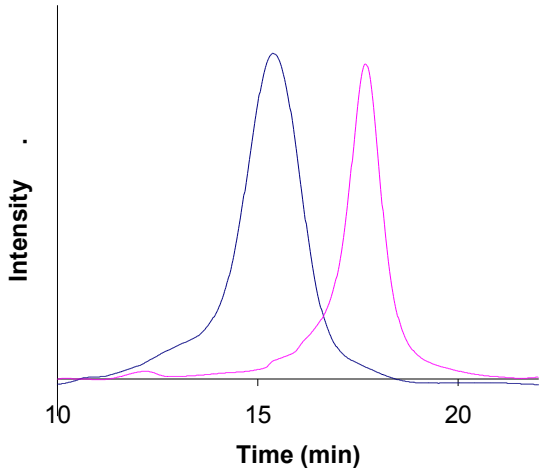

Figure 6.5. GPC traces of 10 % initiator density polymers: **G100** (left), **MI100** (right).

The proton NMR analysis indicated that the monomer conversion had reached 28 % at 24 hours, at which point the reaction was quenched. Based on the initial ratio of monomer:initiator (2000:1), this conversion percentage correlates to a new molecular weight of $3.85 * 10^5$, a significant increase from the molecular weight of the pre-grafted analogue, $2.60 * 10^4$. Additionally, proton NMR analysis suggested that the palladium-pincer moiety was still fully intact following the grafting procedure.

6.7 Cross-Linking Studies

Once the grafted system is created, self-assembly-based cross-linking using the tris-pyridine-functionalized glycerol cross-linker **4** or the pentakis-pyridine galactose-based cross-linker **5** can be carried out via metal coordination. This fully grafted, cross-linked supermolecular network is expected to exhibit a significant increase in viscosity from that of its un-cross-linked counterpart, similar to the behavior reported for the non-grafted analogue.[10] The cross-linking procedures described in this section relate specifically to the **G100**.

Initial cross-linking tests were carried out on the pre-grafted macroinitiator in order to test the efficiency of the cross-linkers. In all cases, addition of cross-linker to **MI100** resulted in full gellation (1:1 Pd-pyridine ratio) or precipitation (Pd-pyridine ratio >2). These results served as an indicator that the cross-linkers were indeed effective, and that the grafted copolymer chains would be necessary in order to keep the cross-linked networks soluble.

Thus cross-linking of **G100** was carried out in an identical manner to that for the pre-grafted version, at various copolymer concentrations. The cross-linking event was monitored via viscometry using a Cannon 150 C330 viscometer, and the relative flow times were monitored (Figure 6.6).

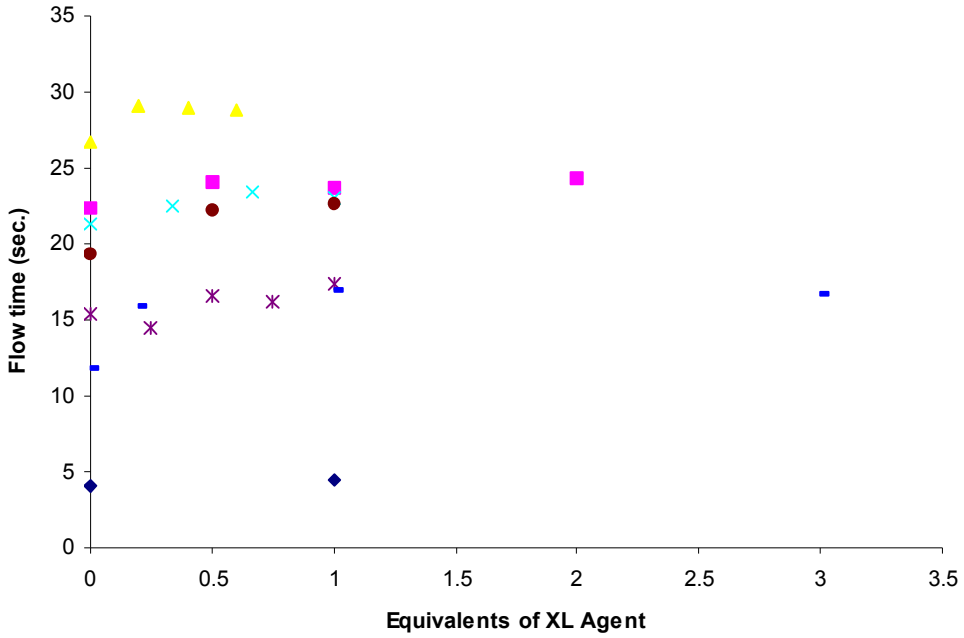

Figure 6.6. Viscosimetry data for cross-linking of **G100**: ♦ **4**, 5mg/mL, $CHCl_3$; △ **4**, 20mg/mL, $CHCl_3$; **4**, 24mg/mL, $CHCl_3$; x **5**, 20mg/mL, $CHCl_3$; * **4**, 20mg/mL, CH_2Cl_2; ♦ **4**, 20mg/mL, CH_2Cl_2 after ion exchange resin; - PVPy, 20mg/mL, CH_2Cl_2.

In all cases, cross-linking attempts did not produce any significant increases in solution viscosity (Figure 6.6), due to the inability to remove residual copper ions left over from the ATRP reaction. By ^{1}H NMR, it can be observed that upon addition of pyridine to **G100** as a control, the ortho-protons that normally appear at 8.6 ppm appear significantly broader, and the remaining signals from the pyridine are shifted slightly downfield (~0.05 - 0.10 ppm) as well. This is indicative of an interaction event occurring between the pyridine and another species in solution. Since the palladium-pincer complex appeared to be still intact after the ATRP process, the pyridine is not able to coordinate to the palladium until after addition of a silver salt, so this interaction must be emanating from another source. The other possibility for this potential interaction with pyridine is that of the copper complex left in solution from the grafting process. In order to remove this copper species, several techniques were employed. First, filtration of a solution of **G100** in methylene chloride through an small column of alumina was carried out, but the ^{1}H NMR pyridine self-assembly experiment again behaved similarly to the initial attempt, suggesting that this method was not successful at removing the copper species from the solution. Second, a solution of the **G100** in methylene chloride was extracted with an aqueous solution of 4,4'-dicarboxy-2.2'-bipyridine buffered at pH 9. This method as well was unsuccessful at removing the copper from solution, as the resulting polymer behaved in the same manner as in the first two attempts. Third, a solution of the **G100** in methylene chloride was stirred with Reillex™ 402 ion-exchange resin, which is poly(vinylpyridine) cross-linked with divinylbenzene to a degree of 2 %. This mixture was stirred for 48 hours, after which time the entire mixture was filtered through a small plug of this same resin followed by celite. Proton NMR experiments with pyridine suggested that this method was somewhat effective, as there was a lessening of the broadening and shifting effects on the pyridine signals prior to addition of the silver salt. However, subsequent cross-linking attempts with this sample using **4** did not show any significant increase in viscosity. It was theorized that if copper was still in solution and

was interfering with coordination attempts, that the graft copolymer might still be capable of undergoing cross-linking via addition of a low molecular weight linear poly(vinlypyridine) (PVPy). This molecule should bind any copper around, as well as functionalize the palladium with additional open pyridine sites along the PVPy. The low molecular weight (ca. 2.0 * 10^4) PVPy was added to the polymer in ½ equivalent increments up to a total of 2 equivalents. However, there was once again no significant increase in solution viscosity.

6.8 Conclusions

In this chapter, a multifunctional polymeric system based on poly(norbornene) modified tri-block copolymers was introduced that employed functional groups along the same backbone that enabled cross-linking via functionalization as well as other functional groups that enabled the initiation of a second type of polymerization via copper(I) catalyzed ATRP to grow graft copolymers in a "grafting-from" motif. In keeping with the major hypothesis and goal of this thesis, engineering multiple functions into a single polymer system enhances the demonstration of the utility and potential of the concept of functionalizing polymers via side-chain metal coordination. It was shown that ATRP was unaffected by the presence of the SCS-palladium-based pincer functional groups, which had never been reported to date. However, the coordination behavior of the palladium-pincer complex did not behave as expected after the ATRP process had taken place, suggesting that some residual copper-based remnants from the ATRP reaction remained and were interfering. This graft co-polymer contains several different types of side-chain functionalities, and demonstrates the utility of side-chain functionalized polymers that perform many functions within the same system. The side-chains include the pincer complex, triethylene glycol spacers, and poly(*tert*-butyl acrylate) chains, and although it is still unclear which one is responsible for binding the residual copper ions, it seems likely that the glycol might be the reason. This situation might be alleviated if

these spacers were converted into non-polar side-chains, although water solubility via cleavage of the *tert*-butyl groups might be more difficult at that point.

No study to date has been published regarding ATRP in the presence of the palladium-pincer complex, and this chapter provides some useful insight into what is still a current challenge.

6.9 Experimental Section

All reagents were purchased either from Acros Organics or Aldrich. Tert-butyl acrylate was purified via extraction from a 6 % NaOH solution (3 x) and distillation from CaH_2. CuBr was purified by stirring in glacial acetic acid, followed by ethanol, and finally diethyl ether to obtain a white powder that was immediately stored in a nitrogen atmosphere. Toluene was dried via passage through copper oxide and alumina columns. NMR spectra were taken using a 300 MHz Varian Mercury spectrometer. All spectra are referenced to residual proton solvent. Mass spectral analyses were provided by the Georgia Tech Mass Spectrometry Facility using a VG-70se spectrometer. Gel-permeation chromatography (GPC) analyses were carried out using a Waters 1525 binary pump coupled to a Waters 2414 refractive index detector with methylene chloride as an eluant on American Polymer Standards 10 μm particle size, linear mixed bed packing columns. All GPCs were calibrated using poly(styrene) standards. Atlantic Microlabs, Norcross, GA, performed all elemental analyses.

Synthesis of bicyclo[2.2.1]hept-5-ene-2-carboxylic acid 2-(2-bromo-propionyloxy)-ethyl ester (2)

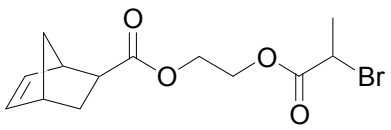

Bicyclo[2.2.1]hept-5-ene-2-carboxylic acid 2-hydroxy-ethyl ester (compound **6**, 3.0 g, 16.5 mmol) was combined with 2-bromopropionic acid (2.52 g, 16.5 mmol) and dimethylaminopyridine (100 mg, 0.82 mmol) in 50 mL CH_2Cl_2 and stirred for two minutes until the solution was homogeneous. Then a solution of dicyclohexylcarbodiimide (3.43 g, 16.6 mmol) in 5 mL CH_2Cl_2 was added, and the reaction mixture was stirred under argon at ambient temperature for four hours. Immediately upon addition the solution became warm and bubbles formed, but ceased after one minute, during which a white cloudy precipitate had begun to form. After four hours, the precipitate was filtered off and the reaction mixture was concentrated and purified by column chromatography (silica gel, hexane/EtOAc 3:1, $R_f = 0.6$). Pure **2** was collected as a clear light yellow oil (4.54 g, 14.3 mmol, 87 %). ^{1}H NMR (300 MHz, $CDCl_3$): δ = 6.15 (dd, 0.8H, J_1 = 5.6 Hz, J_2 = 3.0 Hz, endo vinyl), 6.10 (dd, 0.2H, J_1 = 5.6 Hz, J_2 = 2.9 Hz, exo vinyl), 6.07 (dd, 0.2H, J_1 = 5.4 Hz, J_2 = 3.0 Hz, exo vinyl), 5.89 (dd, 0.8H, J_1 = 5.6 Hz, J_2 = 2.8 Hz, endo vinyl), 4.39 (d, 0.2H, J = 6.9 Hz, exo), 4.35 (d, 0.8H, J = 6.9 Hz, endo), 4.29 (t, 1.6H, J = 4.7 Hz, endo, -C**H**$_2$O(CO)-), 4.22 (t, 1H, J = 4.7 Hz, methine, bromoester), 4.07-4.17 (m, 2H), 3.19 (br, 0.8H, endo, methine, norbornenyl ester), 3.02 (br, 0.2H, exo, methine, norbornenyl ester), 2.92-2.96 (m, 1H, norbornenyl), 2.87 (br, 1H, norbornenyl), 2.22 (dd, 0.2H, J_1 = 9.9 Hz, J_2 = 4.5 Hz, exo, norbornenyl), 1.84-1.91 (m, 1H, norbornenyl), 1.80 (d, 2H, J = 6.9, norbornenyl bridgehead), 1.67 (br, 0.2H, exo, norbornenyl), 1.23-1.40 (m, 3H, norbornenyl). ^{13}C NMR (100 MHz, $CDCl_3$): δ = 176.23, 174.68, 170.28, 138.11, 137.77, 135.68, 132.31, 70.60, 69.29, 68.77, 63.43, 49.57, 46.64, 46.26, 45.70, 43.14, 43.01, 42.47, 41.61, 39.85, 30.33, 29.22, 21.53.

Synthesis of 1,2,3-tris-(pyridine-4-carbonyloxy)-propyl ester (4)

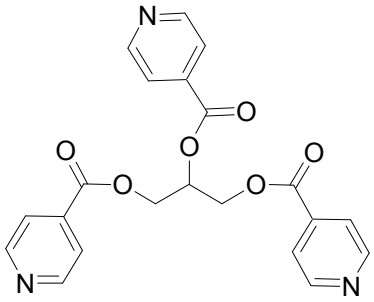

Triethylamine (15 mL) was added dropwise over a period of five minutes to a stirred suspension of glycerol (656 mg, 7.12 mmol) and isonicotinoyl chloride hydrochloride (8.87 g, 49.9 mmol) in THF (110 mL) at ambient temperature under argon, during which the color changed from orange to white, with white gas evolving. After addition was complete, the reaction mixture was refluxed for 18 hours, and the color became rusty orange. The reaction was carefully quenched with 20 mL of distilled water at 0 ^{o}C, and became homogeneous and purple. The solution was diluted with diethyl ether (100 mL) causing two layers to form. Sodium hydroxide (0.1 M) was added until the pH of the aqueous layer was approximately 10, and the layers were separated. The organic layer was saved, washed with brine, dried with $MgSO_4$, and the solvent removed to give a brown oil, which was exposed to vacuum (100 mTorr, 4 hours) to remove most of the residual triethylamine. The resulting brown oil was purified by column chromatography (stationary phase: neutral alumina, 80-200 mesh; mobile phase: 3:2 ethyl acetate/hexanes; R_f = 0.4) to give pure **4** (2.13 g, 5.24 mmol, 74 %) as a light orange oil that solidified upon standing overnight. ^{1}H NMR ($CDCl_3$, 300 MHz): δ = 8.77 - 8.74 (m, 6H, *o*-pyridine); 7.80 - 7.77 (m, 6H, *m*-pyridine); 5.85 - 5.79 (m, 1H, methine); 4.81 - 4.64 (ddd, 4H, J_1 = 31.1 Hz, J_2 = 12.6 Hz, J_3 = 4.2 Hz, methylene). ^{13}C NMR ($CDCl_3$, 100 MHz): δ = 164.83, 164.52, 151.01, 136.48, 122.98, 70.55, 63.47. MS (ESI) 408.2 (M+1). Elemental analysis for $C_{21}H_{17}N_3O_6$ calculated: C, 61.91; H, 4.21; N, 10.31; found: C, 62.28; H, 4.38; N, 10.19.

Synthesis of isonicotinic acid 3,4,5,6-tetrakis-(pyridine-4-carbonyloxy)-tetrahydro-pyran-2-ylmethyl ester (5)

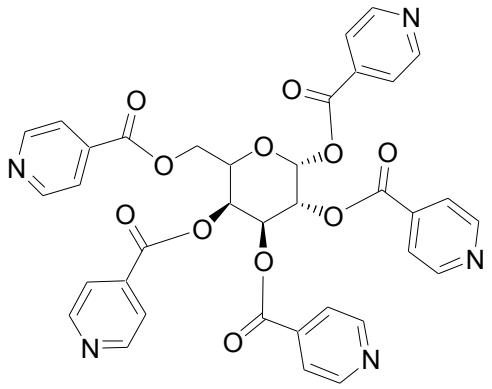

Triethylamine (25 mL) was added dropwise over a period of five minutes to a stirred suspension of D-galactose (686 mg, 3.81 mmol), isonicotinoyl chloride hydrochloride (6.13 g, 34.5 mmol), and dimethylaminopyridine (DMAP) (25 mg) in a solution mixture of THF (10 mL) and pyridine (35 mL) at 0 ^{o}C under argon, and the reaction allowed to stir for 20 minutes, after which the temperature was increased to 60 ^{o}C and the stirring continued for 24 hours. After several hours, the solution had turned red-purple, with a significant amount of precipitate having formed. After 24 hours, the reaction was cooled to ambient temperature and carefully quenched with 1M sodium hydroxide, until the pH of the aqueous phase was approximately equal to 10. The aqueous phase was extracted three times with methylene chloride, and all of the organic fractions combined, washed with twice 1M sodium hydroxide, and dried with $MgSO_4$. The residue was purified by column chromatography (stationary phase: neutral alumina, 80-200 mesh; mobile phase: ethyl acetate) to give pure **5** (457 mg, 0.65 mmol, 17 %) as a white solid. ^{1}H NMR ($CDCl_3$, 300 MHz): δ = 8.91-8.89 (m, 2H, *o*-pyridine); 8.85-8.67 (m, 8H, *o*-pyridine); 7.89-7.87 (m, 2H, *m*-pyridine); 7.73-7.57 (m, 8H, *m*-pyridine); 6.96 (d, 1H, J = 3.2 Hz); 6.85 (d, 0.5 H, J = 3.4 Hz); 6.77 (s, 0.5 H); 6.05 (qd, 2 H, J_1 = 10.4 Hz, J_2 = 2.6 Hz, methylene); 5.79 (m, 1 H, anomeric methine); 4.88-4.83 (m, 1 H, methine); 4.76-4.65 (m, 1H, methine); 4.50-4.44 (m, 1H, methine). MS (ESI) 706.2 (M+1).

Synthesis of macroinitiators

MI100

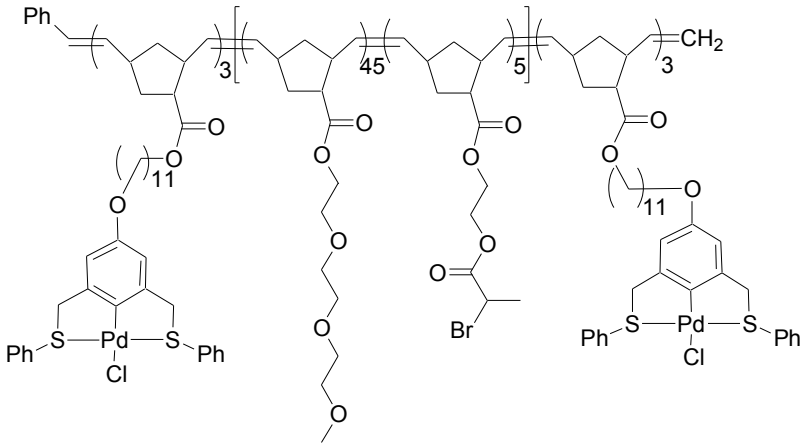

A solution of Grubbs' 3rd generation catalyst (65 mg, 0.07 mmol) in 1 mL of CH_2Cl_2 was added at once to a solution of **3** (170 mg, 0.2 mmol) in CH_2Cl_2, and stirred for one minute. Next, a combined solution of **1** (1.029 g, 3.6 mmol) and **2** (117 mg, 0.4 mmol) in 3 mL CH_2Cl_2 was added slowly over a period of 30 seconds, and stirred for another five minutes. Finally, a solution of **3** (170 mg, 0.2 mmol) in CH_2Cl_2 was added once again and stirred for another five minutes. The polymerization was quenched by addition of 0.3 mL of ethyl vinyl ether, and precipitated into methanol three times to afford **MI100** in 68 % yield. ^{1}H NMR ($CDCl_3$, 300 MHz): δ = 7.81 (s, br, 0.3H); 7.35 (s, br, 0.6H); 6.55 (s, br, 0.2H); 5.42-5.23 (m, br, 2H); 4.53 (s, br, 0.2H); 4.29-4.04 (m, br, 1.4H); 3.84-3.55 (m, br, 7.5H); 3.37-3.18 (s, br, 1.8H); 3.09-2.75 (m, br, 1.3H); 2.60-2.44 (s, br, 0.3H); 2.64-1.66 (m, br, 2.8H); 1.48-1.10 (m, br, 2.1H). Elemental analysis for $C_{17.39}H_{25.84}Cl_{0.11}Pd_{0.11}O_{4.70}S_{0.21}Br_{0.09}$ calculated: C, 61.57; H, 7.68; found: C, 61.55; H, 7.73.

MI25

Synthesis was carried out analogously to that of **MI100**, giving a 71 % isolated yield. The proton NMR spectrum was indistinguishable from that of **MI100**. Elemental

analysis for $C_{17.53}H_{26.52}Cl_{0.11}Pd_{0.11}O_{4.76}S_{0.21}Br_{0.02}$ calculated: C, 62.45; H, 7.87; found: C, 62.56; H, 7.72.

MI50

The synthesis was carried out analogously to that of **MI100**, giving a 58 % isolated yield. The proton NMR spectrum was indistinguishable from that of **MI100**. Elemental analysis for $C_{17.48}H_{26.15}Cl_{0.11}Pd_{0.11}O_{4.74}S_{0.21}Br_{0.04}$ calculated: C, 62.15; H, 7.80; found: C, 61.58; H, 7.57.

Synthesis of graft copolymers: G100

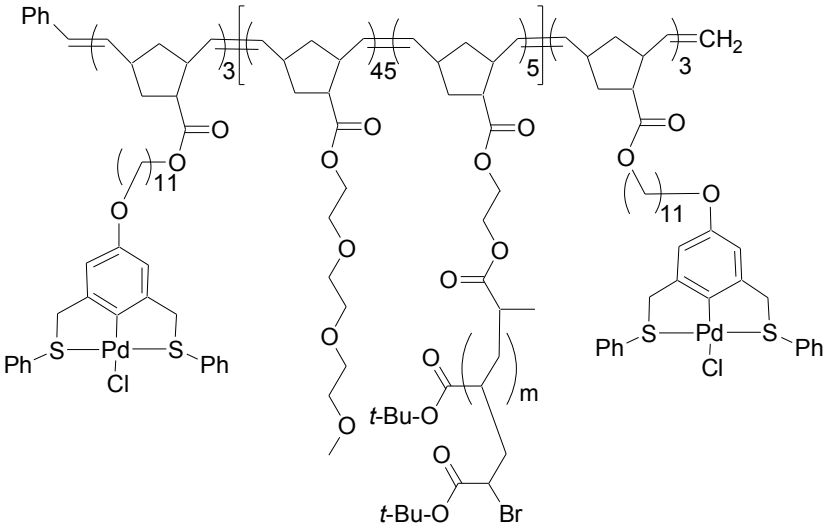

Macroinitiator **MI100** (150 mg) was dissolved in 3 mL toluene and 6 g of *tert*-butyl acrylate in a pre-dried flask, under nitrogen. In a second pre-dried flask was added CuBr (15.3 mg), Me_6TREN (24.6 mg) and *tert*-butyl acrylate (23.5 g), and the mixture stirred at 50 ^oC for 30 minutes under nitrogen to completely dissolve the catalyst. Then, 5 mL of the CuBr/Me_6TREN solution was added to the macroinitiator solution via syringe, and the reaction mixture was then degassed via three freeze-pump-thaw (<50 mTorr) cycles. The solution was then heated to 65 ^oC, and stirred for 24 hours, after which the reaction mixture was quenched by opening to air and cooling to ambient temperature. The

solution was filtered through silica gel, concentrated, and precipitated into a 50/50 mixture of water/methanol to give 1.22 g of **G100** as a light tan solid. ^{1}H NMR ($CDCl_3$, 300 MHz): δ = 7.81 (s, br); 7.36 (s, br); 6.61 (s, br); 5.43-5.16 (m, br); 4.56 (s, br); 4.30-4.03 (m, br); 3.87 (s, br); 3.65 (s, br); 3.55 (s, br); 3.49 (s, br); 3.18 (s, br); 3.09 (m, br); 2.76 (m, br); 2.24 (s, br); 1.89-1.73 (m, br); 1.53-1.29 (m, br).

6.10 References

(1) Matyjaszewski, K. *Macromolecules* **1998**, *31*, 4710-4717.

(2) Pintauer, T.; Matyjaszewski, K. *Coord. Chem. Rev.* **2005**, *249*, 1155–1184.

(3) Queffelec, J.; Gaynor, S. G.; Matyjaszewski, K. *Macromolecules* **2000**, *33*, 8629-8639.

(4) Neugebauer, D.; Matyjaszewski, K. *Macromolecules* **2003**, *36*, 2598-2603.

(5) Neugebauer, D.; Zhang, Y.; Pakula, T.; Matyjaszewski, K. *Macromolecules* **2005**, *38*, 8687-8693.

(6) Kriegel, R. M.; Rees, W. S., Jr.; Weck, M. *Macromolecules* **2004**, *37*, 6644-6649.

(7) Katayama, H.; Yonezawa, F.; Magao, M.; Ozawa, F. *Macromolecules* **2002**, *35*, 1133-1136.

(8) Li, M.-H.; Keller, P.; Albouy, P.-A. *Macromolecules* **2003**, *36*, 2284-2292.

(9) Coca, S.; Paik, H.; Matyjaszewski, K. *Macromolecules* **1997**, *30*, 6513-6516.

(10) Pollino, J. M.; Nair, K. P.; Stubbs, L. P.; Adams, J.; Weck, M. *Tetrahedron* **2004**, *60*, 7205-7215.

(11) Pollino, J. M.; Stubbs, L. P.; Weck, M. *J. Am. Chem. Soc.* **2004**, *126*, 563-567.

(12) Reinhoudt, D. N.; Timmerman, P.; Van Veggel, F. C. J. M. *NATO Ser. C: Math. Phys. Sci.* **1999**, *519*, 51-66.

(13) Pollino, J. M.; Weck, M. *Synthesis* **2002**, 1277-1285.

(14) Higley, M. N.; Pollino, J. M.; Hollembeak, E.; Weck, M. *Chem. Eur. J.* **2005**, *11*, 2946-2953.

(15) Love, J. A.; Morgan, J. P.; Trnka, T. M.; Grubbs, R. H. *Angew. Chem.* **2002**, *114*, 4207-4209.

(16) Jung, J.-C.; Jung, M.-H.; Baik, K.-H. *J. Photopolym. Sci. Tech.* **1998**, *11*, 481488.

CHAPTER 7

POLYMERS WITH SIDE-CHAIN FUNCTIONALIZATION VIA METAL COORDINATION: CONCLUSIONS AND POTENTIAL FUTURE DIRECTIONS

7.1 Abstract

This final chapter outlines the major conclusions and lessons learned from the science presented herein. This includes major advantages and methodologies involved, as well as areas and concepts that still remain a challenge. The second theme of this chapter is to provide an extension to the concepts already presented, with interesting future directions described and highlighted.

7.2 Introduction

The hypothesis addressed by this thesis was that combining multidentate metal complexes with living polymerization is useful for materials applications. Based on this hypothesis, this thesis was designed with the focus of improving and expanding the current technology of developing polymers and materials with useful functionalities, and this strategy was built around the transition metal coordination motif as a means to this goal. This aim was met and the hypothesis supported through the course of the research presented in this thesis, as is evidenced by the selected project highlights that will be discussed below. Several methodologies were employed to obtain the functionalized polymers described in this thesis, including all three of the strategies outlined in Chapter 1: (1) monomer functionalization, (2) polymer functionalization, and (3) various combinations of 1 and 2.

7.3 Overall Summary and Conclusions

Strategy 1, "pre-polymerization functionalization", was utilized by the work in Chapters 3 and 5, for several reasons.[1,2] First, neither the desired ruthenium or iridium coordination complexes form spontaneously under mild conditions. To form the $Ru(bpy)_3(PF_6)_2$ complex typically requires temperatures in excess of 100 ^oC, in a protic solvent such as ethanol or water. Analogously, synthesis of the desired *fac*-$Ir(ppy)_3$ also requires temperatures in excess of 100 ^oC. Thus it was desirable to perform this chemistry on the small molecules to both facilitate the purification of the polymer products, and to ensure full polymer functionalization.

Chapters 3 and 5 both outline the first examples of poly(norbornene)-supported $Ru(bpy)_3(PF_6)_2$ and $Ir(ppy)_3$ – type complexes. The polymeric supported iridium complexes showed adherence to the luminescence data for the small molecule analogues both in solution as well as in the solid state, demonstrating that the method of polymer functionalization described in Chapter 5 is an effective method to transform vacuum-deposited small molecules into solution-processable polymer supported complexes. During the course of the work in Chapter 3, a method for the polymerization of ROMP monomers with the 1st generation Grubbs' catalyst in the presence of 2,2'-bipyridine and other chelating ligands was developed.[2] The presence of ligands of this type typically poisons this catalyst, but it was shown that the addition of a small amount of trifluoroacetic acid to the polymerization mixture enabled full polymerization to take place without any additional modifications or precautions. The ability to carry out polymerizations in the presence of chelating ligands is important and highly relevant in the area of metal coordination-based functionalized polymers and materials design.

Conversely, the guar project described in Chapter 4 was built entirely upon Strategy 2, or "post-polymerization functionalization." As guar is a naturally occurring macromolecule, Strategy 2 was required. This project represented the first time that a naturally occurring polysaccharide such as guar had been modified with a chelating

ligand for the purpose of cross-linking or functionalization through subsequent metal ion chelation.[3] In order to gain an added element of control and minimize covalent chemical reactions on this large macromolecule, it was desirable to combine multiple levels of functionality onto the initial site on the guar molecule. An effective technique, used often by Nature as well as many scientists, is that of engineering multiple levels of functionalization into a single site. The modified guar was capable of again being modified by way of the initial functional group, thus allowing the cross-linking to take place. A limitation of this system exists in the solubility of guar, as it was only soluble in water. However, the functionalization was carried out in dry dioxane, which likely caused the polysaccharide to both aggregate as well as collapse to a smaller size, both of which limit the surface area with which a metal coordination site could be attached. Nonetheless, the functionalization was sufficient to achieve significant viscosity changes, even at the lower ligand loadings reported.

The work reported in Chapter 6 consisted of a substantial amount of both Strategies 1 and 2, and represented the first time that ATRP has been successfully carried out in the presence of the SCS-palladium pincer complex. This work also demonstrated the capability of the Grubbs' 3rd generation catalyst to form triblock copolymers as complex as those reported in Chapter 6, in air, with PDI's as low as 1.05. From a strategic perspective, the first step of synthesizing the functionalized monomers adhered to Strategy 1. Once polymerized, the newly formed macroinitiator was cross-linked via coordination of the pincer groups on the ends of the polymer, consistent at this point with Strategy 2. Additionally, the macroinitiator was used to initiate graft a copolymerization reaction in a "grafting from" methodology via ATRP, also consistent with Strategy 2, unless the perspective of macromonomer is applied in this case to the macroinitiator giving this step the appearance of Strategy 1 again.

The methods described herein to functionalize poly(norbornene)s and other polymers using transition metal coordination as the key step are easily adapted to an enormous

range of systems, as the method of ROMP polymerization used is gentle and tolerant to most ligands and metal complexes, especially with the advent of the 3rd generation Grubbs' catalyst. Metal coordination is a highly versatile method of functionalization as a wide range from very weak to very strong interactions can be achieved. The next section will address some of the ways that the work presented in this thesis can be expanded upon.

7.4 Potential Future Directions

The methodologies involved in the syntheses of the polymers and materials described herein open many doors to achieving further complexity and potential new applications and solutions to currently unsolved challenges. It is often through the creative combination of seemingly simple and common methods that ingenious ideas and designs arise. This section will attempt to describe a few potential extensions of the research in this thesis, as well as other new but related ideas, all within the scope of side-chain transition metal-based polymer functionalization.

7.4.1 Self-Assembly-Based Tuning of Luminescence

As demonstrated in Chapter 5, emissive species such as $Ir(ppy)_3$ and others can be tethered to polymer supports thus enabling solution processibility, etc.[1] However, in order to change the wavelength of the emissive output, a new copolymer formulation is needed, including additives, or changing the ligands altogether to higher or lower field ligands to alter the HOMO-LUMO gap of the complex and thus adjust the emission.[4-7] This raises the question: Is there a simpler way to alter the wavelength of the emission from polymer-bound metal complexes without having to design an entirely new system? To address this question, an initial ligand modification may be all that is required and can be accomplished before the synthesis of the polymer.

The idea combines the concept of self-assembly with the previously described polymer supported emissive complexes in this thesis. It is already well-known that changing the electronics of an emissive species has a great effect on the luminescent output.[6] It follows then that since there is much electronic interaction involved in metal coordination that a stable metal complex flanked with secondary coordination sites might be susceptible to electronic variations based on the self-assembly of various molecules to the secondary coordination sites, thus emitting light than is can be tuned by self-assembly (Figure 7.1).

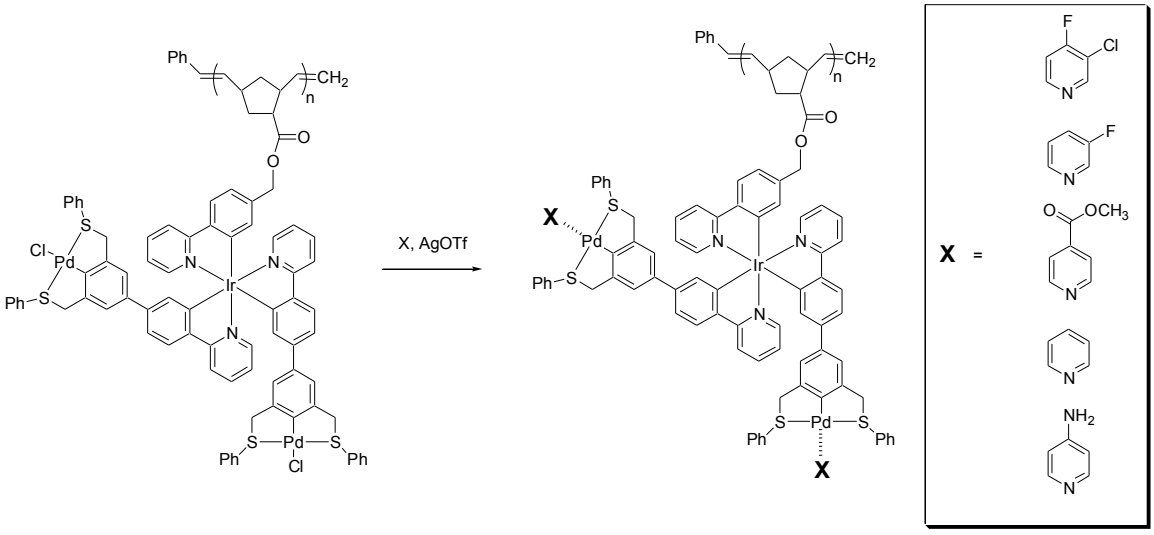

Figure 7.1. Design of self-assembly-tunable emissive polymeric metal complexes.

The design of this system is based on common methods and familiar molecules, combined in a way that might enable the tuning of this phosphorescence emission depending on the relative electron withdrawing or donating ability of the substituted pyridine that is self-assembled to the complex.

What gives this design potential is the robustness of the central iridium complex. Once formed, a wide array of chemical reactions can take place on or around the complex and the species will retain its integrity. As such, the iridium complex can be created prior to metallation with palladium so that there is no interference with the pincer ligand. Both

metal complexes have already been shown to be stable to ruthenium-mediated ROMP,[1,8,9] so once created, this monomer could be easily polymerized. The degree of emission tuning is unknown at this point. The library of potential pyridines might offer different enough electronics to the system to make a significant difference in the output. However, at this point, no report of a self-assembly-based emission tunable polymeric coordination complex has emerged in the literature.

7.4.2 Solving the Problems of Polymer-Bound Alq_3

Since Weck and co-workers reported the synthesis of polymeric Alq_3 complexes, a useful new methodology for spin coating and solution processing of this chromophore has come into being.[10,11] The advantages of tethering species such as Alq_3 to a soluble polymeric support have been described in detail throughout this thesis. However, several drawbacks still remain with this particular material, since it is apparently more labile than the complexes described in Chapters 3 and 5. Once the material is in the solid state, intermolecular cross-links prevent it from being re-dissolved. Additionally, just as is the case with $Ir(ppy)_3$, the facial isomer is more efficient than the meridional isomer,[5,12] and as such, the presence of any meridional isomer decreases the quality of the luminescent output.

These two points lead to the obvious questions of (1) can this cross-linking be eliminated, and (2) can the meriodional isomer also be eliminated? The following proposed system, based on polymeric side-chain functionalized metal complexes, gives a simple, yet efficient solution to both of these problems. It is the tris-hydroxyquinoline "claw" approach outlined in Figure 7.2 below:

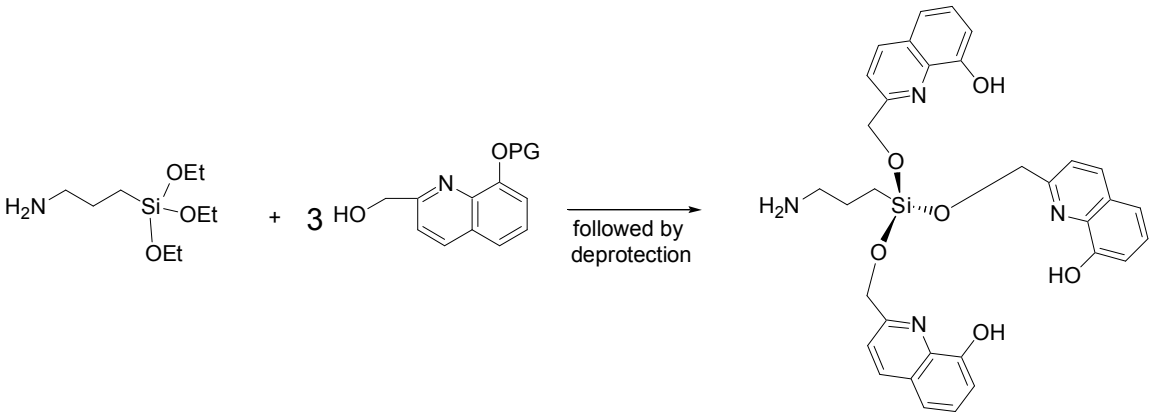

Figure 7.2. Schematic of the "claw" motif for polymer-bound Alq_3 complexes.

This basic idea is then easily functionalized to a norbornenyl ester, followed by alumination with $AlEt_3$, to form the target monomer (Figure 7.3).

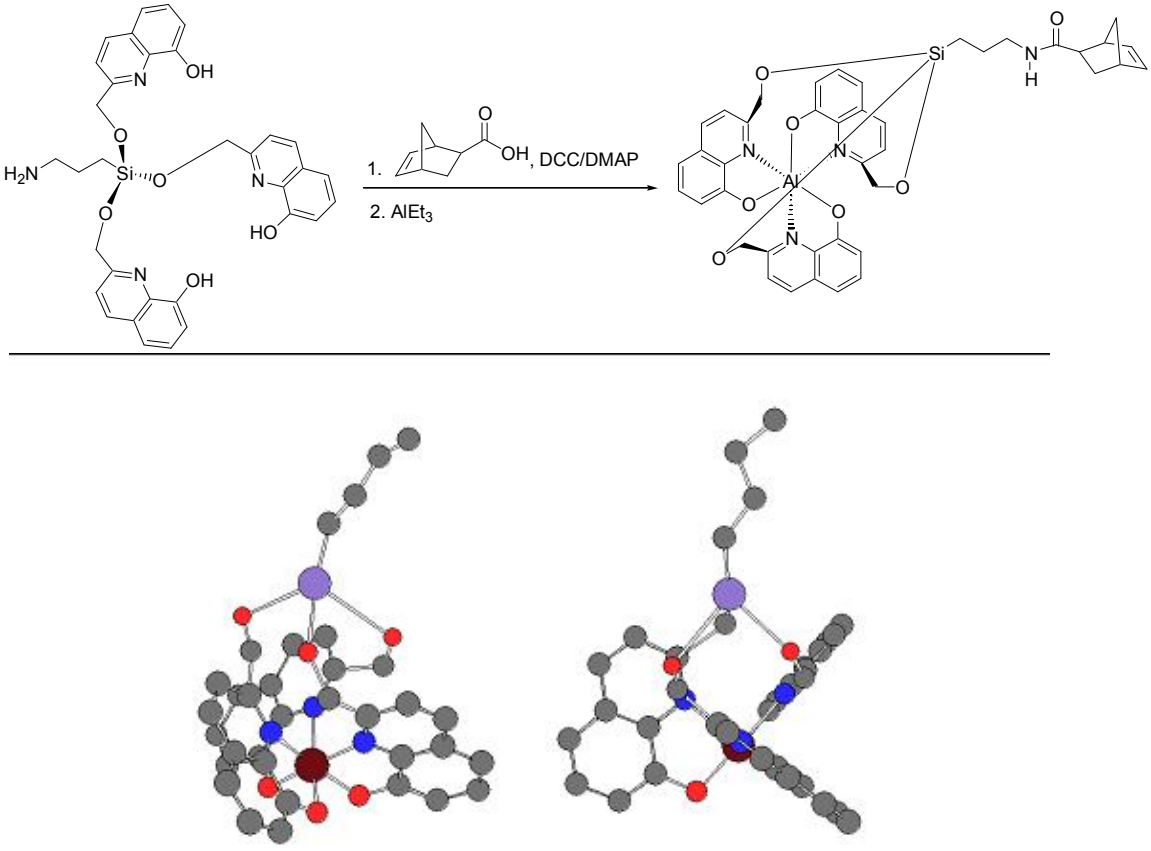

Figure 7.3. Formation of the improved Alq_3 monomer (top); 3-dimensional representation of the coordination environment (bottom) (on bottom picture: norbornenes left out for clarity)

The above picture gives a better idea of the actual benefits that might be gained from this methodology. First, there is a large "chelate effect" for the entire set of three ligands since if one dissociates, it does not go far enough away to allow for cross-linking, so this problem is circumvented by this strategy. Second, by the three-dimensional images it can be seen that this type of tethering does not put any excess strain on the complex that might impede the formation of the chromophore. Finally, it can be seen that the configuration of ligands within the "claw" motif allows solely for the facial isomer to form. There is no potential for meridional isomer formation due to the short linkers between the silicon atom and the ligands, and so the problem of eliminating the meridional isomer is solved as well by this methodology.

7.4.3 Potential Directions for Macromolecular Cross-Linking

High molecular weight polymers are desirable in a number of industrial applications such as paper making, waste water treatment, mining, and a great many others. Lower molecular weight polymers can be transformed into high molecular weight polymers by end-to-end attachment or backbone elongation, as well as intermolecular cross-linking via the side-chains. From the preliminary data described in Chapter 6, the graft copolymers experienced little to no cross-linking upon addition of the cross-linking agent (multi-pyridine molecule) due to residual copper ion from the ATRP process interfering with this incoming base. However, this system still represents a great deal of potential for future development by improving upon the cross-linking motif. Possible improvements include choosing a new metal-ligand couple, that is less sensitive to copper ion, such as replacement of the palladium pincer moiety with a 2,2'-bipyridine or 2,2',2"-terpyridine functionality (Figure 7.4).

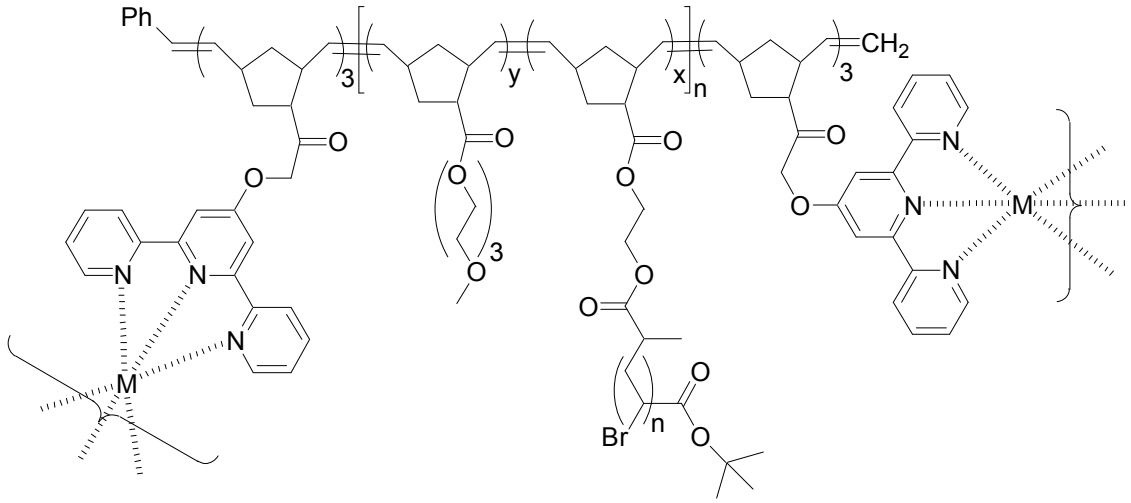

Figure 7.4. Alternative cross-linking methodology using 2,2',2"-terpyridine (shown) or 2,2'-bipyridine units in place of the palladium pincer moiety. (M = transition metal)

The primary way that copper ion might interfere in this case would be coordination with the new ligand and thus spontaneous cross-linking, but this has been shown to be fully reversible by addition of EDTA or HEEDTA,[13,14] thus giving an additional element of control to the cross-linking event.

It is also conceivable that the macromolecules might be large enough as to make it difficult for the end groups to find each other. This possibility might be addressed by placing the cross-linking moieties on the ends of the grafts instead of the backbone, thus creating more easily accessible sites through which to cross-link (Figure 7.5).

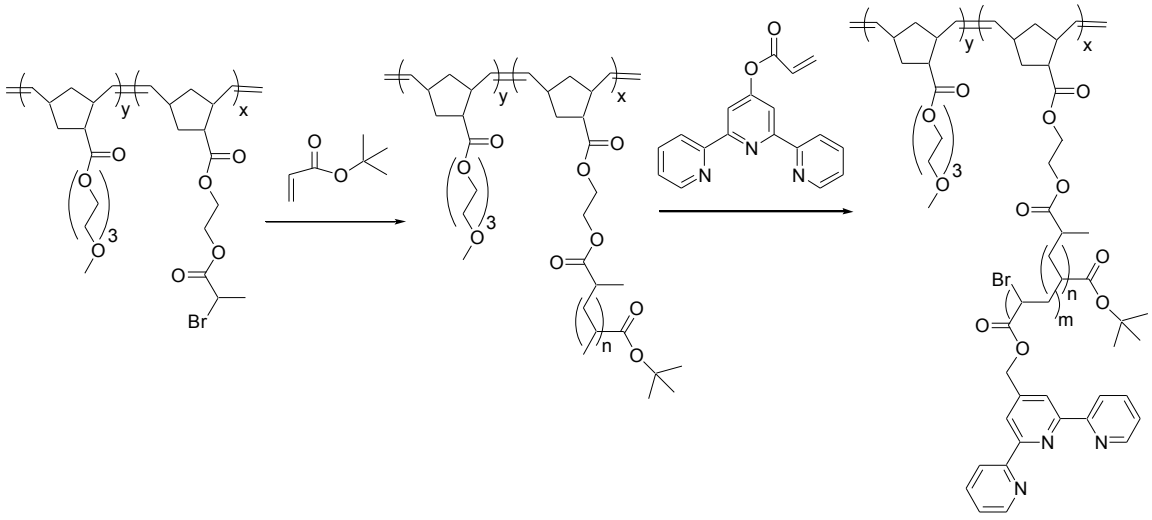

Figure 7.5. Placement of cross-linking moieties on ends of graft chains instead of on the ends of the parent backbone (m = 0-3, n = 100-500).

An interesting tangent to this work arises upon consideration of the hurdles that have arisen with regards to the joining together of very small pieces of rather large structures. Specifically, as polymers increase in size, the probability that two chain ends will come into contact with each other decreases, making it increasingly more difficult to create end-to-end combinations of polymers, such as the one attempted in Chapter 6 using the palladium-based pincer/pyridine couple (although residual copper was likely a major hurdle as well). If high molecular weight polymers are desired by means of end-to-end coordination of ligand-functionalized polymers, it may be possible to increase the efficiency of the process of end-to-end polymeric assembly by harnessing the power of hydrogen-bonding as a type of "guide" that will help long polymer chain ends to find each other, and then once there, create a more permanent linkage via metal coordination (Figure 7.6).

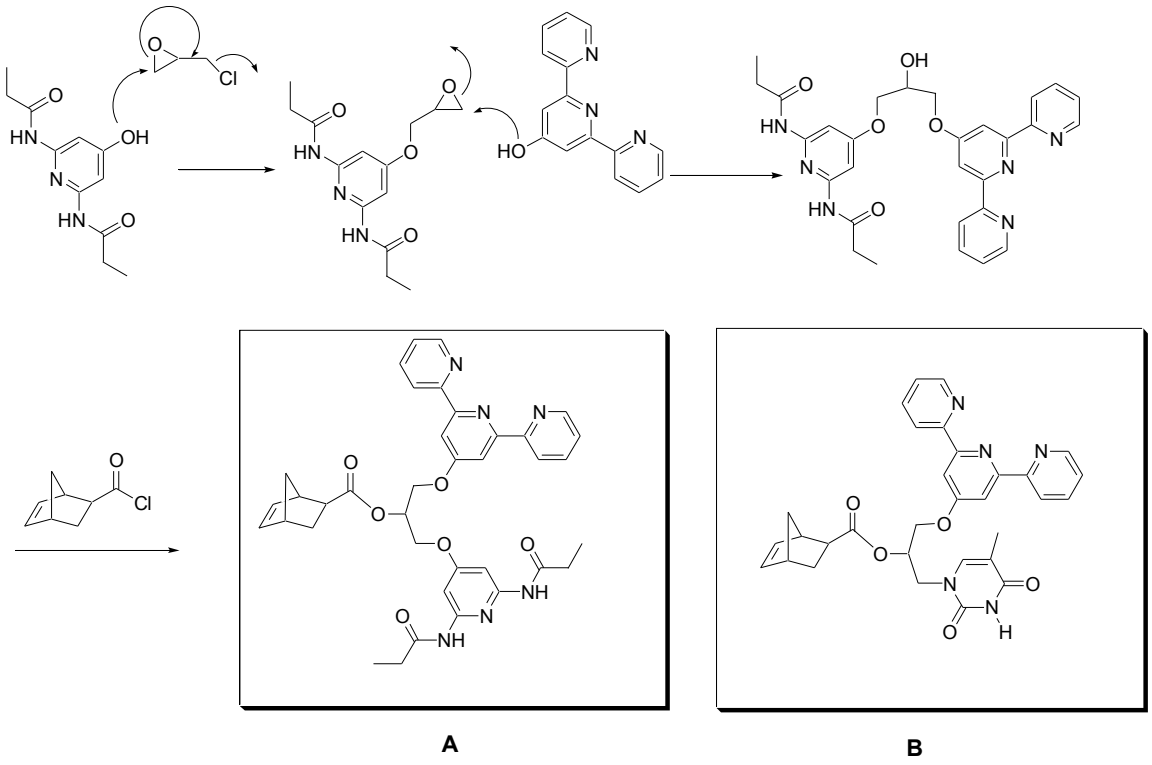

Figure 7.6. Synthesis of potential hydrogen-bond "guided" monomers for use in metal coordinated high molecular weight polymers. Possible sequence order would be (1) diaminopyridine monomer (A) on left (synthesis shown), followed by a water soluble spacer such as a triethylene glycol monomer, followed by thiamine monomer (B) on left (synthesis not shown, analogous to A).

The hydrogen-bonding moiety therefore will act as a type of intermediary structure that helps to bring together the chain ends that are otherwise so far apart that they are much less likely to combine in the absence of the moiety. Once the polymer is created (Figure 7.7), hydrogen bond linkages begin to join the chain ends and increase molecular weight.

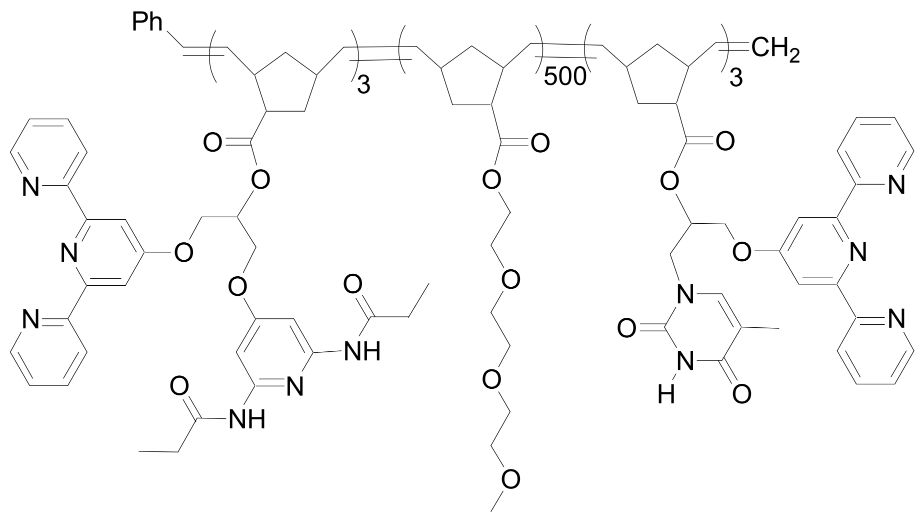

Figure 7.7. Schematic of polymer designed for metal coordination-based chain extension via end-to-end coupling. Hydrogen bonding moieties are included to assist in end-to-end coupling once the chain becomes significantly long.

Then upon addition of a metal ion, stable end-to-end links are formed. The newly formed high polymer should possess water stability, given that the polymer itself is designed to be soluble in water, such as that which uses triethylene glycol spacer units along the bulk of the backbone. This strategy may open a new door to water soluble high polymers.

7.5 Conclusions

The possibilities for interesting polymeric designs with metal coordination as a major theme is limitless. This thesis has demonstrated several circumstances where side-chain functionalization via transition metal coordination was used to create new polymers and materials. By taking Nature's lead, technology has advanced in recent years to the point where multiple tiers of polymer and macromolecular functionalization through various differing modes of interactions are being exploited more successfully. As suggested in this chapter, every new lesson inspires and reveals more than it was thought could be possible. Polymeric supermolecular and supramolecular functionalization has had a profound influenced the world over, and shows no signs of slowing down. Side-chain

functionalized polymeric metal complexes are part of this technology that is becoming more prominent every day. This field, having been so inspired by Nature, has become nearly as ubiquitous in our modern society.

7.6 References

(1) Carlise, J. R.; Wang, X.-Y.; Weck, M. *Macromolecules* **2005**, *38*, 9000-9008.

(2) Carlise, J. R.; Weck, M. *J. Polym. Sci. Part A: Polym. Chem.* **2004**, *42*, 2973-2984.

(3) Norman, L. R.; Carlise, J. R.; Concepcion, J. J. C.; Rees, W. S. j.; Weck, M.; (USA). Application: US
US, 2005; pp 7 pp.

(4) Frampton, M. J.; Namdas, E. B.; Lo, S.-C.; Burn, P. L.; Samuel, I. D. W. *J. Mater. Chem.* **2004**, *14*, 2881-2888.

(5) Segal, M.; Baldo, M. A.; Holmes, R. J.; Forrest, S. R.; Soos, Z. G. *Phys. Rev. B* **2003**, *68*, 075211.

(6) Beeby, A.; Bettington, S.; Samuel, I. D. W.; Wang, Z. *J. Mater. Chem.* **2003**, *13*, 80-83.

(7) Lamansky, S.; Djurovich, P.; Murphy, D.; Abdel-Razzaq, F.; Lee, H.-E.; Adachi, C.; Burrows, P. E.; Forrest, S. R.; Thompson, M. E. *J. Am. Chem. Soc.* **2001**, *123*, 4304-4312.

(8) Pollino, J. M.; Nair, K. P.; Stubbs, L. P.; Adams, J.; Weck, M. *Tetrahedron* **2004**, *60*, 7205-7215.

(9) Pollino, J. M.; Weck, M. *Synthesis* **2002**, 1277-1285.

(10) Meyers, A.; Weck, M. *Macromolecules* **2003**, *36*, 1766-1768.

(11) Meyers, A.; Weck, M. *Chem. Mater.* **2004**, *16*, 1183-1188.

(12) Wang, X.-Y.; Weck, M. *Macromolecules* **2005**, *38*, 7219-7224.

(13) Hofmeier, H.; Hoogenboom, R.; Wouters, M. E. L.; Schubert, U. S. *J. Am. Chem. Soc.* **2005**, *127*, 2913-2921.

(14) Schmatloch, S.; Gonzalez, M. F.; Schubert, U. S. *Macromol. Rapid Commun.* **2002**, *23*, 957-961.

APPENDIX A

SYNTHESIS AND HYDROLYSIS BEHAVIOR OF SIDE-CHAIN FUNCTIONALIZED NORBORNENES

A.1 Abstract

The stabilities of various functionalized norbornenes that are monomers for the ring-opening metathesis polymerization (ROMP) in aqueous solution were evaluated towards hydrolysis under a range of temperatures (37 ^{o}C, 60 ^{o}C, 80 ^{o}C) and pH values (3-9). All monomers contain hydrolysable linkages to pendant functional groups, and conclusions were drawn relating to how the chemical diversity of these pendant functional groups, in accordance with the pH and temperature variations, affect hydrolysis of the aforementioned linkages. The hydrolysis was monitored by reverse phase HPLC analysis, and/or NMR spectroscopy. As expected, monomers containing ester linkages were fairly labile at higher pH values, while acetal-based linkers were cleaved at lower pH values. β-amino ester groups experienced a significant increase in hydrolysis rate, while carboxylic acid containing monomers did not follow any clear trend. Saccharide-containing monomers exhibited unique behaviors for various pH values and temperature ranges. The work presented in this chapter resulted from a collaborative effort with Dr. Robert M. Kriegel (Georgia Inst. of Tech.) who synthesized and measured the hydrolyses of several compounds noted herein.

A.2 Introduction

Norbornene has been used extensively as a monomer for ring-opening metathesis polymerization (ROMP) across a broad spectrum of applications,[1-4] in fields as diverse as drug delivery[5] and biochemical applications,[6-13] luminescent materials and devices,[14-

[21] liquid crystalline[22-29] and non-linear optical materials,[30,31] and polymer-supported catalysis.[32-43] Poly(norbornene) has also constituted the majority of polymeric designs in Chapters 3-6 in this write-up thus far. This is in part due to the fact that ROMP is a highly efficient method of polymerization, both in organic and aqueous media, the latter being a convenient route towards a number of biologically relevant materials.[6-13] For example, poly(norbornene) homo- and co-polymers substituted with oligopeptides have been used to study competitive inhibition of fibroblast cell adhesion.[10] In another example, Kiessling and co-workers have used ROMP for the synthesis of neoglycopolymers to study cellular binding with L-selectin, a surface protein.[12]

It is well-known that polymer degradation is the major cause for change or loss of materials properties in many poly(norbornene) based materials.[44-47] A primary mode of degradation of poly(norbornene)s in biological applications might be the hydrolysis of water-labile moieties within the polymer. In most norbornene monomer designs a linkage between the polymerizable group and the functional moiety is introduced.[4] The choice of linker is crucial since it will influence and partially determine the conditions under which hydrolysis occurs. In the vast majority of cases these linkages are carboxylic esters, with other functionalities such as ethers, pure alkyl chains, amides, etc. being the exception.[1-4] Esters are known to be sensitive to hydrolysis under both acidic and basic conditions, and depending upon the structure can hydrolyze in minutes (esters that give strong acids and stable anions) or be stable for years (hydrophobic esters of weak acids).[48,49] Another important functional group in biomaterials containing biological moieties such as saccharides are acetals. In contrast to esters, acetals can be cleaved rapidly in strongly acidic aqueous media and are stable to basic conditions. Additionally, the structure of a neighboring functional group greatly influences the hydrolysis rate through steric and hydrophobic interactions but also by the stability of the charged intermediates.[50,51]

A detailed study of the hydrolytic stability of functionally diverse norbornene monomers is of utmost importance in order to be able to predict and tailor important

polymer properties in aqueous solution and to relate polymer performance to function. Despite the extensive use of functionalized poly(norbornene)s in biomaterials, no study has been carried out to gain a deeper understanding of the hydrolysis behavior of these materials. This report provides a study of the hydrolysis behavior of various norbornene-base monomers, with a variety of linker choices and pendant functional groups, each one being subject to a range of pH values and temperatures.

A.3 Design Strategy

In order to gain a better understanding of the hydrolysis behavior of norbornene monomers in aqueous media, where hydrolysis may have the most significant influence on polymer performance and properties, linkers and functional moieties had to be chosen that were both water soluble and hydrolysable. All monomers studied herein contain a norbornene as the polymerizable unit. Spacer molecules, such as ethylene glycols and pure alkyl chains are attached to the norbornene via carboxylic ester linkages. Finally, several functional groups are introduced at the end of the spacer molecules. Figure A1 outlines the general monomer design and describes the library of monomers that were studied. Two common functionalities within the linkers were examined: esters and acetals. The terminal functional groups that have been employed in our design include saccharides, acids, esters, and amines. Galactose was chosen as the saccharide functional group because it has been shown by Kiessling and coworkers that 7-oxonorbornene polymers with pendant galactoses are very potent binding agents to cellular recognition sites.[52-54] The use of these oligo- or poly saccharides to deliver drugs to specific sites at cellular surfaces, or to the cellular interior *via* endosomal transport is advantageous, provided that the drug can be cleaved efficiently from the polymer backbone. Other pendant functional groups employed in this study are carboxylic acids, ethers, and tertiary amines. These side-chain models represent a wide range of functional groups and

interactions and will allow for insight into the effect of functional groups on the hydrolysis behavior of functionalized norbornenes.

Table A1. Building blocks **1** and **2**, along with monomers **3 - 9**, for which the hydrolysis behavior was investigated in this study. The compound number on the left corresponds with a specific combination of tethers to norbornene, hydrolysable linkages, and functional groups, which are depicted in Figure A1 († synthesized by R. Kriegel[55]).

Compound	**Tether (R)**			**Linkage (R')**		**Functional Group (R")**		
	type	*n*	*R′*	*type*	*R″*	*type*	*m*	*R‴*
1	I	3	OH	---	---	---	---	---
2	I	2	Cl	---	---	---	---	---
3	I	3	OCH_3	---	---	---	---	---
4, 5†	I	2	R'	III	R"	I	2	OCH_3
6†	I	3	R'	I	R"	I	2	OCH_3
7	I	3	R'	I	R"	II	---	---
8	I	3	R'	I	R"	III	---	---
9†	II	1	R'	II	R"	I	3	OCH_3

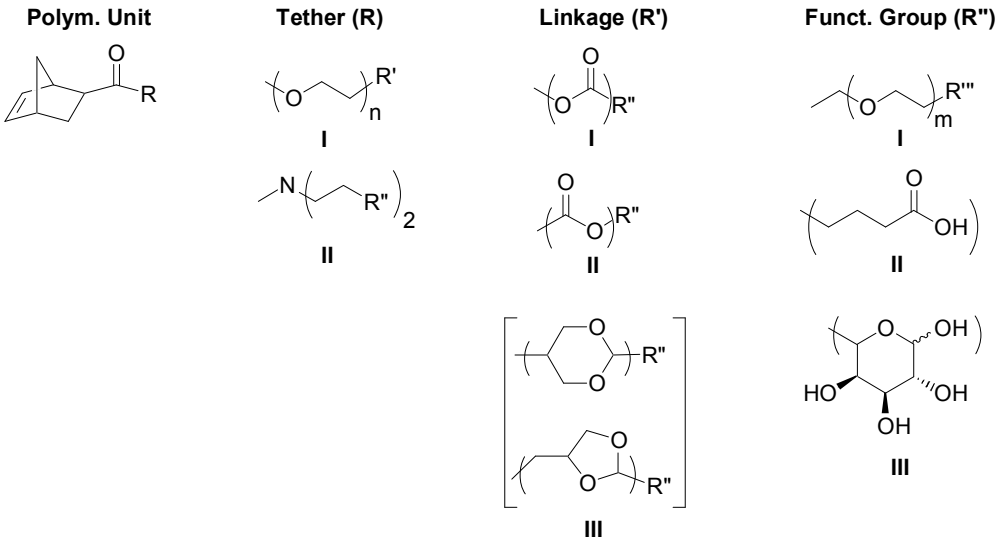

Figure A1. Structures corresponding with combinations in Table A1.

A.4 Monomer Syntheses

A.4.1 Synthesis of Norbornene PEG Esters 1 - 3.

Synthesis of norbornene derivatives **1** - **3**, norbornene triethylene glycol ester derivatives, were accomplished by treatment of the norbornene acyl chloride **10**[56] with triethylene glycol, 2-(2-chloroethyoxy)ethanol, and triethylene glycol methyl ether, respectively (Scheme A1), giving yields in excess of 70%. The synthesis of compounds **1** - **3** resulted in mixtures of *endo*/*exo* isomers in approximately 4:1 ratios.

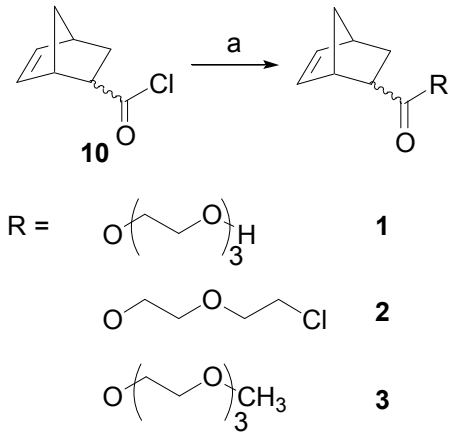

Scheme A1. Synthesis of norbornene spacer molecules **1**, **2**, and **3**. **1**: a = triethylene glycol (excess), THF, triethyamine; **2**: chloroethoxyethanol, triethylamine, THF; **3**: triethylene glycol monomethyl ether, triethylamine, THF.

A.4.2 Synthesis of Norbornene monomers containing PEG-Ester and Acid-Ester in their side-chains: Monomers 6 and 7

The esterfication of **1** with 2-[2-(2-methoxyethoxy)ethoxy]-acetic acid was carried out at ambient temperatures using DCC/DMAP in CH_2Cl_2 to give the PEG-ester monomer **6** in 52% yield (R. Kriegel)[55]. Compound **7** was synthesized by the reaction of **1** with glutaric anhydride in 82% yield (Scheme A2).

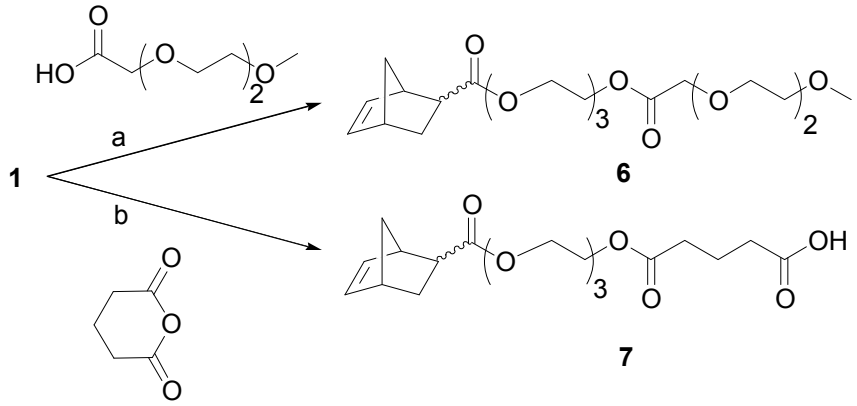

Scheme A2. Synthesis of compounds **6** and **7**: a.) DCC, DMAP, CH_2Cl_2; b.) pyridine, THF.

A.4.3 Synthesis of Norbornene linked to galactose *via* triethylene glycol ester: Monomer 8

The synthesis of **8** started with the oxidation of 1,2:3,4-di-*O*-isopropylidene galactopyranose using Jones conditions to give **14** in 81% yield.[57] Coupling of **14** to **1** using DCC/DMAP gave the acetal protected saccharide ester **15** in 60% yield. Removal of the acetal protecting groups to give the free tetra-ol **8** (Scheme A3) was achieved by treatment of **15** with 80% TFA (aq.). Conversion after one hour is 100% by NMR analysis but isolation and purification of the product resulted in lower yields (84%).

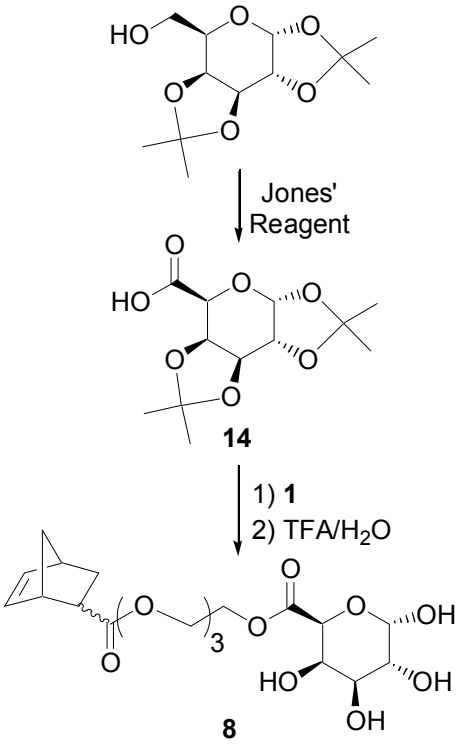

Scheme A3. Synthesis of compound **8**.

A.4.4 Synthesis of Monomer 9

Synthesis of **9** required the triethylene glycol monomethyl ether monoacrylate **16**, which was synthesized from the condensation of triethylene glycol monomethyl ether and acryloyl chloride in 84% yield. Addition of two equivalents of **16** to ethanolamine at

room temperature gave the bis-Michael addition product **17** in nearly quantitative yield (97%) after 24 hours. Coupling of **17** to **10** in THF with triethylamine at ambient temperature gave product **9** in 64% yield after chromatography (Scheme A4).

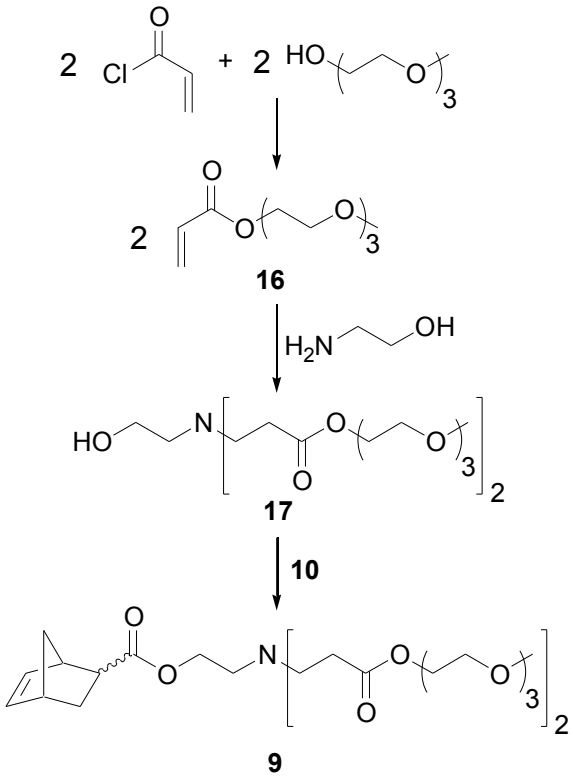

Scheme A4. Synthesis of compound **9**.

A.5 Hydrolysis.

To investigate the effect of pH on the hydrolysis of compounds **3** - **9**, measurements were carried out in the range of pH 3.1 to 8.9. A phosphate/citric acid buffer was used for pH 3.1, acetate buffers were employed for pH 4.6 and pH 5.6, phosphate buffers for pH 6.9 and pH 7.4 and borate buffer for pH 8.9. All buffers were made to 0.1 M ionic strength, with the exception of pH 7.4, which was an isotonic phosphate buffered saline solution. Solutions of 5 mM analyte were employed to give conditions that would result in pseudo-first order kinetics. Temperatures of 80, 60, and 37 °C were investigated to study the influence of temperature on the hydrolysis rate. The hydrolysis rates were

measured by HPLC analysis using refractive index and/or UV detection and/or proton NMR.

A.5.1 Hydrolysis of 4 and 5.

The hydrolysis data for monomers **3**, **4** and **5** (collected by R. Kriegel)[55] are shown below.

Table A2. Hydrolysis data for a mixture of compounds **4** and **5**.

Compounds **4** and **5**, 80 ºC			
pH	k (h^{-1})	R^2	$t_{1/2}$ (h)
3.1	0.341	0.988	2.0
4.6	0.040	0.977	17
5.7	0.030	0.975	23
6.9	0.035	0.976	20
7.4	0.059	0.982	12
8.9	0.850	0.943	0.82
Compounds **4** and **5**, 60 ºC			
3.1	0.215	0.991	3.2
4.6	0.022	0.995	32
5.7	0.012	0.992	58
6.9	0.012	0.996	58
7.4	0.043	0.996	16
8.9	0.513	0.996	1.4

Table A2 (continued). Compounds **4** and **5**, 37 ºC			
3.1	0.079	0.996	8.8
4.6	0.0089	0.994	78
5.7	0.0013	0.942	530
6.9	0.0024	0.996	290
7.4	0.0031	0.988	220
8.9	0.319	0.994	2.2

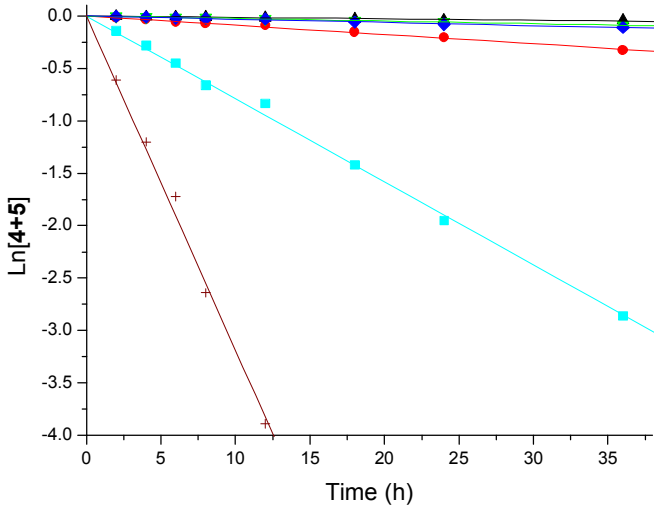

Figure A2. Pseudo-first order hydrolysis kinetics for compounds **4** and **5** at 37 ºC. pH 3.1, • pH 4.6, Δ pH 5.6, ∇ pH 6.9, ♦ pH 7.4, + pH 8.9.

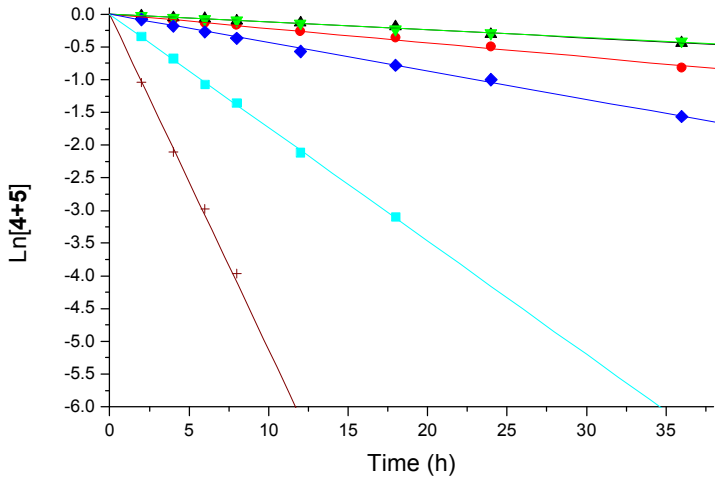

Figure A3. Pseudo-first order hydrolysis kinetics for compounds **4** and **5** at 60 ºC. pH 3.1, • pH 4.6, Δ pH 5.6, ∇ pH 6.9, ♦ pH 7.4, + pH 8.9.

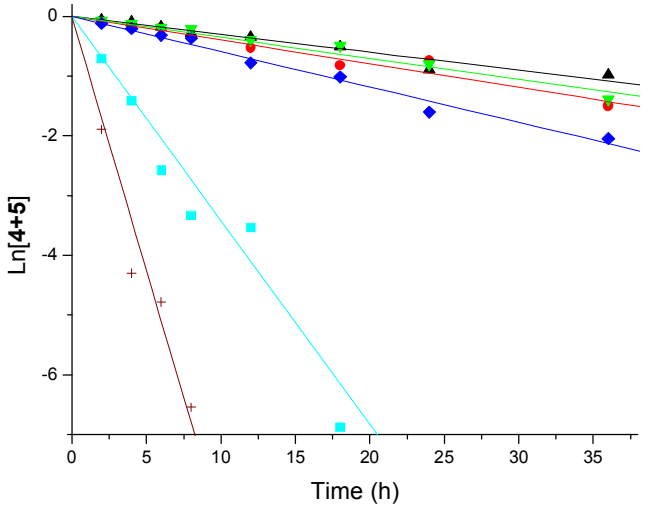

Figure A4. Pseudo-first order hydrolysis kinetics for compounds **4** and **5** at 80 ºC. pH 3.1, • pH 4.6, Δ pH 5.6, ∇ pH 6.9, ♦ pH 7.4, + pH 8.9.

The acetal moiety is well known for its rapid hydrolysis at low pH values, as well as its relative stability in alkaline media. This common characteristic of acetals matches well with our hydrolysis data for compounds **4** and **5**, at all temperature ranges (Figures

A2 – A4), where at low pH, rapid acetal hydrolysis is observed. The monomer was substantially more stable in both weakly acidic, as well as neutral aqueous solutions, but showed rapid decomposition at pH 8.9. In terms of the acetal group, this effect cannot be explained. To investigate if the hydrolysis occurs at the ester linkage to the norbornene instead of at the acetal for this set of circumstances, monomer **3** was synthesized, with a triethylene glycol monomethyl ether chain directly linked to the norbornene polymerizable unit *via* an ester. This monomer models the ester linkage of **4** and **5** without any further hydrolysable moieties. The hydrolysis behavior of this monomer at 60 and 80 ºC correlated closely with the unexpected hydrolysis data observed for **4** and **5** at pH values of 8.9, giving a plausible explanation: cleavage of the base-labile norbornene ester bond is occurring at this slightly basic pH value. In **3** the pH value of 8.9 is the only set of conditions where hydrolysis is achieved fairly rapidly, due to the base-sensitivity of the ester (Figures A5 and A6 and Table A3). This suggests that the same hydrolytic cleavage of the ester may be occurring for **4** and **5**. At low pH, cleavage of the acetal is the dominant decomposition pathway, while at high pH ester hydrolysis predominates.

Table A3. Hydrolysis data of compound **3**.

Compound **3**, 80 ºC			
pH	k (h^{-1})	R^2	$t_{1/2}$ (h)
3.1	0.027	0.943	27
4.6	0.014	0.980	50
5.7	0.010	0.976	70
6.9	0.026	0.990	27
7.4	0.040	0.990	17

Table A3 (continued). Compound **3**, 80 ºC

8.9	2.15	0.996	0.32
Compound **3**, 60 ºC			
3.1	0.018	0.994	39
4.6	0.0071	0.992	98
5.7	0.0069	0.992	100
6.9	0.019	0.982	36
7.4	0.024	0.986	29
8.9	0.632	0.946	1.1

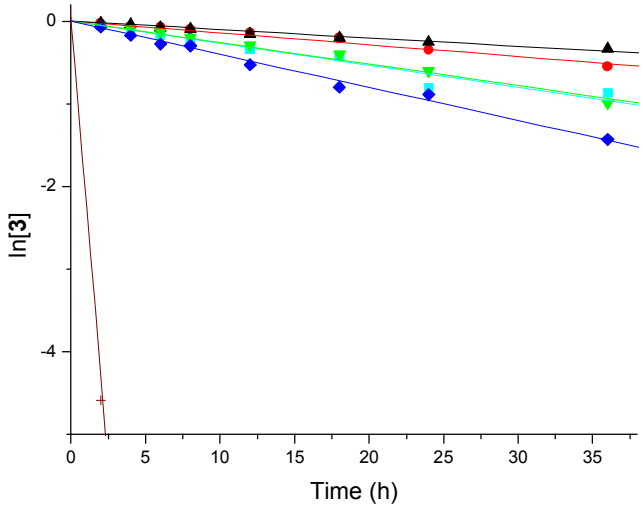

Figure A5. Pseudo-first order hydrolysis kinetics for compound **3** at 80 ºC. pH 3.1, ● pH 4.6, Δ pH 5.6, ∇ pH 6.9, ♦ pH 7.4, + pH 8.9.

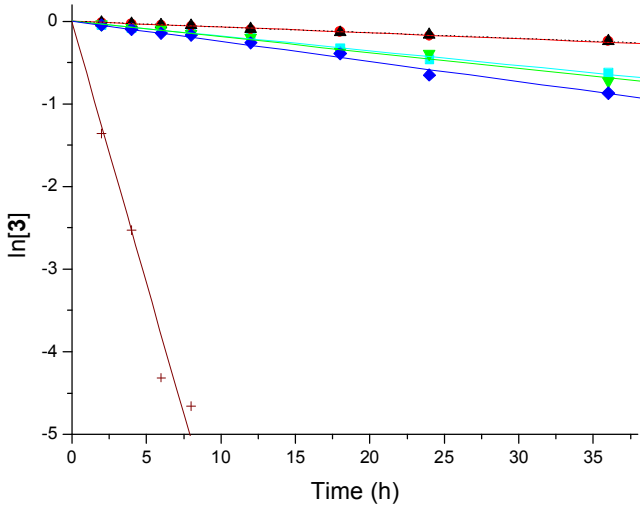

Figure A6. Pseudo-first order hydrolysis kinetics for compound **3** at 60 ºC. pH 3.1, • pH 4.6, Δ pH 5.6, ∇ pH 6.9, ♦ pH 7.4, + pH 8.9.

A.5.2 Hydrolysis of 6

The hydrolysis data for compound **6** was collected by R. Kriegel.[55] The dependence of the hydrolysis of **6** on pH and temperature is shown in Figures 7, 8, and 9 and Table 4. At 80 °C, hydrolysis of **6** at pH 8.9 was rapid, with a 45 to 50% loss in two hours. Under acidic conditions, the rate of hydrolysis is consistent with the expected trend of the rate being inversely proportional to pH. At near neutral or basic pHs, the rates of hydrolysis are greatly enhanced when compared to data collected at low pH conditions (Figure A7). Complete loss of **6** was seen within 18 hours near pH 7 and 80 °C. This does not correlate with the accepted mechanisms of ester hydrolysis under either acidic or basic conditions, which depend upon an increase in electrophilicity of the carbonyl by protonation under acidic conditions, or by the relatively high nucleophilic character of hydroxide compared to water, under basic conditions. The rate would be dependant upon the nucleophilic character of water, which should produce exceedingly slow reactions. The accelerated rates near pH 7 suggest that the buffer identity might play a significant

role in the hydrolysis mechanism at this pH. The same trends were observed for the hydrolysis at 60 °C (Figure A8) and at 37 °C (Figure A9). The pseudo-first order half-lives range from 6-20 hours.

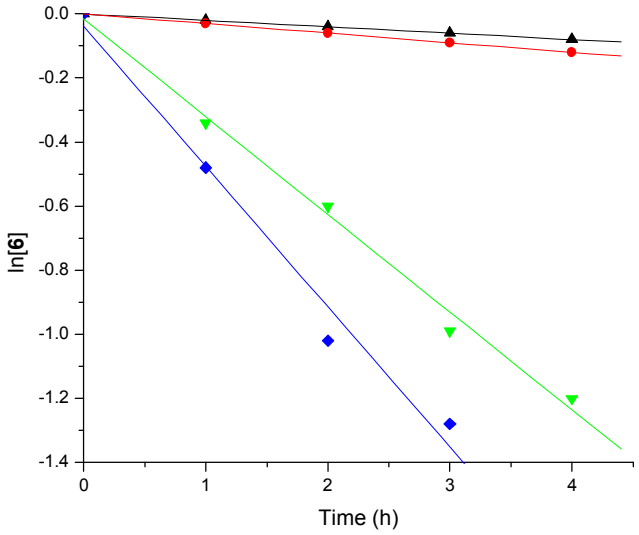

Figure A7. Pseudo-first order hydrolysis kinetics for compound **6** at 80 ºC. • pH 4.6, Δ pH 5.6, ∇ pH 6.9, ♦ pH 7.4.

Table A4. Hydrolysis data for compound **6**.

80 ºC			
pH	k (h^{-1})	R^2	$T_{1/2}$ (h)
4.6	0.044 ± 0.002	0.989	15.8
5.7	0.034 ± 0.001	0.994	20.7
6.9	0.311 ± 0.014	0.994	2.2
7.4	0.443 ± 0.048	0.976	1.6

Table A4 (continued). 60 ºC			
3.1	0.050 ± 0.004	0.940	13.7
4.6	0.032 ± 0.001	0.995	21.9
5.7	0.017 ± 0.001	0.964	41.9
6.9	0.099 ± 0.007	0.950	6.9
7.4	0.121 ± 0.011	0.970	5.7
37 ºC			
3.1	0.006 ± 0.004	---	100
4.6	0.002 ± 0.001	0.933	450
5.7	0.006 ± 0.003	---	100
6.9	0.017 ± 0.004	0.951	40
7.4	0.042 ± 0.006	0.895	17

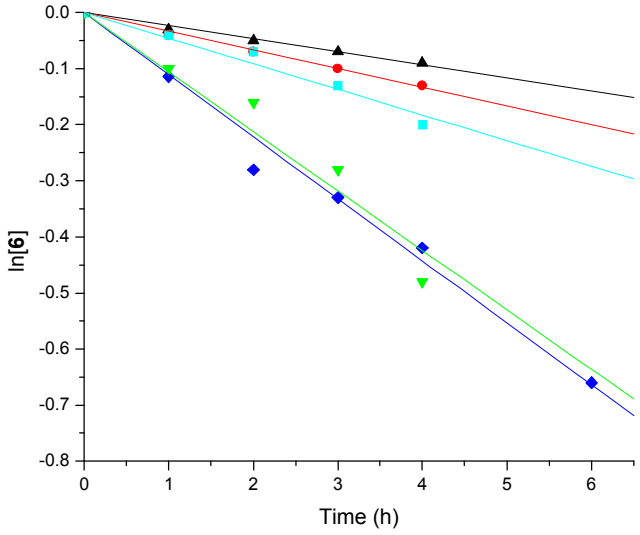

Figure A8. Pseudo-first order hydrolysis kinetics for compound **6** at 60 ºC. pH 3.1, ● pH 4.6, Δ pH 5.6, ∇ pH 6.9, ♦ pH 7.4.

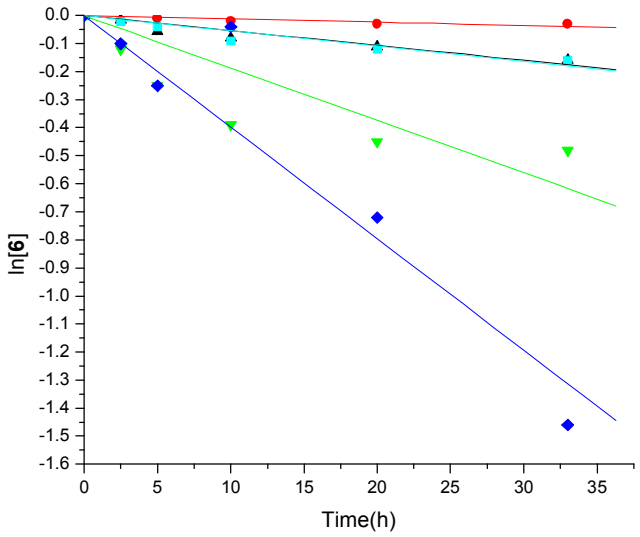

Figure A9. Pseudo-first order hydrolysis kinetics for compound **6** at 37 ºC. pH 3.1, ● pH 4.6, Δ pH 5.6, ∇ pH 6.9, ♦ pH 7.4.

A.5.3 Hydrolysis of 7

By investigating the hydrolysis behavior of compound **7**, virtually no hydrolysis at 37 ^{o}C was observed (half-lives of >200 hours for all pH values) (Figure A10), first-order kinetics at 60 ^{o}C (Figure A11), and finally, great deviations from first-order kinetics at 80 ^{o}C (Figure A12), which are not accompanied by a substantial rate increase. It is clear that this behavior is does not follow a clear hydrolysis trend.

While the reason for this hydrolysis behavior was not unequivocally determined, several possibilities exist. During this study, it was observed that the ester directly next to the norbornene hydrolyzes significantly slower than other hydrolysable sites that are further removed from the norbornene (see study of **3**). This has been evidenced by comparison of the hydrolysis data for monomers **3** – **6**. Hydrolysis data for **3** reflects only hydrolysis at the ester adjacent to the norbornenyl group, since this site is the only water labile site on the molecule. Significant hydrolysis of **3** only occurs at basic pH values. At lower pH values, monomers **4** and **5** exhibited the expected acetal cleavage, but as pH increased, trends began to mimic those of **3**, suggesting that the ester was hydrolyzing instead under that set of conditions. For **6**, faster hydrolysis than that of **3** was observed under all conditions, suggesting that the ester farther removed from the norbornenyl group was more labile under the conditions used in the study. However, one of the initial decomposition products observed for **6** showed subsequently further decomposition on a time scale identical to that of **3**, suggesting that this second hydrolysis step matches with the behavior of **3**. These results thus confirm the identities of the individual hydrolysis sites, recognizable by their own unique characteristic hydrolysis behaviors. The observed rate decrease for the norbornenyl ester is most likely due to the hydrophobic nature of the norbornene, the steric bulk generated by this bridged aliphatic group, or both. In compound **7**, the ester that is not directly attached to the norbornene is partially in a highly hydrophobic environment, potentially shielding it from easy access by water molecules. It is also a common behavior of molecules bearing a

hydrophobic end on one side of the molecule, and an ionic charge on the other, to form aggregates in solution, such is the case with many common surfactants. In aqueous media, the charged end of these molecules appears on the periphery of any aggregates formed, further protecting any hydrophobic esters on the interior from hydrolysis. As the temperature increases, non-covalent forces that aid in the swelling of aggregates or the desolvation of molecules may be overcome, causing the aggregates to collapse. This behavior could potentially lead to a change in mechanism at high temperature.

Table A5. Hydrolysis data for compound **7**.

Compound **7**, 80 ºC			
pH	k (h^{-1})	R^2	$T_{1/2}$ (h)
3.1	0.011 ± 0.003	0.712	61.2
4.6	0.005 ± 0.001	0.794	144
5.7	0.012 ± 0.005	0.227	58.9
6.9	0.013 ± 0.002	0.866	52.0
7.4	0.014 ± 0.005	0.371	50.1
8.9	0.067 ± 0.007	0.929	10.4

Table A5 (continued). Compound **7**, 60 ºC

3.1	0.019 ± 0.004	0.733	32.3
4.6	0.015 ± 0.002	0.904	46.0
5.7	0.060 ± 0.002	0.996	11.6
6.9	0.015 ± 0.003	0.840	45.8
7.4	0.056 ± 0.007	0.929	12.4
8.9	0.043 ± 0.003	0.987	16.3

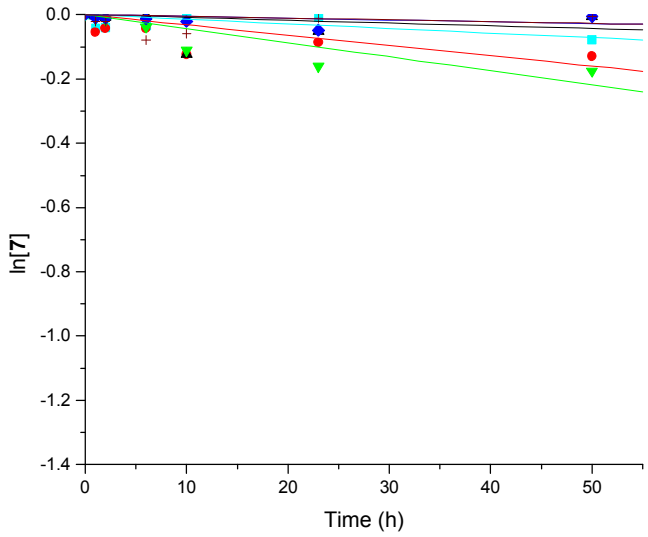

Figure A10. Pseudo-first order hydrolysis kinetics for compound **7** at 37 ºC. pH 3.1, ● pH 4.6, Δ pH 5.6, ∇ pH 6.9, ♦ pH 7.4, + pH 8.9.

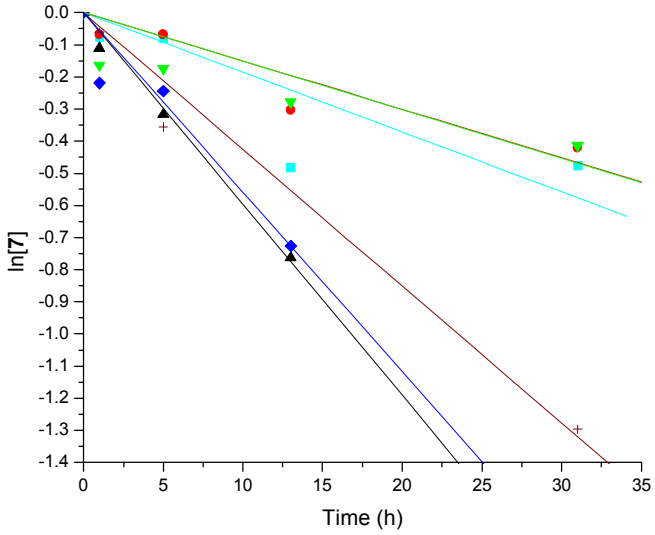

Figure A11. Pseudo-first order hydrolysis kinetics for compound **7** at 60 ºC. pH 3.1, ● pH 4.6, Δ pH 5.6, ∇ pH 6.9, ♦ pH 7.4, + pH 8.9.

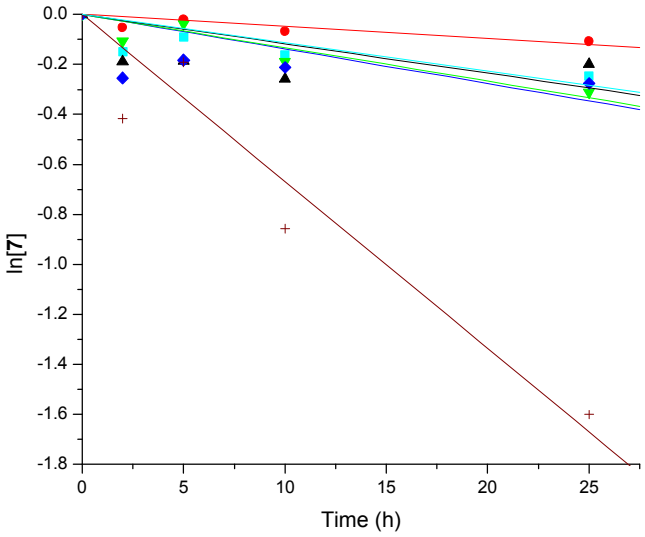

Figure A12. Hydrolysis kinetics for compound **7** at 80 ºC. pH 3.1, ● pH 4.6, Δ pH 5.6, ∇ pH 6.9, ♦ pH 7.4, + pH 8.9.

A.5.4 Hydrolysis of 9

The rate of hydrolysis of **9** at 80 °C and 60 °C at all pH values was too fast to be measured by the methods employed in this study. It is estimated that in buffered aqueous solution the half lives of all monomers are on the order of 5 to 10 minutes at all pH values. While the half-lives are noticeably longer (approximately 20 minutes) at 60 °C, the rate of hydrolysis is still too fast to quantitatively determine rate constants by HPLC analysis. The increased rate of hydrolysis for this compound may be due to several factors. It is hypothesized in the literature that neighboring amine functionalities can act as intramolecular nucleophilic catalysts in ester hydrolysis, thus contributing to higher degradation rates.[58] Langer and Lynn also point out the possibility of a potential retro-Michael addition occurring in molecules synthesized *via* Michael addition reactions.[59] In their study, they employed a polymer containing esters and tertiary amines along the polymer backbone in order to study the cytotoxicity of the degradation products of their polymer as a new transfection vector. They found that hydrolysis occurred faster at pH 7.4 than at 5.1. However, they observed no retro-Michael addition products in their system - only ester hydrolysis products, which suggests that retro-Michael addition is not the primary degradation pathway for **9**. Nucleophilic attack of the amine to the ester carbonyl gives a positively charged quaternary amide, which would be very active toward hydrolysis.

At 37 °C, the rates of hydrolysis are slow enough to observe *via* HPLC analysis, and are described in Table A6 and Figure A13 below. The rate of hydrolysis increases with pH, and was fastest at pH 8.9, consistent with the findings of Langer and Lynn for their similar system.

Table A6. Hydrolysis data for compound **9**.

Compound **9**, 37 ºC			
pH	k (h^{-1})	R^2	$t_{1/2}$ (h)
4.6	0.027 ± 0.001	0.993	26.1
5.7	0.073 ± 0.002	0.995	9.5
6.9	0.095 ± 0.001	0.999	7.3
7.4	0.090 ± 0.002	0.996	7.7
8.9	0.149 ± 0.003	0.997	4.7

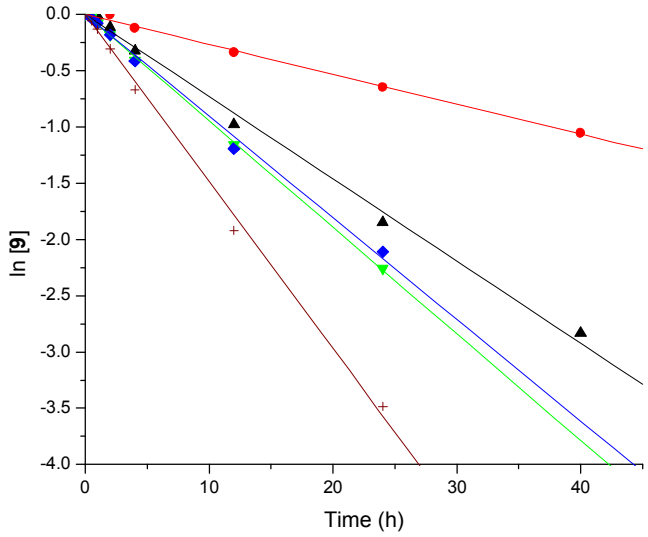

Figure A13. Pseudo-first order hydrolysis kinetics for compound **9** at 37 ºC. • pH 4.6, Δ pH 5.6, ∇ pH 6.9, ♦ pH 7.4, + pH 8.9.

A.5.5 Hydrolysis of 8.

Compound **8** showed no significant hydrolysis at 37 ºC, with the exception of pH 8.9, which appeared to decompose faster than the methods employed in this study are able to measure. At 60 ºC, there was again extremely rapid decomposition at pH 8.9, while pH values of 3.1, 4.6, and 7.4 once again showed no observable hydrolysis. However, pH 5.7 and 6.9 exhibited pseudo first-order kinetics. At 80 ºC, decomposition at pH 8.9 again was too fast to measure, while pH 3.1, 4.6, and 5.7 gave fairly well-behaved pseudo first-order kinetics, displaying half-lives in the range of 5.1 hrs for pH 5.7 to 63 hrs for pH 3.1. As displayed in Figure 16, hydrolysis of pH 6.9 was non-linear. This result suggests the occurrence of side reactions or interactions of **8** with the buffer. Hydrolysis kinetics measured for pH 7.4 did not follow first-order for any temperature range.

Table A7. Hydrolysis data for compound **8**.

Compound **8**, 80 ºC			
pH	k (h^{-1})	R^2	$T_{1/2}$ (h)
3.1	0.011 ± 0.001	0.947	63
4.6	0.012 ± 0.001	0.961	57.8
5.7	0.136 ± 0.006	0.982	5.1
6.9	0.059 ± 0.021	0.272	11.7
7.4	0.020 ± 0.004	0.822	34.7
Compound **8**, 60 ºC			
3.1	0.001 ± 0.001	---	700
4.6	0.001 ± 0.001	---	700
5.7	0.034 ± 0.001	0.985	20.4
6.9	0.053 ± 0.008	0.833	13.1
7.4	0.004 ± 0.001	---	170

Table A7 (continued). Compound **8**, 37 ºC

3.1	0.005 ± 0.001	---	140
4.6	0.001 ± 0.002	---	700
5.7	0.002 ± 0.001	---	350
6.9	0.008 ± 0.004	---	90
7.4	0.003 ± 0.002	---	230

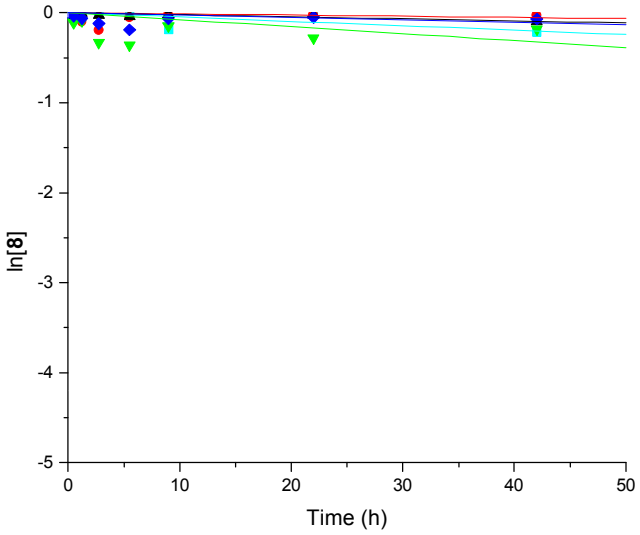

Figure A14. Hydrolysis kinetics for compound **8** at 37 ºC. pH 3.1, • pH 4.6, Δ pH 5.6, ∇ pH 6.9, ♦ pH 7.4.

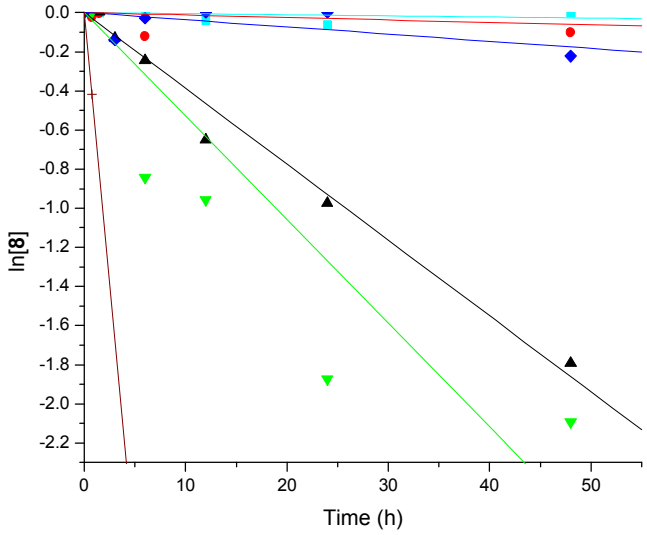

Figure A15. Hydrolysis kinetics for compound **8** at 60 ºC. pH 3.1, • pH 4.6, Δ pH 5.6, ∇ pH 6.9, ♦ pH 7.4, + pH 8.9.

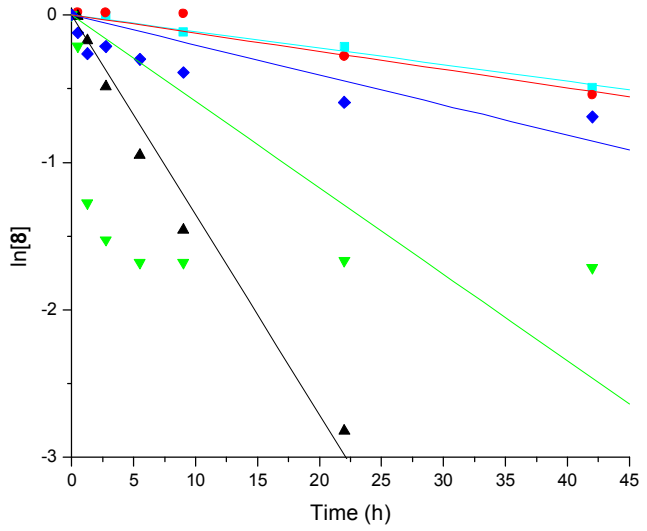

Figure A16. Hydrolysis kinetics for compound **8** at 80 ºC. pH 3.1, • pH 4.6, Δ pH 5.6, ∇ pH 6.9, ♦ pH 7.4.

A.6 Conclusion

In conclusion, a variety of chemically diverse norbornene compounds was synthesized, representing an important class of monomers for ROMP. Furthermore, the decomposition of these monomers via hydrolysis in aqueous solution under a variety of pH and temperature ranges was investigated. The investigated monomers contained either ester and/or acetal linkages, as well as terminal functional groups including esters, acids, ethers, and saccharides. During the hydrolysis studies, the two extremes that were investigated were the amine/ester-based and the saccharides-based monomers. The hydrolysis of tertiary amine/ester-based monomers was very fast with half-lives of below ten hours for all temperatures and pHs investigated. In contrast, the saccharide/ester-based monomer showed the slowest hydrolysis at acidic conditions of any monomer and condition studied.

A variety of important trends were observed during these studies. First, the chemistry of the acetal functional group allows for selective hydrolysis of the side-chain either at the ester linkage of the norbornene at the 2-position (at high pH) or at the acetal group (at low pH). Second, the presence of a beta-amino functionality greatly enhances the rate of hydrolysis and also changes the pH dependence of the rate constants. This suggests a change in the mechanism of hydrolysis by the involvement of intramolecular assistance, but the experiments conducted in this study do not conclusively show which mechanisms may be predominating. Third, the presence of a carboxylic acid in the monomer structure results in the unpredictable hydrolysis of the monomer with non-first-order kinetics. Fourth, saccharide-containing monomers hydrolyze rapidly in alkaline media while they are stable under acidic conditions, an important finding for polymers based on similar monomers have been suggested as biomaterial. Furthermore, it is important to note that the hydrolysis behavior of the monomers under some temperature and pH conditions, in particular at neutral pHs, does not follow the expected trends. It was rationalized that these cases include either the participation of neighboring groups and/or interactions of

the monomers with the buffer. Finally, significant hydrolysis of the ester linkage directly bonded to the norbornene was observed. The use of ester linkages to support side-chains on poly(norbornene)s is the most commonly employed method also for water soluble polymers. Our results clearly demonstrate that these esters are not stable under a wide variety of temperatures and pH values, suggesting that the stability of side-chain functionalized poly(norbornene)s containing ester linkages is limited and this inherent instability must be considered when designing functionalized poly(norbornene)s.

A.7 Experimental Section

Dichloromethane, diethyl ether, THF, and hexanes were dried by passage through columns of alumina and Cuº. Glycols were dried by stirring with sodium under an inert atmosphere and distilled under reduced pressure prior to use. DMSO was refluxed over CaH_2 under an inert atmosphere, distilled and stored in a Schlenk flask at -15 ºC. ^1H and ^{13}C NMR spectra were acquired at 300 MHz for ^1H and 75 MHz for ^{13}C. HPLC data were collected using UV-Vis and RI detection. Compound **1** was synthesized by the method of Jacobine in average of 85% yield and stored under inert atmosphere at -15 ºC.[56]

Synthesis of Bicyclo[2.2.1]hept-5-ene-2-carboxlylic acid 2-[2-(2-hydroxyethoxy)ethoxy ethyl ester (1)

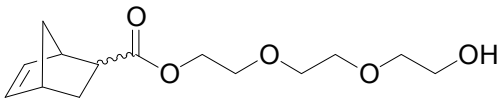

To a solution of triethylene glycol (3.66 g, 24.4 mmol) and triethylamine (4.90g, 48.8 mmol) in THF (200 mL) compound **10** (3.63 g, 23.2 mmol) was added dropwise at 0 °C. The mixture was warmed to ambient temperature and stirred for eight hours. The mixture was diluted with diethyl ether and washed with 5% NaOH (aq.), 5% HCl (aq.), sat. $NaHCO_3$ (aq.), brine and dried over Na_2SO_4. The solvent was removed under

reduced pressure and the residue distilled *in vacuo* to give to give bicyclo[2.2.1]hepta-5-ene-2-carboxlylic acid 2-[2-(2-hydroxvethoxy)ethoxy]ethyl ester as a clear colorless liquid (5.21 g, 83%). ^{1}H NMR (400 MHz, $CDCl_3$): δ 6.15 (m, 0.8H, endo vinyl), 6.10 (m, 0.4H, exo vinyl), 5.90 (m, 0.8H, endo vinyl), 4.14-4.24 (m, 2H, ester O-C**H**$_2$-CH$_2$), 3.72-3.65 (m, 8H, methylene O-C**H**$_2$), 3.60 (m, 2H, terminal methylene CH_3-O-C**H**$_2$-CH_2), 3.19 (br, 1H, O**H**), 3.02 (br, 1H, norbornenyl), 2.94 (m, 1H, norbornenyl), 2.88 (br, 1H, ester methine), 2.22 (m, 1H, norbornenyl), 1.93-1.84 (m, 1H, norbornenyl), 1.49-1.23 (m, 3H, norbornene alkyl). ^{13}C NMR (100 MHz, $CDCl_3$): δ 176.1, 174.6, 137.9, 137.6, 135.6, 132.2, 72.4, 70.4, 70.2, 69.1, 63.2, 63.1, 61.6, 49.5, 46.5, 46.2, 45.6, 43.1, 42.9, 41.5, 30.2, 29.1. IR (neat): 3460 (br, -OH), 3060, 2940, 2870, 1730, 1630 (shoulder), 1450, 1190, 1110, 712 cm^{-1}. MS(EI, 70 KeV): m/z 139, 58 (100). Elem. Anal: Calc. for $C_{14}H_{22}O_5$: C, 62.20, H, 8.20. Found: C, 62.28, H, 8.29.

Synthesis of Bicyclo[2.2.1]hept-5-ene-2-carboxylic acid 2-(2-chloroethoxy)ethyl ester (2)

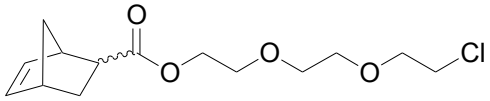

2-Chloroethoxyethanol (14.4 g, 0.12 mol) in triethylamine (40 mL) was added to a solution of **10** (17.3 g, 0.11 mol) in CH_2C1_2 (75 mL) at 0 °C. The reaction mixture was warmed to ambient temperature and stirred for twelve hours. The reaction was washed with aq. NH_4Cl (sat.), the organic layer separated and concentrated, and the residue distilled under reduced pressure to give bicyclo[2.2.1]hept-5-ene-2-carboxylic acid 2-(2-chloroethoxy)-ethyl ester as a clear pale yellow liquid (18.6 g, 69%, 4:1 *endo/exo*). ^{1}H NMR (300 MHz, $CDCl_3$): δ 6.12 (m, 0.8H, endo vinyl), 6.05 (m, 0.4H, exo vinyl), 5.87 (m, 0.8H, endo vinyl), 4.05-4.22 (m, 2H, ester O-C**H**$_2$-CH$_2$), 3.54-3.72 (m, 6H, ether O-C**H**$_2$-CH$_2$), 3.15 (br, 1H, Cl-C**H**$_2$-CH$_2$), 2.98 (br, 1H, CH=CH-C**H**), 2.88-2.94 (m, 1H, CH=CH-C**H**), 2.83 (br, 1H, ester methine), 2.22 (m, 1H, norbornene alkyl), 1.79-1.88 (m,

1H, norbornene alkyl), 1.19-1.38 (m, 3H, norbornene alkyl). ^{13}C NMR (100 MHz, $CDCl_3$): δ 175.8, 174.3, 137.8, 137.5, 135.5, 132.1, 70.9, 69.0, 63.0, 62.9, 49.4, 43.4, 46.1, 45.5, 43.0, 42.8, 42.5, 42.3, 41.4, 31.3, 30.1, 29.0, 22.4. IR (neat): 3052 (br, -OH), 2969, 2872, 1733, 1637 (shoulder), 1458, 1182, 1128, 703 cm^{-1}. MS(EI, 70 KeV): m/z 244 (M^+, 3%), 179, 120, 99, 66 (100), 55. HRMS: Calc. for $C_{12}H_{17}O_3Cl$: 244.0866, Observed: 244.0882.

Synthesis of Bicyclo[2.2.1]hept-5-ene-2-carboxylic acid 2-(2-[2-methoxyethoxy]ethoxy)ethyl ester (3)

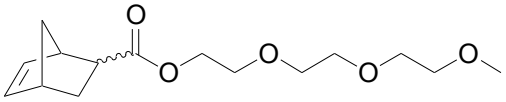

A solution of triethylene glycol monomethyl ether and triethylamine in THF was cooled to 0 ºC and **10** was added dropwise over a period of 30 minutes. The mixture was warmed to ambient temperature and stirred for seven hours. The mixture was diluted with diethyl ether and washed with 5% NaOH (aq.), 5% HCl (aq.), sat. $NaHCO_3$ (aq.), brine and dried over Na_2SO_4. The solvent was removed under reduced pressure and the residue distilled *in vacuo* to give bicyclo[2.2.1]hept-5-ene-2-carboxylic acid 2-(2-[2-methoxyethoxy]ethoxy)ethyl ester as a clear colorless liquid. ^{1}H NMR (300 MHz, $CDCl_3$): δ 6.15 (m, 0.8H, endo vinyl), 6.10 (m, 0.4H, exo vinyl), 5.90 (m, 0.8H, endo vinyl), 4.14-4.24 (m, 2H, ester O-C**H**$_2$-CH_2), 3.72-3.65 (m, 8H, ether O-C**H**$_2$-CH_2), 3.27 (s, 3H, O-C**H**$_3$), 3.19 (br, 1H, CH=CH-C**H**), 3.02 (br, 1H, CH=CH-C**H**$_2$), 2.94 (m, 0.8H, endo ester methine), 2.88 (br, 0.2H, exo ester methine), 2.22 (m, 1H, norbornene alkyl), 1.93-1.84 (m, 1H, norbornene alkyl), 1.49-1.23 (m, 3H, norbornene alkyl). ^{13}C NMR (75 MHz, $CDCl_3$): δ 175.7, 174.2, 137.7, 137.3, 135.4, 132.0, 71.7, 70.4, 70.3, 69.0, 63.2, 63.1, 58.8, 49.4, 46.4, 46.1, 45.5, 43.0, 42.8, 42.3, 41.4, 30.2, 29.1. IR (neat): 3060.6, 2946.9, 2879.6, 1731.9, 1451.3, 1334.6, 1108.9, 714.5 cm^{-1}. MS (EI, 70 KeV): *m/z* 284

(M^+), 239, 219, 165, 120, 99 (100), 66, 55. Elem. Anal.: Calc. for $C_{15}H_{24}O_5$: C, 63.36, H, 8.51. Found: C, 63.31, H, 8.49.

Synthesis of Pentanedioic acid mono-[2-(2-[2-(bicyclo[2.2.1]hept-5-ene-2-carbonyloxy)-ethoxy]ethoxy)-ethyl] ester (7)

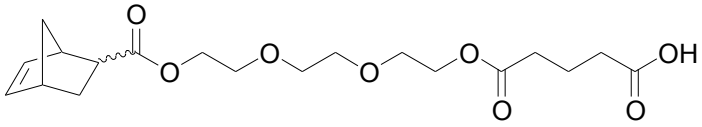

A solution of **1** (1.28 g, 4.75 mmol) and pyridine (3 mL) in THF (20 mL) was added to glutaric anhydride (0.57 g, 4.98 mmol) in THF (10 mL) at ambient temperature and stirred for 12 h. The reaction mixture was diluted with diethyl ether and washed with 10% HCl (aq.), dried over Na_2SO_4, and concentrated under reduced pressure. The residue was purified by column chromatography (1:1 ethyl acetate:hexane, silica) to give pentanedioic acid mono-[2-(2-[2-(bicyclo[2.2.1]hept-5-ene-2-carbonyloxy)-ethoxy]-ethoxy)-ethyl] ester as a clear colorless liquid (1.49 g, 82%). ^{1}H NMR (400 MHz, $CDCl_3$): δ. 6.16 (m, 1.2H, endo/exo vinyl), 5.91 (m, 0.8H, endo vinyl), 4.23-4.14 (m, 2H, ester O-C**H**$_2$-CH$_2$), 3.82-3.73 (m, 8H, ether O-C**H**$_2$-CH$_2$), 3.19 (s, br, 1H, ester methine), 2.98-2.87 (m, 2H, ester methylene C(O)C**H**$_2$), 2.43-2.36 (m, 4H), 2.02-1.84 (m, 3H, norbornene alkyl), 1.42-1.23 (m, 3H, alkyl). ^{13}C NMR (100 MHz, $CDCl_3$): δ 177.7, 174.7, 172.8, 138.0, 137.7, 135.6, 132.3, 72.4, 70.4, 70.3, 69.2, 63.5, 63.2, 61.6, 49.5, 46.6, 46.2, 45.6, 43.1, 43.0, 42.4, 41.5, 33.0, 32.8, 30.3, 29.2, 19.9, 19.7. IR (neat): 3296 (br, -OH), 2963, 2880 (CH stretch), 1760, 1722 (C=0), 1447, 1139, 717 cm^{-1}. MS(El, 70 KeV): m/z 385 (M+H), 367, 301, 247, 205. 159. 120, 99 (100). 66. 55. HRMS: Calc. For $C_{19}H_{28}O_8$: 384.1784, Observed: 384.1779. Elem. Anal.: Calc. for $C_{19}H_{28}O_8$: C, 59.36, H, 7.34. Found: C, 59.31, H, 7.45.

Synthesis of Galactopyranose-6-uronic acid 2-(2-[2-(bicyclo[2.2.1]hept-5-ene-2-carbonyloxy)ethoxy] ethoxy)ethyl ester (8)

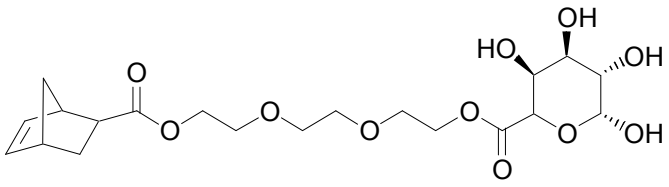

Compound **15** (0.29 g, 0.55 mmol) was dissolved in 8 mL of a solution of 80% TFA (aq.) and stirred for three hours at ambient temperatures. The solvent was removed under reduced pressure and the residue subjected to column chromatography (silica, 1:1 ethanol:ethylacetate) to give galactopyranose-6-uronic acid 2-(2-[2-(bicyclo[2.2.1]hept-5-ene-2-carbonyloxy)ethoxy]ethoxy)ethyl ester as a clear colorless viscous liquid. Yield 0.206 g (84 %). ^{1}H NMR (300 MHz, $CDCl_3$): δ 6.12-6.15 (m, 0.5H, vinyl endo), 6.04-6.08 (m, 1H, vinyl exo), 5.86-5.89 (m, 0.5H, vinyl exo), 5.46 (s, br, 1H, anomeric methine), 5.30 (s, br, 0.5H, galactose methine), 4.86 (m, 0.5H, galactose methine), 4.70 (m, 1H, C**H**-OH), 4.33 (m, 3H, ether O-C**H**$_2$), 4.04 (m, 2H), 3.95 (m, 1H), 3.61 (m, 9H, ether C**H**$_2$-O), 3.16 (s, br, 1H, CH=CH-C**H**), 2.95 (m, 1H, CH=CH-C**H**), 2.85 (s, br, 1H, norbornene alkyl), 2.62, (m, 1H, norbornene alkyl), 2.19 (m, 1H), 1.88 (m, 1H, norbornene alkyl), 1.63 (m, 1H, norbornene alkyl), 1.36 (m, 2H, alkyl), 1.21 (m, 2H, alkyl). ^{13}C NMR (100 MHz, $CDCl_3$): δ 175.1, 138.2, 138.1, 136.2, 132.5, 81.4, 70.6, 70.5, 69.4, 69.3, 65.0, 64.9, 63.6, 49.9, 47.0, 46.0, 44.1, 43.5, 42.6, 40.1, 30.2. IR (KBr): 3379 (br, -OH), 2947, 2877 (CH stretch), 1734 (C=0), 1452, 1340, 1205 (sp^2 C-O), 1105, 1018 (sp^3 C-O), 939, 808 cm^{-1}. Elem.Anal.: Calc. for $C_{20}H_{30}O_{11}$: C, 53.81, H, 6.77. Found: C, 53.74, H, 6.68.

Synthesis of 2:3, 4:5-diisopropylidine galactopyranose-6-uronic acid (14)

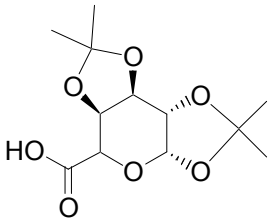

A solution of 2:3, 4:5-diisopropylidine galactopyranose (2.61 g, 10.0 mmol) in acetone (10 mL) was slowly added to a solution of CrO_3 (1.49g, 15.0 mmol) in acetone (30 mL) at 0 ºC. The mixture was warmed to ambient temperature and stirred for five hours. Ethyl acetate was carefully added to the mixture and the reaction was washed with water. The organic layer was washed with brine, dried over Na_2SO_4, and the solvent was removed under reduced pressure. The residue was subjected to column chromatography (silica, 1:1 ethylacetate:hexanes) to give 2:3, 4:5-diisopropylidine galactopyranose-6-uronic acid as a clear, colorless, viscous liquid that crystallized upon standing. Yield 2.23 g (81 %). ^{1}H NMR (400 MHz, DMSO-d_6): δ 5.52 (d, J = 5.0 Hz, 1H, anomeric C**H**), 4.64 (dd, J = 2.4, 7.7, 1H, galactose methine), 4.49 (dd, J = 2.1, 7.7, 1H, galactose methine), 4.39 (dd, J = 2.5, 5.0, 1H, galactose methine), 4.17 (d, J = 2.1, 1H, galactose methine), 1.42 (s, 3H, isopropylidine methyl), 1.31 (s, 3H, isopropylidine methyl), 1.27 (s, 3H, isopropylidine methyl), 1.26 (s, 3H, isopropylidine methyl). ^{13}C NMR (75 MHz, DMSO-d_6): δ 168.9, 108.7, 108.3, 95.8, 71.5, 70.1, 69.6, 67.4, 25.8, 25.7, 24.7, 24.4. IR (KBr): 3491 (br, O-H) 2985, 2937 (sp^3 CH stretch), 1722 (acid C=0), 1456, 1375, 1211, (sp^2 C-O), 1164, 1118, 1070, 1022 (sp^3 C-O), 904, 840, 790, 692, 511 cm^{-1}. Elem.Anal.: Calc. for $C_{12}H_{18}O_7$: C, 52.55, H, 6.62. Found: 52.41, H, 6.63.

Synthesis of (2:3, 4:5-Diisopropylidine)-galactopyranose-6-uronic acid 2-(2-[2-(bicyclo[2.2.1]hept-5-ene-2-carbonyloxy)ethoxy]ethoxy)ethyl ester (15)

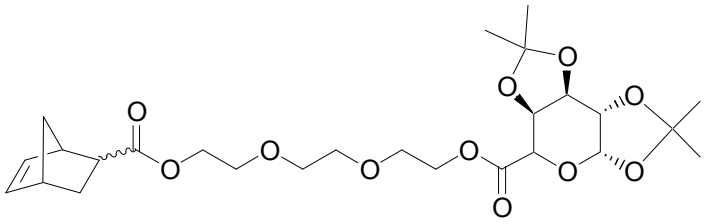

Compound **14** (0.34 g, 1.25 mmol) was dissolved in CH_2Cl_2 (8 mL) at ambient temperature and **1** (0.34 g, 1.25 mmol), pyridine (0.10 g, 1.26 mmol), and dicyclohexylcarbodiimide (0.26 g, 1.25 mmol) were added sequentially. The mixture was stirred for 24 hours at ambient temperature and the resulting white precipitate was removed by filtration. The solvent was removed under reduced pressure and the residue redissolved in benzene. The insoluble white solid was removed by filtration and the solvent removed under reduced pressure and the residue was subjected to column chromatography (silica, 1:1 ethyl acetate:hexanes) to give (2:3, 4:5-diisopropylidine)-galactopyranose-6-uronic acid 2-(2-[2-(bicyclo[2.2.1]hept-5-ene-2-carbonyloxy)ethoxy]ethoxy)ethyl ester as a clear colorless viscous liquid. Yield 0.39 g (60 %). ^{1}H NMR ($CDCl_3$, 300 MHz): δ 6.15 (dd, 0.8H, J = 3.1, 5.7 Hz, endo vinyl), 6.08 (m, 0.4H, exo vinyl), 5.91(dd, 0.8H, J = 2.8, 5.7 Hz, endo vinyl), 5.63 (d, 1H, J = 5.0 Hz, anomeric methine), 4.62 (m, 3H, galactose methine), 4.43 (d, 1H, J = 2.3 Hz, galactose methine), 4.36 (m, 3H), 4.16 (m, 1H, galactose methine), 3.71 (t, 2H, J = 4.9 Hz, ether CH_3-O-C**H**$_2$), 3.60 (m, 6H, ether O-C**H**$_2$-CH_2), 3.19 (s, br, 1H, ester methine), 2.95 (dt, 1H, J = 3.9, 9.3 Hz, norbornenyl alkyl), 2.88 (s, br, 1H, norbornene alkyl), 1.87 (ddd, 1H, J = 3.7, 9.4, 12.7 Hz, alkyl), 1.50 (s, 4H, alkyl), 1.42 (s, 3H, isopropylidine methyl), 1.31 (m, 9H, isopropylidine methyl). Elem.Anal.: Calc. for $C_{26}H_{38}O_{11}$: C, 59.30, H, 7.27. Found: 59.21, H, 7.21.

General Procedure for Hydrolysis

The hydrolysis of all monomers was carried out using 5 mM solutions of analyte in buffers of pH 3.1 (phosphate/citric acid), 4.6 (acetate), 5.7 (acetate), 6.9 (phosphate), 7.4 (phosphate-buffered saline) and 8.9 (borate). The samples were heated to 37, 60, and 80 °C (±0.1 °C) in a thermostatic oil bath and samples (50 μL) were withdrawn and diluted to 1.00 mL in the appropriate mobile phase prior to HPLC analysis. Samples were stored at -15 ºC when not immediately analyzed.

Instrumental Setup for HPLC Analysis:

The kinetics of hydrolysis was investigated via HPLC analysis under isocratic conditions. For monomers **4**, **5**, and **6**, the mobile phase consisted of 1:1 acetonitrile:water, column temperature of 40 °C, and 0.75 mL/min flow rate using a C18 column (25 cm x 4.0 mm, 5 μm particle diameter). For **7**, a mobile phase of 70:30 acetonitrile:water was used with a C18-AI amide functionalized column (25cm x 4.0 mm, 5 μm particle diameter) at a temperature of 40 °C, 1.0 mL/min flow rate using UV detection at 210 nm. For **9**, a mobile phase of 70:30 acetonitrile:pH 6.6 phosphate buffer was employed with a C18 (25 cm x 4.0 mm, 5 μm particle diameter) column at 40 ºC and 1.0 mL/min flow rate with UV detection at 210 nm. Analysis of compound **8** was performed using a MC18-AI amide functionalized column (25 cm x 4.0 mm, 5 μm particle diameter) at a temperature of 40 °C, 1.0 mL/min flow rate using UV detection at 210 nm, and 60:40 methanol:water as the mobile phase.

A.8 References

(1) Barrett, A. G. M.; Hopkins, B. T.; Kobberling, J. *Chem. Rev.* **2002**, *102*, 3301-24.

(2) Furstner, A. *Angew. Chem. Int. Ed.* **2000**, *39*, 3012-3043.

(3) Grubbs, R. H. *Tetrahedron* **2004**, *60*, 7117-7140.

(4) Grubbs, R. H. *Handbook of Metathesis*; Wiley-VCH: Weinheim, 2003; Vol. 3.

(5) Bertin, P. A.; Watson, K. J.; Nguyen, S. T. *Macromolecules* **2004**, *37*, 8364-8372.

(6) Biagini, S. C. G.; Davies, R. G.; Gibson, V. C.; Giles, M. R.; Marshall, E. L.; North, M.; Robson, D. A. *Chem. Commun.* **1999**, 235-236.

(7) Gestwicki, J. E.; Strong, L. E.; Cairo, C. W.; Boehm, F. J.; Kiessling, L. L. *Chem. Biol.* **2002**, *9*, 163-169.

(8) Kiessling, L. L.; Strong, L. E. *Top. Organomet. Chem.* **1998**, *1*, 199-231.

(9) Kiessling, L. L.; Strong, L. E.; Gestwicki, J. E.; (Wisconsin Alumni Research Foundation, USA). Application: WO, 2001; pp 95 pp.

(10) Maynard, H. D.; Okada, S. Y.; Grubbs, R. H. *J. Am. Chem. Soc.* **2001**, *123*, 1275-1279.

(11) North, M. *NATO Sci. Ser. II: Math. Phys. Chem.* **2002**, *56*, 157-166.

(12) Owen, R. M.; Gestwicki, J. E.; Young, T.; Kiessling, L. L. *Org. Lett.* **2002**, *4*, 2293-2296.

(13) Roberts, K. S.; Konkar, S.; Sampson, N. S. *ChemBioChem* **2003**, *4*, 1229-1231.

(14) Boyd, T. J.; Geerts, Y.; Lee, J.-K.; Fogg, D. E.; Lavoie, G. G.; Schrock, R. R.; Rubner, M. F. *Macromolecules* **1997**, *30*, 3553-3559.

(15) Buchmeiser, M. R. *Chem. Rev.* **2000**, *100*, 1565-1604.

(16) Meyers, A.; South, C.; Weck, M. *Chem. Commun.* **2004**, 1176-1177.

(17) Meyers, A.; Weck, M. *Macromolecules* **2003**, *36*, 1766-1768.

(18) Meyers, A.; Weck, M. *Chem. Mater.* **2004**, *16*, 1183-1188.

(19) Myles, A. J.; Gorodetsky, B.; Branda, N. R. *Adv. Mater.* **2004**, *16*, 922-925.

(20) Tsai, M.-L.; Liu, C.-Y.; Wang, Y.-Y.; Chen, J.-y.; Chou, T.-C.; Lin, H.-M.; Tsai, S.-H.; Chow, T. J. *Chem. Mater.* **2004**, *16*, 3373-3380.

(21) Wagaman, M. W.; Grubbs, R. H. *Macromolecules* **1997**, *30*, 3978-3985.

(22) Arehart, S. V.; Pugh, C. *J. Am. Chem. Soc.* **1997**, *119*, 3027-3037.

(23) Demel, S.; Riegler, S.; Wewerka, K.; Schoefberger, W.; Slugovc, C.; Stelzer, F. *Inorg. Chim. Acta* **2003**, *345*, 363-366.

(24) Li, M.-H.; Keller, P.; Albouy, P.-A. *Macromolecules* **2003**, *36*, 2284-2292.

(25) Pasquier, C.; Van der Schaaf, P. A.; (Ciba Specialty Chemicals Holding Inc., Switz.). Application: WO, 1999; pp 35 pp.

(26) Percec, V.; Chu, P.; Asandei, A. D. *Polym. Mater. Sci. Eng.* **1999**, *80*, 223-224.

(27) Ungerank, M.; Winkler, B.; Eder, E.; Stelzer, F. *Macromol. Chem. Phys.* **1997**, *198*, 1391-1410.

(28) Weck, M.; Mohr, B.; Maughon, B. R.; Grubbs, R. H. *Macromolecules* **1997**, *30*, 6430-6437.

(29) Wewerka, K.; Wewerka, A.; Stelzer, F.; Gallot, B.; Andruzzi, L.; Galli, G. *Macromol. Rapid Commun.* **2003**, *24*, 906-910.

(30) Raimundo, J.-M.; Lecomte, S.; Edelmann, M. J.; Concilio, S.; Biaggio, I.; Bosshard, C.; Guenter, P.; Diederich, F. *J. Mater. Chem.* **2004**, *14*, 292-295.

(31) Sattigeri, J. A.; Shiau, C.-W.; Hsu, C. C.; Yeh, F.-F.; Liou, S.; Jin, B.-Y.; Luh, T.-Y. *J. Am. Chem. Soc.* **1999**, *121*, 1607-1608.

(32) Arstad, E.; Barrett, A. G. M.; Tedeschi, L. *Tetrahedron Lett.* **2003**, *44*, 2703-2707.

(33) Krause, J. O.; Lubbad, S.; Nuyken, O.; Buchmeiser, M. R. *Adv. Synth. Catal.* **2003**, *345*, 996-1004.

(34) Krause, J. O.; Lubbad, S. H.; Nuyken, O.; Buchmeiser, M. R. *Macromolecular Rapid Communications* **2003**, *24*, 875-878.

(35) Kroll Roswitha, M.; Schuler, N.; Lubbad, S.; Buchmeiser Michael, R. *Chemical communications (Cambridge, England)* **2003**, 2742-3.

(36) Mayr, M.; Buchmeiser, M. R. *Macromol. Rapid Commun.* **2004**, *25*, 231-236.

(37) Pollino, J. M.; Weck, M. *Org. Lett.* **2002**, *4*, 753-756.

(38) Schubert, U. S.; Weidl, C. H.; Eschbaumer, C.; Kroell, R.; Buchmeiser, M. R. *Polym. Mater. Sci. Eng.* **2001**, *84*, 514-515.

(39) Skaff, H.; Ilker, M. F.; Coughlin, E. B.; Emrick, T. *J. Am. Chem. Soc.* **2002**, *124*, 5729-5733.

(40) Yang, L.; Mayr, M.; Wurst, K.; Buchmeiser, M. R. *Chem. Eur. J.* **2004**, *10*, 5761-5770.

(41) Yu, K.; Sommer, W.; Richardson, J. M.; Weck, M.; Jones, C. W. *Adv. Synth. Catal.* **2005**, *347*, 161-171.

(42) Buchmeiser, M. R.; Lubbad, S.; Mayr, M.; Wurst, K. *Inorg. Chim. Acta* **2003**, *345*, 145.

(43) Buchmeiser, M. R. *Bioorg. Med. Chem. Lett.* **2002**, *12*, 1837.

(44) Liu, C.; Yu, J.; Sun, X.; Zhang, J.; He, J. *Polym. Degrad. Stab.* **2003**, *81*, 197-205.

(45) Thorn-Csanyi, E. *NATO ASI Ser. C: Math. Phys. Sci.* **1998**, *506*, 117-137.

(46) Wang, W.; Qu, B. *Polym. Degrad. Stab.* **2003**, *81*, 531-537.

(47) Wedlake, M. D.; Kohl, P. A. *J. Mater. Res.* **2002**, *17*, 632-640.

(48) Deslongchamps, P.; Dory, Y. L.; Li, S. *Tetrahedron* **2000**, *56*, 3533-3537.

(49) Mabey, W.; Mill, T. *J. Phys. Chem. Ref. Data* **1978**, *7*, 383-415.

(50) Anderson, E.; Capon, B. *J. Chem. Soc., Perkin Trans. (1972-1999)* **1972**, 515-22.

(51) Cordes, E. H.; Bull, H. G. *Chem. Rev.* **1974**, *74*, 581-603.

(52) Gordon, E. J.; Sanders, W. J.; Kiessling, L. L. *Nature* **1998**, *392*, 30-31.

(53) Manning, D. D.; Strong, L. E.; Hu, X.; Beck, P. J.; Kiessling, L. L. *Tetrahedron* **1997**, *53*, 11937-11952.

(54) Smith, E. A.; Thomas, W. D.; Kiessling, L. L.; Corn, R. M. *J. Am. Chem. Soc.* **2003**, *125*, 6140-6148.

(55) Carlise, J. R.; Kriegel, R. M.; Rees, W. S., Jr.; Weck, M. *J. Org. Chem.* **2005**, *70*, 5550-5560.

(56) Jacobine, A. F.; Glaser, D. M.; Nakos, S. T. *Polym. Mater. Sci. Eng.* **1989**, *60*, 211-216.

(57) Godage, H. Y.; Fairbanks, A. J. *Tetrahedron Lett.* **2000**, *41*, 7589-7593.

(58) Lim, Y.-B.; Kim, C.-H.; Kim, K.; Kim, S. W.; Park, J.-S. *J. Am. Chem. Soc.* **2000**, *122*, 6524-6525.

(59) Lynn, D. M.; Langer, R. *J. Am. Chem. Soc.* **2000**, *122*, 10761-10768.